Advances in Science, Technology & Innovation
IEREK Interdisciplinary Series for Sustainable Development

Ana Malheiro · Francisco Fernandes ·
Helder I. Chaminé *Editors*

Advances in Natural Hazards and Volcanic Risks: Shaping a Sustainable Future

Proceedings of the 3rd International Workshop on Natural Hazards (NATHAZ'22), Terceira Island—Azores 2022

IEREK
RESEARCH & KNOWLEDGE ENRICHMENT

Springer

Advances in Science, Technology & Innovation

IEREK Interdisciplinary Series for Sustainable Development

Advances in Science, Technology & Innovation (ASTI) is a series of peer-reviewed books based on important emerging research that redefines the current disciplinary boundaries in science, technology and innovation (STI) in order to develop integrated concepts for sustainable development. It not only discusses the progress made towards securing more resources, allocating smarter solutions, and rebalancing the relationship between nature and people, but also provides in-depth insights from comprehensive research that addresses the **17 sustainable development goals (SDGs)** as set out by the UN for 2030.

The series draws on the best research papers from various IEREK and other international conferences to promote the creation and development of viable solutions for a **sustainable future and a positive societal** transformation with the help of integrated and innovative science-based approaches. Including interdisciplinary contributions, it presents innovative approaches and highlights how they can best support both economic and sustainable development, through better use of data, more effective institutions, and global, local and individual action, for the welfare of all societies.

The series particularly features conceptual and empirical contributions from various interrelated fields of science, technology and innovation, with an emphasis on digital transformation, that focus on providing practical solutions to **ensure food, water and energy security to achieve the SDGs.** It also presents new case studies offering concrete examples of how to resolve sustainable urbanization and environmental issues in different regions of the world.

The series is intended for professionals in research and teaching, consultancies and industry, and government and international organizations. Published in collaboration with IEREK, the Springer ASTI series will acquaint readers with essential new studies in STI for sustainable development.

ASTI series has now been accepted for Scopus (September 2020). All content published in this series will start appearing on the Scopus site in early 2021.

Ana Malheiro • Francisco Fernandes •
Helder I. Chaminé
Editors

Advances in Natural Hazards and Volcanic Risks: Shaping a Sustainable Future

Proceedings of the 3rd International Workshop on Natural Hazards (NATHAZ'22), Terceira Island—Azores 2022

Springer

Editors
Ana Malheiro
Regional Civil Engineering Laboratory (LREC)
Ponta Delgada, Azores, Portugal

Francisco Fernandes
Regional Civil Engineering Laboratory (LREC)
Ponta Delgada, Azores, Portugal

Helder I. Chaminé
Department of Geotechnical Engineering
Laboratory of Cartography and Applied Geology
School of Engineering—ISEP
Polytechnic of Porto
Porto, Portugal

ISSN 2522-8714 ISSN 2522-8722 (electronic)
Advances in Science, Technology & Innovation
IEREK Interdisciplinary Series for Sustainable Development
ISBN 978-3-031-25041-5 ISBN 978-3-031-25042-2 (eBook)
https://doi.org/10.1007/978-3-031-25042-2

This Springer imprint is published by the registered company Springer Nature Switzerland AG
The registered company address is: Gewerbestrasse 11, 6330 Cham, Switzerland

Committees

Scientific Committee

Chairs

Ana Malheiro, LREC, Portugal
Helder I. Chaminé, ISEP, Portugal

Board

Adriano Pimentel, UAç, Portugal
Alberto Gomes, FLUP, Portugal
Annalisa Cappello, INGV, Italy
António Trota, UAç, Portugal
Celeste Jorge, LNEC, Portugal
Chiara Arrighi, UFz, Italy
Dave Chester, UL, UK
Federico Di Traglia, OGS, Italy
Gabriela Queiroz, UAç, Portugal
Gala Avvisati, INGV, Italy
Giuseppe Di Capua, INGV and IAPG, Italy
Giuseppe Sappa, SRU, Italy
Gordon Woo, RMS, UK
Humberto Varum, FEUP, Portugal
Isabel Fernandes, FCUL, Portugal
Joan Martí, CSIC, Spain
João Duarte, FCUL, Portugal
João Carlos Nunes, UAç and INOVA, Portugal
João Luís Gaspar, UAç, Portugal
João Paulo Meixedo, ISEP, Portugal
Joaquim Pombo, IH, Portugal
José Luís Zêzere, IGOT|UL, Portugal
José Martins Carvalho, ISEP, Portugal
José Pacheco, UAç, Portugal
José Teixeira, FLUP, Portugal
José Virgílio Cruz, UAç, Portugal
Kelvin R. Berryman, IKCEST, New Zealand
Luis Hernández-Gutiérrez, INVOLCAN, Spain
Luis González de Vallejo, UCM, Spain
Luís Ribeiro e Sousa, FEUP, Portugal

Manuel Abrunhosa, CITEUC, Portugal
Maria Ferentinou, LJMU, UK
Maria José Afonso, ISEP, Portugal
Maria Pregnolato, UB, UK
Maria Viana-Baptista, ISEL, Portugal
Maurizio Barbieri, SRU, Italy
Nabil Khélifi, Springer Nature, Germany
Nicolau Wallenstein, UAç, Portugal
Pedro JM. Costa, FCTUC, Portugal
Ricardo Garcia, IGOT|UL, Portugal
Rui Coutinho, UAç, Portugal
Rui Marques, UAç, Portugal
Sara Barsotti, IMO, Iceland
Silvia Peppoloni, INGV and IAPG, Italy
Stefano Lorito, INGV, Italy
Teresa Ferreira, UAç, Portugal
Tew-Fik Mahdi, PM, Canada
Tiago Abreu, ISEP, Portugal

Organizing Committee

General Chair

Francisco Fernandes, LREC, Portugal

Local Organizing Committee

Ana Malheiro, LREC, Portugal
Helder I. Chaminé, ISEP, Portugal
Helena Brasil, LREC, Portugal
Letícia Moniz, LREC, Portugal
Roberto Dutra, LREC, Portugal

Foreword by João Luís Gaspar

The geographic location of the Azores in the middle of the Atlantic Ocean, where so often adverse weather conditions occur, and the complex geodynamic environment of the archipelago, characterized by the interaction of the American, Eurasian, and Nubian lithospheric plates under the influence of a mantelic plume, make this Portuguese region an exceptional natural laboratory for the development and promotion of Earth and Space Sciences, namely in what concerns the study of Natural Hazards.

Volcanic eruptions, earthquakes, steam explosions, gaseous emanations, landslides, floods, and tsunamis, among other occurrences, marked the History of the Azores since its discovery and settlement by the Portuguese in the mid-fifteenth century, causing deaths, severe injuries, and extensive property destruction.

These events often occurred in association, ones facilitating or even triggering others, posing special challenges to risk assessment and spatial planning, monitoring and surveillance of natural systems, and emergency response. In this context, the 3rd International Workshop on Natural Hazards (NATHAZ'22) took place on Terceira Island, in the Azores, aimed at scientific advances and human response to Natural Hazards and Volcanic Risks.

The observation and attempt to understand natural hazards were always present in the Azoreans' conscience. The testimonies reported by Gaspar Frutuoso, in the sixteenth century, and the famous works of naturalists Afonso Chaves and José Agostinho, from the end of the nineteenth century to the first decades of the twentieth century, testify to it. But, the introduction of Volcanology as a Science in the Azores is due to Frederico Machado, considering the remarkable scientific and technical work he carried out during the Capelinhos volcanic eruption, on the island of Faial, in 1957/58, and his scientific papers published in national and international journals.

The creation of the Azores Meteorological Service, in 1901, the installation of the Magnetic and Seismological Observatory on the island of São Miguel, in 1911, the emplacement of the first seismological stations in the islands of Faial and Terceira, in the mid-1950s, and the creation of the Azores University Institute, in 1976, which would acquire the name of the University of the Azores in 1980, were decisive steps towards the observation framework that currently exists in the Azores concerning natural phenomena.

However, it was only after the earthquake of 1 January 1980, which particularly affected the island of Terceira, but had significant repercussions on the entire central group of the archipelago, that the course of the Azores' response to the problems posed by natural hazards gained special expression. Civil Protection in the Azores, as a public service for responding to disasters and safeguarding people and goods, was created after this earthquake, and the concept of civil protection was gradually extended to local authorities. Furthermore, the Regional Civil Engineering Laboratory (LREC) was also created in 1980 for technical support, assessment, and quality control of civil construction in the Azores, and in the scope of the

regional administration, planning bodies were then reinforced to apply public prevention policies in spatial planning and water resources management.

In terms of technical and scientific advice to civil protection authorities, the Portuguese Institute for the Sea and Atmosphere (IPMA), formerly the Institute of Meteorology, guarantees in our days the meteorological and geophysical observation of the archipelago on a national scale. In addition, the University of the Azores, through the Institute for Research in Volcanology and Risk Assessment (IVAR) and the Center for Seismovolcanic Information and Surveillance of the Azores (CIVISA), is responsible for managing the multiparametric surveillance network of the active volcanic systems of the archipelago.

The articulation between the monitoring and scientific research structures and the entities responsible for civil protection is fundamental regarding crisis management, and their actions must be developed with total independence. World history shows us that decision-making has been impaired whenever this has not happened, communication to the public has been deficient, and the response of populations has been insufficient. The 3rd International Workshop on Natural Hazards (NATHAZ'22), organized by LREC (Regional Civil Engineering Laboratory—Azores), allowed an integrated approach to these topics, based on the experience of experts from various scientific fields and the practical knowledge acquired in different regions and countries.

While this event took place on Terceira Island, the Azores were facing an important seismovolcanic crisis on the island of S. Jorge. This fact limited the participation in NATHAZ'22 of some of the scientists and civil protection officials directly involved in the management of the crisis, but it underlined the relevance of the matters under analysis in the field of risk mitigation. From the discussion, it remained clear that although the human response to paroxysmal events requires a global approach, it also must consider regional and local specificities and constraints.

July 2022

João Luís Gaspar
Institute for Research in Volcanology
and Risk Assessment (IVAR)
University of the Azores
Ponta Delgada, Azores, Portugal

Preface

The morning was cool, but the dawn slowly began to reveal the curves of the mountains and the contours of the sea cliffs. Despite the choppy seas and a little veil of fog hovering over the mountain, the day looked promising.

—Nemésio 1944 (translated by Fagundes 2019)

This volume comprises the proceedings of the 3rd International Workshop on Natural Hazards (NATHAZ'22), held in Angra do Heroísmo City, Terceira Island, Azores, during 26–27 May 2022. The book follows the second edition of the NATHAZ'19 Workshop (Pico Island, Azores) successfully published, in 2020, by IEREK Springer ASTI Series (details in Fernandes et al., 2020). Thus, both spots are unique for discussing and sharing problems to advance knowledge of natural hazards and risks.

The Azores plateau is positioned as a unique geodynamic framework at the triple junction among the American, Eurasian, and African tectonic plates (e.g., Self 1976; Kueppers and Beier 2018). Many natural hazards impact the geodynamic setting of the Azores archipelago in the middle Atlantic Ocean, such as earthquakes, volcanic eruptions, landslides, floods, coastal erosion, and damage to engineering works (e.g., Malheiro 2006; Malheiro and Nunes 2007; Fernandes et al., 2020; and Chester et al., 2022). The volcanological testimonies from 1586 to 1590 by Gaspar Frutuoso (1522–1591) remain a crucial milestone in the natural framework of the Azores and Macaronesian region (see Frutuoso 2022). Terceira island includes various volcanic systems and a fissural deep zone delineated by alignments of small volcanic cones, lava domes, and fault zones. Terceira island is also unique because of the rural landscape, the natural reserves, and the natural lakes. Additionally, the historic downtown of Angra do Heroísmo city has been a UNESCO world heritage since 1983.

The book provides a comprehensive overview of topical advances on multi-hazard issues highlighting volcanic contexts, including the bridges between volcanic crisis, disaster management, societal concerns, and geoethics. In addition, the 3rd edition NATHAZ international workshop offered an excellent chance to debate natural hazards, particularly volcanic risks and other hazards, such as seismological, hydrological, and geotechnical issues. Finally, the volume underlines current volcanic risks and other hazards research trends, i.e., risk mapping, assessment and management, forecasting catastrophic events, societal impacts, and geoethical issues. That approach is the key milestone in the natural hazards studies pointing out a harmonious design with nature, sustainability, and society, but with geoethics (McHarg 1992, González de Vallejo 2010, Pepolloni and Di Capua 2022).

Natural hazards result from a threat of natural events that will endanger societies and ecosystems. Risks underline processes or actions, natural or technological, that gain socio-economic significance and territorial representation. However, until the 1970s, the international community understood natural and technological disasters as exceptional circumstances to which it was generally necessary to respond with emergency foreign aid. Natural disasters have a destructive impact. The natural hazards and disasters are various, such as earthquakes, volcanic eruptions, landslides, rock falls, floods, and coastal erosion.

Anthropogenic hazards result from anthropic interactions with nature. Finally, technological hazards happen because of exposure to hazardous substances (IASC 2006).

The data, processes, and dynamics of geosystems in a volcanic context include a thorough knowledge and assessment of climate, geology, morphotectonics, hydrology, volcanology, and social sciences. Hence, it is essential to encourage comprehensive studies on hazard and risk assessment and disaster management to undertake multi-hazard mitigation. Also, it underlined the climate variability and change in Earth's systems. Furthermore, the book highlights the role of geoethics and social geosciences as the missing piece to a clear understanding of the responsibility between hazard volcanologists and policy and decision-makers dealing with natural crises.

This volume is expected to outline natural hazard learnings from Europe, America, Asia, and the Atlantic islands. The case studies highlight new understandings of the description, evaluation, and modelling of georisks, multi-hazard systems, engineering, and geoethical issues. The scientific committee comprises lead geoscientists, natural hazards-related practitioners, and academics worldwide.

Key topics comprise the following: (i) Multi-hazards and risks: sustainable society and disasters; (ii) Natural hazards and assessment: rock falls, landslides, and urban planning and management; (iii) Sustainable Earth systems, hazards, and climate change; (iv) Terceira island geology and geodiversity: volcanological hazards.

The volume has a set of 37 chapter books, including the field trips around geology, geodiversity, and natural hazards of Terceira island led by João Carlos Nunes and Adriano Pimentel and four remarkable keynote lectures by Silvia Pepolloni (Italy), Joan Martí (Spain), Gordon Woo (UK), and David Chester (UK). The book was assembled over 154 authors from the academy, research centres, agencies, and companies. In addition, it was involved in a peer-review process with more than 68 reviewers.

The volume is a useful source for researchers and professionals in geosciences, volcanology, natural hazards, geomorphology, geotechnics, engineering, geoethics, and social sciences. So, it is a valuable asset to experts, students, and natural hazard-related practitioners.

Ponta Delgada, Azores, Portugal — Ana Malheiro
Ponta Delgada, Azores, Portugal — Francisco Fernandes
Porto, Portugal — Helder I. Chaminé
July 2022

References

Chester, D., Duncan, A., Coutinho, R., Wallenstein, N. (2022). Earthquakes and volcanic activity on islands: history and contemporary perspectives from the Azores. In *Routledge studies in hazards, disaster risk and climate change*. Routledge, London.

Fernandes, F., Malheiro, A., Chaminé, H. I. (Eds.) (2020). Advances in natural hazards and hydrological risks: meeting the challenge. In *Proceedings of the 2nd International Workshop on Natural Hazards (NATHAZ'19), Pico Island—Azores 2019. Interdisciplinary Series for Sustainable Development (IEREK), Advances in Science, Technology & Innovation (ASTI)*. Cham: Springer.

Frutuoso, G. (2022). Saudades da terra. Letras Lavadas Edições, Ponta Delgada.

González de Vallejo, L. I. (2010). Design with geo-hazards: an integrated approach from engineering geological methods. *Soils and Rocks, International Journal of Geotechnical Engineering, 31*(1), 1–28.

IASC (2006). Protecting persons affected by natural disasters. In *IASC operational guidelines on human rights and natural disasters*. Washington, DC [https://www.preventionweb.net/files/1617_2006IASCNaturalDisasterGuidelines.pdf]

Kueppers, U., Beier, C. (Eds.) (2018). *Volcanoes of the Azores: revealing the geological secrets of the Central Northern Atlantic Islands*. Berlin: Springer.

Malheiro, A. (2006). Geological hazard in the Azores archipelago: volcanic terrain instability and human vulnerability. *Journal of Volcanology and Geothermal Research*, 156, 158–171.

Malheiro, A., Nunes, J. C. (Eds.) (2007). Volcanic rocks. In *Proceedings of the International Workshop on Volcanic Rocks, Workshop W2, 11th Congress ISRM, Ponta Delgada, Azores*. London, UK: CRC Press, Taylor & Francis Group.

McHarg, I. L. (1992). *Design with nature. 25th anniversary edition, Wiley series in sustainable design*. New York: Wiley.

Nemésio, V. (1944). Stormy isles: an Azorean tale. Bellis Azorica Series 1, Translation, Revised edition (May 20, 2019) by Fagundes FC, Tagus Press, Gávea-Brown Publications, Providence, Rhode Island.

Peppoloni, S., Di Capua, G. (2022). *Geoethics: manifesto for an ethics of responsibility towards the Earth*. Cham: Springer.

Self, S. (1976). The recent volcanology of Terceira, Azores. *Journal of the Geological Society London* 132, 645–666.

Acknowledgements

We thank the authors, keynote speakers, field trip coordinators, and delegates of the NATHZ'22 Workshop for making high-quality full extended abstracts. Also, we appreciate the scientific committee's enrolment in careful reviews helping the authors to improve the final texts. The book earned hugely from their suggestions, corrections, and commentaries.

We deeply thank Letícia Moniz, who thoroughly managed the submission system, and Helena Brasil and Roberto Dutra for their skilled permanent support. Thanks to João Carlos Nunes (University of Azores) and Adriano Pimentel (CIVISA and IVAR, University of Azores) for guiding the field trips around Terceira Island. Also, we thank the convener Annalisa Cappello (INGV, Italy), for promoting a special session about volcano-related multi-hazard at Mount Etna. In addition, our thanks are due to Regional Secretariat for Tourism, Mobility and Infrastructure (SRTMI) of Government Azores, Angra do Heroísmo Conference Centre, and Angra do Heroísmo Municipality for supporting the event.

Our warmest gratitude to João Luís Gaspar for the insightful foreword and Paulo Melo for the stunning cover photo. A word of appreciation to all assistance of the IEREK and the Springer production team.

Contents

About the Editors

Ana Malheiro is a skilled Geologist with 38 years of experience in practice and research in engineering geology, geotechnics, natural hazards, and geological risks. She studied Geology at the Faculty of Sciences of the University of Lisbon in 1983 and received her master's degree at the University of Azores in Volcanology and Geological Risks in 2002.

She has worked since 1984 in the Regional Laboratory of Civil Engineering (LREC) in the Azores, where she is responsible for engineering geology, in situ geotechnical investigations, volcanic geotechnics, natural hazards, and geological risk studies. She was Head of the Division of Ports (1995/1998), and from 1998 until now, she has been Director of Services of the Department of Geotechnics, Sustainability and In Situ Investigations at LREC—Azores. She participated in several Coordination Commissions for Management Plans (namely Regional Plans and Municipal Plans). In addition, she was also invited assistant lecturer (1985/1990; 1996/1999) at Azores University.

She has co-authored several publications in indexed journals, conference proceedings/full papers, book chapters, technical and professional papers, and technical reports. In addition, she co-edited 2 special volumes, "Volcanic Rocks" (Balkema+Taylor & Francis) and "Advances in Natural Hazards and Hydrological Risks: Meeting the Challenge" (IEREK+ASTI Springer). In general, technical reports focus on the field of in situ geological-geotechnical investigations to support the larger constructions built in the Azores region, coastal erosion, and slope stability, as well as the evaluation of resources in quarries, evaluation of geological and/or geotechnical problems and the assessment of geological hazards. In addition, she has integrated some research projects in the geotechnical characterization and evaluation of volcanic materials, slope stability, unstable areas monitoring, etc.

She participated in several organizing committees for national and international Conferences and Workshops, as well as Scientific Committees (e.g., 15th World Conference on Seismic Engineering, 2012; 5th, 9th, and 10th Portuguese Congress of Seismology and Seismic Engineering, respectively in 2001, 2014, and 2016; 16th Portuguese Congress of Geotechnics, 2018; 1st, 2nd, and 3rd International Workshop on Natural Hazards, Azores, NATHAZ'2016, 2019, and 2022). Currently, she is the Chair of the scientific committee of the 4th

International Workshop on Natural Hazards—NATHAZ'25 (Azores, May 2025), focused on geotechnical hazards and risks.

Francisco Fernandes is a skilled Engineer with over 26 years of experience in practice and research in civil engineering. After an internship at the "Sociedade de Empreitadas e Trabalhos Hidráulicos", he began his career in 1997 in budgeting and cost control at Engil. He was also a controller and was responsible for several management areas at Eng. Luís Gomes company. He worked as a project manager in the Marques, Engil, and Eng. Luís Gomes companies, and as director of production.

Senior Member of the Institution of Portuguese Engineers, he has a master's degree in Business Administration and Management from the University of the Azores (2003), and is a Qualified Expert in the Energy Certification System (SCE—RCCTE) and ADENE (Agency for Energy and Technical Superior of Safety and Hygiene of Work—Level 5). Other activities include participation in various courses, seminars, and vocational training actions in engineering, safety and hygiene at work, energy certification, and management as a designer and qualified expert in the energy certification system.

Presently, since 2012 he has been Head of the Regional Laboratory of Civil Engineering (LREC) in the Azores. Currently, he is a board member of the Portuguese Seismic Engineer Society (SPES), the Fiscal Council president at the Portuguese Geotechnical Society (SPG), and a Fiscal Council member of the Fund for the Development of Construction Sciences (FUNDCIC). In addition, he has been responsible for some research projects in monitoring unstable areas, masonry wall reinforcement, endogenous construction materials catalogue and idea contest, energy and water efficiency in public buildings, and circular economy and waste management in construction.

He has co-authored publications in journals, conference proceedings, book chapters, professional papers, and technical reports. Furthermore, he co-edited the special volume of the Springer ASTI series (Advances in Natural Hazards and Hydrological Risks: Meeting the Challenge—Proceedings of the 2nd International Workshop on Natural Hazards (NATHAZ'19), Pico Island—Azores 2019).

As president of the organizing committee, he was responsible for several scientific events, namely the 10th Portuguese Congress of Seismology and Earthquake Engineering, the 16th Portuguese Geotechnical Congress, the 6th Luso-Spanish Geotechnical Conference, and the 1st, 2nd, and 3rd International Workshop on Natural Hazards (NATHAZ'2016, 2019, and 2022). He also participated in the workshop "Azores Earthquakes, Rocks and Volcanoes" organized in the Azores, part of the 15th World Conference on Seismic Engineering, Lisbon, 2021, and in the 43rd World Symposium on building water networks CIB W062, Azores, 2018. Presently, he is the

Head of the organizing committee of the 4th International Workshop on Natural Hazards—NATHAZ'25 (Azores, May 2025), focused on geotechnical hazards and risks.

Helder I. Chaminé is a skilled Geologist and Professor of engineering geosciences at the School of Engineering (ISEP) of the Polytechnic of Porto, with over 32 years of experience in multidisciplinary geosciences research, consultancy, and practice. He studied geological engineering and geology (B.Sc., 1990) at the Universities of Aveiro and Porto (Portugal), respectively. He received his Ph.D. in geology at the University of Porto in 2000 and spent his postdoctoral research in applied geosciences at the University of Aveiro (2001–2003). In 2011, he received his Habilitation (D.Sc.) in geosciences from Aveiro University. Before joining the academy, he worked for over a decade on international projects for mining, geotechnics, and groundwater industry and/or academia related to geodynamics and regional geology, hard-rock hydrogeology and water resources, engineering geosciences and applied geomorphology, rock engineering, and georesources. His research interests span fundamental to applied fields: GIS mapping techniques for applied geology, structural geology and regional geology, engineering geosciences and rock engineering, slope geotechnics, mining geology and hydrogeomechanics, hard-rock hydrogeology, exploration hydrogeology, urban groundwater, and hydromineral resources. In addition, he has interests in mining geoheritage, history of cartography, military geosciences and higher-education dissemination, skills, and core values.

He is Head of the Laboratory of Cartography and Applied Geology (LABCARGA|ISEP), the Senior Researcher at Centre GeoBioTec|U.Aveiro and Centre IDL|U.Lisbon, and also belongs to the executive board of the M.Sc. + B.Sc. Geotechnical and Geoenvironmental Engineering programmes (OE+EUR-ACE Label) and the Department of Geotechnical Engineering (ISEP). Furthermore, he belongs to the board of the Technical Committee of Environmental Geotechnics of SPG (2020–2024). Moreover, he was a board member of APGeom—Portuguese Association of Geomorphologists (2009–2013), SPG—Portuguese Geotechnical Society (2016–2020), and AIH-GP—Portuguese Chapter of the International Association of Hydrogeologists (2019–2023).

Furthermore, he was a consultant and or responsible for over 70 projects of applied geology, hydrogeomechanics, slope geotechnics, mining geology, exploration hydrogeology, hard-rock hydrogeology, water resources, urban groundwater, and applied mapping (Mozambique, Portugal, and Spain).

He co-authored over 220 publications in indexed journals, conference proceedings/full papers, book chapters, and technical and professional papers. He co-edited over 15 special volumes and is presently involved in editing themed issues for some international journals or ASTI Springer Series (e.g.,

Springer Nature Applied Sciences, Water MDPI, Arabian Journal of Geosciences—Springer). In addition, he has wide activity as a reviewer for several international journals. In 2021, Springer Nature Applied Sciences awarded him an outstanding guest editor and editorial board member. Furthermore, he served as invited Expert Evaluator of the Bologna Geoscience programme for DGES (Portugal) and Scientific Projects Evaluation for NCST, 2017–2019 (Kazakhstan), and NRF|RISA, 2019 (South Africa), as well as Coordinator of "Geology on Summer/Ciência Viva" programme at ISEP (2005–2019) for geoscience dissemination. He has also been active in teaching and supervising many Ph.D., M.Sc., and undergraduate students.

He has been on the editorial board, among others, of the *Springer Nature Applied Sciences, Arabian Journal of Geosciences, Hydrogeology Journal, Geotechnical Research, Mediterranean Geoscience Reviews, Discover Water, Euro-Mediterranean Journal for Environmental Integration, Journal of Geoethics and Social Geosciences, Revista Geotecnia, and Geología Aplicada a la Ingeniería y al Ambiente*. In addition, he integrates as a moderator or session chair in several conferences, workshops, and meetings. Currently, he co-chairs the scientific committee of the 4th International Workshop on Natural Hazards—NATHAZ'25 (Azores, May 2025), focused on geotechnical hazards and risks.

Multi-hazards and Risks: Sustainable Society, Disasters and Geoethics

Geoethics to Face Natural Risks by Improving Societal Resilience

Silvia Peppoloni

Abstract

Risks determined by natural phenomena cannot be cancelled entirely but can be reduced by minimizing their destructive effects. At present, scientists can predict, though with a certain degree of uncertainty, the onset and the evolution over time of most natural events. Scientific progress provides societies with advanced tools and methods to defend people, such as predictive models, monitoring instruments, early warning systems, and safe building standards. Nevertheless, the defence against natural risks should consider the ethical and social aspects involved in a risk scenario: this is fundamental to help the human community recover after a disaster and support science to identify possible solutions for an acceptable living with natural phenomena. Geoethics promotes the reflection on values that should guide human interaction with the territory and the associated and interlinked individual and collective responsibilities. Geoethics discusses issues and practices in natural risk management and fosters geoeducation and risk communication as a means to improve societal resilience.

Keywords

Geoethics • Natural risks • Prevention • Resilience • Geoeducation

1 Introduction

Natural events that take place on Earth, such as volcanic eruptions, tsunamis, floods, earthquakes, landslides, degassing, and extreme meteorological phenomena, are an expression of the continuous dynamics and transformation that characterize our planet, which occur inside and on its surface, to achieve transitory balances. In many cases, these phenomena are a threat to people's lives and the social equilibrium of the affected communities, as well as to the historical and cultural heritage and economic activities present in the area. Therefore, the defence of the population and the territory must be the priority goal of scientists, experts in the field, professional technicians, and political authorities. The effective integration of their skills and respectful cooperation between them can really contribute to reducing the risk and the probability of such phenomena turning into disasters.

Who is responsible for addressing these problems, and through what tools? And what criteria should guide decisions on the safety and health of human communities?

The safety of people and the protection of the territory must be guaranteed with the responsible involvement of every component of society, including every single citizen whose life is directly affected by natural phenomena. The most efficient human communities in risk prevention, such as the orderly Japanese society, teach us that the risk, even if not entirely eliminable, can be reduced by following discipline, virtuous behaviours, and correct practices, which, together with a high sense of individual and social responsibility, contribute to increasing the resilience of the community.

Due to their enormous impact, those events can seriously condition the development of many societies worldwide, determining high societal costs, which may have direct and indirect repercussions on local and global economic situations. In particular, regarding climate change, as reported by AON (2022), "costs of climate change extend beyond physical damage; larger-scale events can amplify humanitarian aid needs; investment in infrastructure or other adaptation methods can reduce long-term costs; data and analytics will aid increasingly mandated climate-related regulatory disclosures." In 2021, global economic losses were mostly due to flooding, tropical cyclone, severe winter

S. Peppoloni (✉)
Istituto Nazionale di Geofisica e Vulcanologia, Rome, Italy
e-mail: silvia.peppoloni@ingv.it

A. Malheiro et al. (eds.), *Advances in Natural Hazards and Volcanic Risks: Shaping a Sustainable Future*,
Advances in Science, Technology & Innovation, https://doi.org/10.1007/978-3-031-25042-2_1

weather, drought, and to a lesser extent, wildfires and earthquakes.

Dealing with natural risks also includes examining the ethical and social aspects involved in their management, such as the proper risk communication towards different stakeholders, the effective education and training to prepare the population to address and react to those events, and the awareness that actors involved in a risk scenario should have about their responsibilities. All these aspects contribute to increasing societal safety, which is why this issue is of primary importance for geoethics.

2 The Concepts of Hazard and Risk

Hazard and risk are often used synonymously, while they have different meanings. Hazard is an intrinsic characteristic of an area, depending on its geomorphological, geotechnical, and climatic peculiarities, while the risk is connected to the presence in that area of damageable "elements" (people, residential buildings, economic activities, infrastructures, and historical heritage). Therefore, it is necessary to estimate the value and vulnerability of the assets present in the territory to quantify the risk in addition to the hazard. Paradoxically, in an area where people, buildings, and other assets that can be damaged are absent, the risk can be minimal, even if the hazard is high. So, only by acting on the risk through prevention strategies, we can defend our lives and secure our urban centres.

In the last 40 years, the sharp increase in population (Ripple et al., 2020) and the need to increase agricultural (Kopittke et al., 2019), industrial, and energy production (Ripple et al., 2021) have led to the expansion of urbanized areas, greater soil consumption, and an increase in soil erosion (Borrelli et al., 2020; UNEP, 2014). "Megacities" of millions of inhabitants have also reached areas that are potentially dangerous for humans, which in the past would not have been built due to their bad geomorphological or climatic characteristics. In fact, there has been a greater exposure to the risk of societies: we are more than in the past and more vulnerable to natural events, also and above all in consideration of the fact that globalization creates conditions of ever greater interdependence between countries. Hence, a disturbance caused by a natural phenomenon can produce harmful effects even far from the place where it occurred (Peppoloni & Di Capua, 2021a). In this context, it is clear that an effective risk reduction policy should be based on an overall prevention strategy capable of addressing all the elements that contribute to the definition of the risk itself, from the local to the transnational scale, with multidisciplinary and interdisciplinary approaches to problems, which include engineering, geological, urban-architectural aspects, as well as sociological, economic, and political ones.

Even if the risk is not entirely eliminable, we can reduce it to a minimum by applying knowledge made today available by scientific and technical progress. Even if only in probabilistic terms, geoscientists can predict the occurrence and development over time of some natural phenomena that can contribute to counteracting their negative effects. Nowadays, we can defence ourselves by monitoring those phenomena accurately and continuously, setting up warning networks, using reliable forecasting models and construction methods, and implementing information campaigns for the population: ultimately developing prevention programs aimed at more effective risk management. Science helps us identify effective solutions, which allow to live even in highly dangerous areas when the possible expected phenomena are well known. As a result, the vulnerability of the elements at risk can be reduced below thresholds considered acceptable by society.

3 Prevention: Roles and Responsibility

Prevention of that set of actions aimed at reducing risk is possible only if the roles and responsibilities of scientists, technicians, local administrators, politicians, mass media, and citizens are clearly defined.

The task of scientists is to do good science, study and model natural reality, transfer knowledge to the various components of society, and orient those who have to make decisions regarding the territory.

Politicians have the duty to activate new government actions to protect citizens responsibly and strengthen the initiatives already in place by equipping themselves with valid regulatory tools that guarantee compliance with adequate levels of safety and are calibrated on reliable and shared scientific knowledge.

The mass media is entrusted with the delicate work of mediating between scientists and society, which requires verifying the quality of the information collected and disseminated to the reliability and authority of the sources from which data, models, theories, and news come. While, on the one hand, the media denunciation of political inefficiencies is a fundamental civil mission, on the other hand, the media should give greater prominence to the positive results achieved in the defence against risks so that the population can understand the value of science, prevention and the results that can be obtained by wisely investing collective economic resources.

Citizens themselves must become more aware of the possibility of affecting individual and social safety. Finding out about the hazards of the territory and ensuring that the buildings in which one lives have adequate safety features, and knowing the behaviours that can save lives during an emergency means contributing to the resolution or

containment of the problems that can afflict the entire community. Citizens have the right to expect the state to work to ensure their safety, but they also have the duty to be more informed, and become more aware of the value of scientific knowledge, territorial planning, prevention, and the importance of investing in their own safety. More aware citizens will be able to more effectively assess and monitor the work of those responsible for managing the territory.

4 Prevention: A Cultural Issue

Prevention is not a simple matter: it consists of a set of actions which need careful planning of human and economic resources for their implementation to be put into practice. Furthermore, having concrete results of their effectiveness can take long periods of time. Therefore, starting from the identification of areas at risk, prevention strategies should include methods and technologies for monitoring phenomena and for early warning ever more effective, the organization of educational campaigns for the population, the use of pre-alert methods, interventions to secure the heritage construction, the development of regulatory frameworks, and the strong coordination between the various actors involved in the defence from risks. These modalities to implement prevention should be the basis of every local policy.

The term prevention means precisely the set of all these activities that should be carried out before the expected event (e.g., Peppoloni & Di Capua, 2016, 2021a, 2022; Peppoloni et al., 2019). However, these actions remain insufficient if there is no simultaneous action on a cultural level. Most modern societies are unprepared to see prevention as the best way to protect human life from natural disasters, namely to consider it one of the most topical values of our times. There seems to be a lack of recognition of the values on which to base our actions in terms of prevention. Prevention, in fact, is not only an advantage in economic terms, but it is above all the modern, rational, and responsible response to the right to safety, which we must ethically pursue ourselves and the community we are part of, assuming a share of responsibility, from politicians to technicians, from scientists to individual citizens (Peppoloni & Di Capua, 2022).

5 Resilience of Human Communities

The concept of risk also includes social vulnerability and, thus, a community's resilience (Cutter, 2020; Ride & Bretherton, 2011). Each human community has its intrinsic capacity for resistance to natural events, which may depend on different factors (social, historical, cultural, psychological, and economic). The resilience of a community is its ability to face disastrous events, recover both materially and spiritually, and reorganize its life, structure, and activities.

Defending against natural risks means improving the resilience of human communities, an objective that can be achieved through prevention.

However, has society an adequate perception of potential or impending risks? For example, when we consider the causes of death that occur on the occasion of a disaster, we realize that they often occur due to superficial behaviours or lack of information about the minimum safety rules that should instead be well known to the population.

It is a fact that the population, with some exceptions, is never sufficiently aware of the risks to which it is subject, although life itself has intrinsic risks that cannot be eliminated. To date, the knowledge widespread among the population generally does not include adequate basic information on hazards and risks associated with natural events. While peasant civilization had and still has a greater perception of the occurrence of directly or indirectly dangerous natural phenomena, urbanized and/or technologized human beings are increasingly disconnected from a concrete perception of natural processes and dynamics. This determines an increase in social vulnerability and a consequent increase in risk, with the same expected hazard. It is, therefore, necessary to work on increasing the physical perception of natural reality and the dangers that can arise from it.

An effective risk reduction strategy must therefore start from education in schools and information to the population and systematically provide for emergency training, the planning of interventions to reduce the vulnerability of built-up areas, the preparation and rigorous application of "ad hoc" building regulations, and the relocation of strategic buildings, public utility buildings, and industrial plants from areas at higher risk.

School programs should favour understanding the importance of knowledge, the scientific method, and the technological applications that allow people to defend themselves effectively. School education is the foundation of a knowledgeable society, increasingly capable of scientifically analysing disasters and of facing the natural events that, sooner or later, will undoubtedly occur again if geological, geomorphological, and climatic conditions "favourable" to their occurrence will remain.

6 The Ethical Duty of Prevention

Often, a difficult and vulnerable physical environment is combined with negligence, inattention, or even rash human interventions that further increase risk exposure. Unfortunately, in many cases, this increasing risk is not accompanied by an increase in the risk perception by the population,

which consequently cannot fully understand the importance of pretending from the public authorities the development of defence and prevention policies.

Prevention, which is implemented by adopting risk reduction strategies that improve the resilience of human communities and reduce the extent of economic intervention by states to restore the status quo as far as possible, is primarily an ethical duty, for which everyone should assume responsibility, out of respect for their human nature. Already in the 1500s, the Italian architect Pirro Ligorio affirmed this concept in his "Libro dei diversi terremoti" ("Book on Different Earthquakes") (Guidoboni, 2005), when he emphasized that "*earthquakes are not obscure and ineluctable accidents but phenomena within reach of human reason*", and that "*trying to achieve housing security is a necessity and a duty of the human intellect*". His reference to the responsibility of humans is evident when they do not use their rational capabilities to defend their life, assets, and activities, and so turn earthquakes into disasters.

However, in its historical evolutionary dimension, science has always benefited from the lessons of the past, from all the disastrous events that have occurred over the centuries (floods, earthquakes, volcanic eruptions, etc.), reviewing and putting into question its models based on direct observation. Otherwise, modern society and politics always seem to quickly forget the events experienced in the present and postpone the adoption of long-term intervention strategies. Once, the closer relationship with one's territory and widespread popular wisdom meant that several times in the past, houses were not built where unfavourable geomorphological and geotechnical conditions and geological instability were present. On the contrary, modern society's temporal perspective of action seems to have shrunk to a very short period, constantly determined by the run-up to the contingent problem. Therefore, the so-called "culture of emergency" that characterizes current human societies does not seem to be the cause but the effect of our laziness, negligence, and inability to think about the future. Furthermore, in the defence against risks, our inability to rationally prefigure a possible future event causes our constant passive attitude towards phenomena that often have return periods of even more than ten years. In this context, prevention loses its meaning and value.

To change this attitude, it is perhaps necessary to place a framework of reference values at the centre of every human community that cements its relationships because of a common good.

7 Territory of Belonging and Memory of the Past

The territory is not simply the place where one was born or lives by chance, but it is the physical, cultural, and valuable support of one's life, a valuable resource, and, above all, one of the founding values of human identity, thus a good to be preserved. Furthermore, rediscovering the identity value of the territories can lead to cultural change and a growth in responsibility in most of societies, thus understanding the importance of developing policies for land protection and prevention of risks (Peppoloni & Di Capua, 2022).

The awareness of the value of the territory should be a training goal in our schools for a more responsible future, in which a new way of thinking and managing land can be established. Educating to respect the territory and its care already means taking action to prevent disasters.

A solid culture of prevention must be founded on an idea of the territory as a collective good, resource, and advantage. To respect, defend, and safeguard that common good, to ensure its enjoyment for future generations, it is necessary to strengthen social relationships within communities, starting from the sharing and practice of fundamental ethical principles. Moreover, these relationships can be further consolidated by recovering the collective memory of a place, the past history of the natural events that affected it, and the human actions that have shaped the local ecosystem over time.

The ease with which a human community loses the memory of past disasters is one of the causes of a lack of attention towards the defence against risks. There are natural events of great energy, such as strong earthquakes or the most paroxysmal volcanic eruptions, which can have very long return time periods, of several tens if not hundreds of years. Similar return time periods exceed the lifespan of a human being, and it only takes a few years for those events to be forgotten. Time dilutes the memory and also removes the fear of the event. Moreover, while that memory is erased, the need to pay due attention to those particularly hazardous areas of the territory also vanishes from the collective memory.

Thinking about the possibility of natural events having very long return time periods is against the common human experience. Furthermore, the lability of memory is strongly accentuated in the richest and most technologized (and virtualized) societies. At the same time, in the indigenous communities, which maintain a profound material and

spiritual bond with the territory to which they belong, this phenomenon is less present, if not absent (Conversi, 2021).

Memory is indispensable to entering the temporal dimension of natural phenomena and understanding them. Nevertheless, to nourish and preserve it, it is necessary to build new forms of storytelling, which, although based on scientific knowledge, draw insights and forms from the communicative mechanisms of the human sciences.

8 Geoethics and Defence from Natural Risks

Geoethics, although born and developed in the more strictly scientific context to analyse the ethical, social, and cultural aspects that accompany geoscientific activity (e.g., Bobrowsky et al., 2017; Bohle & Di Capua, 2019; Di Capua et al., 2021; Peppoloni & Di Capua, 2012, 2015, 2022; Peppoloni et al., 2019), is now extended to include problems that affect society as a whole (e.g., Bohle & Marone, 2021; Di Capua et al., 2021; Peppoloni & Di Capua, 2021a, 2021b; Peppoloni & Di Capua, 2022), proposing new perspectives for analysing the humans-Earth system relationship (Peppoloni & Di Capua, 2021c). For geoscientists, addressing the issue of disaster risk reduction from the perspective of geoethics means putting awareness of their responsibility first, since each of their actions has implications not only scientific and technical but also ethical and social. This translates into the duty to produce and implement valid scientific results, to know how to develop geo-educational tools for the population, and to commit to cooperating with other professionals involved in risk management at all stages of the disaster cycle, from prevention to emergency up to the recovery phase (Di Capua & Peppoloni, 2014, 2020; Guzzetti, 2015; Peppoloni, 2015). Geoethics provides categories and values capable of creating an ethical framework to build behaviours and policies to reduce risks.

For the geoethical thought, the defence from natural risks is a path of scientific knowledge that takes the form of a social pact based on the dignity of human reason and the scientific method. Rationality and science are irreplaceable tools at the service of the common good.

In this perspective, the work of geoscientists and their social commitment to the community takes on particular relevance. From the point of view of geoethics, their activities should consider the following:

- Cooperating in developing synergies with government agencies and local administrations through the definition of operational procedures and protocols, encoded stream of information between authorities and scientists, and *ad hoc* strategies to face natural risks.
- Helping policymakers make decisions, supporting them with reliable and updated science-based information, keeping scientific observations and achievements distinct from working hypotheses, being aware of their social role in the risk decision chain, and avoiding replacing decision-makers in making choices.
- Making geoscience research outcomes public, but taking into account the final users of that information, so using a language that can be understood adequately while respecting scientific accuracy and informing on the uncertainty of the scientific methods used.
- Contributing to developing a real risk perception in the population by developing educational campaigns on natural hazards and risks to transfer scientific data and increase social awareness and responsibility. This includes, for example, avoiding both prolonged alarmism and excessive reassurance, with consequent loss of trust in science by the population.

9 Conclusions

Investing in research and technological innovation of risk defence interventions can significantly reduce the societal and economic costs of the risk. However, the implementation of widespread and continuous educational and information campaigns for the population (through the construction of storytelling that is capable of linking science and humanities) is fundamental for raising awareness among the population and facilitating new ways to address these risks and promote a culture of prevention.

Nowadays, defence against natural hazards is possible and can be really effective. However, it is implemented through prevention, which should be considered a set of actions and tools helpful in reducing the economic costs inflicted by a possible disaster and, above all, a significant social value. This value, if practised, can lead the entire human community hit by a disaster to a social and cultural attitude that puts safety, sustainability, knowledge, and responsibility first. These concepts are fundamental to building safer and more economically resilient societies.

The ethical commitment of geoscientists to appropriately disseminate their scientific knowledge and adequately and preventively prepare the population to face disastrous circumstances can help improve resilience and, therefore, reduce risk.

In this way, the relationship between the scientific community, political authority, and the population is consolidated, an indispensable prerequisite for developing truly effective strategies and overcoming critical emergency conditions determined by natural phenomena. The increase in the resilience of every human community also depends on improving the relationship between institutions, citizens, and scientists, a relationship of mutual trust and interaction

functional to the safety of the inhabitants and the protection of the territory.

Prevention involves the social body as a whole and every single individual at the same time. Everyone has their share of responsibility in caring for the territory and the communities that inhabit it. Nevertheless, prevention is not just a technical issue; it is a cultural fact that must be realized through close cooperation between geoscience, engineering, and humanities. Furthermore, prevention is a necessary and ethical action, which allows today's communities not to irresponsibly increase the risks and probabilities of disaster for future generations.

References

AON (2022). 2021 Weather, climate and catastrophe insight. Retrieved February 18, 2022, from https://www.aon.com/weather-climate-catastrophe/index.aspx.

Bobrowsky, P., Cronin, V. S., Di Capua, G., Kieffer, S. W., & Peppoloni, S. (2017). The emerging field of geoethics. In L. C. Gundersen (Ed.), *Scientific integrity and ethics in the geosciences* (pp. 175–212). American Geophysical Union, Wiley. https://doi.org/10.1002/9781119067825.ch11.

Bohle, M., & Di Capua, G. (2019). Setting the scene. In M. Bohle (Ed.), *Exploring geoethics: ethical implications, societal contexts, and professional obligations of the geosciences* (pp. 1–24). Cham: Palgrave Pivot. https://doi.org/10.1007/978-3-030-12010-8_1.

Bohle, M., & Marone, E. (Eds.). (2021). *Geo-societal narratives: Contextualizing geosciences*. Cham: Palgrave Macmillan.

Borrelli, P., Robinson, D. A., Panagos, P., Lugato, E., Yang, J. E., Alewell, C., Wuepper, D., Montanarella, L., & Ballabio, C. (2020). Land use and climate change impacts on global soil erosion by water (2015–2070). *PNAS, 117*(36), 21994–22001. https://doi.org/10.1073/pnas.2001403117.

Di Capua, G., & Peppoloni, S. (2014). Geoethical aspects in the natural hazards management. In G. Lollino, M. Arattano, M. Giardino, R. Oliveira, & S. Peppoloni (Eds.), *Engineering geology for society and territory* (Vol. 7, pp. 59–62). Cham: Springer. https://doi.org/10.1007/978-3-319-09303-1_1159-62.

Di Capua, G., & Peppoloni, S. (2020). Geoethics and georisks. In C. Vasconcelos, S. Schneider-Voß, & S. Peppoloni (Eds.), *Teaching geoethics: Resources for higher education* (pp. 97–109). Porto: U. Porto Edições.

Di Capua, G., Bobrowsky, P. T., Kieffer, S. W., & Palinkas, C. (2021). About this title-geoethics: Status and future perspectives. In G. Di Capua, P. T. Bobrowsky, S. W. Kieffer, & C. Palinkas (Eds.), *Geoethics: Status and future perspectives, geological society* (Vol. 508, NP). London: Special Publications. https://doi.org/10.1144/SP508.

Conversi, D. (2021). Exemplary ethical communities. A new concept for a livable Anthropocene. *Sustainability, 13*(10), 5582. https://doi.org/10.3390/su13105582.

Cutter, S. L. (2020). Community resilience, natural hazards, and climate change: Is the present a prologue to the future? *Norwegian Journal of Geography, 74*(3), 200–208. https://doi.org/10.1080/00291951.2019.1692066.

Guidoboni, E. (2005). *Pirro Ligorio, Libro di Diversi Terremoti*. Roma: De Luca.

Guzzetti, F. (2015). Forecasting natural hazards, performance of scientists, ethics, and the need for transparency. *Toxicological & Environmental Chemistry, 98*(9),1043-1059. https://doi.org/10.1080/02772248.2015.1030664.

Kopittke, P. M., Menzies, N. W., Wang, P., McKenna, B. A., & Lombi, E. (2019). Soil and the intensification of agriculture for global food security. *Environment International, 132*, 105078. https://doi.org/10.1016/j.envint.2019.105078.

Peppoloni, S., & Di Capua, G. (2012). Geoethics and geological culture: awareness, responsibility and challenges. *Annals of Geophysics, 55*(3), 335–341. https://doi.org/10.4401/ag-6099.

Peppoloni, S., & Di Capua, G. (2015). The meaning of geoethics. In M. Wyss, & S. Peppoloni (Eds.), *Geoethics: Ethical challenges and case studies in earth sciences* (pp. 3–14). Elsevier. https://doi.org/10.1016/B978-0-12-799935-7.00001-0.

Peppoloni, S., & Di Capua, G. (2016). Geoethics: Ethical, social, and cultural values in geosciences research, practice, and education. In G. R. Wessel, & J. K. Greenberg (Eds.), *Geoscience for the public good and global development: Toward a sustainable future, special papers 520* (pp. 17–21). Boulder: Geological Society of America. https://doi.org/10.1130/2016.2520(03).

Peppoloni, S., & Di Capua, G. (2021a). Geoetica: un'etica per la relazione tra gli esseri umani e la terra (Geoethics: An ethics for the relationship between humans and the earth). *The Future of Science and Ethics, 6*, 42–53. https://doi.org/10.53267/20210104.

Peppoloni, S., & Di Capua, G. (2021b). Geoethics as global ethics to face grand challenges for humanity. In G. Di Capua, P. T. Bobrowsky, S. W. Kieffer, & C. Palinkas (Eds.), *Geoethics: Status and future perspectives, geological society* (Vol. 508, pp. 13–29). London: Special Publications. https://doi.org/10.1144/SP508-2020-146.

Peppoloni, S., & Di Capua, G. (2021c). Geoethics to start up a pedagogical and political path towards future sustainable societies. *Sustainability, 13*(18), 10024. https://doi.org/10.3390/su131810024.

Peppoloni, S., & Di Capua, G. (2022). *Geoethics: Manifesto for an ethics of responsibility towards the earth*. Cham: Springer, pp. XII +123. https://doi.org/10.1007/978-3-030-98044-3.

Peppoloni, S., Bilham, N., & Di Capua, G. (2019). Contemporary geoethics within geosciences. In M. Bohle (Ed.), *Exploring geoethics: Ethical implications, societal contexts, and professional obligations of the geosciences* (pp. 25–70). Cham: Palgrave Pivot. https://doi.org/10.1007/978-3-030-12010-8_2.

Peppoloni, S. (2015). Geoethics: A framework for the management of the geosphere and geo-risks. In J. Marino, & S. Villacorta (Eds.), *Libro de Resumenes–Foro Internacional sobre Gestion del Riesgo Geologico* (pp. 259–263). Peru: Arequipa.

Ride, A., & Bretherton, D. (Eds.). (2011). *Community resilience in natural disasters*. New York: Palgrave Macmillan. https://doi.org/10.1057/9780230339323.

Ripple, W. J., Wolf, C., Newsome, T. M., Barnard, P., & Moomaw, W. R., et al. (2020). World scientists' warning of a climate emergency. *BioScience, 70*(1), 8–12. https://doi.org/10.1093/biosci/biz088.

Ripple, W. J., Wolf, C., Newsome, T. M., Gregg, J. W., & Lenton, T. M., et al. (2021). World scientists' warning of a climate emergency 2021. *BioScience, 71*(9), 894–898. https://doi.org/10.1093/biosci/biab079.

UNEP. (2014). Assessing global land use: Balancing consumption with sustainable supply. *A Report of the Working Group on Land and Soils of the International Resource Panel, UNEP*. Retrieved February 18, 2022, from https://www.resourcepanel.org/reports/assessing-global-land-use.

Multi-Hazard Risk Assessment at the Canary Islands

Marta López-Saavedra and Joan Martí

Abstract

The term "multi-hazard" is a concept that is increasingly gaining ground in national and international disaster reduction policies. However, its implementation is still timid, and the initiatives that have been carried out are important but insufficient. Multi-hazard scenarios are still difficult to implement due to the complexity of the interactions between the different hazards, the lack of addressed research on this topic, and the uncertainty of their consequences at different spatial and temporal scales. Due to their intrinsic multi-hazard nature and their social, economic, and political context, volcanic islands are particularly vulnerable to these scenarios. These environments require adopting a multi-hazard perspective to design new multi-risk management programmes to reduce risk effectively. The case of the Canary Islands, an active volcanic archipelago that also suffers from multiple non-volcanic geohazards, is a clear example of such complex multi-hazard scenarios. With a worrying overpopulation and tourism that make this management difficult, and with emergency plans that do not consider this multi-hazard perspective, natural disasters may accentuate in the near future. This is also applicable to other volcanic islands in similar situations.

Keywords

Multi-hazard • Multi-risk • Cascading • Volcanic islands • Canary Islands

1 Introduction

In the last decade, the concept of "multi-hazard" has progressively emerged among national and international disaster reduction policies. However, conflicts in terminology and the complexity of the concept make it difficult to fully enter into risk management plans. Increasingly, some countries are implementing multi-hazard early warning systems and are undertaking the design of risk reduction strategies considering multi-hazard scenarios. However, not all regions with multi-hazard potential are implementing this concept, and those that are implementing or have implemented it have only applied this concept to some aspects of the entire risk management framework or only to some regions from their entire territory. Occasionally, this implementation is done on an individual level, ignoring the scope of the consequences of some events, so that international cooperation is necessary, and those that consider an international level, sometimes, for political reasons, only take into account those regions with which they have signed agreements or have some relationship.

The assessment of multi-hazard scenarios is complex due to the uncertain interrelationships between the different hazards. For this reason, it is often difficult to analyse such scenarios, causing problems in implementing this multi-hazard approach in hazard assessment and risk analysis. For example, volcanic islands are environments that are more susceptible to receive the impact of multiple natural hazards that sometimes may show cascading effects. In addition, they are, in many cases, highly vulnerable areas due to their demographic expansion in a small space and the reception of a large number of tourists, which cause problems of supply, pollution, and, above all, increasing exposure to risk, and also making emergency management difficult in terms of evacuation and assistance. On the other hand, most of their inhabitants live from local commercial activities, such as fishing, agriculture, and tourism, making them even more vulnerable to the long-term effects of certain

M. López-Saavedra · J. Martí (✉)
Geosciences Barcelona, CSIC, Barcelona, Spain
e-mail: jmarti@geo3bcn.csic.es

M. López-Saavedra
Department of Earth and Ocean Dynamics, Earth Sciences Faculty, University of Barcelona, Barcelona, Spain

A. Malheiro et al. (eds.), *Advances in Natural Hazards and Volcanic Risks: Shaping a Sustainable Future*,
Advances in Science, Technology & Innovation, https://doi.org/10.1007/978-3-031-25042-2_2

natural hazards. Furthermore, their location, sometimes former colonies of countries located far away from them, makes it difficult to receive external aid.

For this reason, multi-risk management plans should be mandatory in these special regions. In this contribution, we review the evolution of the multi-hazard concept and its most important aspects. We then focus on the situation of volcanic islands and the multiple hazards to which they are subject. Finally, we end by analysing the Canary Islands' situation in terms of multi-hazard assessment and management in that region.

2 The "Multi-Hazard" Concept

The first reference to the term multi-hazard appeared in the international policy with the United Nations' Agenda 21 for sustainable development (United Nations Homepage, 2022). They called for multi-hazard research for pre-disaster plans for any human settlement. This claim is made again with the Johannesburg Plan (UN, 2002). However, the action was not taken until the Second World Conference on Disaster Risk Reduction (held in Japan in 2005); when the Hyogo Framework for Action 2005–2015 (United Nations for Disaster Risk Reduction Homepage, 2022) was adopted, implementation of the multi-hazard concept began. Nevertheless, the real actions in those ten years were driven by two major events with extensive damage: Hurricane Katrina in 2005 and the tsunami in Japan in 2011.

Despite this slow awakening, the engineering field has the greatest awareness (Ellingwood, 2010). Fortunately, with the Third World Conference on Disaster Reduction, the Sendai Framework for Disaster Risk Reduction 2015–2030 (UN-ISDR, 2015) was adopted with seven objectives and four priorities for action that advocate for a multi-hazard approach to the management of disaster risk through developmental planning and practices across all the sectors involved (United Nations for Disaster Risk Reduction Homepage, 2022). Some countries and regions have developed multi-hazard forecasting and early warning system initiatives to meet these objectives.

The UN Sustainable Development Summit was held in the same year, culminating in adoption of the 2030 Agenda for Sustainable Development, with 17 Sustainable Development Goals (SDGs). One of these goals highlights the importance of multi-hazard early warning systems. This goal emphasises climate-related hazards and disasters in the context of climate change. In this sense, other multi-hazard scenarios, such as those caused by some geohazards (volcanic eruptions, earthquakes, tsunamis, etc.), are sidelined and comparatively do not receive the same attention when some of them may be aggravated by global change.

Despite all these efforts, basic conflicts such as contradictory terminology, lack of uniformity, and lack of consensus among researchers and users of the concept hinder the efficient implementation of such a multi-hazard approach (Kappes, 2011). From all definitions, it is clear that the concept of multi-hazard refers to multiple hazards occurring simultaneously or separated in time in a given region. Whether or not they occur simultaneously determines whether or not they are related to each other. These relationships may be of different types, such as cascading effects. Due to the complexity of these interactions and the wide range of consequences depending on their combination, some authors have tried to classify them into broad groups (e.g., Kappes et al., 2010; Gill & Malamud, 2016): (1) those events that are triggered by others, (2) those events that maintain some relationship and alter in frequency or magnitude mutually, (3) those that are unrelated or independent even though they coincide in space and time, and (4) those that exclude each other.

From a management point of view, we can distinguish between multiple extreme and non-extreme event scenarios. The former cannot normally be managed due to the magnitude of the impact, but they can be foreseen and prevented. The latter are scenarios for which good risk and emergency management plans can be designed, considering the possible interactions and interrelationships that may arise.

3 Multi-Hazard on Volcanic Islands

Volcanic islands are fragile economic systems and highly vulnerable communities due to their social, political, and economic context. Their main monetary income is from tourism and local economic activities, such as fishing and agriculture. Therefore, many are former colonies dependent on a sovereign country, usually far away from them. However, most volcanic islands are self-governing territories with their own management of natural hazards, which exerts greater local pressure. On the other hand, volcanic islands are prone to experience complex successions of disastrous events, as is evident from any examination, for instance, of the geological record of regions such as Hawaii, the Canary Islands, Reunion, and Indonesia. Created by the growth of volcanoes in the sea and modified by natural and anthropogenic processes, volcanic islands are subject to the impact of multiple natural hazards, including extreme geohazards and wildfires, cyclones, and floods. In this context, climate change may increase the number and intensity of these events, and population expansion and increased tourism elevate exposure and vulnerability. The result is a tendency to increase risk in the future, so the need to devise new strategies to manage multi-hazard and multi-risk is

becoming increasingly evident. In this review, we will focus only on geohazards, although it should not be forgotten that many are caused and/or altered by climatic hazards and/or human action and, in turn, also affect the environment and human health.

3.1 Geohazards: Volcanic and Non-volcanic Events

The rapid growth and configuration of volcanic islands, by the successive accumulation of magma, solid rock, altered rock, volcanic sediments, and hydrothermal systems, together with their steep slopes, favour the instability of these terrains compared to many continental areas. In addition, they are weak structures affected by intense faulting, alteration, and avalanche structures resulting from constructive and destructive processes that account for their entire evolution. In addition, many of them are seismically and volcanically active areas. Therefore, we must distinguish between volcanic events, associated hazards, and non-volcanic geohazards.

Volcanic activity and eruptions themselves are sources of multiple hazards and are susceptible to cascading effects. Sequences involving an eruption, seismicity, mega-landslide, and tsunami are, fortunately, a non-frequent but common multi-hazard scenario in volcanic islands. Some examples are the last caldera-forming eruption that occurred 180 ka ago in Tenerife, the Santorini caldera-forming eruption in 1610 BCE $\pm$14 years, the tsunami and the pyroclastic flow associated with the eruption of Krakatoa in 1883, and the dome collapse in Montserrat island in 2003. Other associated hazards are, for example, lava flows and related wildfires (e.g. Kilauea eruption in 1983), and rockfall and landslides (e.g. flank collapse at Stromboli in 2002), among many others. In the long term, extreme events can cause climatic effects that, in turn, cause famine and disease (e.g. the year after the Tambora eruption in 1815).

On the other hand, the geodynamic context of these types of islands makes them seismically active areas, so they may also suffer the effects of large tectonic earthquakes and those of volcanic origin. An example is a seismic crisis in the Azores in 2005 or the Indonesia earthquake in 2004. Some of these earthquakes, as happened in the last example, are tsunamigenic, so these regions, either because they are in the tsunami source areas or because they are in the tsunami path, and surrounded by the ocean, are severely affected by this derived hazard (e.g. effects of the Japan tsunami in 2011 in the Galápagos Islands). Landslides can also result from this seismicity, and heavy rainfall events (e.g. the Vila Franca 1522 earthquake or the Azores landslide in 2013) and can also trigger tsunamis (e.g. the landslide in the Azores in 1847). Landslides, in turn, can block river channels and cause flooding, another common event following extreme rainfall and torrential downpours (e.g. the landslide in Mt. Pelee in 2010). Torrential floods are accentuated in these environments due to the steep slopes. It should be added that, on the one hand, their geographical location means that these areas are frequently in the path of cyclones (e.g. cyclone Pam as it passed through Vanuatu in 2015), and, on the other hand, their topography may cause large local climatic differences with some extreme episodes of rainfall (e.g. Madeira in 2010) and, finally, they are also sometimes the target of pests (e.g. Lanzarote in 2004) and epidemics (e.g. Cape Verde dengue epidemic in 2009) due to this geographical-climatic combination.

4 The Case of the Canary Islands

The Canary Islands is an active volcanic archipelago in the Atlantic Ocean off the coast of southern Morocco. It is a group of eight islands whose origin is still a subject of debate. Some of these islands have experienced extreme events that can occur again in the future (López-Saavedra et al., 2021) and are, in turn, susceptible to practically all the hazards mentioned in the previous section.

Since its colonisation by the Spanish in the fifteenth century, the Canarian Archipelago has undergone an intense demographic expansion, especially in the coastal areas, and receives millions of tourists yearly. This increase in exposure and pressure on local resources, combined with climate change, has increased risk in all senses, both for the Canarian population and tourists. As an autonomous community of the Spanish State, it is responsible for its natural risk management, so they are obliged to develop the corresponding emergency plans against natural impacts.

Local and regional emergency plans have been developed during the last decades, each facing one particular hazard. In this sense, the Municipal Emergency Plan (PEMU) is activated at a municipal level. Likewise, each Island Council must develop its island plan. Emergencies at the regional level affect more than one island of the Archipelago or those whose magnitude of the incident requires using means from outside the affected island. The Territorial Civil Protection Plan of the Autonomous Community of the Canary Islands (PLATECA) is activated when an emergency is declared at the Autonomous Community level. The PLATECA includes all the previous territorial plans and, in addition, the different Special Plans. These plans are divided into Basic Plans (nuclear and war emergencies, both of which are the responsibility of the Spanish State), and Special Plans for other risks (floods, earthquakes, chemicals, transport of dangerous goods, forest fires, and volcanic). If we focus on geohazards, this last category includes the following Special Plans for the Canary Islands:

- Special Plan for Civil Protection and Attention to Emergencies due to volcanic risk in the Autonomous Community of the Canary Islands (PEVOLCA).
- Special Plan for Civil Protection and Emergency Attention due to seismic risk in the Autonomous Community of the Canary Islands (PESICAN).
- Special Plan for Civil Protection and Emergency Attention due to Forest Fires in the Autonomous Community of the Canary Islands (INFOCA).
- Special Plan for Civil Protection and Emergency Attention due to Flood Risk in the Autonomous Community of the Canary Islands (PEINCA).

In addition to these, there are two Specific Plans:

- Specific Plan for Civil Protection and Emergency Attention of the Autonomous Community of the Canary Islands due to risks of adverse meteorological phenomena (PEFMA).
- Specific Plan for accidental marine pollution emergencies in the Canary Islands (PECMAR).

Focusing on volcanic risk, PEVOLCA considers volcanic earthquakes, pyroclast projection, ash fall, pyroclastic flows, lava flows, structural collapse, lahars, and volcanic gases. It also includes self-protection measures for ash fall. On the other hand, the PEVOLCA includes a "volcanic traffic light" consisting of four colours (green—pre-alert, yellow—alert, orange—maximum alert, and red—emergency) corresponding to four risk situations that serve to inform the population, as well as 3 levels within the emergency situation (0–1—island level, 2—autonomous, and 3—national). However, PEVOLCA does not contemplate any possible interaction between any of these processes or with other processes unrelated to volcanism itself (e.g. forest fires and floods) to which a volcanic eruption could interact or trigger. In the same way, the other Spatial Plans are restricted to the corresponding individual hazard, not assuming any possible interaction with other hazards.

5 Discussion

Multi-risk management is a problem facing society. The complexity of the relationships between the different possible hazards that can impact a territory makes it difficult to implement a multi-hazard concept into risk reduction programmes. The obstacles are accentuated if the lack of research for developing multi-hazard assessments is added. For this reason, although the concept of "multi-hazard" is increasingly being discussed and considered, from its inception to the present day, it has only been used in non-binding agreements and frameworks. Although sometimes big steps are taken, such as some multi-hazard early warning systems or some multi-hazard risk reduction strategies, these are still a few and are often triggered by a disaster that has affected society's economy. In addition, many of these initiatives are geared towards climate-related hazards, as the main focus is now on climate change. However, many other hazards have always been there and will continue to cause millions of losses and many deaths, which the global change may also accentuate. Therefore, it is unnecessary to wait for an event to occur before taking action, and we already have sufficient examples of multi-hazard natural disasters with human losses, which should be reason enough to start taking action at all political levels.

Change must begin by building consensus around the multi-hazard concept and developing competent studies to understand better the possible succession of events, their relationships, and the consequences of multi-hazard scenarios. These studies must not only consider the intrinsic nature of the hazards and their impacts individually but how they may interact and how this interaction may condition the final impact. Also, it is necessary to consider how human pressures through population growth and tourism may influence the occurrence and impact of multi-hazard events. Finally, we must also investigate how global change may influence multi-hazard scenarios. In this respect, volcanic islands are particularly vulnerable to these situations. For this reason, natural risk management must go hand in hand with proper territorial and tourism planning, as resources are scarce in these environments and hazards are manifold. This overpopulation also makes risk management more difficult, as it requires a greater effort and mobilisation of resources during an emergency in a limited space compared to the mainland.

In the case of the Canary Islands, volcanic risk management was again tested during the eruption of 19 September 2021 at La Palma Island. The strengths of this management were highlighted in how an efficient evacuation and confinement of the population at risk was carried out. As a result, there were no direct casualties from the eruption, and the necessary resources were mobilised to attend to the affected population. Nevertheless, the lack of a multi-hazard perspective in the PEVOLCA made the Scientific Committee fearful of the risk of triggering other events, such as lahars or blockages of sewage and other municipal facilities due to the threat of heavy rainfall following the deposition of large thicknesses of ash. The Canarian emergency plan does not cover this scenario. However, some problems were difficult to manage, such as the excessive pressure from media and social networks, and the lack of clear protocol in certain scientific actions (e.g. sample collection and analysis) and communication strategies. Also, the lack of a long-term

hazard assessment for the whole Canary Islands does not help define precise emergency plans and implement risk reduction programmes.

As for non-volcanic risks, the Canary Islands are subject to floods and landslides every year, as well as sometimes to forest fires (e.g. the fires of 2019) or earthquakes (e.g. the seismic crisis in Tenerife in 2004). Despite this, disaster reduction initiatives and strategies do not keep pace with the occurrence of these events, and every year the same towns continue to be flooded, the same bridges continue to be washed away, the same seafronts continue to be affected, and the same roads continue to be cut.

With unstoppable climate change and repeating the same mistakes despite our globalisation and technological development, it is time to become aware of the risk posed by these multi-hazard scenarios and invest effort and money in foresight, prevention, and mitigation in front of such complex situations.

6 Concluding Remarks

This paper has reviewed the evolution and status of the multi-hazard concept and its application to volcanic islands. With a high vulnerability and exposure to multi-hazard scenarios, the need for multi-hazard management becomes more evident in these environments. A consensus must be reached on this emerging but increasingly topical perspective and the necessary investment in research to better understand the interactions between events and the regional and global consequences of such scenarios. In addition, awareness must be raised of the increasing difficulties volcanic islands encounter when facing multi-hazards due to overpopulation. If we add to this the responsibility that many of these regions have to manage their own emergencies with their own local resources, and the added difficulty of managing them with an excess of tourism from different origins, other needs such as territorial planning and a redesign of risk management policies are highlighted.

A clear example is the case of the Canary Islands, a region susceptible to multiple geohazards and with a worrying overpopulation. The eruption of September 2021 in La Palma allowed us to see the strengths and weaknesses of the management plans in this territory. However, like many others, this region suffers from hazards of lesser media interest but with equal or greater impact. The solution is not to wait until they occur and the population becomes temporarily aware but to invest in prevention and preparedness. Moreover, for this to happen, the multi-hazard perspective needs to be fully integrated into disaster risk reduction policies in a binding way.

Acknowledgements Marta López-Saavedra received an FPU Ph.D. grant (FPU19/02413). This research was partially funded by the EC Grant EVE (DG ECHO H2020 Ref: 826292).

References

Ellingwood, B. R. (2010). Performance-based engineering for multiple hazards: the role of risk assessment. In J. Li, Y. G. Zhao, J. B. Chen, & Y. B. Peng (Eds.), *Reliability engineering and risk management, proceedings of the international symposium on reliability engineering and risk management (ISRERM2010)*. Shanghai: Tongji University Press.

Gill, J. C., & Malamud, B. D. (2016). Hazard interactions and interaction networks (cascades) within multi-hazard methodologies. *Earth System Dynamics, 7*(3), 659–679. https://doi.org/10.5194/esd-2015-94.

Kappes, M. S. (2011). *Multi-hazard risk analyses: a concept and its implementation*. Ph.D. thesis, The University of Vienna, Vienna.

Kappes, M. S., Keiler, M., & Glade, T. (2010). From single- to multi-hazard risk analyses: a concept addressing emerging challenges. In *Proceedings of the "Mountain Risks" international conference*, Firenze.

López-Saavedra, M., Martí, J., Rubio, J.L., & Kelfoun, K. (2021). Cascading effects of extreme geohazards on Tenerife (Canary Islands). *Journal of Geophysical Research: Solid Earth 126*(9), e2021JB022294. https://doi.org/10.1029/2021JB022294.

UN. (2002). *Johannesburg plan of implementation of the world summit on sustainable development*. Technical Report, United Nations, Johannesburg. http://www.un.org/esa/sustdev/documents/WSSD_POI_PD/English/WSSD_PlanImpl.pdf.

UN-ISDR. (2015). Sendai framework for Disaster Risk Reduction 2015–2030. In *Third United Nations world conference on disaster risk reduction*, Sendai, Miyagi, Japan. https://www.undrr.org/publication/sendai-framework-disaster-risk-reduction-2015-2030.

United Nations for Disaster Risk Reduction Homepage. Retrieved January 23, 2022, from https://www.undrr.org/.

United Nations Homepage. Retrieved February 14, 2022, from http://www.un.org/esa/dsd/agenda21/res_agenda21_07.shtml.

Risk-Informed Decision-Making on Volcanic Hazards

Gordon Woo

Abstract

The safety of residents and tourists in volcanic regions is traditionally managed through an alert system with discrete levels ranging from no unrest to a major volcanic eruption. In recent years, substantial progress has been made in quantitative volcano risk modelling, which can generate estimates of eruption probability that can refine the discrete alert levels. The estimation of eruption probability is an important scientific interface between the volcanological community and public officials. It can help inform important safety decisions such as when to call a population evacuation or restrict tourist access, or conversely, when to allow people to return home or tourists to visit. The concept of risk-informed decision-making on volcanic hazards is explained and motivated by the need for all stakeholders to be more knowledgeable about the risk assessment process. Illustrations of the application of risk-informed decision-making are given, including the 2022 volcanic crises in Tonga and the Azores.

Keywords

Volcanic • Hazards • Risk • Decisions • Evacuation

1 Introduction

During a period of volcanic unrest, public officials need to make decisions which balance two objectives: protecting against casualties arising from a volcanic event; protecting the livelihoods and way of life of the surrounding population.

Public officials are entrusted with making safety-critical decisions for all kinds of risks. For risks that pose a finite short-term threat, such as a leak from a chemical plant, the precautionary principle is often invoked. All those who might be impacted are evacuated until the source of the leak has been found and fixed. However, the precautionary principle does not work well for volcanic crises, which can persist for many months, and where the hazard source is beyond human control.

The evacuation time for a threatened population is comparatively short. Therefore, an evacuation decision often may be delayed until the probability of an imminent eruption is high. This may be effective in regions with good transport logistics, but the transport infrastructure might not allow for timely evacuation for many densely populated volcanic regions. This applies especially to the infirm and elderly who need more time to evacuate safely.

The task of balancing the advantages and disadvantages of any decision is part of the routine of daily life. For difficult, complex decisions, decision-making can be supported by risk analysis which assesses the pros and cons in a methodical and systematic manner, transparent to scrutiny, facilitating risk-informed decision-making.

Within their core education in the geological sciences, most volcanologists are not trained in the formalism of risk analysis, which is peripheral to the career path of most Earth scientists, but is more familiar to engineering geologists. Hence, the practical adoption of risk-informed decision-making around the world has been limited. However, it should evolve with further progress in training volcanologists and experience gained from actual crises. For example, a survey of crisis management performance of volcano observatories (Winson et al., 2014) indicated a tendency towards greater hesitation in calling for an evacuation than might be optimal for safety.

G. Woo (✉)
RMS, Minster Building, 21 Mincing Lane, London, EC3R 7AG, UK
e-mail: Gordon.Woo@rms.com

A. Malheiro et al. (eds.), *Advances in Natural Hazards and Volcanic Risks: Shaping a Sustainable Future*, Advances in Science, Technology & Innovation, https://doi.org/10.1007/978-3-031-25042-2_3

2 The Need for Quantitative Volcano Risk Assessment

Quantitative risk assessment for natural hazards began in the 1960s with the pioneering work of Cornell on seismic hazards. Deterministic earthquake scenario analysis had been in use by civil engineers for decades earlier, but it was computer power which allowed multiple scenarios to be considered. Instead of a single maximum credible earthquake scenario, the whole spectrum of earthquake sizes could be considered, as well as the stochastic variability in the level of seismic ground motion.

In the 1980s, the eruption of Mt. St. Helens established the value of volcano event-tree analysis, considering a sequential array of alternative eruption outcomes. In the 1990s, the eruption of Mt. Pinatubo in 1991, the third largest in the twentieth century, provided further opportunities for deploying event-tree analysis to estimate the chance of an eruption impacting distant areas. For any volcanic crisis, there is a multitude of alternative realisations of its evolution, as well as the societal response. Newhall (2021), one of the principal Pinatubo volcanologists, has given an insightful counterfactual account of the various ways in which the successful evacuation might have been derailed. For any historical eruption, a counterfactual analysis of what else might have happened is instructive for future disaster preparedness, as well as quantitative risk assessment (Woo, 2019).

A major advance in the practical use of quantitative volcano risk assessment came in the mid-1990s with the involvement during the Montserrat volcanic crisis of Willy Aspinall and Barry Voight, both very knowledgeable and experienced in seismic risk analysis. Following the start of the Soufrière Hills eruption in July 1995, management of the Monserrat crisis was fraught with episodic dome building and collapse. Quantitative volcano risk assessment played an important role in crisis communication and management. One of the key metrics calculated is the probability of exceedance of multiple fatalities from a large eruption. This metric could be used for comparative purposes, such as with earthquake risk. It could also be used to gauge the tolerability of this societal risk.

One of the practical innovations introduced by Aspinall (2006) was structured elicitation of expert judgement for probabilistic hazard and risk assessment. It is quite common for the eruption probability associated with a given period of unrest to be poorly defined and assessed. The structured elicitation process provides a way of gauging this probability methodically, using the collective knowledge and wisdom of the volcanological community.

Geological sciences are specialised as academic disciplines, and few volcanologists are experienced as seismic hazard analysts, and vice versa. In his book on the mathematics of natural catastrophes, Woo (1999) surveyed the general framework for risk assessment of geological, meteorological, and hydrological hazards. This framework has proved useful for the academics at Bristol University, a mainstay of the Montserrat Volcano Observatory (Rougier et al., 2018). With the expanded international education of volcanologists to include academic postgraduate courses in multi-hazard risk assessment, decision support during volcanic crises may increasingly be risk-informed.

During the Montserrat crisis, good communication between volcanologists and the governor of Montserrat was enabled and maintained by being risk-informed. The continuous pressure on decision-makers during a volcanic crisis is alleviated if a risk-informed viewpoint is adopted in situations of high uncertainty—which is often the case. An evacuation decision may be quite straightforward if a sizeable eruption is clearly imminent. However, if there is considerable uncertainty over whether an eruption will occur at all, and if so, how large, then any thought about evacuation has to be balanced by considering the societal implications of the consequences of a false positive. The designation of any exclusion zone is fraught with objections and displeasure from property owners denied access to their homes. Balancing the pros and cons of actions to mitigate volcano risk lies at the heart of volcano crisis decision-making.

3 Volcano Crisis Decision-Making

Adaptive behavioural decisions have always been essential for human survival. Paying a sum now to avert payment of a larger sum later, contingent on the occurrence of a rare event, is the kind of dilemma faced intermittently by those living near an active volcano.

Consider a hazardous situation where one has to choose between two actions: either protect, or do not protect (Woo, 2008). The cost of protection is C. Without protection, the decision-maker incurs a loss L which exceeds C if an adverse hazard state arises. Denote by P the probability of the adverse hazard state arising within a specified time window. To minimise the expected expense, the optimal policy is to protect, if P exceeds C/L; but not to protect if P is less than C/L. The minimal expense is then min [C, PL].

If the cost of protection C is very low compared with the potential loss L, then paying for this protection will be eminently sensible, even if the probability P of an adverse

hazard state is small. However, if the cost of protection C is quite high compared with the potential loss L, then paying for this protection may not be worthwhile unless the probability of an adverse hazard state P is significantly high.

The loss/cost ratio L/C of action to mitigate volcano risk varies significantly from one community to another. Most in a community would be willing to suffer dislocation and loss of livelihood for a few months to avoid some potentially lethal threat. This is the predicament commonly experienced by war refugees.

By contrast, consider the predicament of farmers whose entire wealth is represented by the value of their farm animals. This dilemma is personified by the refusal in May 2013 of a chicken farmer to leave her chickens even though there was a mandatory evacuation from the Copahue volcano in the Andes Cordillera. In the absence of a trusted government compensation scheme, farmers face financial ruin if their animals are lost. As a result, farmers may be extremely reluctant to leave their animals, even if the perceived probability of personal harm is quite high. However, the cost C to farmers of protective action can be reduced if farm animal evacuation schemes complement human evacuation, as has been established for some Asian volcano crises, such as Mt. Agung, Bali, in September 2017.

The management of a volcanic crisis by public officials may extend to providing evacuated residents with security guarantees in circumstances where residents may be loathed to leave their homes for fear of looting. Such security guarantees would be an effective way of 'nudging' urban populations to evacuate (Thaler & Sunstein, 2008), where some residents with valuable heirlooms at home may have a low perception of the probability of harm from a potential eruption, cognitively biased by a preoccupation with theft from an unattended property.

Before deciding how to react to a hazard warning, people watch the reaction of others: family, neighbours, friends, etc. Psychologists refer to this tendency to conform as social proof. This social phenomenon gives rise to a substantial degree of self-organisation in the way that individuals take decisions when facing a perceived threat. Therefore, the public dissemination of hazard warnings should aim to elicit a cohesive public response. Where the loss cost ratio L/C is widely perceived to be high, then self-evacuation may occur provided the eruption probability P is perceived to be significant.

The problem is that public communication of the state of a volcano is typically not given through probability assessment, but rather through a discrete set of alert levels, which may obscure the actual volcano hazard level.

Papale (2017) has pointed out that there is no equivalent discretisation in the underlying volcanic processes. Consequently, it is not uncommon for significant eruptive events to occur, without a corresponding change in alert level.

In an assessment of the U.S. use of volcano alert systems, Fearnley et al. (2012) have noted that the decision to move between alert levels is based upon a complex negotiation of perceived risks. Nevertheless, Papale (2017) has argued for a separation of roles, with scientists basing their evaluations exclusively on scientific knowledge, providing decision-makers with clear, unambiguous information.

The provision by scientists of eruption probabilities, with associated uncertainties, would help decision-makers make optimal decisions in the public interest. This would also help individual public members make their own personal evacuation decisions that depend on their own self-assessed loss cost ratio L/C.

4 Recent Case Studies and Final Remarks

The value of risk-informed decision-making is illustrated by the eruption of the Hunga Tonga-Hunga Ha'apai volcano on 15 January 2022. There had been volcanic activity for several weeks beforehand, but this had significantly decreased by 3 January 2022. On 10 January, with no further activity, the Tonga Geological Services declared the volcano dormant. Volcanic activity was considered to have ceased, and the volcano had reverted to its normal state.

Fundamental to any decision about the state of a volcano should be a quantitative risk assessment. A description of the prevailing observed state of the volcano does not itself provide guidance as to the imminent probability of an eruption. As remarked above, this is a basic deficiency of the volcano alert level system, which is not informative of the underlying volcano dynamics. A quantitative risk assessment can address the driving mechanism of a possible eruption.

Hunga Tonga has a major eruption about every 900–1000 years, the most recent being in 1100 CE. So when the moderate 14 January 2015 eruption occurred, the volcano was primed for a large eruption. Geodetic data gathered afterwards indicated that the surrounding coral reef was lifting up, suggesting the magma was building beneath the volcano and could cause an eruption in the near future. Counterfactually, this January 2015 event might have triggered an event, such as that occurred seven years later in January 2022. The elapsed time of seven years is only 0.8% of the return period.

On 10 January 2022, after a week of quiescence, the volcano was still in a critical state, where the imminent probability of a large eruption was non-zero, even if no

precursory activity was currently evident. Fortunately, the surprisingly large eruption on 15 January occurred outside the evening hours of darkness. Otherwise, the tsunami would have claimed more casualties. A structured expert elicitation of the Hunga Tonga eruption probability on 10 January 2022 would have been valuable for decision-making.

The same applies to the volcanic island of Sao Jorge in the Azores archipelago after nearly 27,000 small tremors of tectonic origin had been recorded, at an average depth of 8–12 km, in a period of several weeks up to 5 April 2022. As a result, the volcano alert level was set at Level 4, indicative of a real possibility of an eruption.

The seismic activity in Sao Jorge was somewhat reminiscent of the seismicity detected prior to the first eruption of the Cumbre Vieja volcano on La Palma island in September 2021. Elderly people and those with reduced mobility were evacuated from Velas, the western area of the Sao Jorge island, where most of the seismic activity has been recorded. A sudden eruption might have left them stranded in danger. In 1808, a series of explosions took place from vents along the south-central crest of the island.

Emergency services established safe corridors for traffic and temporary accommodation on the island's eastern side. Hundreds of others amongst the 8,400 population of Sao Jorge self-evacuated the island by air out of fear and caution. This would be a rational risk-informed response to the perceived imminence of an eruption and the comparatively moderate cost of evacuation.

References

Aspinall, W. P. (2006). Structured elicitation of expert judgement for probabilistic hazard and risk assessment in volcanic eruptions. In H. M. Mader, S. G. Coles, C. B. Connor, & L. J. Connor (Eds.), *Statistics in volcanology*. London: Geological Society.

Fearnley, C. J., McGuire, W. J., Davies, G., & Twigg, J. (2012). Standardisation of the USGS volcano alert system (VALS): Analysis and ramifications. *Bulletin of Volcanology, 74*, 2023–2036.

Newhall, C. (2021). Volcanic risk mitigation that could have been derailed but wasn't: Pinatubo, Philippines 1991. Frontiers in Earth Science. https://doi.org/10.3389/feart.2021.743477.

Papale, P. (2017). Rational volcano hazard forecasts and the use of volcano alert levels. *Journal of Applied Volcanology, 6*, 13.

Rougier, J. C., Sparks, R. S. J., & Cashman, K. V. (2018). Regional and global under-reporting of large explosive eruptions in the last 1000 years. *Journal of Applied Volcanology, 7*, 1.

Thaler, R. H., & Sunstein, C. R. (2008). *Nudge*. New Haven: Yale University Press.

Winson, A. E. G., Costa, F., Newhall, C. G., & Woo, G. (2014). An analysis of the issuance of volcanic alert levels during volcanic crises. *Journal of Applied Volcanology, 3*, 14.

Woo, G. (1999). *The mathematics of natural catastrophes*. London: Imperial College Press.

Woo, G. (2008). Probabilistic criteria for volcano evacuation decisions. *Natural Hazards, 45*(1), 87–97.

Woo, G. (2019). Downward counterfactual search for extreme events. *Frontiers in Earth Science*. https://doi.org/10.3389/feart.2019.00340.

Geoethics: The Missing Piece in the Separation of Responsibility Between Volcanologists and Decision-Makers

Silvia Peppoloni, Gordon Woo, Joan Martí, and Giuseppe Di Capua

Abstract

In a volcanic crisis, authorized decision-makers must balance the social and economic costs of mitigating actions, such as evacuation, against the potential human losses if such actions are insufficient. In making their decisions, advice is needed from volcanologists on the eruption probability. Therefore, there should be a clear separation in the roles of volcanologists and decision-makers; the volcanologists should advise on the volcano hazard and alternative potential scenarios but refrain from involvement in making decisions. Currently, volcanologists are responsible for setting volcano alert levels. Given the small handful of distinct alert levels, there is inherent ambiguity and substantial uncertainty in the interpretation of individual levels. Furthermore, changing an alert level may automatically trigger actions by decision-makers. This would violate the principle of separation of responsibility and may result in unwelcome pressure being applied to volcanologists. Just as physicians can invoke medical ethics in resisting pressure to alter their advice, so volcanologists can invoke geoethics. Freedom to abide by their scientific beliefs is a basic tenet of geoethics.

Keywords

Volcano • Crisis • Evacuation • Geoethics • Responsibility

S. Peppoloni · G. Di Capua (✉)
Istituto Nazionale di Geofisica e Vulcanologia, Rome, Italy
e-mail: giuseppe.dicapua@ingv.it

International Association for Promoting Geoethics, Rome, Italy

G. Woo
Risk Management Solutions, London, UK

J. Martí
Geosciences Barcelona, CSIC, Barcelona, Spain

1 Introduction

The role of volcanologists during a volcanic crisis varies quite widely around the world. Quite apart from variable standards of staff training and monitoring capability at a volcano observatory, there are substantial national and cultural differences in how crisis decisions are made.

Even in the most deprived areas of the world, physicians should abide by the principles of medical ethics, as originally formulated by Hippocrates. Similarly, volcanologists with only primitive technical support and monitoring equipment should abide by the principles of geoethics in being free to express their true scientific opinions without being pressured to change them. Under circumstances where officials resort to pressure, geoethics provides a solid universal defence.

2 Geoethical Aspects in Decision-Making on Natural Hazards

The fear of dangerous natural phenomena has always accompanied the life of human beings and shaped the human-nature relationship over the centuries. However, the progress of modern science has changed the perspective of this relationship. Human rationality has developed methods for investigating natural phenomena, created mathematical tools for their modelling, identified laws that control their evolution, and produced technological devices to support human beings in defending against natural hazards. Nevertheless, this does not mean that society has reached full awareness of what can and must be done to reduce the impact on humans of the negative effects of natural phenomena. In fact, in most cases, human communities remain particularly vulnerable to natural hazards.

The growth in the world population, the expansion of urbanized areas and the consequent anthropic occupation of hazardous zones (such as those around active volcanoes), as

A. Malheiro et al. (eds.), *Advances in Natural Hazards and Volcanic Risks: Shaping a Sustainable Future*,
Advances in Science, Technology & Innovation, https://doi.org/10.1007/978-3-031-25042-2_4

well as the increase in the intensity of some natural phenomena linked to climate change (such as extreme meteorological events) and the appearance of other man-induced phenomena (for example, the average sea-level rise), are increasing the risk to which humans are exposed.

Human communities are complex realities, made up of a network of relations of cooperation and subordination, establishing roles and consequently different responsibilities in decision-making processes (Peppoloni, this volume). From this perspective, managing natural hazards is a sensitive issue, as it concerns the interaction between science and society, particularly the relationship between scientists and decision-makers. This relationship exists during all the different stages of the disaster cycle. If this relationship is set up correctly and guided by a clear distinction in roles and responsibilities, we can expect positive effects on the health and safety of citizens. On the other hand, pitfalls and ambiguity in the interaction between scientists and decision-makers can lead to dire consequences for society. In fact, even though the wealth of knowledge acquired on natural phenomena is considerable compared to the past, often, human communities do not receive precise and unambiguous information on what to do during an emergency phase and may find themselves unable to establish priorities in the implementation of risk mitigation strategies and crisis management, capable of minimizing the number of victims and damage to property.

The lack of clarity on the roles and responsibilities of the actors involved in the risk scenario can lead to tragic consequences for people's lives and the economic activities of an area.

The "L'Aquila earthquake case" in 2009, Italy (Cocco et al., 2015), is a paradigmatic case in the relationship between science and society that clearly did not work properly in managing a seismic crisis. Seven scientists were convicted for negligence in assessing seismic hazards after the city of L'Aquila had been extensively damaged in 2009 by an earthquake, and three hundred people died. The lack of clarity on the responsibility of the various actors involved (decision-makers, scientists, mass media and the population), the lack of protocols and procedures during the seismic swarm, which had lasted for four months, and the interference of media in search of scoops led to confused messaging to citizens about the risk they were running and about the preventative actions to be adopted by local administrative managers. However, with the third and final judgement, six out of seven scientists were acquitted because they had the role of "scientific advisors" and not decision-makers. The conviction was confirmed only for one of them, the representative of the Civil Protection Department, who was responsible for risk management.

In geoethics, the principle of responsibility is the ethical criterion of agency (Peppoloni et al., 2019). It is articulated according to different levels of interaction, or domains of human experience, that become gradually wider, more complex and intricate: the self, the social group(s) to which individuals belong (including professional ones), society and future generations, and the environment. The principle of responsibility expresses the commitment of the human agent to answer for the agent's actions and consequences. Making responsible choices requires evaluating the possible repercussions of the agent's decisions/actions. Therefore, scientists are called to adopt responsible behaviours towards stakeholders. In fact, they should consider that there are objective difficulties by scientists in relating to a perception of risk by the population that differs from theirs, consequently in communicating the hazard and risk to citizens.

From a scientific point of view, the geoethical approach to risk management is based on four considerations (Peppoloni & Di Capua, 2022, pp. 35–43):

(a) Scientists must be aware of their social role in collecting observations and data and developing models, techniques and scenarios for the benefit of society, assuring a high level of scientific preparation and updated knowledge to provide their best support in complex situations, like during dangerous natural and anthropogenic phenomena occurrence.
(b) Scientific and decision-making roles must be kept separate to avoid societal pressures and conditioning on scientists and technicians who have to provide scientific data to decision-makers. The responsibility of those assessing hazards, vulnerabilities and exposures is different from that of those who are in charge of making decisions based on a complex and holistic evaluation of all elements at risk, by taking into account technical, environmental, economic, cultural and political aspects, in the awareness that the same risk may require different solutions in different contexts due to diverse hazards, vulnerabilities or exposures.
(c) Hazard and risk communication is a delicate matter (Fearnley et al., 2018) that needs preventative preparation by those who will be in charge of transferring information to a population during a crisis and an emergency phase (Cauzzi et al., 2018). Scientists must inform citizens about the characteristics, dynamics and evolution of phenomena, but civil protection agencies/departments must make decisions about mitigation strategies leading up to evacuation.
(d) Mitigation strategies have to be consequent to cost-benefit analyses.

An orderly and effective decision-making process should be based on the following:

- Carrying out an operational organization chart that establishes the roles and responsibilities of the various actors involved in the crisis and emergency phase, including the decision-making chain.
- Creating operational protocols to codify the collection, storage and assessment of data, situation analyses and the decision-making process.
- Defining the acceptable level of risks for reference communities (politicians being in charge) (Peppoloni & Di Capua, 2021, p. 73) by assessing uncertainties (Doyle et al., 2014) and establishing probability hazard thresholds (scientists being in charge) (Geller, 2015).
- Building an encoded stream of information between scientists and decision-makers, which defines the timing and methods of communication in the crisis and emergency phase, including communication of mitigation actions to the population, considering the variability of the probability of occurrence of natural phenomena during their evolution (Marzocchi & Bebbington, 2012; Peppoloni, this volume).
- Establishing a legal framework that gives scientists full autonomy in the study, discussion and communication of scientific results within the codified decision-making process.

From their side, individual scientists and research teams have ethical obligations towards society, and their behaviours must be based on the following:

- To cooperate with colleagues to find an operational synthesis of results which should inform the decision-making process. In the crisis and emergency phase, cooperation is one of the keys to success in mediating different visions and evaluations in a complex scenario.
- To provide raw and analysed data, and probability scenarios to decision-makers, with explanations about their reliability and uncertainties.
- To strengthen trust in science by the population by informing transparently and using a language that maintains scientific accuracy while simplifying knowledge without trivializing it. Citizens must receive clear information on what is certain and what is possible. This implies avoiding the "medialization" of the scientific debate within the community of experts. The strictly scientific discussion among scientists cannot become public, especially during a crisis or an emergency phase; otherwise, the trust in science in facing/solving problems is inevitably undermined by legitimate scientific controversies with the consequent affirmation of pseudo-scientific theories based on non-existent cause-and-effect links, and/or of legal implications for scientists of being accused of misleading hazard communication. Neuberg (2015) pointed out, "*Alternative models and explanations do not need to confuse. Different opinions can be explained and expressed as a form of uncertainty, but the essential difference is to avoid debating in the full glare of the media in an ego-serving, allegedly scholarly discourse*".

3 Rational Crisis Decision-Making and Responsibility Separation

There is a rational way of making decisions in a volcanic crisis. This involves weighing the pros and cons of mitigating action, such as evacuation. The optimal decision would favour mitigating action if the ratio of the cost C to the potential loss L, without mitigating action, is less than the eruption probability P (Marzocchi & Woo, 2007). Thus if the cost of evacuation is low, evacuation makes obvious sense even when the hazard level is low. However, if the evacuation cost is high, decision-makers would be justified in delaying an evacuation decision until the eruption probability, (which may increase with time in accord with volcano dynamics), becomes substantial. Even if this elementary algebraic statement of the decision-making process is not explicit in the minds of decision-makers, it is always implicit. If no mitigating action is taken, the hope must be that the odds of an eruption are low. On the other hand, if an evacuation is called, the thinking must be that the odds of an eruption are sufficient to justify it. Cost-benefit analysis is a methodical extension of this basic thought process.

Apart from its expression of rationality, this formalism has the important advantage of expressing transparently and readily comprehensibly the separation of responsibilities between volcanologists and authorized decision-makers. Volcanologists are responsible for estimating the eruption probability P, leaving C and L to others. Of course, volcanologists need to share with decision-makers their insights on the impacts of potential eruption scenarios, their uncertainties and likelihoods, but estimating the societal costs and losses and issuing the call for evacuation ultimately are matters for the decision-makers.

If the scientific evidence and best judgement indicate that the eruption probability has increased by an amount ΔP, this should be communicated to decision-makers freely, without considering any societal or economic consequences. It is not for volcanologists to ponder such consequences, let alone be legally responsible for them.

Especially after the 2009 L'Aquila earthquake legal proceedings, it should be clear that hazard scientists have a professional duty to undertake their hazard assessment with due diligence, which means providing their informed estimate of the event occurrence probability, but not making any specific forecasting statements about what will or will not happen. Decision-makers should have the responsibility for setting and enforcing population exclusion zones. Residents denied access to their property inside an exclusion zone or who have suffered volcanic harm outside it should not have legal redress against the scientists themselves.

Traditionally, volcanologists have had responsibility for volcano alert level systems, and changing levels, as and when such a change seems warranted. However, the transition between a handful of levels is highly ambiguous, e.g. the change from minor to moderate volcanic unrest. No equivalent discretization in the natural processes leads to volcanic hazards (Papale, 2017). Such ambiguity can lead to a contentious and protracted debate with decision-makers, which is antithetical to the separation of responsibility.

A volcano alert system serves a useful, practical purpose in providing a general guide to a volcano's status. However, rational decision-making dictates that any actions taken to mitigate volcanic risk at a given time should be based not directly on the volcano alert level per se but rather on C/L and the perceived value of P.

To take a 2022 South Pacific example, the Hunga Tonga-Hunga Ha'apai volcano erupted on 15 January. It had exhibited unrest for several weeks beforehand, although activity had ceased for a week on 3 January, and the volcano was declared dormant by Tonga Geological Services on 10 January. The declaration about the absence of activity was not equivalent to a statement of the null probability of an eruption. What is clear from the earlier eruption of 14 January 2015 is that the volcano remained in a critical state, during which the eruption probability was small—but non-zero. Even a low eruption probability may justify a low-cost action, such as issuing a general tsunami preparedness warning. Had the eruption on 15 January 2022 occurred in hours of darkness, there might have been more than three Tongan fatalities.

The most vexing crisis situations arise in areas with poor transport infrastructure where the evacuation time may be slow or where many elderly or infirm residents require extra time to evacuate. In such situations, decision-makers may need to call for evacuation even when the eruption probability is comparatively low. In situations of uncertainty, scientists are trained to wait to gather further information. The separation of responsibility is especially crucial here; otherwise, in discussion with decision-makers, scientists may be inclined to involve themselves in the decision to delay. The historical record on alert level changes is that the change has very often come late (Winson et al., 2014).

4 A Volcanologist's Perspective

Volcanoes are complex, non-linear geological systems that drive magma from the Earth's interior to the surface. This process is governed by numerous physical laws that depend on many variables. This makes each volcanic system different and difficult to predict. In an attempt to find reproducible patterns that could make volcanic behaviour predictable, volcanologists tend to make comparisons among volcanoes. Unfortunately, the amount of available observational data is still insufficient to apply modern data analysis methods, which could ensure reliable results in forecasting the future behaviour of volcanoes. This is why volcano forecasting is still subject to great uncertainties that need to be incorporated as part of the process description.

From a volcanologist's perspective, the role of a volcanologist during a volcanic crisis is to provide probabilities of eruption (during the unrest phase) and probabilities of eruption changes (during the eruption phase). Eruption probabilities include providing an estimate of where, when and how the next eruption may be, while probabilities of eruption changes refer to potential variations in the eruptive behaviour that may imply changes in eruption scenarios. In both cases, probability estimates should be based on the integration of good knowledge of the past eruptive behaviour of the volcano with a precise interpretation of the monitoring data. These probabilities will provide information not only on the possible evolution of the volcanic process but also on the degree of uncertainty that volcanologists have regarding this process.

This information needs to be well understood by decision-makers in order for them to make the most appropriate decisions in each situation. During a volcanic crisis, volcanologists must obtain scientifically accurate information about the process and communicate it to those responsible for managing the crisis clearly and concisely. However, volcanologists should not become part of the decision-making process.

One of the main problems for volcanologists who advise on a volcanic crisis is to reach a consensus on the information to be communicated to decision-makers. Scientific advisory groups during a volcanic crisis are composed of different experts who have different backgrounds, information and opinions, and not everyone may share the same view on the red lines that should not be crossed during the management of a volcanic crisis. This is why a consensus based on geoethics is fundamental to avoid venturing beyond the strictly scientific advice required by the decision-makers.

When scientific information is used to make a decision, even if this is simply to upgrade the traffic light system, as mentioned above, scientists tend to become part of the decision-making process and, therefore, are subject to

societal and legal compromises these may imply. Scientists are responsible for providing the most accurate information on the current volcanic process, which is essential for crisis management. Nevertheless, scientists should not be responsible for the consequences of how a crisis has been managed when they have avoided involvement in the decision-making process, as justified by the principles of geoethics.

5 Concluding Remarks

In a review of the emerging field of geoethics, Bobrowsky et al. (2018) have observed that: "*In conducting their activities, geoscientists should consider if they are free from compromises and (or) conflicts of interest, including political, social and psychological pressures*."

Now that geoethics has emerged, it may be regarded as the longstanding missing piece of the volcano crisis management puzzle, justifying the separation of responsibility between volcanologists and decision-makers unequivocally and freeing volcanologists from becoming entangled in public policy issues which are outside their domain of professional expertise.

Acknowledgements The authors would like to express their gratitude to the organizers of NatHaz22 for proposing this chapter.

References

Bobrowsky, P., Cronin, V. S., Di Capua, G., Kieffer, S. W., & Peppoloni, S. (2018). The emerging field of geoethics. In L. C. Gundersen (Ed.), *Scientific integrity and ethics with applications to the geosciences* (pp. 155–173). American Geophysical Union, John Wiley and Sons Inc., Special Publication 73. https://doi.org/10.1002/9781119067825.ch11.

Cauzzi, C., Haslinger, F., Marti, M., & Zechar, J. D. (2018). White paper on general guidelines, recommendations, and best practices on communication and decision making under uncertainty for environmental hazards and natural disasters. Deliverable D12.2, ENVRIplus project (p. 31). Retrieved June 20, 2022, from https://www.envriplus.eu/wp-content/uploads/2015/08/D12.2-White-paper-on-general-guidelines-recommendations-and-best-practices-on-communication-and-decision-making-under-uncertainty-for-environmental-hazards-and-natural-disasters.pdf.

Doyle, E. E. H., McClure, J., Paton, D., & Johnstone, D. M. (2014). Uncertainty and decision making: Volcanic crisis scenarios. *International Journal of Disaster Risk Reduction, 10*, 75–101. https://doi.org/10.1016/j.ijdrr.2014.07.006.

Fearnley, C., Winson, A. E. G., Pallister, J., & Tilling, R. (2018). Volcano crisis communication: Challenges and solutions in the 21st century. In C. J. Fearnley, D. K. Bird, K. Haynes, W. J. McGuire, & G. Jolly (Eds.), *Observing the volcano world. Advances in volcanology* (pp. 3–21). Cham: Springer. https://doi.org/10.1007/11157_2017_28.

Geller, R. J. (2015). Geoethics, risk-communication, and scientific issues in earthquake science. In M. Wyss, & S. Peppoloni (Eds.), *Geoethics: Ethical challenges and case studies in earth sciences* (pp. 263–272). Elsevier. https://doi.org/10.1016/B978-0-12-799935-7.00022-8.

Marzocchi, W., & Bebbington, M. S. (2012). Probabilistic eruption forecasting at short and long time scales. *Bulletin of Volcanology, 74*, 1777–1805. https://doi.org/10.1007/s00445-012-0633-x.

Marzocchi, W., & Woo, G. (2007). Probabilistic eruption forecasting and the call for an evacuation. *Geophysical Research Letters, 34*, L22310. https://doi.org/10.1029/2007GL031922.

Neuberg, J. (2015). Thoughts on ethics in volcanic hazard research. In M. Wyss, & S. Peppolon (Eds.), *Geoethics: Ethical challenges and case studies in earth sciences* (pp. 305–312). Elsevier. https://doi.org/10.1016/B978-0-12-799935-7.00024-1.

Papale, P. (2017). Rational volcanic hazard forecasts and the use of volcanic hazard levels. *Journal of Applied Volcanology, 6*, 13. https://doi.org/10.1186/s13617-017-0064-7.

Peppoloni, S. (this volume). Geoethics to face natural risks by improving societal resilience. In A. Malheiro, F. Fernandes, H. I. Chaminé (Eds.), *Advances in natural hazards and volcanic risks: Shaping a sustainable future, proceedings of the 3rd international workshop on natural hazards (NATHAZ'22), Terceira Island-Azores 2022, ASTI*. Cham: Springer.

Peppoloni, S., & Di Capua, G. (2022). *Geoethics: Manifesto for an ethics of responsibility towards the earth*. Cham: Springer. https://doi.org/10.1007/978-3-030-98044-3.

Peppoloni, S., Bilham, N., & Di Capua, G. (2019). Contemporary geoethics within the geosciences. In M. Bohle (Ed.), *Exploring geoethics: Ethical implications, societal contexts, and professional obligations of the geosciences* (pp. 25–70). Cham: Palgrave Pivot. https://doi.org/10.1007/978-3-030-12010-8_2.

Winson, A. E. G., Costa, F., Newhall, C. G., & Woo, G. (2014). An analysis of the issuance of volcano alert levels during volcanic cries. *Journal of Applied Volcanology, 3*, 14. https://doi.org/10.1186/s13617-014-0014-6.

Earthquakes, Volcanoes and God: Changing Perspectives on the Importance of Religion as an Important Influence in Cultural Responses

David K. Chester and Angus M. Duncan

Abstract

During the past thirty years, the authors have been engaged in researching the influence of religious belief on responses to earthquakes and volcanic eruptions. As late as the 1990s, the prevailing attitude within both the academic and disaster planning communities was that such responses, though important historically, had been progressively replaced since the Eighteenth-Century Enlightenment by notions of scientific contingency operating within largely secular frames of reference. Such attitudes where they remained were either those of a small minority in economically more advanced countries, or represented the last redoubts of superstition and irrationality in societies untouched by the forces of modernism. In this work, it is argued that academic and disaster planning perspectives have changed profoundly in recent years, and there is now recognition that, in many societies, not all of them economically less developed, there is a widespread religious framing of responses. Using examples from Christian, Judaic, Islamic, Hindu, Buddhist and Shinto traditions, the authors propose that religious believers and their resources (e.g. buildings, wealth and access to indigenous and foreign aid networks) may assist in the achievement of successful disaster risk reduction (DRR) policies.

Keywords

Earthquakes • Volcanoes • Religion • Responses • Policy development

1 Introduction

Volcanology, seismology and hazard planning have their roots in the *Enlightenment*, and until the late 1990s, practitioners had little time for mythological or faith-based understandings of disasters and their consequences. This fostered a scholarly consensus that was unwilling to accept the notion that religion was a vital part of the cultures that affect responses to and recovery following emergencies caused by earthquakes and eruptions. Indeed it has been frequently maintained in histories of research that statements contained in religious scriptures, in which catastrophes are assumed to be under deistic control, are of historical curiosity only and rarely impinge on post-eighteenth-century understandings of either physical processes or the formulation of policies concerned with Disaster Risk Reduction (DRR). It has been maintained that where they do occur, such attitudes represent the last redoubts of superstition and irrationality in both economically less developed countries that have been relatively unaffected by forces of modernism; and amongst a decreasing number of religious believers in more economically advantaged states. The position up to the closing years of the United Nations' *International Decade for Natural Disaster Reduction (IDNDR)* 1990–2001 "was even more extreme and … (the)… predominant attitude to faith-based responses to disasters was at best dismissive, at worst hostile and on occasions even involved such attitudes … being equated with backwardness" (Chester et al., 2019a, p. 446).

2 A New Consensus

Since the late 1990s, the authors and others (e.g. Abbott, 2019) have argued against the previously dominant post-Enlightenment secularist view by proposing an alternative which maintains that religious explanations of disasters are not just to be found historically, but are frequently encountered across a range of countries and regions at

D. K. Chester (✉) · A. M. Duncan
Department of Geography and Planning, University of Liverpool, Liverpool, UK
e-mail: jg54@liverpool.ac.uk

A. Malheiro et al. (eds.), *Advances in Natural Hazards and Volcanic Risks: Shaping a Sustainable Future*, Advances in Science, Technology & Innovation, https://doi.org/10.1007/978-3-031-25042-2_5

differing levels of economic development. However, making a case for a widespread religious framing of historical eruptions and earthquakes has not proved to be straightforward because secularist perspectives have been so pervasive that any references to spirituality have been effectively "written out" of eruption and earthquake narratives (Chester & Duncan, 2007). This "hidden history" is recoverable by interrogating a wider range of source materials than is customary in disaster inquiries. These comprise published research in anthropology, area studies and theology; newspapers of record; newsreel film; television programmes and web-based source materials. By using these "unconventional" sources, we have compiled several catalogues of historic religious responses over the past two decades (e.g. Chester & Duncan, 2007, p. 213), the latest iteration being presented as in Table 1.

Not only has there been an increasing recognition that religious responses are important, but, over the past twenty years, hazard research has also changed. Beliefs are now regarded as being a crucial component of culture, and comprehension of culture is accepted as essential in building policies of DRR. This is clear from policies advocated by United Nations' Hyogo's (2006) and Sendai's (2015) *Frameworks for Action*. Publication of the *World Disasters Report* (2014) by the International Federation of Red Cross and Red Crescent Societies reinforces this new awareness (Chester et al., 2019a, p. 446).

Over the same time interval of approximately two decades, during which attitudes of academic researchers and disaster risk reduction planners towards religious interpretations of earthquake and eruption losses changed fundamentally, the major religions of the world have witnessed transformations in their approaches towards catastrophes. Changes in attitudes occurred first within the Judaeo/Christian tradition and are so deep-seated that they represent a Kuhnian paradigm shift in the manner in which suffering in disasters is perceived. Developments in Islamic theology occurred later yet have been equally significant in allowing policies of risk reduction to be proposed, which are in line with Islamic doctrine (Chester et al., 2013). Finally, for adherents of Hinduism, Buddhism, Shinto and other "eastern" faiths, the issue of divine agency in human suffering has never been so acute because these are not monotheistic faiths with all-powerful deistic figures who may or may not share some, or indeed all, the responsibility for human suffering.

All traditions of faith have one feature in common that there are few historic examples where religious views have prevented adherents from co-operating with the authorities at times of disaster, accepting help and embracing future disaster risk reduction policies. The possession of seemingly incompatible views of the world, and holding opinions and acting contrary to them, is known in the literature as *parallel practice* or *cognitive dissonance*, and this is important when future planning policies are proposed.

2.1 The Judaeo/Christian Tradition

Theodicy attempts to reconcile the notion of an almighty, loving and omniscient God with the concurrent reality of evil and suffering. In Judaism and Christianity, three models have predominated: the *free-will* (i.e. *Augustinian*); the *retributive* and the so-called "*best of all possible worlds*"—or *Irenaean*. The *free-will* approach holds that human beings have a choice, with suffering not just being the consequence of the exercise of choice but also involves sinfulness because a person may act contrary to the divine purpose. This understanding segues into the second model, where notions of divine punishment and retribution are stressed. Such an understanding has been used to explain many disasters in the Hebrew Scriptures and Christian Bible, and many that have occurred over the past 2000 years. Although this defence has been far less prominent since the Enlightenment, disasters

Table 1 Historic earthquakes and volcanic eruptions show a marked religious response. Earthquakes included are those with a death toll of over 1000. Volcanoes include those with a VEI of 4 or greater

Historical earthquakes 1900–1921	Religious framing	
	Number	Percent (%)
1900–1949	20	37
1950–1999	24	43
2000–2021	7	88
Large historical eruptions 1850–2021		
1850–1899	4	50
1900–1949	7	58
1950–1999	13	46
2000–2021	9	60

Note True figures are likely to be higher because the table only includes sources available internationally; and there are many areas and countries where information was either not recorded until recently (e.g. some Middle East States) or deliberately withheld (e.g. the former Soviet Union and China)

are still viewed as divine punishment by some conservative and traditional believers. The "*best of all possible worlds*" model proposes that it is not possible to create any natural system that does not have the capability to inflict harm on injure human beings. God uses natural processes to secure the greater good: for example in a world without earthquakes, there would be no global tectonics; and in a world without volcanoes, there would be no atmosphere.

Over the past twenty-five years, a majority of Christian and Jewish theologians have argued that this traditional approach to theodicy is deficient. A key concept in this new thinking is collective as opposed to individual guilt, and this notion is alluded to but not developed in many reports on historical earthquake and eruption-related disasters (Chester et al., 2019a). Traditional models of theodicy attempted to place responsibility for disasters with God so reducing human responsibility, with the divine becoming the scapegoat for what are essentially acts of human collective sinfulness. Putting together notions of human responsibility, societal culpability and collective sinfulness has allowed a liberationist model to be put forward (Sobrino, 2004; Abbott, 2019, p. 3). "This not only represents a re-formulation of the free-will defence, because freedom and the possibility of sinful conduct is shifted from the individual to the institution (e.g. the State, a system of international trade and/or local administration), but structural sinfulness also lies at the heart of global differences in wealth, power and unequal disaster outcomes" (Chester et al., 2019a, p. 453–4).

The implication of this new thinking is that the role of the Christian when confronting disasters changes from trying to explain catastrophes in theological terms to attempting to relieve suffering by being involved in relief, recovery and planning to reduce future risks. It is notable that in our historical archive upon which Table 1 is based, post-2000 events have seen Christian responses that are increasingly characterised by: pastoral concern; care for victims; the widespread use of church buildings and seeking and then mobilizing financial resources from indigenous and foreign aid donors.

2.2 Islamic Perspectives

Islam is defined as submission to the will of Allah, and in the *Qur'an*, *Hadith* and many subsequent doctrinal statements, suffering is viewed as either a test of devotion, as an instrument by which God may achieve some outcome, or as a punishment for sin (Akasoy, 2007). The early history of Islam was not wholly consistent regarding what causes suffering in disasters. However, from the tenth century, an orthodox position evolved which viewed disasters as being wholly under the control of God, with the majority of Muslims accepting that disasters were instrumental to the divine purpose. It has been argued that this may encourage fatalism, but research by the authors and others (e.g. Acevedo, 2008) has uncovered few actual instances.

There is rich literature on historical and contemporary disasters in Islamic countries in which disaster losses have been ascribed to divine displeasure because of what were considered sinful actions on the part of a population or group within a society (Akasoy, 2007, p. 403–4). In more recent years, attitudes have changed. Even though many Muslims including scholarly elites continue to maintain theological opinions focused on retribution and godly wrath, today this is not the only or indeed the dominant perspective. In writing about the 2010 eruption of the Merapi volcano in Indonesia, Bagir (2012, p. 363) notes that "natural events turn to disaster when there are negative impacts on people because of their vulnerability… In this understanding, the question of *natural* evil becomes less relevant, because much if not all the evil coming from disasters … is non-natural." In common with the spread of new thinking within Christian theology, a contemporary Islamic scholar puts forward the view that suffering in disasters is associated with vulnerability produced by poverty, deficient planning and a lack of effective mitigation (Bagir, 2012).

In Islam, there is an apparent dilemma between God controlling everything and the extent of human responsibility. In attempting to resolve this predicament, some scholars have presented proposals that include assertions that catastrophes are only disastrous from the human point of view; and that people make themselves vulnerable because they contravene the divine laws that govern actions and conduct in the world. This standpoint is grounded in an Islamic perspective that the purpose of nature is ultimately good, even when it occasionally leads to a bad result (Solihu, 2007, p. 62). Such conclusions are very similar to the "best of all possible worlds" theodicy developed within Christianity and represent a convergence of perspectives between the two faiths. With respect to Iranian earthquake losses, Ghafory-Ashtiany (2009) puts forward the view that disregard by the state of awkward scientific truths and inconvenient civil engineering knowledge equates to corporate sinfulness, which increases vulnerability. Indeed there are many examples of instances where scholars have argued that sinfulness is collective and resides in the state and amongst developers, architects and builders.

Islamic theology strikes a balance between notions of an almighty deity, on the one hand, and characteristics of mercy and concern on the other. The *Qur'an* describes a God who shows empathy towards the human condition. This empathy should stimulate a benevolent response on the part of the believer, with all Muslims being under an obligation to assist the poor and destitute.

2.3 South Asian Religions

Hinduism, Buddhism and Shinto share a belief that a person's behaviour leads irrevocably to a future reward or punishment in a subsequent existence. This may encourage a fatalistic attitude to disasters (Kogen, 1987, p. 261), although in common with many Muslim believers, this is often exaggerated and may reflect the perspectives of outsiders (Burke, 2015). The notion of *Karma* holds that current actions produce the seeds of future happiness or suffering and within these faiths, there is no doctrine of innocent suffering. In theory, *karma* represents a complete solution to the problem of theodicy, because it constructs a "self-contained cosmos of ethical retribution", but in all three traditions orthodoxy is often compromised by outbreaks of popular devotion, heterodox beliefs and pastoral concerns (Merli, 2010, p. 106). Table 2 summarises features of orthodoxy and heterodoxy in Buddhism, Hinduism and Shinto.

In spite of a greater sense of detachment than is present in Judaism, Christianity and Islam, there are numerous examples where strong elements of pastoral concern and a willingness to aid relief efforts are in evidence, and it is on these foundations that policies to develop future relief efforts are focused (see below). For instance, in Buddhism, commitments to social welfare and concern were shown in the aftermath of the 2004 Asian tsunami in Malaysia and Thailand; the 2014 Yushu earthquake in the largely Tibetan area of Qinghai Province in China; the 2011 Japanese earthquake and tsunami and the Nepalese earthquake of 2015. Examples from Hindu majority countries and regions include the 1993 Latur earthquake; the Gujarat earthquake in 2001; the Nepalese earthquake in 2015. The Japanese earthquake and tsunami also brought forth pastoral responses from both Shinto and Buddhist believers.

3 Religion and Policies of Disaster Risk Reduction

Only c.16% of the world's population may be classified as religiously "unaffiliated", and since the 1970s, there has been not just a resurgence of religion in the post-Communist world, but in-migration to economically developed countries of people with strongly held religious convictions from Africa, the Middle East, the Indian sub-continent and the Far East. For the development of DRR policies, this is highly fortuitous for, as we have argued, the major faiths and their leaders are today far more receptive to the introduction of measures designed to help victims and allow planning for the future. Hence, a *rapprochement* is possible between religion and secular disaster planning which only a short time ago were considered incompatible.

It does not follow that policy development is straightforward and that there are both benefits and potentially problematic issues involved when DRR planners interact with religious groups. In reviewing popular Catholicism in southern Italy and the Azores, the authors concluded that there is no evidence that religious beliefs "have been: associated with debilitating fatalism; served to inhibit successful responses; have increased vulnerability and/or offered an 'alternative reality', where measures of risk

Table 2 Examples of variations from orthodoxy and pastoral focus in Buddhism, Hinduism and Shinto. Based on Chester and Duncan (2007) and many other sources

Religion	Orthodox and heterodox characteristics
Buddhism	Buddhism arose from a desire to find an answer to human suffering. In Buddhism *anicca* (impermanence) is central to orthodox faith and, following the Indian Ocean tsunami of 2004, many survivors including the bereaved perceived the event as a dramatic example of *anicca*. Following the 2010 earthquake in Tibet, some people viewed the earthquake as divine punishment, a view far removed from orthodox Buddhism. In "popular" Buddhism in southern Thailand, there are deities, magic and other manifestation forms of idolatry which are also theologically heretical.
Hinduism	Hinduism is less certain about deserved suffering and a sense that the gods might participate in and be recruited to assist in the conquest of evil and suffering. Orthodox Hinduism, with its focus on acceptance and detachment, is balanced by obligations of duty (*dharma*) and virtues including those of generosity (*dāna*). More negatively low-caste status may be conceived as a special form of misfortune or suffering, entailing a social, religious and ritual marginalisation position of economic under-privilege. Prejudice against lower castes is frequently encountered.
Shinto	Shinto is more syncretic than the other South Asian faiths, showing not only many common features with Buddhism but also unique traits as well. The latter includes the notion of *kami*: being and existence are mysterious and there is harmony in creation. Humans are children of *Kami* and the lives of all people are sacred. The concept that *kami* resides in shrines and in some cases is permanently present, is a prominent feature in *Shinto*. Shrine worship of mountains (especially Fuji) is strongly developed, and ancestors have a special role in the collective memory of Japanese people. There is a minority view that *tenbatsu* (i.e. heavenly punishment) is an element in Shinto.

reduction are opposed because disasters are viewed as being in God's hands with any intervention perceived as blasphemous" (Chester et al., 2019b, p. 50). This conclusion applies, with only a few minor exceptions, across the gamut of religious beliefs. When combined with the notion of *cognitive dissonance* (see above) this means that, even in regions where there are devote people who believe in notions of divine punishment such as in the southern Italian peninsula, Sicily and many Islamic countries (Chester et al., 2013), there is overwhelming support for assisting victims and embracing DRR planning policies.

In our bibliographic research, we have identified two negative features associated with some manifestations of religious practice, although both are exceptions rather than the general rule: discrimination in favour of co-religionists and using aid provision and alignment with DRR policies as levers for conversion. With respect to discrimination, most international religious charities are signatories of the *1994 Code of Conduct for International Red Cross and Red Crescent Movements and Non-Governmental Organisations in Disaster Relief*, which mandates aid provision on a non-discriminatory basis, although there is some evidence that these high ideals are not always put into practice in the field. This is a particular case in India and Nepal, where in spite of legislation to the contrary, there is some evidence of discrimination against low-caste Hindus (i.e. *Dalits*), Muslims and Christians following recent earthquakes. With regards to using disaster and relief efforts to proselytise and so encourage conversion, there are a small number of examples from within Christian communities, but these remain aberrations (Chester & Duncan, 2007).

In recent disasters, religious institutions, their leaders and members have, in contrast, shown many positive characteristics which are already assisting DRR planning. These include the use of sacred buildings (e.g. synagogues, churches, mosques, and temples) as community centres; leaders, many of whom are embedded in and respected by local people; willing volunteers inspired by notions of vocation and altruism; and access to resources—financial and personnel—to be found locally, nationally and internationally. There is much potential for further collaboration.

References

Abbott, R. P. (2019). "I Will Show You My Faith by My Works": Addressing the nexus between philosophical theodicy and human suffering and loss in contexts of 'Natural' disaster. *Religions, 10*, 213.

Acevedo, G. A. (2008). Islamic fatalism and the clash of civilisations: An appraisal of a contentious and dubious theory. *Social Forces, 86* (4), 1711–1752.

Akasoy, A. A. (2007). Islamic attitudes to disasters in the Middle Ages: A comparison of earthquakes and plagues. *The Medieval History Journal, 10*(1–2), 387–410.

Bagir, Z. A. (2012). Nidhal Guessoum's reconciliation of Islam and science: Practice and agenda of Islam and science. *Zygon, 47*(2), 354–366.

Burke, D. (2015). *How Hindus and Buddhists view Nepal's devastating earthquake*. CNN News May 1 2015.

Chester, D. K., & Duncan, A. M. (2007). Geomythology, theodicy and the continuing relevance of religious worldviews on responses to volcanic eruptions. In J. Grattan & R. Torrence (Eds.), *Living under the shadow* (pp. 1–13). Left Coast Press.

Chester, D. K., Duncan, A. M., & Dhanhani, H. A. G. (2013). Volcanic eruptions, earthquakes and Islam. *Disaster Prevention and Management, 22*(3), 278–292.

Chester, D. K., Duncan, A. M., & Speake, J. (2019a). Earthquakes, volcanoes and God: Comparative perspectives from Christianity and Islam. *GeoHumanities, 5*(2), 444–467.

Chester, D. K., Duncan, A. M., Coutinho, R., & Wallenstein, N. (2019b). The role of religion in shaping responses to earthquakes and volcanic eruptions: A comparison between Southern Italy and the Azores, Portugal. *Philosophy, Theology and the Sciences, 6*, 33–45.

Ghafory-Ashtiany, M. (2009). View of Islam on earthquakes, human vitality and disaster. *Disaster Prevention and Management, 18*(3), 218–232.

Kogen, M. (1987). Karman. In M. Eliade (Ed.), *The encyclopedia of religion* (Vol. 8, pp. 261–268). New York: Macmillan.

Merli, C. (2010). Context-bound Islamic theodicies: The tsunami as supernatural retribution vs. natural catastrophe in Southern Thailand. *Religion 40*(2), 104–111.

Sobrino, J. (2004). *Where is God? Earthquakes, terrorism, barbarity, and hope*. New York: Orbis, Maryknoll.

Solihu, A. K. H. (2007). Making sense of natural disasters: An Islamic hermeneutics of malevolent phenomena in nature and its implication for sustainable development. *The American Journal of Islamic Social Sciences, 24*(1), 46–72.

Towards a Multi-Hazard Assessment at Etna Volcano (Italy): The PANACEA Project

Raffaele Azzaro, Salvatore D'Amico, Tomaso Esposti Ongaro, Gaetana Ganci, Alexander Garcia, Simona Scollo, Marco Aliotta, Boris Behncke, Andrea Bevilacqua, Giuseppe Bilotta, Stefano Branca, Carmelo Cassisi, Mauro Coltelli, Paola Del Carlo, Mattia de' Michieli Vitturi, Alessio Di Roberto, Luigi Lodato, Luigi Mereu, Michele Prestifilippo, Cristina Proietti, Laura Sandri, Tiziana Tuvè, Francesco Zuccarello, and Annalisa Cappello

Abstract

This work presents the first results of the PANACEA project regarding the assessment of different volcano-related hazards at Mt. Etna (lava and pyroclastic flows, tephra fallout and earthquakes) by exploiting data deriving from the volcano's history with accurate physical–mathematical models. Volcano-related hazards are distributed differently on Etna—from the deserted summit area down to the densely populated flanks—but must be considered together for long-term territorial planning.

Keywords

Lava flows • Tephra • Pyroclastic flows • Earthquakes • Hazard assessment

1 Introduction

Natural hazards cannot be stopped or eliminated, but their effects can be mitigated by careful planning and data-assisted decision-making. Mt. Etna is one of the most active volcanoes globally, which produces effusive and explosive eruptions and frequent seismic activity, significantly affecting territory and human society.

The PANACEA project aims at assessing hazards and risks at Etna by using a huge amount of data—historical, volcanological, and seismological—and physics-based models. The objectives include improving knowledge of the long-term seismic and eruptive history of Etna and the numerical modelling of geophysical phenomena. Probabilistic maps combine the long-term probability of future events with numerical simulations. In case of volcanic unrest, short-term scenarios can be produced using real-time monitoring data. Here is presented the first estimates of volcano-related individual hazards at Etna, i.e. lava and pyroclastic flows, tephra fallout, and earthquakes.

2 Materials and Methods

Volcanoes are intrinsically multi-hazard systems that impact the surrounding environment at different levels, ranging from mild economic and social losses to fatalities and total destruction (Deligne et al., 2017). Volcanic eruptions can last minutes to decades, rarely even centuries, and produce cascading and/or concurrent hazards, amongst others, lava flows, tephra fallout, pyroclastic flows, and earthquakes. Modelling hazardous volcanic phenomena has not been fully resolved and requires implementing different physical models, and proper numerical codes specialized to each hazardous event. The following sections briefly present state of the art and preliminary results to assess the different hazards at Etna.

R. Azzaro (✉) · S. D'Amico · G. Ganci · S. Scollo · M. Aliotta · B. Behncke · G. Bilotta · S. Branca · C. Cassisi · M. Coltelli · L. Lodato · M. Prestifilippo · C. Proietti · T. Tuvè · F. Zuccarello · A. Cappello (✉)
Istituto Nazionale di Geofisica e Vulcanologia, Osservatorio Etneo, Catania, Italy
e-mail: raffaele.azzaro@ingv.it

T. Esposti Ongaro · A. Bevilacqua · P. Del Carlo · M. de' Michieli Vitturi · A. Di Roberto
Istituto Nazionale di Geofisica e Vulcanologia, Sezione di Pisa, Pisa, Italy

A. Garcia · L. Mereu · L. Sandri
Istituto Nazionale di Geofisica e Vulcanologia, Sezione di Bologna, Bologna, Italy

A. Malheiro et al. (eds.), *Advances in Natural Hazards and Volcanic Risks: Shaping a Sustainable Future*, Advances in Science, Technology & Innovation, https://doi.org/10.1007/978-3-031-25042-2_6

3 Results

3.1 Lava Flow Hazard

The lava flow hazard has been assessed using GPUFLOW (Cappello et al., 2022; Rogic et al., 2022; Zuccarello et al., 2022), which includes a new thermo-rheological model (with a variable emissivity and cooling by atmospheric convection), and a correction factor that scales the diagonal neighbour contributions, calibrated to achieve a circular emplacement on a flat topography.

As input data, a Digital Surface Model (DSM) was used and updated to 2019 and the typical parameters for a'a lavas: 1360 and 1143 K respectively as extrusion and solidification temperatures, 2600 kg m^{-3} as density, and 0.05 wt% as water content. The effusion rate was derived from a statistical analysis of the flank eruptions of the last 4 ka, which provided 9 eruptive classes. The eruptive vents are the grid's nodes shown in Fig. 1, from which 9 simulations were ran (one per eruptive class).

The preliminary hazard map (Fig. 1) was obtained by overlapping about two-thirds of the total lava flow simulations, using the same probability for all eruptive vents and eruptive classes. Since the temporal recurrence rate has been neglected, our investigation was limited to assessing constrained hazards, i.e. probabilities upon the occurrence of an eruption. We are currently running the remaining simulations and performing statistical analyses to estimate probabilities of vent opening, occurrences for the nine eruptive classes, and a temporal recurrence rate.

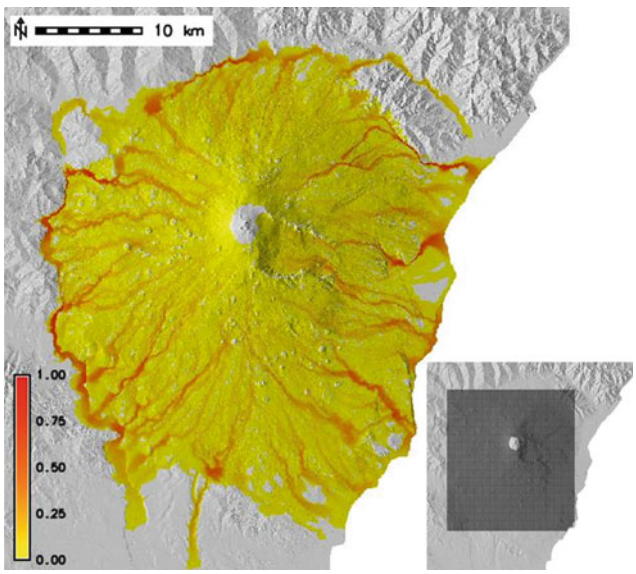

Fig. 1 A preliminary lava flow hazard map obtained by overlapping 151,770 GPUFLOW numerical simulations starting from 25,295 potential eruptive vents. The nodes of the 200-m regular grid are shown in the bottom-right inset. The legend shows relative probabilities

3.2 Tephra Fallout Hazard

Tephra fallout hazard has been assessed (Scollo et al., 2013) using the 2-D advection–diffusion TEPHRA model (Bonadonna et al., 2005). Input data, i.e. column height, total grain size distribution, total erupted mass, and density of lithics and pumices, were estimated for selected test cases. Hazard maps were developed considering eruptions forming both strong and weak short-lived plumes.

All lava fountains that occurred in the last two decades (Andronico et al., 2021) were selected and complemented with new field-based and remote sensing data by radar, camera, and satellite (Fig. 2). Thus, the main eruption source parameters of 270 events to perform the new TEPHRA simulations were estimated and the associated hazard assessed. Also, the correlations, distinguishing between long-lasting and short-lasting events, were statistically analysed.

3.3 Pyroclastic Flow Hazard

For pyroclastic flows we improved the IMEX-SfloW2D model (de'Michieli Vitturi et al., 2019; Gueugneau et al., 2021) and a workflow for probabilistic hazard assessment was created. The model is based on the depth-averaged equations of an incompressible granular flow, accounting for non-hydrostatic effects associated with the steep and irregular topography. It considers non-linear dissipative terms and non-Newtonian rheologies with a mixed implicit-explicit numerical scheme, accurately tracking the front propagation and properly modelling steady conditions. IMEX-SfloW2D has been re-engineered by including several rheological models, routines for solving thermodynamics equations of gas, liquid, and particle mixtures, deposition of a polydispersed mixture, erosion from a substrate, and variable density flows.

For the hazard assessment from pyroclastic flows at Mt. Etna, a statistical calibration of rheological parameters was performed and a parallel computing workflow for Monte Carlo simulations and post-processing to run on CPU clusters was developed. The workflow implements several procedures for pre- and post-processing, suitable for the numerical simulation of crater collapse events at the volcano's summit. In particular was developed an automatic procedure to define collapsing geometry over the DSM and an ensemble of numerical runs that span a wide range of volumes and rheological parameters was created (Fig. 3a, b). In addition, automatic post-processing and generation of probabilistic hazard maps have also been implemented, considering the potential variability of the position of the collapsing niche (Fig. 3c).

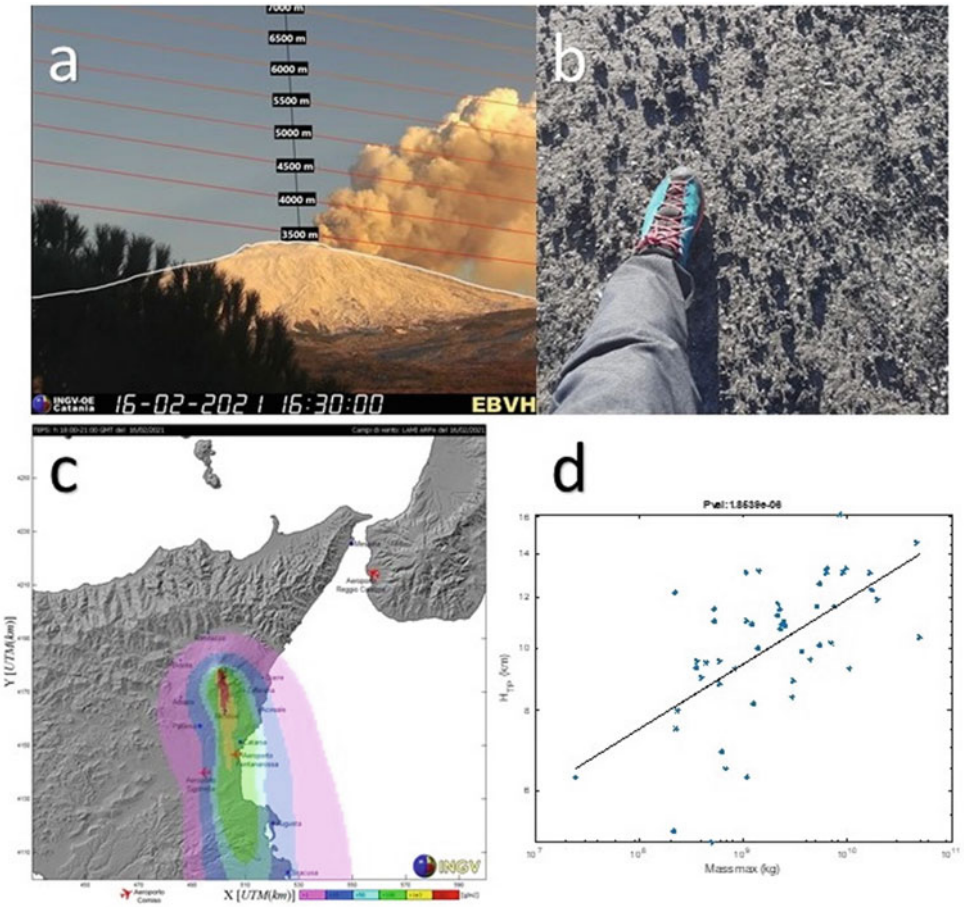

Fig. 2 The lava fountain of 16 February 2021 observed by **a** visible camera and **b** on the field; **c** simulation of the deposit using the TEPHRA model; and **d** example of the statistical analysis carried out amongst the column heights and the total masses of the investigated events

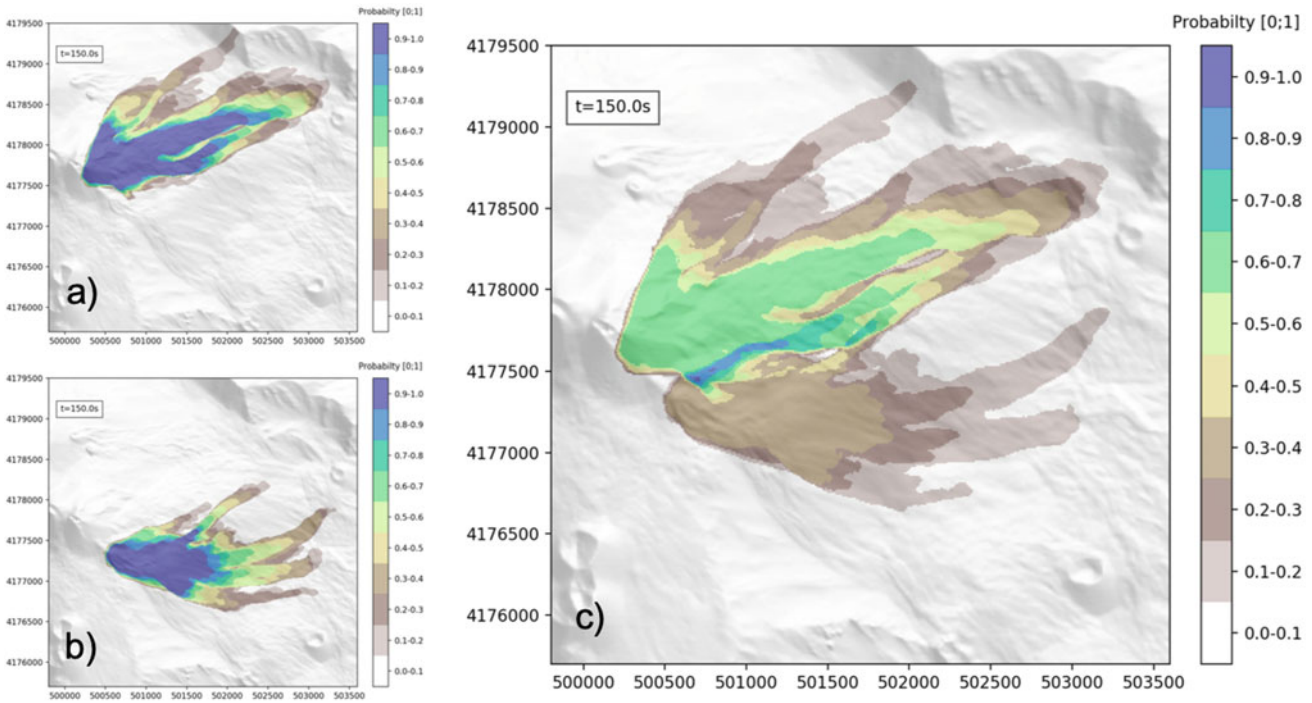

Fig. 3 **a**–**b** Example of probabilistic pyroclastic flow hazard maps from two independent collapse niches on Etna, accounting for volume variability. **c** Example of the weighted probability of invasion considering both collapse locations and volume variability

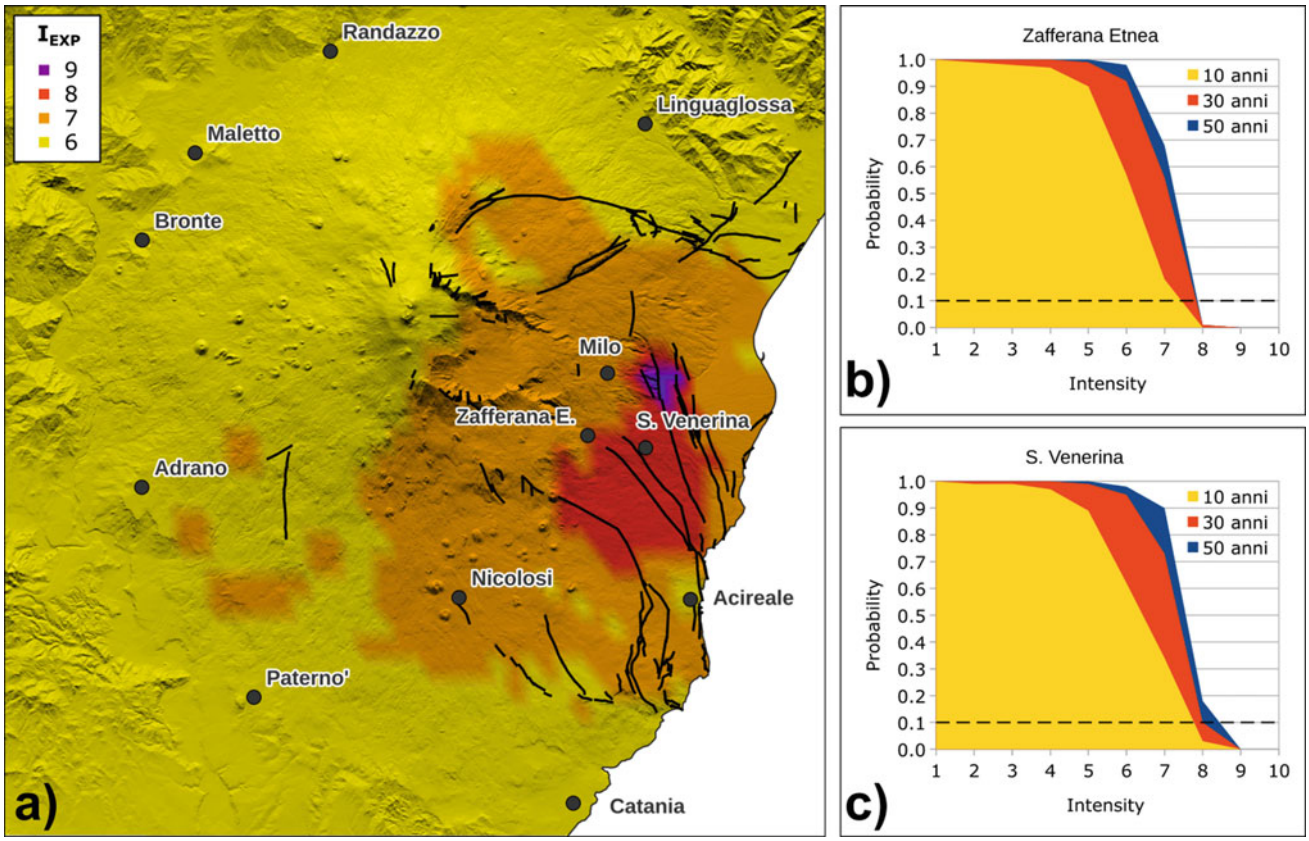

Fig. 4 **a** Seismic hazard estimated for an exposure time of 30 years; the values of expected intensity (I_{EXP}) refer to an exceedance probability of 10%. **b**, **c** Hazard curves for exposure times of 10, 30, and 50 years referring to the towns of Zafferana Etnea and S. Venerina

3.4 Seismic Hazard

The probabilistic seismic hazard assessment (PSHA) considers only the local volcano-tectonic seismicity to improve the knowledge for short exposure times. The final PSHA estimations, based on the SASHA code (D'Amico & Albarello, 2008), have been computed by integrating the observed data taken from the Catalogo Macrosismico dei Terremoti Etnei (CMTE, Azzaro & D'Amico, 2014) and intensity calculated (Rotondi et al., 2016) by applying an anisotropic attenuation model. Figure 4a shows the map of expected intensities (I_{EXP}) for an exposure time of 10 years with a 10% of exceedance probability, while Figs. 4b, c represent the hazard curves for exposure times of 10, 30, and 50 years in two municipalities of the study area.

4 Preliminary Considerations and Concluding Remarks

The PANACEA project aims to solve challenging issues related to the probabilistic mapping of volcano-related hazards at Etna without overlooking the basic processes associated with the numerical modelling of complex geophysical flows in conceptual and technological terms. The main goal is to develop a flexible framework of tools and procedures for assessing long- and short-term multi-hazard and the quantification of multi-risk (see Pessina et al., 2023).

Thus, the assessment of different hazards at Etna was introduced, including lava flows, tephra fallout, pyroclastic flows, and earthquakes. Our evaluations have been constrained by a deep knowledge and characterization of the eruptive and seismic activity, the development of physical models to simulate different scenarios, and the probabilistic combination of their potential risks. From this perspective, Mt. Etna offers great opportunities for testing methodological approaches due to the high number of monitoring networks installed, as well as the availability of long-term volcanic and seismic catalogues, which are very rare features for other volcanoes worldwide.

Based on a modular structure (hazards can easily be added or removed) and the ability to rapidly update outputs by revising the inputs without modifying the tool structure, PANACEA will provide a powerful instrument to develop effective and operational strategies to enhance safety and reduce the risk associated with eruptive or seismic crises at Etna.

Acknowledgements This work was supported by the INGV project Pianeta Dinamico (CUP D53J19000170001) funded by MIUR ("Fondo finalizzato al rilancio degli investimenti delle amministrazioni centrali dello Stato e allo sviluppo del Paese," legge 145/2018), Tema 8—PANACEA 2021-2023.

References

Andronico, D., Cannata, A., Di Grazia, G., Ferrari, F. (2021). The 1986–2021 paroxysmal episodes at the summit craters of Mt. Etna: Insights into volcano dynamics and hazard. *Earth-Science Reviews*, *220*, 103686.

Azzaro, R., D'Amico, S. (2014). Catalogo Macrosismico dei Terremoti Etnei (CMTE), 1633-2022. Istituto Nazionale di Geofisica e Vulcanologia (INGV), https://doi.org/10.13127/cmte.

Bonadonna, C., Phillips, J. C., & Houghton, B. F. (2005). Modeling tephra sedimentation from a Ruapehu weak plume eruption. *Journal of Geophysical Research, 110*, B08209.

Cappello, A., Bilotta, G., & Ganci, G. (2022). Modeling of geophysical flows through GPUFLOW. *Applied Sciences, 12*, 4395. https://doi.org/10.3390/app12094395.

D'Amico, V., & Albarello, D. (2008). SASHA: A computer program to assess seismic hazard from intensity data. *Seismological Research Letters, 79*, 663–671.

de' Michieli Vitturi, M., Esposti Ongaro, T., Lari, G., Aravena, A. (2019). IMEX_SfloW2D 1.0: a depth-averaged numerical flow model for pyroclastic avalanches. *Geoscientific Model Development*, *12*, 581–595.

Deligne, N. I., Horspool, N., Canessa, S., Matcham, I., Williams, G. T., Wilson, G., & Wilson, T. M. (2017). Evaluating the impacts of volcanic eruptions using RiskScape. *Journal of Applied Volcanology, 6*, 18.

Gueugneau, V., Charbonnier, S., Esposti Ongaro, T., Vitturi, M. M., Peruzzetto, M., Mangeney, A., Bouchut, F., Patra, A., & Kelfoun, K. (2021). Synthetic benchmarking of concentrated pyroclastic current models. *Bulletin of Volcanology, 83*, 75.

Pessina, V., Garcia, A., Meroni, F., Sandri, L., Selva, J., Azzaro, R., Bilotta, G., D'Amico, S., de Michieli Vitturi, M., Esposti Ongaro, T., Ganci, G., Mereu, L., Scollo, S., Cappello, A. (2023). From multi-hazard to multi-risk at Mount Etna: approaches and strategies of the PANACEA project. In: A. Malheiro, F. Fernandes, H. I. Chaminé (Eds.), *Advances in natural hazards and volcanic risks: shaping a sustainable future – proceedings of the 3rd international workshop on natural hazards (NATHAZ'22), Terceira Island - Azores 2022*, ASTI Series. Cham : Springer (this volume).

Rogic, N., Bilotta, G., Ganci, G., Thompson, J. O., Cappello, A., Rymer, H., Ramsey, M. S., & Ferrucci, F. (2022). The impact of dynamic emissivity-temperature trends on spaceborne data: applications to the 2001 Mount Etna Eruption. *Remote Sensing, 14*(7), 1641.

Rotondi, R., Varini, E., & Brambilla, C. (2016). Probabilistic modelling of macroseismic attenuation and forecast of damage scenarios. *Bulletin of Earthquake Engineering, 14*, 1777–1796.

Scollo, S., Coltelli, M., Bonadonna, C., & Del Carlo, P. (2013). Tephra hazard assessment at Mt. Etna (Italy). *Natural Hazards and Earth Systems Sciences, 13*, 3221–3233.

Zuccarello, F., Bilotta, G., Cappello, A., Ganci, G. (2022). Effusion rates on Mt. Etna and their influence on lava flow hazard assessment. *Remote Sensing*, *14*(6), 1366.

From Multi-Hazard to Multi-Risk at Mount Etna: Approaches and Strategies of the PANACEA Project

Vera Pessina, Alexander Garcia, Fabrizio Meroni, Laura Sandri, Jacopo Selva, Raffaele Azzaro, Giuseppe Bilotta, Salvatore D'Amico, Mattia de' Michieli Vitturi, Tomaso Esposti Ongaro, Gaetana Ganci, Luigi Mereu, Simona Scollo, and Annalisa Cappello

Abstract

Managing multiple hazards simultaneously affecting a territory is a challenge for effective risk mitigation. This is particularly true on active volcanoes like Mt. Etna, characterized by effusive and explosive eruptions, often coupled with intense seismic activity. This work presents the PANACEA project's approach to treating multi-hazards in terms of risk, which requires a common definition of the exposed elements and their vulnerability. Another aspect emerging from the recent and historical volcanic crises at Etna is the cascading effects and the problem of assessing their short-term interactions. A risk model is presented considering a set of sequences of hazardous events that may result from volcano unrest to possible impacts on some infrastructural elements. The project's outcomes are intended to be a significant step toward a more comprehensive resilience to volcanic disasters, leading to a safer society.

Keywords

Volcanic eruptions • Earthquakes • Cascading hazards • Vulnerability • Damage

V. Pessina (✉) · F. Meroni
Istituto Nazionale di Geofisica e Vulcanologia, Sezione di Milano, Milano, Italy
e-mail: vera.pessina@ingv.it

A. Garcia · L. Sandri · J. Selva · L. Mereu
Istituto Nazionale di Geofisica e Vulcanologia, Sezione di Bologna, Bologna, Italy

R. Azzaro · G. Bilotta · S. D'Amico · G. Ganci · S. Scollo · A. Cappello
Istituto Nazionale di Geofisica e Vulcanologia, Osservatorio Etneo, Catania, Italy

M. de' Michieli Vitturi · T. Esposti Ongaro
Istituto Nazionale di Geofisica e Vulcanologia, Sezione di Pisa, Pisa, Italy

1 Introduction

Etna volcano (Sicily, Italy) looms over a densely urbanized territory, and its phenomena (e.g. lava flows, earthquakes, tephra and pyroclastic flows) severely affect built-up locations' lifelines and communication systems at very different scales, from local to sub-regional. Therefore, to move from hazard to risk, it is necessary to identify the elements exposed to the volcano's effects and assess their vulnerability to the different hazards. In general, the loss estimation is mainly performed in structural damage, victims, loss of functionality, economic effects on activities, and environmental damage and requires the definition of proper risk indicators common to all the elements exposed. Finally, it is possible to proceed to more complex risk analyses, such as multi-risk and cascading assessments (e.g. Garcia-Aristizabal et al., 2015; Marzocchi et al., 2012; Neri et al., 2008; Zuccaro & De Gregorio, 2019; Zuccaro et al., 2008).

Figure 1 shows the structure of the logic tree defined for Etna, representing a set of sequences of events happening and the possible impact on some infrastructural elements. Such structure splits the problem into possible phenomenological pathways according to the hazard events (or sequences) and the potentially impacted elements involved in a given scenario. In this way a set of multi-risk scenarios was hypothesized by considering as reference the impact on a given infrastructural element (e.g. damage to houses' roofs, in black in Fig. 1) and reconstructing the series of events potentially driving impacts on it (e.g. seismic activity, and ashfall or ballistics from the summit or lateral vents). Moreover, once the series of events of interest are identified, the model for risk assessment can be outlined by defining the scenarios for the analysis, considering both independent and interacting risks. For example, in the case of roofs before mentioned, one could assess the risk by considering (i) the seismic load only (independent), (ii) the ash load only (independent), or their combined effects acting

A. Malheiro et al. (eds.), *Advances in Natural Hazards and Volcanic Risks: Shaping a Sustainable Future*, Advances in Science, Technology & Innovation, https://doi.org/10.1007/978-3-031-25042-2_7

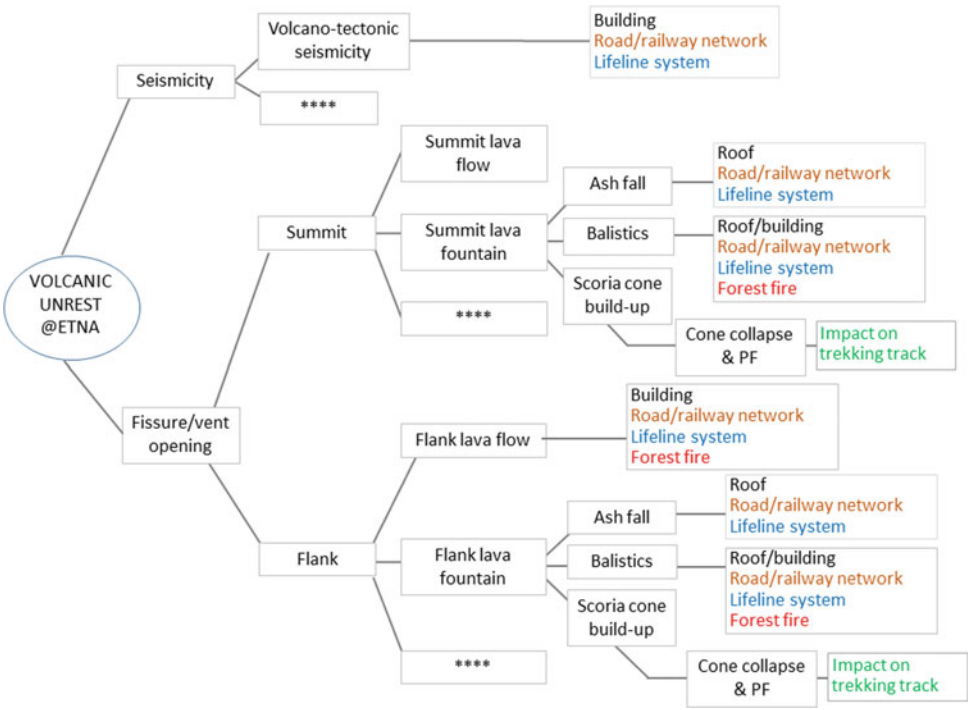

Fig. 1 Example of a possible set of sequences of events resulting from volcano unrest at Etna and possible impact on some infrastructural elements. PF stands for pyroclastic flow

simultaneously. This model provides modular and scalable solutions for assessing risk levels, including analyses carried out at different geographical scales and levels of detail.

2 Elements Exposed to Volcano-Related Hazards

The complex and huge dataset of exposed elements (Table 1) was collected from regional or provincial government offices and organized in a GIS, as shown in Fig. 2.

The census data collected by the Italian Institute of Statistics (ISTAT, 2011) provides a valuable source of information on building stock and demographic data, updated and spatially detailed. The calibration of the models at a local scale is performed through satellite images or the AeDes data ("post-earthquake damage and safety assessment and short-term countermeasures" provided by the regional department of Civil Protection; see Torrisi, 2018), i.e. a set of data collected in the field after the strong earthquakes occurred during the 2002 eruption.

3 Vulnerability Assessment

The logic tree model in Fig. 1 calculated the risk for residential buildings hit by earthquakes and loaded by volcanic particles (tephra). In addition, the case of a fire triggered by burning clasts during a lava fountain was also considered. In particular, it focuses on three municipalities—Zafferana Etnea, Santa Venerina and Milo (Fig. 3, left)—that are often affected by these kinds of hazards.

Different examples of vulnerability assessment for buildings are available in the literature, but they are often limited to specific areas or single volcanic hazards (Jenkins et al., 2014; Marti et al., 2008; Pomonis et al., 1999).

Table 1 Inventory assets of elements at risk

Themes	Data
Demographics	Population
Building stock	Residential, commercial, industrial
Essential facilities	Hospital, schools, police and fire stations, hotels, municipal offices
Transportation	Highways and bridges, state/provincial/city roads, railways and stations
Lifeline utility	Potable water, wastewater, oil, gas, electric power, communication
Hazardous material	Facilities housing industrial and hazardous material

Fig. 2 Example of the inventory assets organized in a dedicated GIS

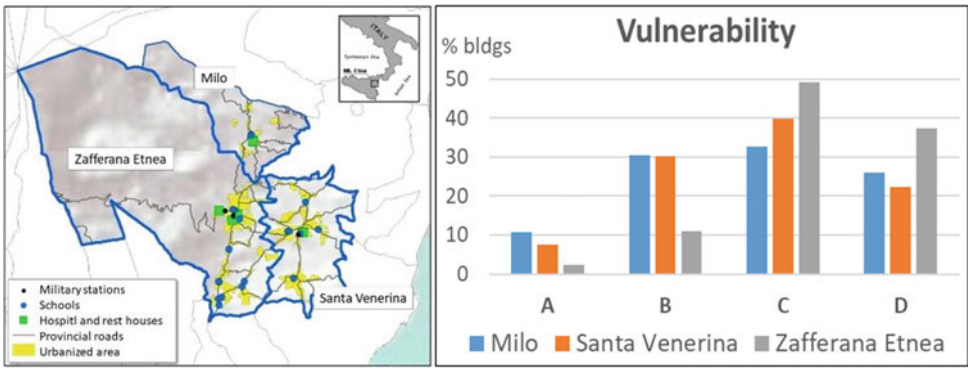

Fig. 3 Map of the three Etnean municipalities chosen as test areas (left) and percentage distribution of the buildings (right) into the four seismic vulnerability classes: A—weak, B—medium weak, C—medium strong and D—strong

Adopting the recent models of Lagomarsino et al. (2021) for masonry buildings and Rosti et al. (2021) for reinforced concrete ones, the residential stock can be grouped into six vulnerability classes according to the EMS-98 scale definition (from the most vulnerable A to the less vulnerable E; see Grünthal, 1998) (Fig. 3, right). The model proposed by Spence et al. (2005) is used to assess the vulnerability of building roofs, classified into four classes (weak, medium-weak, medium strong and strong).

4 Risk Assessment

As a preliminary step, it was decided to elaborate the first urban risk scenario for the residential building stock, considering the territory affected by a fallout of tephra and earthquake shaking. In a more advanced phase of the PANACEA project, our analyses will be extended to include lava flow hazards and other exposed elements, such as road network, power network and people's health.

4.1 Single Risk

As for earthquakes, the probabilistic damage distribution was evaluated for the expected intensity value equal to I_{EMS} VII, with a return period of 78 years, equally distributed over the considered area. As a result, the average annual number of heavily damaged buildings is 0.39, which of unusable buildings is 2.6.

Damage to the building roofs due to ash accumulation is calculated by assuming a load equal to 200 kg/m^2 and 300 kg/m^2 (Scollo et al., 2013). Since the distribution of roofs in vulnerability classes was not locally characterized, the hypothetical distribution "Median roofing stock" was assumed, according to Spence et al. (2005), to better

reproduce the real distribution observed in the field. As a result, the number of buildings with complete roof collapse and severe damage ranges from 18 to 36%, respectively.

4.2 Multi Risk

The multi-risk evaluation is complex because of the interaction among single risks, such as both independent events and cascading effects, e.g. when one event triggers another one (Marzocchi et al., 2012).

Analyzing the interaction of the effects caused by the accumulation of ashes and the occurrence of the earthquake, according to Zuccaro et al. (2008), a threshold value of 300 kg/m^2 of ash is needed to weaken the resistance of the most vulnerable buildings affected by the seismic event. In particular, those with class A vulnerability will behave as if affected by an additional degree (+1) of intensity. It is challenging to foresee larger ash accumulations in this area, such as weakening other classes of buildings.

5 Concluding Remarks

The theme of the multi-risk in a complex and highly active volcano such as Etna being the new frontier to be developed. Although the PANACEA project started just one year ago (April 2021), it has demonstrated the actual chance of aggregating research groups working on different themes. Even if Etna is not among the most dangerous volcanoes, the first estimates show that the risk is significant due to the dense urbanization of the area and the interaction of different hazards.

Lastly, an adaptive risk model was conceived to consider the full range of potential hazards (such as fires, floods, health and regional earthquakes) that may interact with the prevailing ones (see, for example, Azzaro et al., 2023). Moreover, a flexible model can adopt different loss estimation methods and implement the area of analysis and procedures to make the risk estimation procedure ordinary.

Acknowledgements This work was carried out within the PANACEA project that benefited from funding provided by the MIUR (Ministero Istruzione Università e della Ricerca)—Decreto MIUR 1118 del 04/12/2019, within the Pianeta Dinamico project. We acknowledge A. Torrisi of the Department of Civil Protection of Sicily (DPCR) for providing the 2002 AeDES data.

References

Azzaro, R., D'Amico, S., Esposti Ongaro, T., Ganci, G., Garcia, A., Scollo, S., Aliotta, M., Behncke, B., Bevilacqua, A., Bilotta, G., Branca, S., Cassisi, C., Coltelli, M., Del Carlo, P., de Michieli Vitturi, M., Di Roberto, A., Lodato, L., Mereu, L., Prestifilippo, M., Proietti, C., Sandri, L., Tuvè, T., Zuccarello, F., Cappello, A. (2023). Toward a multi-hazard assessment at Etna volcano (Italy): the PANACEA project. In: A. Malheiro, F. Fernandes, H. I. Chaminé (Eds.), *Advances in natural hazards and volcanic risks: Shaping a sustainable future, Proceedings of the 3rd International Workshop on Natural Hazards (NATHAZ'22), Terceira Island - Azores 2022*, ASTI Springer Series, Cham (this volume)

Garcia-Aristizabal, A., Gasparini, P., Uhinga, G. (2015). Multi-risk assessment as a tool for decision-making. In: S. Pauleit, A. Coly, S. Fohlmeister, et al. (Eds.), *Urban Vulnerability and Climate Change in Africa. Future City*, vol 4, (pp. 229–258). Cham: Springer

Grünthal, G. (1998). European macroseismic scale 1998 (EMS-98). In: *Cahiers du Centre Européen de Géodynamique et de Séismologie*, Vol. 15. Luxembourg: Conseil de l'Europe

ISTAT (2011) 15° Censimento generale della popolazione e abitazioni. Retrieved February, 2022, from http://dati-censimentopopolazione.istat.it/Index.aspx?lang=it

Jenkins, S. F., Spence, R. J. S., Fonseca, J. F. B. D., Solidum, R. U., & Wilson, T. M. (2014). Volcanic risk assessment: Quantifying physical vulnerability in the built environment. *Journal of Volcanology and Geothermal Research, 276*, 105–120.

Lagomarsino, S., Cattari, S., & Ottonelli, D. (2021). The heuristic vulnerability model: Fragility curves for masonry buildings. *Bulletin of Earthquake Engineering, 19*(8), 3129–3163.

Martí, J., Aspinall, W. P., Sobradelo, R., Felpeto, A., Geyer, A., Ortiz, R., Baxter, P., Cole, P., Pacheco, J., Blanco, M. J., & Lopez, C. (2008). A long-term volcanic hazard event tree for Teide-Pico Viejo stratovolcanoes (Tenerife, Canary Islands). *Journal of Volcanology and Geothermal Research, 178*(3), 543–552.

Marzocchi, W., Garcia-, A., Gasparini, P., Mastellone, M. L., & Di Ruocco, A. (2012). Basic principles of multi-risk assessment: A case study in Italy. *Natural Hazards, 62*(2), 551–573.

Neri, A., Aspinall, W. P., Cioni, R., Bertagnini, R., Baxter, P. J., Zuccaro, G., Andronico, D., Barsotti, S., Cole, P. D., Esposti, T., Hincks, T. K., Macedonio, G., Papale, P., Rosi, M., Santacroce, R., & Woo, G. (2008). Developing an event tree for probabilistic hazard and risk assessment at Vesuvius. *Journal of Volcanology and Geothermal Research, 178*(3), 397–415.

Pomonis, A., Spence, R., & Baxter, P. (1999). Risk assessment of residential buildings for an eruption of Furnas Volcano, São Miguel, the Azores. *Journal of Volcanology and Geothermal Research, 92*(1–2), 107–131.

Rosti, A., Del Gaudio, C., Rota, M., Ricci, P., Di Ludovico, M., Penna, A., & Verderame, G. M. (2021). Empirical fragility curves for Italian residential RC buildings. *Bulletin of Earthquake Engineering, 19*(8), 3165–3183.

Scollo, S., Coltelli, M., Bonadonna, C., & Del Carlo, P. (2013). Tephra hazard assessment at Mt. Etna (Italy). *National Hazards and Earth System Sciences, 13*, 2945–2981.

Spence, R., Kelman, I., Petrazzuoli, S., & Zuccaro, G. (2005). Residential buildings and occupant vulnerability to Tephra fall. *National Hazards and Earth System Sciences, 5*(4), 1–18.

Torrisi, A. (2018). Esiti di agibilità e danno nell'emergenza sismica (schede AeDES) in occasione dei terremoti etnei del 2002 e 2008. Regione Siciliana, Dipartimento della Protezione Civile, Servizio Rischio Sismico e Vulcanico S.03, Nicolosi, Italy

Zuccaro, G., Cacace, F., Spence, R. J. S., & Baxter, P. J. (2008). Impact of explosive eruption scenarios at Vesuvius. *Journal of Volcanology and Geothermal Research, 178*(3), 416–453.

Zuccaro, G., De Gregorio, D. (2019). Impact assessments in volcanic areas: the Vesuvius and Campi Flegrei cases studies. *Annales Geophysicae*, *62*(1), doi: https://doi.org/10.4401/ag-7827

The Role of the Individual in Successful Disaster Management in *Pre-industrial* Societies: The Cases of Southern Italy and the Azores

Angus Duncan, Rui Coutinho, David K. Chester, Nicolau Wallenstein, Stefano Branca, and Alessandra Lotteri

Abstract

We contend that the leader was often the key actor in determining whether responses to disasters were successful in the *pre-industrial* societies of Southern Italy and the Azores (Portugal). We examine how leaders emerged and the ways in which they operated in the context of two similar, but in detail, very different societies shaped by a common Catholic ethos.

Keywords

Volcanoes • Earthquakes • Responses • Leadership • S. Italy • Sicily • Azores

1 Introduction

Gilbert White drew a distinction between *pre-industrial* and more economically developed *industrial* societies in the ways in which they respond to environmental disasters (White, 1974). White recognised that in *pre-industrial societies*, leadership by an individual is often the key factor in determining the success of responses to disasters, and this is exemplified by the situation in Southern Italy and the Azores. In Italy and Portugal, change from *pre-industrial* to *industrial* responses was gradual. In Southern Italy, State control over disaster management is usually dated from the 1908 Messina earthquake and, with respect to volcanic eruptions, to the 1928 destructive eruption of Etna which destroyed the town of Mascali. Earlier emergencies in the late nineteenth and early twentieth centuries show the increasingly important role of the State. For instance, responses to the 1906 eruption of Vesuvius were transitional. Whilst still being classifiable as *pre-industrial*, responses exemplified for the first time a major relief effort on the part of central government in Rome and also involved an international dimension, with moral empathy and financial support from abroad.

In Portugal, a powerful centralised political system emerged during the late eighteenth century associated with the dictatorship of Marquês de Pombal and caused the State to assume an atypical role in what was otherwise still a *pre-industrial* society, with the effects of centralised disaster and post-disaster planning being felt, not only in Lisbon and its region following the 1755 earthquake but also in the Algarve. Following the dismissal of Pombal in 1777, Portugal reverted once more to a typical *pre-industrial* society with respect to disasters.

2 Examples of Leadership in *Pre-Industrial* Southern Italy

The 1669 eruption This was the largest historical eruption of Etna and its lava field impacted an area of ca.40 km^2. It was also the widest and longest historic lava field of Etna and affected the highly urbanised and agriculturally productive area on the lower southeast flank of Etna. Volcanic eruptions damaged many agricultural villages, and earthquakes plus lava devastated 8 large and 14 smaller settlements, including part of the city of Catania (Branca et al., 2015). In the 1669 eruption, the Spanish Viceroy of Sicily was based in Palermo. The city authorities were unable to cope with the unfolding emergency, and the government in Palermo was

A. Duncan (✉) · D. K. Chester
Department of Geography & Planning, University of Liverpool, Liverpool, UK
e-mail: amduncan1951@gmail.com

R. Coutinho · N. Wallenstein
IVAR, Universidades Dos Açores, Ponta Delgada, Azores, Portugal

S. Branca
Istituto Nazionale di Geofisica e Vulcanologia, Osservatorio Etneo, Catania, Italy

A. Lotteri
Department of Geography & Environmental Science, Liverpool Hope University, Liverpool, UK

A. Malheiro et al. (eds.), *Advances in Natural Hazards and Volcanic Risks: Shaping a Sustainable Future*, Advances in Science, Technology & Innovation, https://doi.org/10.1007/978-3-031-25042-2_8

forced to dispatch cavalry in order to quell lawlessness. The Viceroy appointed an administrator with wide powers, the Sicilian aristocrat Prince Stefano Reggio (1610–1678), to manage the emergency. When Reggio arrived on 18 April with funds and troops, the city was soon pacified. He erected barracks for refugees to the north of the city, salvaged the city archives and organised supplies. Poorer people were temporarily re-housed, and Reggio used political skill in negotiating with and reconciling the conflicting interests of local elites and those of the central authorities. City walls were reinforced, gates blocked and, where lava did penetrate, barriers were constructed (Branca et al., 2015).

The 1693 Val di Noto earthquake In 1693, Catania had to face a second major catastrophe. An earthquake on 11 January had an estimated magnitude (M) of 7.4 and caused devastation across the Etna region. Catania was reduced to rubble, with SE Sicily and Malta also being affected (Branca et al., 2015). In Catania, the 1693 earthquake struck parts of the mediaeval city that had survived the 1669 eruption. At the time Catania had an urban form typical of a Mediaeval southern European city, with a network of narrow streets and a high-density built-up area surrounded by a system of defensive walls. The 11 January earthquake impacted Catania whose buildings, already weakened by an earlier earthquake two days before, collapsed. In the week following the earthquake, there was another breakdown in law and order and the unplanned evacuation of much of the city's population. The total death toll in Sicily exceeded 50,000 and in Catania estimates range from a probable 11,000 to a maximum of 20,000, out of a total population of 23–27,0000 (Branca et al., 2015). The initial response was the construction of temporary shelters outside the walled city to avoid disease because thousands of bodies remained buried under rubble. The Viceroy sent supplies, troops and an administrator, Giuseppe Lanza, Duca di Camastra, to co-ordinate both the immediate response and longer-term reconstruction across southeast Sicily. Immediately, he exempted the worst affected areas from taxation and drafted in labour to clear the rubble. In Catania, his subsequent initiatives included the provision of food; the re-establishment of law and order; prevention of epidemic disease, by recovering and interring bodies from within the ruined city; and locating doctors who formed an emergency health service. It is because of these actions that before the end of the year many evacuees had returned to the city. The Duke planned for reconstruction across the devastated region, and Catania was rebuilt on the same site but with a new plan. The newly planned city was notable for its wide streets, aligned in a 'grid pattern', and the insertion of squares. By 1695, Catania was under local control, but the urban plan plus the desire of local elites to 'build back better' ensured that a fine city was constructed, with new districts being built outside the former city walls, mainly to the north and towards the sea. By 1737, Catania's population had reached 26,000—probably higher than its pre-earthquake total.

The 1631 eruption of Vesuvius In the seventeenth century, Naples was the major city and principal port in Spanish-ruled Southern Italy. For many years, Naples had proved difficult to rule and when the new Spanish Viceroy, the Count of Monterrey, arrived in May 1631, he was confronted with the need to maintain a working relationship with powerful elites, especially those of the ecclesiastical hierarchy led by Cardinal Archbishop Boncompagni. The eruption of December 1631 came as a surprise to the people in Naples. The 1631 event was the largest eruption of Vesuvius since AD 79. The Viceroy was forced to cope with the demands of the emergency whilst at the same time balancing the concerns of those who sought, on the one hand, to make sense of the catastrophe in theological terms—particularly by embracing a theodicy of divine punishment of sins—and, on the other, a desire to respond to the emergency through policies of mitigation based on empirical observation. The Viceroy achieved this balance using political skill and organisation ability. Despite more than 200 contemporary accounts of the 1631 eruption, it was only in the 1990s that, by reconciling historic records with both field evidence and what at the time were new understandings of Plinian eruptive processes (Rosi et al., 1993), a new understanding of events emerged. Previously, it was assumed that rapid lava flow emplacement was responsible for the devastation, but highly destructive Pyroclastic Density Currents (PDCs) are now viewed as being critical, which makes Monterrey's achievements even more significant. After a month of warnings, including felt earthquakes, Vesuvius erupted on 16 December with a Plinian column rising to a height of 21 km, with the whole area being affected by earthquakes. On 17, there were loud explosions, the column collapsed and PDCs swept down the southern flanks causing widespread destruction. After 48 h, activity waned and the eruption ended in January 1632. The eruption killed ca. 4,000 people, devastated productive land and caused major damage to towns and villages on the flanks of the volcano. The total financial loss was estimated at 25 million ducats. Led by the Cardinal Archbishop, the principal response of the clergy was to combine the provision of shelter, food for the destitute and the provision of alms together with liturgical actions to appease divine wrath. Several processions were organised, involving sacred relics, including the head and a phial of blood from the martyred San Gennaro, patron saint of Naples. These processions were supported by the Viceroy. The Viceroy committed himself to remain at his post and if necessary die with his people, forcing the Cardinal Archbishop and senior clergy to do likewise. He also organised the supply of provisions to stricken communities

and established a *Public Health Commission* to assess the impact of the eruption and help clear the roads and bury the dead.

3 Leadership in the Azores During *Pre-Industrial* Times

Located 1,500 km west of Portugal, isolation is a feature of the geography and history of the Azores, which has forced the islands to cope with using their own resources of people and matériel until the middle of the twentieth century. All islands are volcanic, but since they were first settled by the Portuguese in the fifteenth century, only Faial, Pico, São Jorge, Terceira and São Miguel have been affected by onshore eruptions. Major earthquakes have affected these islands together with Graciosa. In the *pre-industrial* era, the Azores were particularly isolated. Before the arrival of steamships and the telegraph in the nineteenth century, communications with Europe and the Americas took weeks or months. This meant that for most of the *pre-industrial* era the islands depended on local leadership. Initially, the Azores were ruled by hereditary *capitães* (i.e. captains), but in the eighteenth century Marquis de Pombal reorganised the administration, and by 1835 this comprised three districts: Angra Do Heroismo (capital of Terceira, with responsibility for São Jorge and Graciosa); Ponta Delgada (on São Miguel, also in charge of Santa Maria) and Horta (capital of Faial and administering Pico, Flores and Corvo). Each district was ruled by a governor who was assisted by a *Junta Geral* (general council).

1522 Vila Franca do Campo Earthquake Vila Franca do Campo, then the capital of São Miguel island, was destroyed in what was the most destructive earthquake to have affected the archipelago. A combination of seismic activity and the triggering of a destructive landslide killed ca.3,500–5,000 inhabitants in Vila Franca do Campo and other settlements, mainly along the south coast (Chester et al., 2022). The Captain, Rui Gonçalves da Câmera II, proved to be the most effective leader, with a new capital being established at Ponta Delgada. He also planned for Vila Franca to be rebuilt.

1841 Terceira Earthquake The best recorded example of impressive leadership in the *pre-industrial* era is that of José Silvestre Ribeiro (1807–1891) and his role in managing the aftermath of the 1841 earthquake on Terceira. This earthquake caused 2,100 houses to collapse with the greatest damage being centred on Praia da Vitória (Chester et al., 2022). At the time, José Ribeiro was General Administrator of the District of Angra do Heroísmo 1839–1844. Amongst his actions were the establishment of local relief committees (*Comissões de Soccorros*), chaired by parish priests who knew the people; ensuring that contractors 'built back better' by controlling the quality of re-development; responding to the needs of the poor; obtaining funds, not only from Horta and other districts but also from the central government in Lisbon and expatriate communities in Brazil and Europe. Ribeiro was interested in both architectural and urban planning and developed a distinctive style in which reconstructed buildings were symmetrical, uniform and proportional. Ribeiro hoped in vain that the lessons learnt from this disaster would inform subsequent emergencies.

1672–73 Pico Eruption An earlier example of firm leadership occurred after the 1672/3 eruption on Faial when it became clear that, as a result of large areas of land being rendered sterile by lava inundation, the island could no longer support its pre-eruption population. It was concluded that the excess population could not be supported, and its unnamed leader successfully petitioned Lisbon to support the emigration of approximately 200 people to Brazil (Chester et al., 2022).

4 Discussion and Concluding Remarks

Common features emerge in the ways in which leaders successfully managed disasters in the Azores and Southern Italy: **First**, a desire for human betterment which involved a personal obligation to work tirelessly for the people. Examples have been quoted of leaders, who not only successfully handled the challenges that occurred in the immediate aftermath of disasters but also initiated post-disaster recovery. The **second** feature is that effective leadership displayed empathy with the people affected. Leaders were not just aware of material requirements but also displayed well-honed understanding of local culture. The **third** element is the successful direction of a post-disaster response. Effective leaders, **fourth**, displayed political acumen and were able to work with and, indeed, liberate the latent potential found within local elites.

As discussed above, the development of *industrial responses* was transitional and for much of the twentieth century, notwithstanding state control, responses were in many respects still ad hoc affairs. Under such circumstances, there was often a role for an effective individual leader. In Southern Italy during the 1944 eruption of Vesuvius, Prof. Imbò (scientific monitoring) and Colonel Kincaid (Allied Control Commission) played critical roles in ensuring an effective response under difficult wartime conditions. This was also the case in the 1957–58 Capelinhos eruption on Faial island (Azores), where the Governor, António Freitas Pimentel, put in place an effective response in disaster management during and following the eruption (Chester et al., 2022). By the end of the twentieth century, proactive policies in disaster planning were extant, and hazard assessment, training and monitoring with effective civil defence procedures were in place. There is not the same need

for individuals to take the initiative and develop procedures in response to an eruption or earthquake, but there is still a requirement for disaster managers to display administrative skills, empathy with the people affected and, not least, political insight and judgement.

References

Branca, S., Azzaro, R., De Beni, E., Chester, D., & Duncan, A. (2015). Impacts of the 1669 eruption and the 1693 earthquakes on the Etna Region (Eastern Sicily, Italy): An example of recovery and response of a small area to extreme events. *Journal of Volcanology and Geothermal Research, 203*, 25–40.

Chester, D. K., Duncan, A. M., Coutinho, R., & Wallenstein, N. (2022). *Earthquakes and Volcanic activity on islands history and volcanic perspectives from the Azores*. Routledge.

Rosi, M., Principe, C., & Vecci, R. (1993). The 1631 Vesuvius eruption. A reconstruction based on historical and stratigraphical data. *Journal of Volcanology and Geothermal Research, 58*, 151–182.

White, G. F. (1974). Natural hazards research: Concepts, methods, and policy implications. In G. F. White (Ed.), *Natural Hazards: Local, National, Global* (pp. 3–16). Oxford University Press.

Historical Volcanism as a Source of Knowledge to Assess the Vulnerability of Population Settlements in the Azores: Some Thoughts

Fernando Pereira, Ana Oliveira, Ana Botelho, Paula Cabral, Luísa Magalhães, and Tomás Medeiros

Abstract

There are records of more than two dozen volcanic eruptions since the settlement of the islands of the Archipelago of the Azores, some submarine, but many on land, subaerial. The recorded eruptions are centred on or close to São Miguel, Terceira, São Jorge, Pico and Faial islands. For the populations, eruptions are a source of concern and fear, transforming the landscape radically with the coverage of built elements and fields by ash deposits and other projected materials or lava flows, destroying their belongings and social environment. Nevertheless, over time, these new lands become sources of materials, new fertile lands, new geological and landscape elements with scientific and tourist potential and, consequently, urban reoccupation. This work starts with an analysis of the historical eruptions recorded in the Azores, types of activity and affected areas and seeks to assess the vulnerability of current populations to similar situations prospectively.

Keywords

Volcanic hazards • Historical volcanism • Azores vulnerability • Impacts of volcanic eruptions

1 Introduction

To live in volcanic areas, and more significantly on volcanic islands, is to live, even unconsciously, with the presence that an eruption can occur, as well as significant changes in its social and environmental context. At a time when communities, in general, depend heavily on communications and transport networks, for global mobility of people and products, with special emphasis on supply chains, volcanic eruptions can cause significant disturbances in this model of social sustainability, either by direct changes in the places themselves, either indirectly, by the dispersion of ash and dust in the atmosphere, which affects air transport, or by ejected materials, which can affect the operation of infrastructures and land and sea transport routes.

Even those who have not experienced any volcanic eruptions are a constant presence, either because of the marks on the landscape, of which some receive very specific local names and the cultural manifestations preserved and passed on from generation to generation.

2 Methods and Concepts

For the present work, an analysis was made of scientific works from the last three decades on historical volcanic activity on the Azores islands, with a special focus on the impacts on critical infrastructure and the social structure of communities. Moreover, as a way of framing how populations have responded to crises, it stands out that three terms and two cultural manifestations with terminology and local presence in popular culture show how populations adapt and reinforce their resilience:

"***Fajã***"—Area of low land, usually by the sea, created by lava flows (*lavic fajã*) or by materials from the collapse of the overlying slopes (*detritic fajã*).

"***Lagido***"—Area by the sea, characterized by smooth or wavy rock surfaces resulting from the flow of Pahoehoe lava.

"***Mistério***"—It corresponds to basaltic lava flows of type *aa* or *pahoehoe*, which cover extensive fields.

"***Romeiros***"—The pilgrims of São Miguel who, in Lent, in groups of several people, go around, passing by the churches and chapels devoted to Our Lady and which has its

F. Pereira (✉) · A. Oliveira · A. Botelho · P. Cabral · L. Magalhães · T. Medeiros
Secretaria Regional do Turismo, Mobilidade e Infraestruturas, Ponta Delgada, Portugal
e-mail: fdpereira@sapo.pt

A. Malheiro et al. (eds.), *Advances in Natural Hazards and Volcanic Risks: Shaping a Sustainable Future*, Advances in Science, Technology & Innovation, https://doi.org/10.1007/978-3-031-25042-2_9

origin according to current conviction in the earthquakes and volcanic eruptions of the sixteenth century.

"***Império dos Nobres***"—It is the vow instituted by the people of Faial island during the volcanic eruption of 1672. It was then assumed the perpetual commitment to annually organize a religious act consisting of procession, mass and distribution of alms to the population.

3 Results

3.1 Historic Overview

The first historical record of an eruption in the Azores refers to the one that occurred at the Furnas Volcano, with its final phase between 1439 and 1443, contemporaneous with the beginning of the settlement (Queiroz et al., 1995). Since then, about thirty eruptive events have been recorded (Fig. 1), causing several human victims and destroying built structures and productive lands in the islands of S. Miguel, Terceira, S. Jorge, Pico and Faial.

Many of the recorded eruptions were of submarine origin (Table 1). Nevertheless, some of them are well present in people's memories and stories, such as the eruptions of 1963 and 1964, in which people from the islands of Faial, Pico and S. Jorge, at night, saw the plume of fire over the sea, or the emergence of a new island, in 1811, visible from S. Miguel, Ilha Sabrina, which disappeared in a short time.

In recent times, the Capelinhos Volcano, 1957–58, whose first manifestation was bubbling and jets of water in the ocean, leaving an extensive area covered by projection materials, burying houses, fields and roads (Silva, 2005), is still the primary reference.

However, looking further back, several eruptions had exclusively subaerial origin (Table 2), which highlights what happened in 1563, when the Fogo volcano in S. Miguel island began with almost continuous tremor and created a high black column of fire and ash that later fell to the earth, causing no deaths. However, some people were left with burns (Silveira, 2002), and three days later, at Pico do Sapateiro or Queimado, another eruption began, first with ejections of pyroclastic material, but changed characteristics,

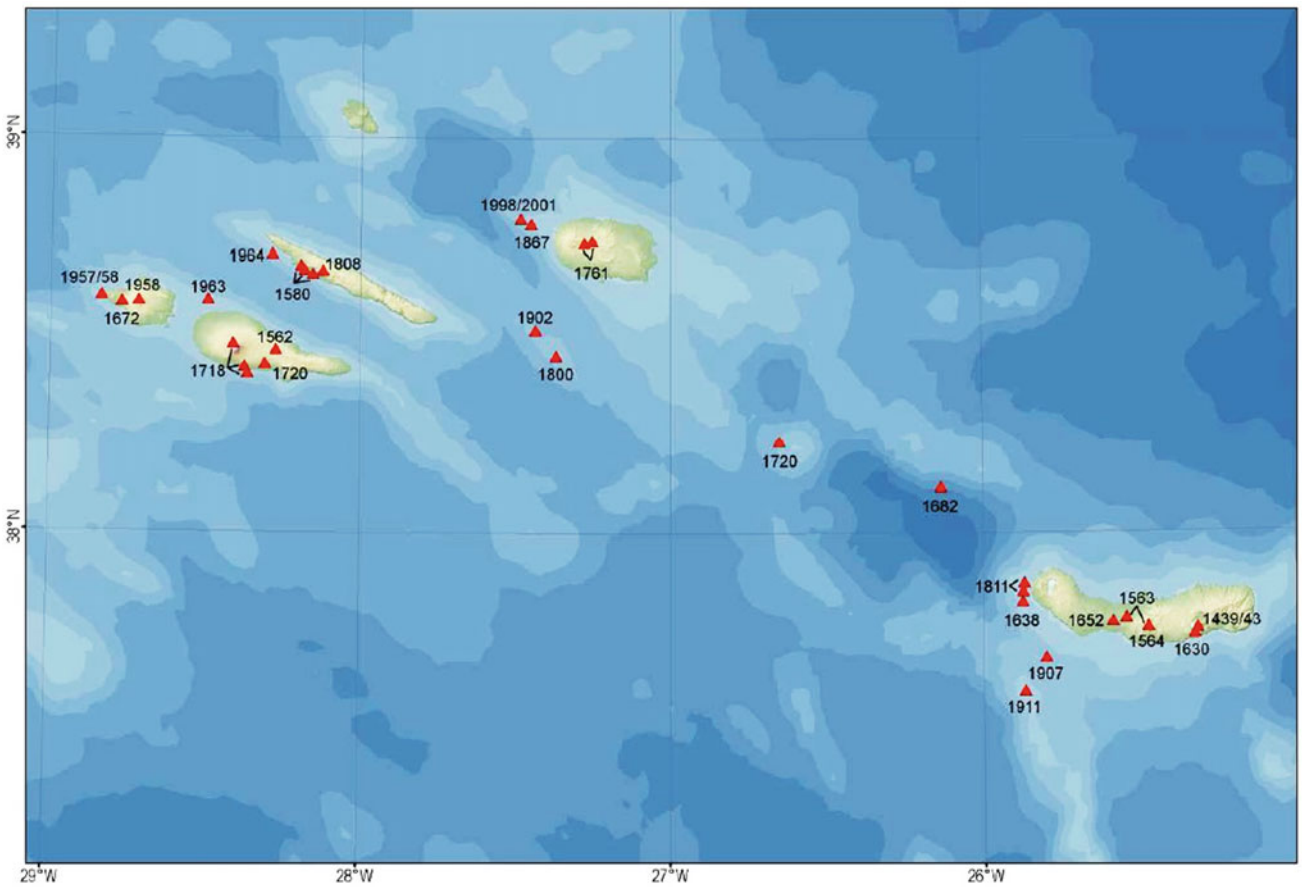

Fig. 1 Historical eruptions in Azores Archipelago area (Medeiros, 2009)

Table 1 Historic eruptions in Azores (submarine origin)

Year	Location	Eruptive type
1638	Off Ponta da Candelária, S. Miguel	Surtseyan
1682	Off Mosteiros, S. Miguel	
1720	D. João de Castro Bank	Surtseyan
1800	Off Ponta do Topo, S. Jorge	
1811	Off Ponta da Ferraria, S. Miguel	Surtseyan
1867	Off Ponta da Serreta, Terceira	
1902	Off Ponta do Topo, S. Jorge	
1904	South of Ponta da Ferraria, S. Miguel	
1907	Near the south coast, S. Miguel	
1911	Monaco Bank	
1957/58	Capelinhos, Faial	Surtseyan, Hawaiian and Strombolian
1963	Off Cachorro, Pico	
1964	West of Velas, S. Jorge	
1981	Monaco Bank	
1998/01	WNW of Ponta da Serreta, Terceira	

Modified from Madeira (2005) and Medeiros (2009)

Table 2 Historic eruptions in Azores (subaerial origin)

Year	Location	Eruptive type
1439–43	Pico do Gaspar, S. Miguel	Subplinian and Phreatomagmatic
1562/63	Cabeços do Fogo, Pico	Hawaiian and Strombolian
1563	Pico Queimado, S. Miguel	Hawaiian
1563/64	Lagoa do Fogo, S. Miguel	Plinian and Phreatomagmatic
1580	Ribeira do Almeida and other vents, S. Jorge	Hawaiian and Strombolian
1630	Lagoa Seca-Furnas, S. Miguel	Subplinian and Phreatomagmatic
1652	Picos de João Ramos and other vents, S. Miguel	Vulcanian
1672/73	Cabeço do Fogo and Pincarito, Faial	Hawaiian and Strombolian
1718	Lomba de Fogo and other vents, Pico	Hawaiian and Strombolian
1720	Cabeços do Fogo, Pico	Hawaiian and Strombolian
1761	Picos das Caldeirinhas and other vent, Terceira	
1761	Pico Vermelho, Terceira	Hawaiian and Strombolian
1808	Pico do Pedro and other vents, S. Jorge	Hawaiian, Strombolian and Phreatomagmatic
1957/58	Capelinhos, Faial	Surtseyan, Hawaiian and Strombolian
1958	Caldeira, Faial	Phreatic explosion

Modified from Madeira (2005) and Medeiros (2009)

and a stream of fire started to flow and reached the sea (Silveira, 2002), and these are the eruptions that will give rise to the "*Romeiros*".

Furthermore, those that took place on Pico Island, in 1718, at Lomba de Fogo, Cabeço de Cima and Cabeço de Baixo generated lava flows to both flanks of the central mountain, cutting terrestrial routes, almost dividing the island into two parts (Fig. 2), originating two "*Mistérios*".

3.2 Impacts on Critical Infrastructures and Social Structures

The eruption of the Eyjafjallajökull volcano in Iceland in 2010 created an extensive plume of ash in the atmosphere (Fig. 3) which affected air traffic, leading to the cancellation of many flights, including to and from the Azores and even the closure of many airports in Europe.

Other infrastructures such as communication networks, roads and seaports are also vulnerable, and there are reports about a submarine cable rupture associated with a submarine eruption off the west coast of S. Miguel in 1904, and ruptures of submarine cables that occurred in the area S. Jorge channel in the beginning of 1964 are also associated with a submarine eruption (Madeira, 1998). Also concerning critical infrastructure, the first damages near the Capelinhos Volcano were the destruction of windows and the perforation of roofs in constructions by projected materials (Silva & Gaspar, 2007) and the abandonment of fishing activities due to water toxicity (Cunha 1959; in Coutinho et al., 2017). In addition, the seaport of Capelo remained inoperative for some decades, covered by pyroclastic materials, and there were water sources and wells dried up (Silva, 2005).

One of the most decisive social impacts was the displacement of populations, followed by the emigration of about 5,000 people from the then-District of Horta to the United States of America (Coutinho et al., 2017), most of them from Faial island, representing a significant reduction in the active population of the island.

4 Discussion

There are several types of hazards associated with volcanic eruptions, depending on the volcano and the type of volcanism, and they can often coincide. Potential hazards are ashfalls, pyroclastic flows, lava flows, volcanic gases, electrical storms, lahars, mixtures of volcanic ash, blocks and water formed in volcanoes, landslides, and hydrothermal eruptions and eventually tsunamis.

Looking at the historical records, volcanic events did occur in all centuries, and there were events of almost all types and in all active areas. So, there is no standard; therefore, almost all potential hazards could be expected. So, the concept of "Build Back Better" can not only be an essential tool to reduce disaster risk and implement measures to prevent new types of risk (Pereira et al., 2020), but it also aims to reinforce the resilience of populations by preserving elements of their cultural and social identity.

5 Concluding Remarks

Unlike other events associated with natural disasters, volcanic eruptions usually have impacts that are reduced in terms of victims but very high in individual and social terms due to the prolonged time of occurrence or the changes in the surrounding landscape communities and their livelihoods.

Even considering the great technological development and the globalization of communications and supply chains, volcanic eruptions can disrupt their functioning, requiring local response capacity. Therefore, it will be essential to

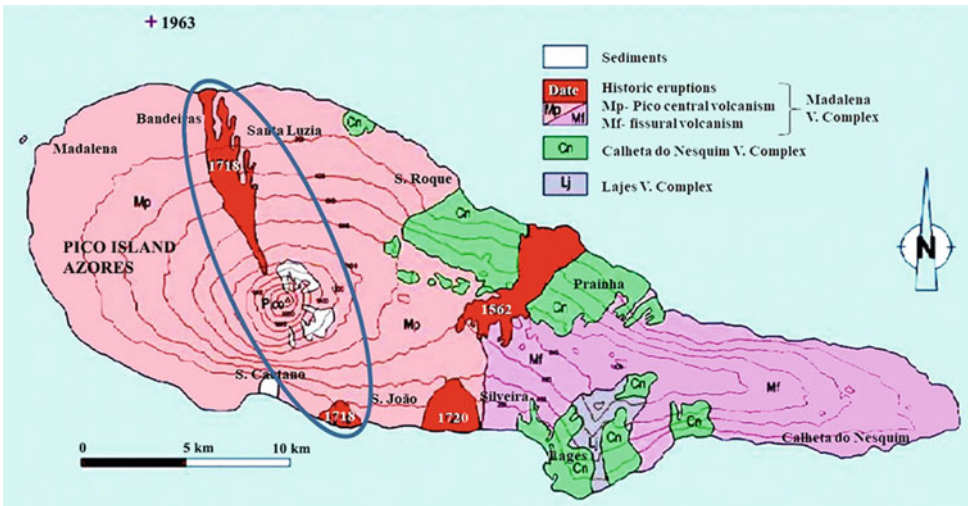

Fig. 2 Volcanologic map of Pico Island showing in red the four "*mistérios*" or "mysteries" (adapted from Madeira, 2005). The blue ellipsis: 1718 eruptions

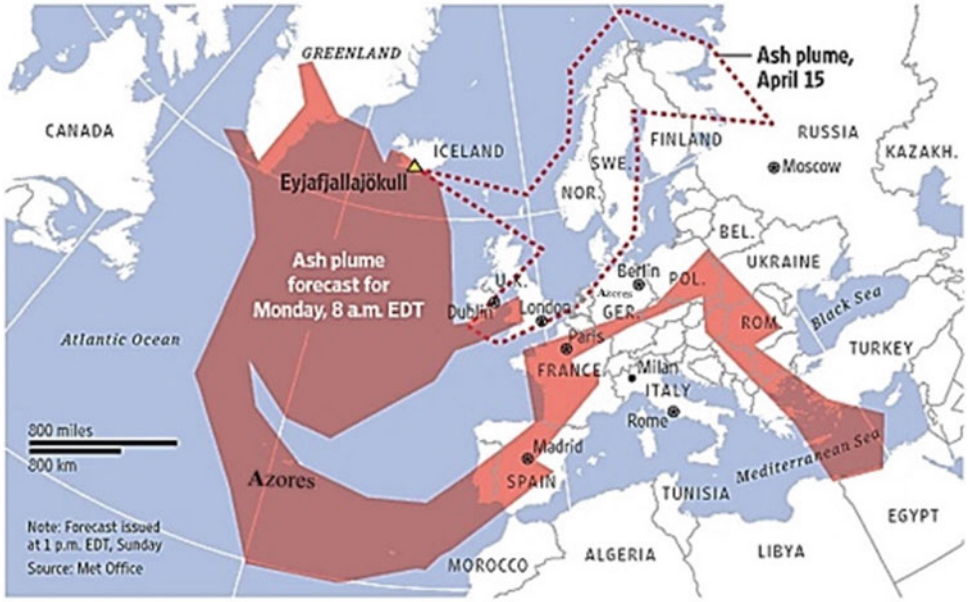

Fig. 3 The extent of the ash cloud across Europe directly after the first explosive eruption of the Eyjafjallajökull volcano (adapted from IB Geography: www.thegeographeronline.net, last accessed 2022-02-22)

have various basic infrastructures scattered around each island to support emergency actions.

Acknowledgements We want to thank Ana Carvalho, Regional Secretary for Public Works and Communications, and Berta Cabral, Regional Secretary for Tourism, Mobility and Infrastructure, of the Government of the Azores, for the conditions provided to develop this work and for all the co-workers who supported us and, even indirectly, contributed to the final result.

References

Coutinho, R., Chester, D., Wallenstein, N., & Duncan, A. M. (2017). Impactes a curto e longo prazo da erupção dos Capelinhos e respostas à crise. *Boletim do Núcleo Cultural da Horta, 26*, 557–589.

Madeira, J. (1998). *Estudos de neotectónica nas ilhas do Faial, Pico e S. Jorge: uma contribuição para o conhecimento geodinâmico da junção tripla dos Açores*. Ph.D. thesis, Lisbon University, Lisbon.

Madeira, J. (2005). The volcanoes of Azores island: A world-class heritage. *Field Trip Guide Book of IV International Symposium ProGEO on the Conservation of the Geological Heritage*, organized by European Association for the Conservation of the Geological Heritage and Earth Sciences Center of University of Minho, Braga (LATTEX ed.).

Medeiros, A. (2009). *Base de dados para a divulgação da Geologia dos Açores*. M.Sc. dissertation, University of the Azores, Ponta Delgada.

Pereira, F., Oliveira, A., Santos, M., Aguiar, M., & Magalhães, L. (2020). Build back better: Rebuild to preserve. In F. Fernandes, A. Malheiro, H. I. Chaminé (Eds.), *Advances in natural hazards and hydrological risks: Meeting the challenge.* (pp. 101-104), ASTI Springer Series, Cham

Queiroz, G., Gaspar, J., Cole, P., Guest, J., Wallenstein, N., Duncan, A., & Pacheco, J. (1995). Erupções Vulcânicas no Vale das Furnas (ilha de S. Miguel, Açores) na primeira metade do Sec XV. *Açoreana, 8*(1), 159–165.

Silva, M. (2005). *Caracterização da sismicidade histórica dos Açores com base na reinterpretação de dados macrossísmicos: contributo para a avaliação do risco sísmico nas ilhas do Grupo Central*. M. Sc. dissertation, University of the Azores, Ponta Delgada.

Silva, M., & Gaspar, J. (2007). Seismic activity associated to volcanic events. The Capelinhos Volcano case-study. *Boletim do Núcleo Cultural da Horta, 16*, 45–59.

Silveira, D. (2002). *Caracterização da sismicidade histórica da ilha de S. Miguel com base na reinterpretação de dados macrossísmicos: contributo para a avaliação do risco sísmico*. M.Sc. dissertation, University of the Azores, Ponta Delgada.

A Proposal for Systematisation of Vulnerability Elements and Parameters in Volcanic Risk Assessment

Ana Malheiro, João Luis Gaspar, Gabriela Queiróz, Teresa Ferreira, Paulo Amaral, Filipe Marques, and Letícia Cunha

Abstract

This work is part of the broader context of volcanic risk assessment, focusing on the identification, characterisation, and systematisation of the vulnerability elements and parameters to be considered for its determination. An extensive set of specialised bibliography was analysed to identify and characterise the various volcanic hazards (direct—lava flows, pyroclastic fall, pyroclastic flows and surges, lahars, and volcanic gases; and indirect—earthquakes, ground deformation, landslides, and tsunamis), and also the different elements of vulnerability (people, animals, all types of buildings, infrastructures, cultures, and all other economic activities). The global analysis allowed the identification and systematisation of vulnerability parameters to be built into a table in which general critical values are proposed, which can be used to determine vulnerabilities. Any analysis of this type must also include applying critical values specific to the area under study, considering each volcanic system's specificity. This methodology was applied to Terceira Island to simulate two basaltic volcanic eruptions.

Keywords

Volcanoes • Volcanic risks • Volcanic hazards • Vulnerability assessment

1 Introduction

Over time, natural hazards have been a permanent threat to humanity, annually causing high loss of human lives and substantial material damage. Its unpredictable, frequently sudden, and violent character determined an attitude of impotence by part of society when facing something considered inevitable.

From these facts stems the growing importance that the treatment of natural hazards, particularly the treatment of geological hazards, occupies or should occupy in the different planning stages of land use and environmental preservation. Furthermore, the regularity in the occurrence of catastrophic events requires a response from the entities involved in planning and those responsible for the safety of populations in the preparation and implementation of mitigation strategies appropriate to the hazards.

Due to its geodynamic and geographic context, the Azores archipelago has suffered the adverse effects of multiple geological hazards over the years. The frequency of these catastrophic events leads to the need for adequate mitigation strategies, including characterising the various hazards likely to occur and assessing vulnerabilities. In this context, defining a methodology that includes identifying parameters that can contribute to quantifying risk as objectively as possible is crucial.

2 Methodology

Assessing volcanic risk has two main components: identifying the volcanic hazards to which a given area is subject and recognising the vulnerable elements. In the present work, the elements of vulnerability for each volcanic hazard are identified and characterised, bearing in mind that the latter contain decisive specificities in this domain.

The lack of knowledge of many of the parameters that rule the phenomenon causing the disaster, or the structures'

A. Malheiro (✉) · P. Amaral · F. Marques · L. Cunha
Regional Laboratory of Civil Engineering of Azores (LREC), Ponta Delgada, Portugal
e-mail: Ana.MM.Malheiro@azores.gov.pt

J. L. Gaspar · T. Ferreira
Geosciences Department, Azores University, Ponta Delgada, Portugal

J. L. Gaspar · G. Queiróz · T. Ferreira
Institute of Volcanology and Risk Assessment, Azores University, Ponta Delgada, Portugal

A. Malheiro et al. (eds.), *Advances in Natural Hazards and Volcanic Risks: Shaping a Sustainable Future*, Advances in Science, Technology & Innovation, https://doi.org/10.1007/978-3-031-25042-2_10

behaviour and the population exposed to it, significantly hinders the analysis of vulnerabilities. Unfortunately, it appears that the existing data for this purpose are scarce and stem, fundamentally, from duly documented historical cases.

The analysis of direct and indirect volcanic hazards in this work allowed us to identify some measurable parameters for which critical values in terms of vulnerabilities were estimated based on data available in the bibliography. In some cases, it was possible to verify the frequency with which each of these hazards, with specific characteristics, occurs typically. On the other hand, the respective impact of the various vulnerability elements was identified for each hazard, which varies according to the parameters in some cases.

The main types of volcanic products to be taken into account for the calculation of vulnerabilities were considered as lava flows, pyroclastic falls, pyroclastic density currents (pyroclastic flows and surges), lahars, volcanic gases, and also the indirect hazards arising from the volcanic activity, such as earthquakes, soil deformation, landslides, and tsunamis.

As elements of vulnerability were considered people, animals, housing, commercial and industrial buildings, and all other constructions (e.g. hospitals, schools, and services), infrastructure (e.g. roads, bridges, airports, ports, and telecommunications), crops, and other economic activities.

The vulnerability of the same exposed element varies depending on the type of volcanic hazard. For each type of exposed element, the impacts of the various hazards were identified based on the analysis of occurrences described in the bibliography. This made it possible to define for each hazard which volcanological parameters should be considered and the respective critical values that can be used to assess vulnerabilities. The cases reported in the bibliography typically had the most significant impact or showed a specific particularity, so the proposed critical values should be understood only as limiting reference values. This research culminated in elaborating a summary table with critical values of a general nature (details in Malheiro, 2002). Please see Table 1.

To assess the vulnerabilities of a given region, the following steps were defined:

(a) concerning hazard analysis:
  - study and definition of its eruptive history;
  - identification of existing volcanic hazards;
  - characterisation of volcanic hazards, as well as the assessment of the frequency with which they occur and their magnitude;
  - characterisation of the type of the most probable event (MPE) and the most significant magnitude event (GME);
  - simulation of eruptions for each of the volcanic hazards in question, assuming the critical values for the MPE and the GME;

(b) concerning the exposed elements:
  - a survey of their physical, social, economic, cultural, and environmental reality;
  - identification of vulnerability elements;
  - characterisation of vulnerability elements in terms of exposure and behaviour;
  - mapping of vulnerability elements.

For each scenario, preferably using a geographic information system, overlapping the affected area by a given hazard with the elements of vulnerability allows for calculating the percentage of losses.

For each scenario, the general critical values must be considered (see Table 1), even though a detailed and specific analysis is carried out on the different characteristic parameters of the volcanic system under analysis.

The described methodology was applied to Terceira island with the simulation of two volcanic eruptions of Hawaiian and Strombolian (s.l.) type, whose location was defined based on the density of the volcanic vents mapped by Self (1974) for the last 20,000 years.

3 Results

The maximum slope model developed by Felpeto et al. (1996) was used to simulate the progression of lava flows. This model applies a Monte Carlo algorithm to calculate the possible paths for the flows based on a digital terrain model. In our study, two eruptive vents (F1 and F2) and two scenarios were considered: the worst situation for the range of most frequent cases reported in the bibliography (More Probable Event—MPE—General), and the most likely situation, given the values observed for the island (MPE—Region). In the case of basaltic pyroclastic fall, the same eruptive vents were considered, using dispersion values based on the isopachs traced by Self (1974) for scoria cones from Terceira Island. The maximum distances observed for each range of thickness of the deposits (200, 50, 25, and 10 cm) were determined through these isopachs.

Figure 1 shows the overlap of the area covered by lava flows and basaltic pyroclasts, taking the F1 vent as an example.

Table 1 Critical parameters of volcanic vulnerability materials: general character (details in Malheiro, 2002)

Volcanic phenomenon	Parameters		Critical values	Frequency	Danger	Impact	References
Lava flows	Low viscosities	Thickness	<20 m	Very frequent	Very high	Lava flows can cause the collapse or burying of all vulnerable elements in their passage and cause fires. However, as for people and animals and any movable property, vulnerability is usually low insofar as they can be evacuated promptly, given the generally low speeds of the lava flows	Walker (1973), Crandell et al. (1984), Fisher et al. (1997), Blong (1984)
			20–25 m		High		
			25–35 m		Moderate		
			35–50 m		Low		
			>50 m	Less common	Very low		
		Length	<10 km	Very frequent	Very high		
			10–15 km		High		
			15–20 km		Moderate		
			20–45 km		Low		
			>45 km	Less common	Very low		
	High viscosities	Thickness	<200 m	Very frequent	Very high		
			200–300 m		High		
			300–500 m		Moderate		
			500–800 m		Low		
			>800 m	Less common	Very low		
		Length	<3 km	Very frequent	Very high		
			3–5 km		High		
			5–8 km		Moderate		
			8–11 km		Low		
			>11 km	Less common	Very low		
Lahars	Thickness		<10 m	Very frequent	Very high	They can cause severe injury and death by burying or suffocating people and animals. The other elements of vulnerability can destroy by collapse, burying, displacement, or flooding	MacDonald (1972), Francis (1976) in Blong (1984), Baxter (2000)
			10–20 m		High		
			20–30 m		Moderate		
			30–40 m		Low		
			>40 m	Less common	Very low		
	Length		<20 km	Very frequent	Very high		
			20–50 km		High		
			50–100 km		Moderate		
			100–300 km		Low		
			>300 km	Less common	Very low		

(continued)

Table 1 (continued)

Volcanic phenomenon	Parameters		Critical values	Frequency	Danger	Impact	References
Surges	Length		<10 km	Very frequent	Very high	They cause death by asphyxiation, heat, severe burns, and throat and nostril irritations in people and animals. The remaining elements of vulnerability cause destruction by impact, collapse, burial, displacement, or fire	Crandell et al. (1984), Tilling (1989), Carey (1991)
			10–20 km		High		
			20–30 km		Moderate		
			30–40 km		Low		
			>40 km	Less common	Very low		
Pyroclastic flows	Obstacles		<100 m	Very frequent	Very high	They cause death by asphyxiation and heat, severe burns, and throat and nostril irritations in people and animals. The remaining elements of vulnerability cause destruction by impact, collapse, burial, displacement, or fire	Crandell et al. (1984)
			100–500 m		High		
			500–750 m		Moderate		
			750–1000 m		Low		
			>1000 m	Less common	Very low		
	Length		<50 km	Very frequent	Very high		
			50–75 km		High		
			75–100 km		Moderate		
			100–200 km		Low		
			>200 km	Less common	Very low		
Gases	Soil	CO_2	>50%			High risk of suffocation	Baubron et al. (1994)
			50–25%			Moderate risk of suffocation	
			5–25%			Low risk of suffocation	
			1.5–5%			No risk of suffocation	
			<1.5%			CO_2 concentrations equal to non-volcanic areas	
	Air	CO_2	5000 ppm (for a maximum of 8 h)			Permissible exposure limits for living beings. When any of the limits are exceeded, living beings are affected according to the toxicity of the gases	Williams-Jones and Rymer (2000)
		SO_2	5 ppm				
		Rn	200 Bq/m^3				
		H_2S	20 ppm (for na average of 10 min)				
		HCl	5 ppm				
		HF	3 ppm				
		H_2SO_4	20 ppm				
Acid rain			2000 km			Acid rain can cause skin irritation and burns, sore lips, eye irritation, and hair loss in people within this range. In addition, they cause damage to vegetation and can cause corrosion of metal components in buildings, infrastructure and equipment	Erskine (1962) in Blong (1984), MacDonald (1975) in Crandell et al. (1984)

(continued)

Table 1 (continued)

Volcanic phenomenon	Parameters		Critical values	Frequency	Danger	Impact	References
Gases/Ashes			>10 km			Events rich in SO_2 and/or with eruptive columns that penetrate in the stratosphere are likely to cause global climate change	Stothers and Rampino (1983) in Chester (1993)
Tephra falls	Ashes and volcanic dust	Thickness	<1 mm			They can cause respiratory problems and eye irritation in people and animals	Blong (1984)
	Volcanic ash and *lapilli*	Thickness	>200 cm			Death of all vegetation	Blong (1984)
			200–50 cm			Death of medium-sized and large-sized vegetation that is not very resistant	
			50–15 cm			Death of poorly resistant medium-sized vegetation	
			15–10 cm			Death of low-resistant small vegetation	
			<10 cm			Death of small vegetation	
	Dry volcanic ash and lapilli	Thickness	>400 cm			Total collapse of all types of structures	Crandell et al. (1984), Booth et al. (1983), Walker (1982), Blong (1984)
			400–100 cm			Total collapse of type 1 structures and partial collapse of structures 2 and 3	
			100–20 cm			Partial collapses of type 1 structures	
			>20 cm			The collapse of roofs with a load capacity of less than 100 kg/m^2	
	Moist volcanic ash and lapilli	Thickness	>50			Total collapse of all types of structures	
			50–15 cm			Total collapse of type 1 structures and partial collapse of structures 2 and 3	
			15–10 cm			Partial collapse of type 1 structures	
			>10 cm			Collapse of roofs with a load capacity of less than 100 kg/m^2	
	Volcanic ashes	Thickness	>1 mm			They can cause problems in various infrastructures and the economy	Blong (1984), Crandell et al. (1984), Blong (1984), Crandell et al. (1984)
	Lithics	Dimensions	>5 cm			They can cause injury or even death to people and animals and puncture ceramic tiles	
	Pumice	Dimensions	>10 cm			They can cause injury or even death to people and animals and cause fires	

The modelling of lava flows assuming critical values of a general and regional nature made it possible to estimate the areas likely to be affected. Furthermore, its intersection with the elements of vulnerability, using a geographic information system for this purpose, made it possible to assess the foreseeable losses qualitatively, given the absence of significant quantitative data.

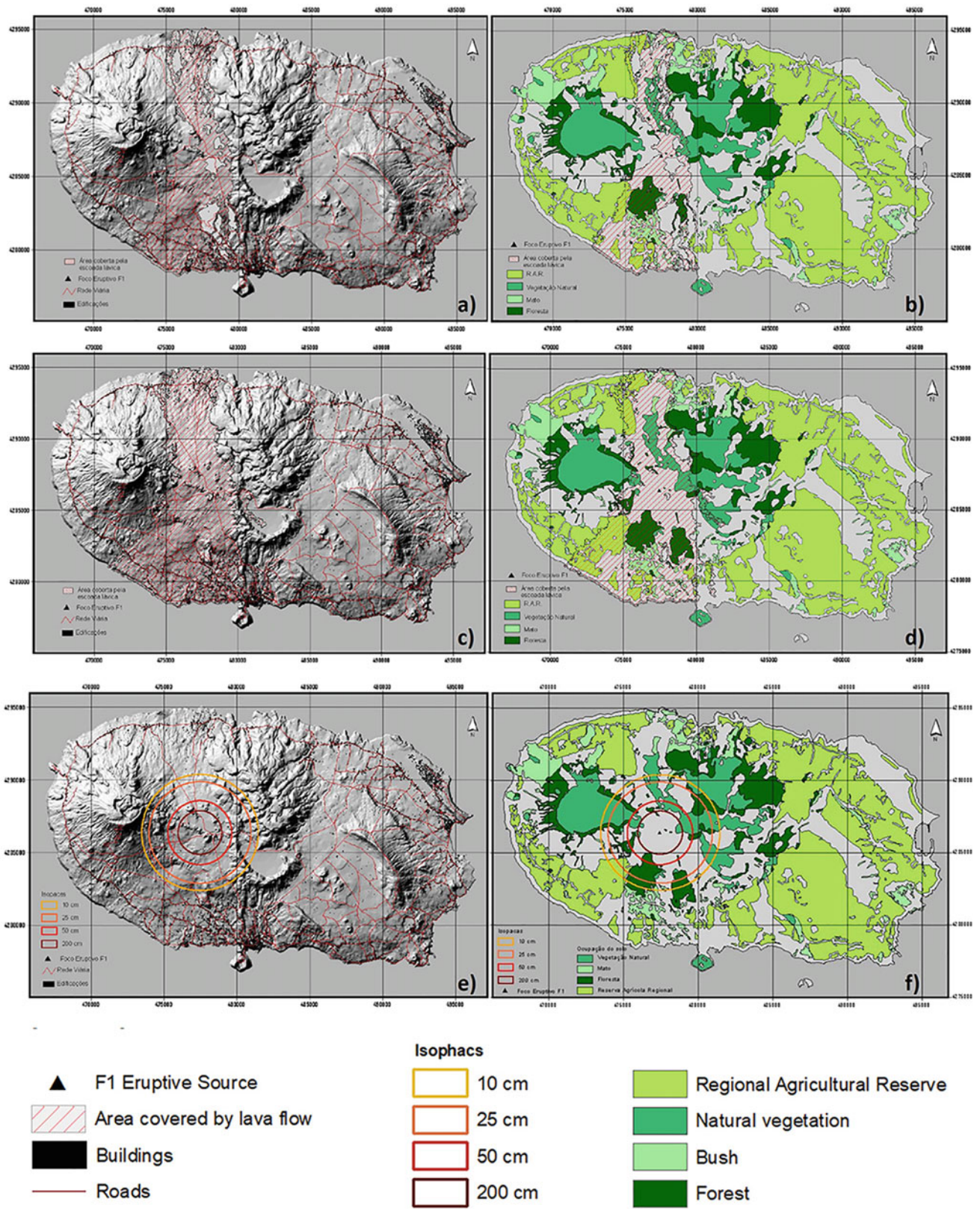

Fig. 1 Overlapping of the area covered by lava flows resulting from the simulation carried out for the F1 vent, located in the fissure zone of Terceira Island: **a** for a critical height of 3 m, with the urban areas and the road network; **b** for a critical height of 3 m, with the different types of land occupation; **c** for a critical height of 20 m, with urban areas and the road network; **d** for a critical height of 20 m, with the different types of land occupation; **e** intersection of areas potentially subject to the fall of basaltic pyroclasts resulting from a Hawaiian/Strombolian eruption (focus F1) with the housing stock and road network; **f** intersection of areas potentially subject to the fall of basaltic pyroclasts resulting from a Hawaiian/Strombolian eruption (focus F1) with land occupation

4 Concluding Remarks

The analysis of geological hazards in the Azores islands is fundamental, taking into account their impacts through history concerning the occurrence of volcanic eruptions, earthquakes, landslides, coastal erosion, and floods.

This study showed that the number of variables involved in estimating vulnerabilities is high, which is reflected in the difficulty in obtaining an objective and desirable overall assessment. Additionally, the unpredictability of the volcanic phenomenon must be taken into account. In order to try to approximate the analysis, as much as possible, to the reality of the studied region, it is also essential to consider its eruptive particularities, which will translate into identifying and applying specific critical values.

It was verified that the suggested procedure is effective for the intended objectives, and the acquisition of the necessary information must be continued to define the critical values for the different volcanic systems of the archipelago.

It is considered that this methodology should be improved as the modelling of eruptions is developed and optimised. So, new data are acquired to assess critical values of a general and regional nature. The test proved suitable for elaborating risk scenarios and, consequently, of interest for planning, land use planning, emergency planning, and Civil Protection actions.

Acknowledgements The authors would like to thank the Regional Laboratory of Civil Engineering and the Regional Secretary for Public Works and Communications of the Government of the Azores for the conditions provided to develop this work.

References

Baubron, J.-C., Baxter, P., Coutinho, R., Allard, P., Ferreira, T., & Gaspar, J. L. (1994). *Gas hazard in dwellings Furnas map*. EC—Environment Programme Furnas Laboratory Volcano, Health aspects.

Baxter, P. (2000). Impacts of eruptions on human health. In H. Sigurdsson, B. Houghton, S. McNutt, H. Rymer, & J. Stix (Eds.), *Encyclopedia of volcanoes* (pp. 1035–1043). Academic Press.

Blong, R. J. (1984). *Volcanic hazards*. Academic Press.

Booth, B., Croasdale, R., & Walker, G. (1983). Volcanic hazard on São Miguel, Azores. In H. Tazieff & J.-C. Sabroux (Eds.), *Forecasting volcanic events* (pp. 99–109). Elsevier.

Carey, S. N. (1991). Transport and deposition of tephra by pyroclastic flows and surges. In *Sedimentation in volcanic settings* (Vol. 45, pp. 39–57). SEPM Special Publication.

Chester, D. (1993). *Volcanoes and society*. Chapman and Hall Inc.

Crandell, D., Booth, B., Kusumadinata, K., Shimozuru, D., Walker, G., & Westercamp, D. (1984). *Source book for volcanic-hazards zonation*. UNESCO.

Felpeto, A., Garcia, A., & Ortiz, R. (1996). Mapa de riesgo. Modelizácion. In R. Ortiz (Ed.), *Riesgo Volcánico Série Casa de los Volcanes, Lanzarote, Canarias* (Vol. 5, pp. 67–98).

Fisher, R. V., Heiken, G., & Hulen, J. B. (1997). *Volcanoes. Crucibles of change*. Princeton University.

Macdonald, G. (1972). *Volcanoes*. Prentice-Hall Inc.

Malheiro, A. (2002). *Identificação, caracterização e proposta de sistematização dos elementos e parâmetros de vulnerabilidade a considerar no âmbito da avaliação de riscos vulcânicos*. Master dissertation, Azores University, Ponta Delgada.

Self, S. (1974). *Recent volcanism on Terceira, Azores*. Ph.D. thesis, Imperial College, London. http://hdl.handle.net/10044/1/20874

Tilling, R. I. (Ed.). (1989). Volcanic hazards and their mitigation: Progress and problems. *Reviews of Geophysics, 27*(2), 237–269.

Walker, G. P. L. (1973). Lengths of lava flows. *Philosophical Transactions of the Royal Society London, 274*, 107–118.

Walker, G. P. L. (1982). Volcanic hazards. *Interdisciplinary Science Reviews, 7*(2), 148–157.

Williams-Jones, G., & Rymer, H. (2000). Hazards of volcanic gases. In H. Sigurdsson, B. Houghton, S. McNutt, H. Rymer, & J. Stix (Eds.), *Encyclopedia of volcanoes* (pp. 997–1004). Academic Press.

Natural Hazards and Assessment: Rock Falls, Landslides, Urban Planning and Management

Specific Characteristics of Volcanic Materials in Landslides: A Geotechnical Outlook

Celeste Jorge

Abstract

Volcanism is related to active seismic tectonic areas. Numerous islands resulted from submarine volcanic eruptions. Different volcanic materials with specific characteristics (intrinsic parameters) are acted by seismic activity and extreme weather events (external parameters) interacting and generating landslide risks. Anthropic actions also contribute to the destabilization. Therefore, landslides are a destructive natural hazard. To mitigate or control the risk related to this type of hazard, it is necessary to understand the geotechnical properties of volcanic materials, which are very heterogeneous. Besides, there is less information about these geologic environments. On the other hand, geotechnicians with no experience in volcanic materials should not carry out this type of study without prior preparation. For this reason, a compilation of the generic properties of these materials, which contribute to the peculiarities of landslides in a volcanic environment, is made.

Keywords

Volcanic-materials • Characteristics • Geotechnics • Landslides

1 Introduction

There are basaltic and andesitic/dacitic/rhyolitic islands in the oceans, mainly grouped in archipelagos. The basaltic or andesitic nature of the magmas results from the conditions of the seismic tectonic zone; essentially, if they are at the axis of the oceanic ridge system (e.g., Azores Archipelago—low silica lava) or the tectonic plates convergence boundaries (e.g., New Zealand Archipelago—higher silica lava). Vulcanism also occurs within the plates, as is the case of Hawaii islands (basaltic magma). These islands result from submarine eruptions that emerge from the ocean, and subaerial volcanism occurs. On the surface, volcanoes are formed by the deposition and accumulation of lava and ash expelled from craters and vents during explosive and non-explosive eruptions.

Volcanic materials/rocks shape volcanic structures and surrounding volcanic ring plateaux composed of volcanic ash, slag, pumice deposits, and compact volcanic rocks, for example, lava flows, lava domes, dykes, sills, laccoliths (Liu et al., 2012). The transformation of a volcano into a mountain or plateau is determined by the balance between the deposition of lava and ash during eruptions and its subsequent weathering and erosion by external geological agents (e.g., wind, rain, and sea action). The action of the external geological agents on the rocks results in more weathered and eroded situations, with more scenarios of multi-hazard natures.

Volcanoes generate several significant natural hazards; among them, large volcanic landslides are the most dangerous. This partly results from the fact that volcanic soils can often support very steeply to near-vertical slopes. These steep slopes frequently have a partial or total absence of vegetation and consequently are susceptible to unexpected and tragic failure (Bommer et al., 2002). These authors considered that "the engineering characterization of volcanic soils is needed for general application. Understanding the geotechnical properties of volcanic materials (soils/rocks) is very important and challenging under static and dynamic conditions when subjected to infiltration due to rainfall". Bommer et al. (2002) also emphasize the "need to increase the exchange of data, experiences, and knowledge among the experts in the characterization and engineering of volcanic soils, to bridge gaps in creating appropriate engineering solutions for these difficult materials".

C. Jorge (✉)
Advisory Group of Board of Directors, Laboratório Nacional de Engenharia Civil (LNEC), Lisboa, Portugal
e-mail: cjorge@lnec.pt

A. Malheiro et al. (eds.), *Advances in Natural Hazards and Volcanic Risks: Shaping a Sustainable Future*,
Advances in Science, Technology & Innovation, https://doi.org/10.1007/978-3-031-25042-2_11

2 Volcanic Hazards/Landslides

Volcanoes produce many natural hazards that can injure or kill people and destroy assets. Figure 1a shows a typical volcano and the respective risks associated. Volcano landslides are one of the main hazards in the not eruptive phase of a volcano (USGS, 2008) (Fig. 1b, c), and all volcanic edifices are susceptible to landslides. Landslides are critical processes in composite and shield volcanoes (NPS, 2021). Composite volcanoes are steep and have weakened areas due to clay minerals, where hydrothermal alteration occurs. Most composite volcanoes also have high volumes of fractured rock or loosely consolidated pyroclastic deposits (NPS, 2021; USGS, 2014). Shield volcanoes are also subject to mass wasting and large landslides or slumps (NPS, 2021).

A landslide is a mass movement controlled by rock fragments, soil, and debris downslope gravity. Volcanic landslides are usually substantially deeper and less influenced by stratigraphy than nonvolcanic landslides. They tend to be dramatically larger and more mobile than their nonvolcanic counterparts and are characterized by a low-angle basal failure plane (Siebert, 2002). They range in size from less than 1 km^3 to more than 100 km^3.[1] On the shoreline, the mass movements associated with volcanoes can generate tsunamis.

3 Volcanic Materials Characteristics Contributing to Landslide

Complex geological systems represent the volcanic environment. Valerio et al. (2012) point out that the following "volcanoclastic deposits have a wide range in their granulometry, degree of consolidation, and geomechanical characteristics. The potential type of movement in volcanic materials is determined by the form and size of the blocks, their position within the rock mass, and the relative orientation of the discontinuities concerning the slopes. These features control destabilizer processes, including falls of rock or granular material landslides and flows".

Bommer et al. (2002) and Siebert (2002) assumed the key issues: "volcanic soils are a special group of deposits that create particular engineering problems related to slope stability. In addition, morphology, textures, and emplacement mechanisms vary widely with water content. They can be relatively dry or sufficiently wet".

Consequently, all relevant geological and geophysical information is essential for understanding the behavior of volcanic materials. According to Molist (2017), this information includes stratigraphic studies, geological mapping, sedimentological studies, petrological studies, and structural studies.

Most of the volcanic materials described in the literature (e.g., Fisher, 1961; Fisher & Schminke, 1984; Bommer et al., 2002) are composed of "fragments produced in volcanic vents, fragments formed from the break-up of moving lava, or fragments of dust, ash, or pumice that fall around or are carried to a distance by the wind". They also include volcano-sedimentary materials and deposits resulting from solidified lava or consolidated pyroclastic debris when weathering and erosion agents act upon them. From the facts stated above, it is easy to understand that volcanic materials have specific features. These features are regarding plasticity, particle size, and mineral composition. Moreover, the volcanic soils have relatively high shear strength and permeability, while their compressibility is quite low under relatively low-stress increments (e.g., Gonzalez de Vallejo et al., 1981; Bommer et al., 2002).

Some researchers (e.g., Wesley, 1973; Belloni et al., 1988) assumed that the resistance of this type of soil results from a rocky skeleton surrounded by clay particles and a cementing agent, which behaves as a viscous gel, what Bommer et al. (2002) reinforce by mentioning that most volcanic deposits have relatively weak cementation. However, the data of Wesley (1973) tested for two allophanic soils (young soils derived mainly from volcanic ash) shows only small differences between peak and residual strengths.

According to several authors, two main factors that play an essential role in the slope stability of volcanic soils and explain their steep slopes are (i) an open metastable structure and (ii) a relatively low moisture content, which is reflected in soils with negative pore-water pressures.

When acted by external agents, Belloni and Morris (1991) concluded that "sloping areas slipped, after a prolonged period of heavy rainfall, when an earthquake later acted upon them. So, neither the saturation of the slopes due to rain nor earthquake shaking alone would have caused extensive damage, but the combination of both factors resulted in extensive mass movements".

In the opinion of the author of the present paper, this is not true, as extreme weather events can cause slope destabilization on their own, as, under heavy rainfall events, the pore water pressure increases, leading to the loss of shear strength and subsequent slope instability (agreeing with Putra et al., 2020).

Smith et al. (2015) confirm it, essentially in shallow landslides. These authors found slope geometry, rainfall totals, and initial groundwater table location significantly affect stability, as is common in all landslides. However, lithology is fundamental in the mechanisms developed in mass movements on slopes. Among the parameters

[1] https://courses.lumenlearning.com/geo/chapter/reading-lahars-landslides-and-lavaflow/ (accessed in April 2022).

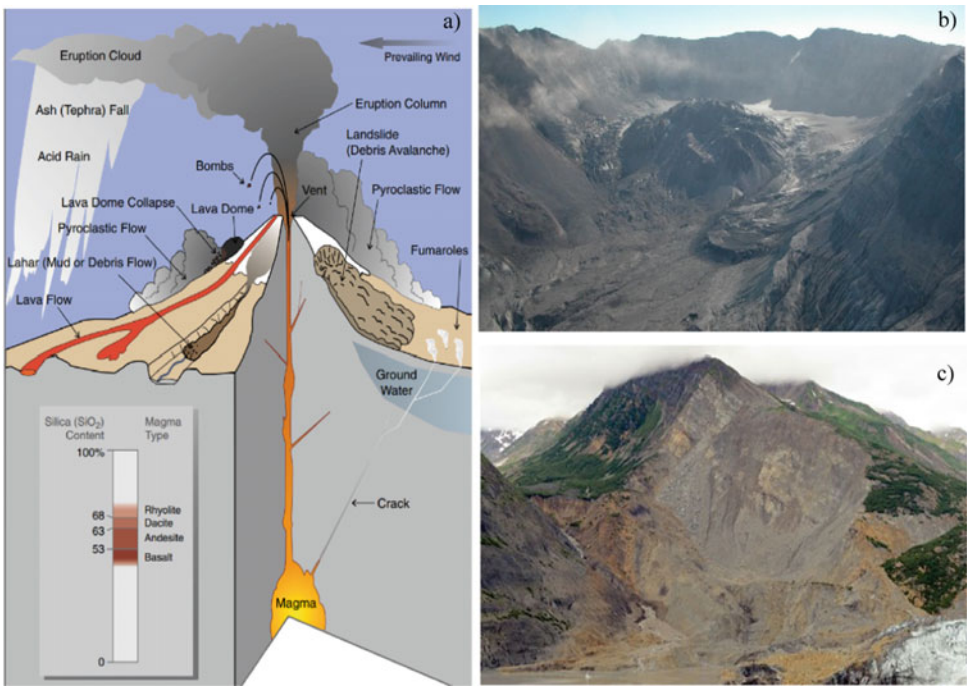

Fig. 1 **a** Volcanic hazards (USGS, 2008), **b** landslides on the crater of Mount St. Helens (USGS, 2022), and **c** landslides on volcanic material (NPS, 2021)

associated with the lithologic characteristics are resistance to compression, tension and cutting force, degree of disturbance, porosity, permeability, and discontinuities associated with the formation of the material. According to Valerio et al. (2012), "the discontinuities can be related to sequences of lava intercalated with pyroclastic deposits, which gives the rocky masses a heterogeneous and anisotropic character. This heterogeneity implies the existence of zones with different mechanical and hydraulic properties, degree of alteration, and water content, among other characteristics".

Wong and Baud (2012) state that "volcanic rock's mechanical behavior and failure modes of volcanic rock are qualitatively similar to sedimentary rocks. Nevertheless, volcanic rocks are much more complex than sedimentary rocks. For example, their porosity can vary from almost 0 to almost 1; they often contain both microcracks and pores; their pore shapes are more complex, and their pore size distributions are much wider than most sedimentary rocks; they can contain crystals characterized by different shapes, sizes, and size distributions; they can be granular or characterized by a groundmass that hosts pores and crystals; their compositions and glass contents can vary; they are often variably affected by hydrothermal alteration". However, understanding how these attributes and others influence volcanic rock's mechanical behavior and failure modes is still poorly understood. Another topic that requires attention is that laboratory data necessitate upscaling to the rock mass or volcano scale (Heap & Violay, 2021).

4 Concluding Remarks

Their varied and complex micro- and macrostructures control volcanic materials' mechanical behavior and failure modes. To understand and mitigate the risk of landslides in volcanic materials, it is necessary to comprehend the geotechnical properties of these materials (soils/rocks), but they remain not fully known. An unfamiliar geotechnician with these materials and their characteristics may not be able to deal with the particularities of volcanic materials, which must be considered. In situ and laboratory tests must also consider all the features mentioned and others that may be site-specific. For all that can be mentioned, the complexity of volcanic materials needs further studies to better adapt these engineering approaches to volcanic systems, as was already mentioned by Miranda et al. (2018), among other authors.

References

Belloni, L., & Morris, D. (1991). Earthquake-induced shallow landslides in volcanic debris soils. *Géotechnique, 41*(4), 539–551.

Belloni, L., Morris, D., Bellingeri, G. A., & Purkowo, I. (1988). Compaction and strength characteristics of a residual clay from Bali, Indonesia. In *Proceedings of 2nd International Conference on Geomechanics in Tropical Soils*, Singapore (pp. 343–349).

Bommer, J. J., Rolo, R., Mitroulia, A., & Berdousis, P. (2002). Geotechnical properties and seismic slope stability of volcanic soils. *Paper Reference 695, 12th European Conference on Earthquake Engineering*. Elsevier Science Ltd.

Fisher, R. V. (1961). Proposed classification of volcaniclastic sediments and rocks. *Geological Society of America Bulletin, 72*(9), 1409–1414.

Fisher, R. V., & Schminke, H. U. (1984). *Pyroclastic rocks*. Springer.

Gonzalez de Vallejo, L. I., Jimenez Salas, J. A., & Leguey Jiminez, S. (1981). Engineering geology of the tropical volcanic soils of La Laguna, Tenerife. *Engineering Geology, 17*, 1–17.

Heap, M. J., & Violay, M. E. S. (2021). The mechanical behaviour and failure modes of volcanic rocks: a review. *Bulletin of Volcanology 83,* 33.

Liu, J., Chen, X., & Guo, W. (2012). Volcanic natural resources and volcanic landscape protection: An overview. In K. Nemeth (Ed.), *Updates in volcanology—New advances in understanding volcanic systems* (43 pp.). Intech Open.

Miranda, T., Sousa, L. R., Gomes, A. T., Tinoco, J., & Ferreira, C. (2018). Geomechanical characterization of volcanic rocks using empirical systems and data mining techniques. *Journal of Rock Mechanics and Geotechnical Engineering, 10*(1), 138–150.

Molist, J. M. (2017). *Assessing volcanic hazard: A review*. Oxford Handbooks Online.

NPS. (2021). *Volcanic processes—Landslides*. U.S. National Park Service, U.S. Department of the Interior.

Putra, O. A., Yasufuku, N., Alowaisy, A., Ishikura, R., Rifa'I, A., & Kawaguchi, Y. (2020). Shear strength characteristic of unsaturated undisturbed black volcanic ash soil in Kumamoto under static and cyclic loading. *Lowland Technology International, 22*(3), 280–289.

Siebert, L. (2002). Landslides resulting from structural failure of volcanoes. In S. G. Evans & J. V. Degraff (Eds.), *Catastrophic landslides: Effects, occurrence, and mechanisms* (Vol. XV). Geological Society of America, Reviews in Engineering Geology.

Smith, D. M., Oommen, T., Bowman, L. J., Gierke, J. S., & Vitton, S. J. (2015). Hazard assessment of rainfall-induced landslides: A case study of San Vicente volcano in central El Salvador. *Natural Hazards, 75*, 2291–2310.

USGS. (2008). *What are volcano hazards? Reducing the risk from volcano hazards*. USGS Fact Sheet 002-97, U.S. Geological Survey, U.S. Department of the Interior.

USGS. (2014). *Volcanic processes. Living with a volcano in your backyard—An educator's guide with emphasis on Mount Rainier*. General Information Product 19, National Park Service, U.S. Geological Survey, U.S. Department of the Interior.

USGS. (2022). *Mount St Helens—Analysis of photographs and other images for monitoring purposes*. U.S. Geological Survey, U.S. Department of the Interior.

Valerio, V. C., López, M. C., & Alcántara, A. I. (2012). Mass movement processes associated with volcanic structures in Mexico City. *Investigaciones Geográficas (Mx), 79,* 48–74.

Wesley, L. D. (1973). Cluster hypothesis and the shear strength of a tropical red clay. *Géotechnique, 23*(1), 109–113.

Wong, T., & Baud, P. (2012). The brittle-ductile transition in porous rock: A review. *Journal of Structural Geology, 44*, 25–53.

A Decade of Monitoring and Research on the San Andrés Megalandslide on El Hierro, Canary Islands, Spain

Jan Blahůt, Jan Klimeš, Stavros Meletlidis, Jan Balek, Matt Rowberry, and Ivo Baroň

Abstract

Precise 3D dilatometric monitoring began on the San Andrés megalandslide detachment plane on El Hierro, Canary Islands, during the winter of 2013. It has been found that this presumably aborted giant landslide creeps progressively at rates of up to 0.5 mm a^{-1}, with accelerations following periods of seismicity and extreme rainfall. In addition, a detailed multidisciplinary investigation of the landslide detachment plane has found that silica and cataclastic layers were produced during a pair of discrete slip events at 545–430 ka and 183–52 ka. Furthermore, slope stability analysis has suggested that creep may result from the deformation of sedimentary layers in the ocean, while destabilisation of the volcanic flank would require an earthquake with an intensity of at least VII. Finally, simple tsunami modelling based on conservative scenarios has shown that even a comparatively small event could have severe ramifications along the coasts of northwest Africa and southwest Europe.

Keywords

Volcanic collapse • Displacement monitoring • Stability modelling • San Andrés Landslide • El Hierro • Canary Islands

1 Introduction

Massive volcanic collapses usually result in large debris avalanches (Blahůt & Klimeš, 2022). However, a detailed assessment of all known megalandslides from volcanic islands has revealed that only a small number of collapses result in deep-seated gravitational slope deformations with visible morphology (Blahůt et al., 2018a, 2019). Instead, most collapses create large, horseshoe-shaped source areas that resemble part of a caldera or crater and lack an onshore sliding mass. One conspicuous exception is located on the volcanic island of El Hierro in the Canaries Archipelago, Spain.

The San Andrés Landslide (SAL) is a megalandslide situated on the island's east coast. It has been interpreted as either an anchored mass associated with the Las Playas I debris avalanche or an enormous aborted landslide (Day et al., 1997). However, geological clues indicate that the landslide is steadily progressing to the east and southeast (Troll & Carracedo, 2016).

During 2013, three dilatometers were installed (Fig. 1) on its supposed detachment planes (Klimeš et al., 2016). This was accompanied by detailed geomorphological analysis and structural geological mapping. Since then, the exposed fault plane has been studied through microstructural analysis, petrological characterisation, and cosmogenic exposure dating (Blahůt et al., 2020a). In addition, a simple slope stability analysis has been conducted (Blahůt et al., 2020b), followed by tsunami modelling (Blahůt & Quan Luna, 2021).

2 Settings and Methods

El Hierro is a composite volcano in the Atlantic Ocean whose most recent rocks, represented by the Rift Series, have a maximum age of 0.16 Ma and whose oldest subaerially exposed rocks have been dated to 1.12 Ma (Guillou

J. Blahůt (✉) · J. Klimeš · J. Balek · M. Rowberry · I. Baroň
Department of Engineering Geology, Institute of Rock Structure and Mechanics, Czech Academy of Sciences, Prague, Czechia
e-mail: blahut@irsm.cas.cz

S. Meletlidis
Centro Geofísico de Canarias, Instituto Geográfico Nacional, Santa Cruz de Tenerife, Spain

A. Malheiro et al. (eds.), *Advances in Natural Hazards and Volcanic Risks: Shaping a Sustainable Future*,
Advances in Science, Technology & Innovation, https://doi.org/10.1007/978-3-031-25042-2_12

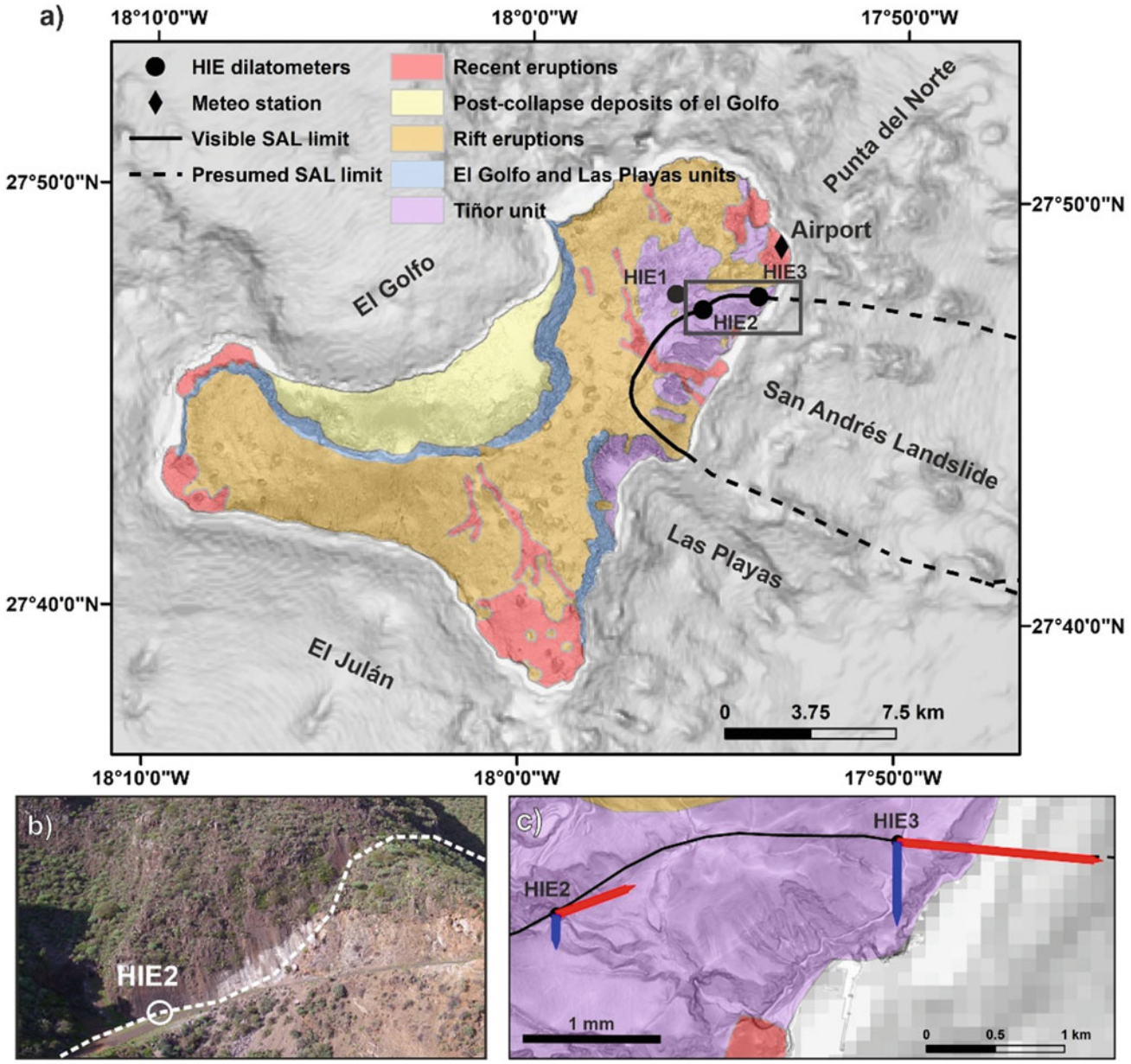

Fig. 1 **a** Simplified geological map of the island of El Hierro presenting an outline of the San Andrés Landslide and the locations of monitoring gauges HIE1, HIE2 and HIE3 (black box outlines the area shown in panel (**c**); **b** aerial photograph of the landslide detachment plane, indicated by the dashed line, at dilatometric monitoring point HIE2; **c** interpretation of the long-term monitoring results (the red arrow indicates horizontal movement while the blue arrow indicates vertical movement). Updated and modified from Blahůt et al. (2020c)

et al., 1996). The present, ongoing phase of volcanic activity started about 2.5 ka (Carracedo et al., 2001). Intense seismicity characterised the period between July 2011 to 2014 (López et al., 2012; Benito-Saz et al., 2017). At this time, a submarine eruption began on 10 October 2011 and stopped in March 2012 (Meletlidis et al., 2015). Comprehensive information about the island's geological history can be found elsewhere (Carracedo & Troll, 2016).

In February 2013, three precise 3D dilatometers, referred to as TM-71s (Klimeš et al., 2012), were installed in the island's northeastern part. Two are located on the head scarp and lateral scarp, respectively, while one is located on a fault plane in an underground dry gallery, around 900 m to the west of the head scarp. These dilatometers are precise (±0.007 mm) and facilitate automatic image interpretation (Martí et al., 2013). The actual dilatometric gauges are based on optical-mechanical interferometry and record data in three axes: X—compression or extension; Y—strike-slip; Z—vertical movement. This enables the interpretation of three-dimensional vector movements on the instrumented

fault or sliding plane. Data are collected daily at 00:00 UTC. However, due to the lack of GSM coverage, they are not transmitted online and must be downloaded regularly, usually once a year, during routine maintenance. A fully quantitative approach to analysing the data has been developed amid our research on El Hierro (Blahůt et al., 2020c), while it has also been possible to interrogate single displacement events to compute different landslide stress states (Blahůt et al., 2018b).

Apart from continuous monitoring, several other methods have been employed to unravel the history of the San Andrés Landslide. First, its distinctive detachment plane has been thoroughly studied to determine whether this feature was exposed during a single geological moment, as suggested by previous studies (Day et al., 1997), or whether exposure represents a series of accelerations. This has been achieved by integrating rock weathering studies using a Schmidt hammer, cosmogenic 3He surface exposure dating, and microstructural and structural analyses (Blahůt et al., 2020a).

The limit equilibrium Morgenstern-Price method has been used to evaluate the current stability conditions of the San Andrés Landslide. This geotechnical model has been constructed based on analysed rock parameters (Blahůt et al., 2020b) coupled with information gleaned from the published literature (e.g., Huusgard et al., 2015; León et al., 2017; Masson et al., 2002; Stow, 2009). A conservative tsunami scenario has been prepared (Blahůt & Quan Luna, 2021). In this scenario, two empirical approaches were used to create the critical initial wave (Noda, 1970; Huber & Hager, 1997). The DELFT 3D model determined the consequent wave propagation.

3 Results

3.1 Monitoring

The long-term monitoring results are presented in Fig. 2. The gauge HIE1, located in a dry gallery beyond the limits of the landslide, has not exhibited any movements since its installation. In contrast, HIE2 and HIE3 evidence the progressive evolution of the sliding plane. On both gauges, a continuous sinistral strike-slip movement is visible (Y-axis, red line), although the actual rates are somewhat dissimilar (0.635 mm on HIE2 and 2.04 mm on HIE3). Except for a small uplift towards the end of 2013, the downslope movement of the landslide mass is also visible on both gauges (Z-axis, blue line). This reaches 0.27 mm in the case of HIE2 and 0.666 mm at HIE3. However, these movements are subject to a seasonal influence, most probably caused by atmospheric temperature changes influencing the thermal expansion of the rock blocks (the gauges themselves are temperature compensated) (Klimeš et al., 2012). Unfortunately, the long-term monitoring has been disrupted by the malfunction of the automatic recordings in 2019 at HIE2 and in 2020 at HIE3. The loggers were replaced in June 2021 and February 2022, respectively.

Detailed analysis of the data from HIE3, combined with information about specific seismic and rainfall events, has revealed that the behaviour of the landslide at any moment in time is likely to reflect any one of six short-term activity modes, each corresponding to a specific stress state (Fig. 3). Its reaction to rainfall events is seen to be immediate, assumed to reflect increasing levels of saturation within the landslide mass. However, its reaction to geophysical perturbations is more complicated as periods of gravitational relaxation often come after the compressional pulses (Blahůt et al., 2018b).

3.2 History and Future of the SAL

Analysis of the San Andrés Landslide detachment plane revealed two main sets of slickenlines plunging with azimuths of 111° and 125–134°. Microstructural investigations identified a later silica layer with flow bands and clast-cortex aggregates overlying an earlier foliated cataclastic layer. Cosmogenic 3He surface exposure dating along two vertical profiles did not provide evidence for a gradual decrease in the exposure ages, indicating that movements on the detachment plane were accomplished over short periods. The more recent reactivation occurred between 183 ± 17 and 52 ± 17 ka, while an older active phase occurred between 545 and 430 ka (Blahůt et al., 2020a).

The current stability state of the landslide has been assessed by a limited model developed based on numerous assumptions (Blahůt et al., 2020b). Nevertheless, the results point to the overall stability of the flank during periods of low volcanic and seismic activity. They also point to the possibility of reactivation during earthquakes with intensities of at least VII. The monitoring results—emphasising slow creep—are in good agreement with the analysis of deep-sea sediment stability, characterised by low shear resistance and softening of the toe of the slope. Limited tsunami scenario modelling, considering only the subaerial part of the landslide (6 km^3), has shown that a minimum sliding velocity of 94.5 m/s is needed for critical wave generation. This will result in an initial wave reaching approximately 80 m and lead to severe consequences for the Canary Islands as well as along the coasts of northwest Africa and southwest Europe, with waves reaching more than 3.5 and 2 m, respectively (Blahůt & Quan Luna, 2021).

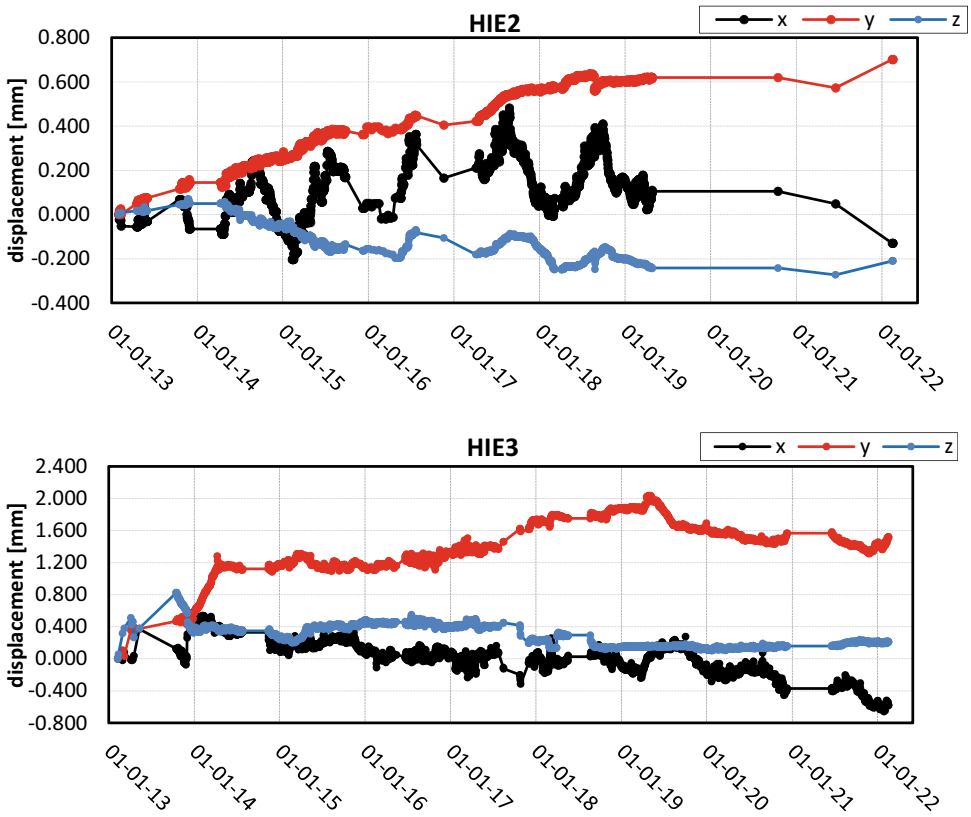

Fig. 2 The long-term 3D dilatometric monitoring results at points HIE2 (upper figure) and HIE3 (lower figure)

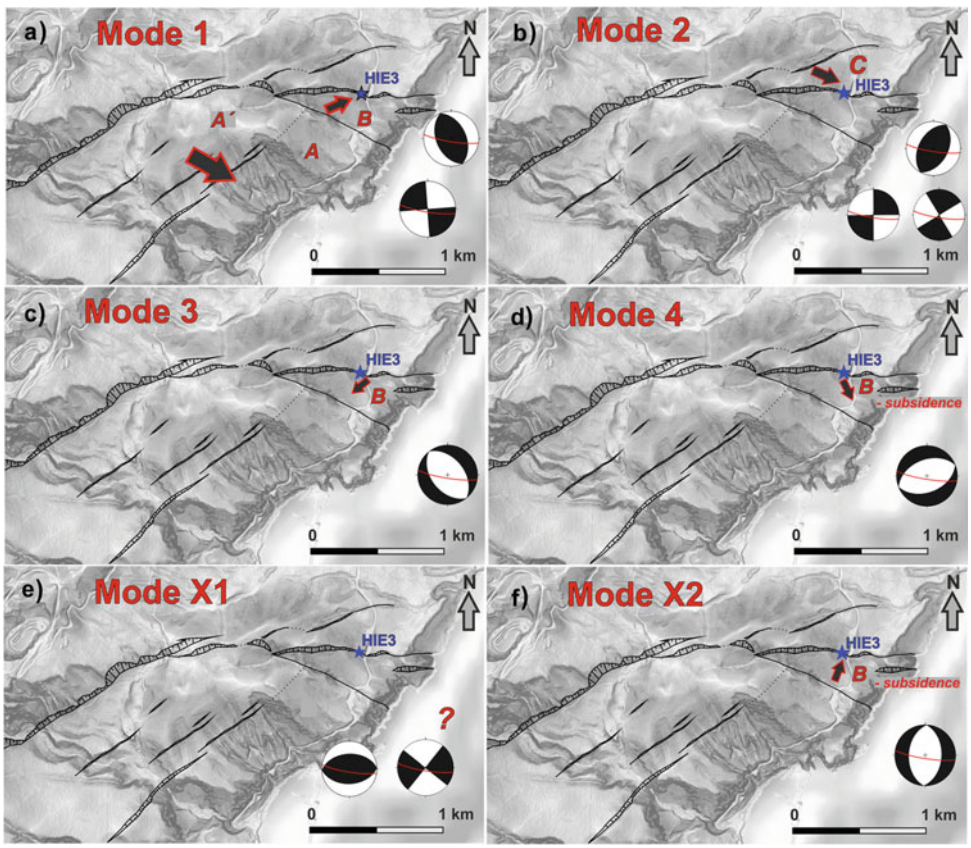

Fig. 3 Interpretation of the landslide's six main short-term activity modes in response to specific stress states. Please refer to Blahůt et al. (2018b) for more details about each mode

4 Discussion

Even at the global scale, there are only a small number of instances of long-term instrumental monitoring on large volcanic flank collapses. Examples include monitoring the Hilina slump on the Big Island of Hawai'i (Cannon & Bürgmann, 2001; Owen et al., 2000) and Pico Island in the Azores (Hildebrand et al., 2012). However, in these cases, the observed horizontal and vertical motions are up to two orders of magnitude greater than those measured on El Hierro. Such monitoring is usually performed using GNSS, which has much lower accuracy than the dilatometric gauges used in this study (Klimeš et al., 2012). This raises the question of whether very slow creep is, in fact, a common phenomenon on volcanic flanks. The answer might lie in implementing other types of monitoring, including undersea (Urlaub et al., 2018). Satellite interferometry has a large and growing potential (Blahůt et al., 2021). However, this promise is constrained because it is difficult to differentiate between creep and movements associated with the internal activity of the volcano, which is often greater in magnitude.

The stability of the San Andrés Landslide remains an open question because the modelling is based on numerous assumptions. However, the results are in good agreement with other research, such as studies from Stromboli (Apuani et al., 2005), Teide (del Potro et al., 2013), and La Palma (Ferrer et al., 2014). Tsunami simulation showed that a high failure velocity is needed to achieve the critical speed. Although seemingly improbable given the current stability state, recent volcanic collapses such as Anak Krakatau and Hunga Tonga-Hunga Ha'apai show that such speeds are easily achieved during violent eruptions and may lead to severe damage.

5 Concluding Remarks

Over the last decade, research and monitoring on the San Andrés Landslide have demonstrated that this megalandslide is characterised by active, ongoing creep. As a result, it has been possible to study its response to seismicity and rainfall events in considerable detail and perform stability calculations and tsunami modelling. Very few flank collapses are subject to long-term instrumental monitoring, so these results significantly contribute to our understanding of volcanic flank collapses on a global scale.

Acknowledgements The authors are grateful for support from Mobility Plus Project no. FNRS-20-01, "Investigation, monitoring and modelling of the eastern incipient flank collapse of El Hierro volcano, Canary Islands", 2020–2022.

References

Apuani, T., Corazzato, C., Cancelli, A., & Tibaldi, A. (2005). Stability of a collapsing volcano (Stromboli, Italy): Limit equilibrium analysis and numerical modelling. *Journal of Volcanology and Geothermal Research, 144*, 191–210. https://doi.org/10.1016/j.jvolgeores.2004.11.028

Benito-Saz, M., Parks, M., Sigmundsson, F., Hooper, A., & García-Cañada, L. (2017). Repeated magmatic intrusions at El Hierro Island following the 2011–2012 submarine eruption. *Journal of Volcanology and Geothermal Research, 344*, 79–91. https://doi.org/10.1016/j.jvolgeores.2017.01.020

Blahůt, J., Balek, J., Eliaš, M., & Meletlidis, S. (2020a). 3D dilatometer time-series analysis for a better understanding of the dynamics of a giant slow-moving landslide. *Applied Sciences, 10*, 5469. https://doi.org/10.3390/app10165469

Blahůt, J., Balek, J., Klimeš, J., Rowberry, M., Kusák, M., & Kalina, J. (2019). A comprehensive global database of giant landslides on volcanic islands. *Landslides, 16*, 2045–2052. https://doi.org/10.1007/s10346-019-01275-8

Blahůt, J., Baroň, I., Sokoľ, L., Meletlidis, S., Klimeš, J., Rowberry, M., Melichar, R., García-Cañada, L., & Martí, X. (2018a). Large landslide stress states calculated during extreme climatic and tectonic events on El Hierro, Canary Islands. *Landslides, 15*, 1801–1814. https://doi.org/10.1007/s10346-018-0993-1

Blahůt, J., Jaboyedoff, M., & Thiebes, B. (2021). Novel approaches in landslide monitoring and data analysis. *Applied Sciences, 11*, 10453. https://doi.org/10.3390/app112110453

Blahůt, J., & Klimeš, J. (2022). Causes and triggers of mass-movements: Volcanic activity. *Treatise in Geomorphology, 5*, 254–282. https://doi.org/10.1016/B978-0-12-818234-5.00121-8

Blahůt, J., Klimeš, J., Rowberry, M., & Kusák, M. (2018b). Database of giant landslides on volcanic islands: First results from the Atlantic Ocean. *Landslides, 15*, 823–827. https://doi.org/10.1007/s10346-018-0967-3

Blahůt, J., Mitrovic-Woodell, I., Baroň, I., René, M., Rowberry, M., Blard, P.-H., Hartvich, F., Balek, J., & Meletlidis, S. (2020b). Volcanic edifice slip events recorded on the fault plane of the San Andrés Landslide, El Hierro, Canary Islands. *Tectonophysics, 776*, 228317. https://doi.org/10.1016/j.tecto.2019.228317

Blahůt, J., Olejár, F., Rott, J., & Petružálek, M. (2020b). Current stability modelling of an incipient San Andrés giant landslide on El Hierro, Canaries, Spain: First attempt using limited input data. *Acta Geodynamica et Geomaterialia, 17,* 89–99. https://doi.org/10.13168/AGG.2020.0006

Blahůt, J., & Quan Luna, B. (2021). Tsunami from the San Andrés Landslide on El Hierro, Canary Islands: First attempt using simple scenario. In K. Sassa, M. Mikoš, S. Sassa, P. Bobrowsky, K. Takara, & K. Dang (Eds.), *Understanding and reducing landslide disaster risk. Volume 1: Sendai partnerships and Kyoto landslide commitment* (pp. 369–376). Springer. https://doi.org/10.1007/978-3-030-60196-6_27

Cannon, E., & Bürgmann, R. (2001). Prehistoric fault offsets of the Hilina fault system, south flank of Kilauea Volcano, Hawaii. *Journal of Geophysical Research, 106*(B3), 4207–4218. https://doi.org/10.1029/2000JB900412

Carracedo, J.-C., Rodríguez Badiola, E., Guillou, H., de la Nuez, H., & Pérez Torrado, F. (2001). Geology and volcanology of the western Canaries: La Palma and El Hierro. *Estudios Geológicos, 57*, 171–295. https://doi.org/10.3989/egeol.01575-6134

Carracedo, J.-C., & Troll, V. (2016). *The geology of the Canary Islands* (622 pp.). Elsevier. https://doi.org/10.1016/C2015-0-04268-X

Day, S., Carracedo, J.-C., & Guillou, H. (1997). Age and geometry of an aborted rift flank collapse: The San Andres fault system, El Hierro, Canary Islands. *Geological Magazine, 134*, 523–537. https://doi.org/10.1017/S001675689700724

del Potro, R., Hürlimann, M., & Pinkerton, H. (2013). Modelling flank instabilities on stratovolcanoes: Parameter sensitivity and stability analyses of Teide, Tenerife. *Journal of Volcanology and Geothermal Research, 256*, 50–60. https://doi.org/10.1016/j.jvolgeores.2013.02.003

Ferrer, M., González de Vallejo, L., González, S., & Jimenéz, E. (2014). Stability and failure mechanisms of large land-slides in the volcanic islands flanks of the Canary Islands. In G. Lollino, D. Giordan, G. Crosta, J. Corominas, R. Azzam, J. Wasowski, & N. Sciarra (Eds.), *Engineering geology for society and territory. Volume 2: Landslide processes* (pp. 915–919). Springer. https://doi.org/10.1007/978-3-319-09057-3_158

Guillou, H., Carracedo, J.-C., Pérez Torrado, F., & Rodríguez Badiola, E. (1996). K-Ar ages and magnetic stratigraphy of a hotspot-induced, fast grown oceanic island: El Hierro, Canary Islands. *Journal of Volcanology and Geothermal Research, 73*, 141–155. https://doi.org/10.1016/0377-0273(96)00021-2

Hildebrand, A., Marques, F., Catalão, J., Catita, C., & Costa, A. (2012). Large-scale active slump of the southeastern flank of Pico Island, Azores. *Geology, 40*, 939–942. https://doi.org/10.1130/G33303.1

Huber, A., & Hager, W. (1997). *Forecasting impulse waves in reservoirs* (pp. 993–1005). Commission Internationale des Grands Barrages, 19 Congres des Grands Barrages.

Huusgard, P., Caycedo, A., & Cai, M. (2015). *Diamond impregnated drillbit performance in the lower basalt series offshore the Faroe Islands. A case study based on basalt outcrop testing* (22 pp.). Conference Paper SPE-175880-MS, Society of Petroleum Engineers. https://doi.org/10.2118/175880-MS

Klimeš, J., Rowberry, M., Blahůt, J., Briestenský, M., Hartvich, F., Košťák, B., Rybář, J., Stemberk, J., & Štěpančíková, P. (2012). The monitoring of slow-moving landslides and assessment of stabilisation measures using an optical-mechanical crack gauge. *Landslides, 9*, 407–415. https://doi.org/10.1007/s10346-011-0306-4

Klimeš, J., Yepes, J., Becerril, L., Kusák, M., Galindo, I., & Blahůt, J. (2016). Development and recent activity of the San Andrés Landslide on El Hierro, Canary Islands, Spain. *Geomorphology, 261*, 119–131. https://doi.org/10.1016/j.geomorph.2016.02.018

León, R., Somoza, L., Urgeles, R., Medialdea, T., Ferrer, M., Biain, A., García-Crespo, J., Mediato, J., Galindo, I., Yepes, J., González, F., & Gimenez-Moreno, J. (2017). Multi-event oceanic island landslides: New onshore-offshore insights from El Hierro Island, Canary Archipelago. *Marine Geology, 393,* 156–175. https://doi.org/10.1016/j.margeo.2016.07.001

López, C., Blanco, M., Abella, R., Brenes, B., Cabrera Rodríguez, V., Casas, B., Domínguez Cerdeña, I., Felpeto, A., Fernández de Villalta, M., del Fresno, C., et al. (2012). Monitoring the volcanic unrest of El Hierro (Canary Islands) before the onset of the 2011–2012 submarine eruption. *Geophysical Research Letters, 39*, L13303. https://doi.org/10.1029/2012GL051846

Martí, X., Rowberry, M., & Blahůt, J. (2013). A MATLAB code for counting the moiré interference fringes recorded by the optical-mechanical crack gauge TM-71. *Computers & Geosciences, 52*, 164–167. https://doi.org/10.1016/j.cageo.2012.09.029

Masson, D., Watts, A., Gee, M., Urgeles, R., Mitchell, N., Le Bas, T., & Canals, M. (2002). Slope failures on the flanks of the western Canary Islands. *Earth-Science Reviews, 57*, 1–35. https://doi.org/10.1016/S0012-8252(01)00069-1

Meletlidis, S., Di Roberto, A., Domínguez Cerdeña, I., Pompilio, M., García-Cañada, L., Bertagnini, A., Benito-Saz, M., Del Carlo, P., & Sainz-Maza Aparicio, S. (2015). New insight into the 2011–2012 unrest and eruption of El Hierro Island (Canary Islands) based on integrated geophysical, geodetical, and petrological data. *Annales Geophysicae, 58*, S0546. https://doi.org/10.4401/ag-6754

Noda, E. (1970). Water waves generated by landslide. *Journal of the Waterways, Harbors and Coastal Engineering Division, Proceedings of the American Society of Civil Engineers, 96*, 835–855.

Owen, S., Segall, P., Lisowski, M., Miklius, A., Denlinger, R., & Sako, M. (2000). Rapid deformation of Kilauea Volcano: Global Positioning System measurements between 1990 and 1996. *Journal of Geophysical Research, 105*(B8), 18983–18998. https://doi.org/10.1029/2000JB900109

Stow, D. (2009). *Deep-water turbidite systems*. International Association of Sedimentologists Series (483 pp.). Wiley. https://doi.org/10.1002/9781444304473

Troll, V., & Carracedo, J.-C. (2016). The geology of El Hierro. In J.-C. Carracedo & V. Troll (Eds.), *The geology of the Canary Islands* (pp. 43–99). Elsevier. https://doi.org/10.1016/B978-0-12-809663-5.00002-5

Urlaub, M., Petersen, F., Gross, F., Bonforte, A., Puglisi, G., Guglielmino, F., Krastel, S., Lange, D., & Kopp, H. (2018). Gravitational collapse of Mount Etna's southeastern flank. *Science Advances, 4,* eaat9700. https://doi.org/10.1126/sciadv.aat9700

Pico Volcano Flank Landslides and Hazard Implications: Preliminary Results

Fernando Marques

Abstract

In the Pico volcano (Pico Island, Azores) flank, there is evidence of 8 major landslides that were the object of back analysis using the Generalized Limit Equilibrium method. The analyses yielded a close range of strength parameters for a safety factor equal to 1, with $c' = 10$ kPa and average friction angle, $\phi' = 40.1°$ (38.7–41.1°), for wet conditions, and similar values for the dry condition pseudo-static analysis, with $c' = 10$ kPa and average $\phi' = 40.2°$ (39.0–40.9°). The landslide's shadow angle varied between 31.7 and 34.0° and showed no relation with the landslide's scar elevation or planimetric area. Considering the numerous tension cracks at the upper part of the southern flank of the Pico volcano and the steep down-slope angle, there is the possibility of a large landslide developing and the debris travelling down to the S. Caetano cliff crest and village. These preliminary results suggest that this problem requires further studies to prevent or minimize the possible related hazards.

Keywords

Landslides • Volcano instability • Back analysis • Strength parameters • Azores • Pico Island

1 Introduction

Landslides are the more visible process of volcanoes' erosional evolution, including large failures which can generate debris avalanches with high mobility and velocity (e.g., Siebert, 1996) and large flank collapses that can generate tsunamis with devastating effects even on distant coasts (e.g., McGuire, 2006).

Volcanic edifices stability analysis requires a good knowledge of the rock masses' strength properties, groundwater levels, and the presence of low strength zones, among other factors. However, acquiring reliable strength estimates is a challenging task due to the large volumes of rock involved and the uncertainties on the presence and position of low-strength layers, which may be weak pyroclastic deposits, weathered rock, or interbedded soil beds. In fact, in volcanic complexes, the strength differences between the rock samples and the weaker zones or layers tend to be very high, the latter the main conditioning factor in slope failure (Thomas et al., 2004).

To improve the knowledge on this topic, the study case of the steep volcanic edifice of the Pico stratovolcano (Pico Island, Azores) was considered. There is well-preserved evidence of 9 major landslides in the volcano flank, which top is located at the upper part of the volcano, and their deposits extend to its base. Of these landslides, the smaller one also has less preserved field evidence and was discarded for further analysis. The remaining 8 landslides were an object of a geometrical reconstruction of the initial topographic surface to enable systematic back analyses to obtain estimates of the failure strength parameters. These landslides correspond to the failure of the superficial parts of the volcanic edifice, mainly controlled by the separation surfaces of the different lava flows that build up the volcano. Furthermore, the angle of reach of the downslope landslide debris was also estimated to calculate the potential run-out distance of future slope failures, which are likely to occur due to several open tension cracks in the upper part of the volcano. The results obtained and the preliminary hazard implications are presented in this work.

F. Marques (✉)
Departamento de Geologia, Instituto D. Luiz (IDL), Faculdade de Ciências da Universidade de Lisboa, Lisboa, Portugal
e-mail: fsmarques@fc.ul.pt

A. Malheiro et al. (eds.), *Advances in Natural Hazards and Volcanic Risks: Shaping a Sustainable Future*, Advances in Science, Technology & Innovation, https://doi.org/10.1007/978-3-031-25042-2_13

2 Setting and Methods

A near conical shape characterizes the Pico stratovolcano with a slight bulge in the southern flank (Fig. 1). It is built over a plateau at an elevation of circa 1000 m, with flanks rising steeply (mainly 32–38°) to the border of the former crater, located at near 2250 m, which is filled by lavas that flowed out to the east and SSE, overlain by a small cone which rises to 2351 m. The Pico volcano is part of the youngest volcanic complex on the island, the Montanha Volcanic Complex (Fig. 1), with the Pico volcano probably younger than 5k years and is mainly composed of pahoehoe basalt lava flows with interbedded pyroclasts and breccias (Nunes, 1999). The available information suggests several faults cut the volcano with dominant directions NNW-SSE, NE-SW, and E-W. Also, Nunes (1999) suggested that they may have some relations with the generation of some landslides (landslides 1, 6 and 9, Fig. 1).

The landslides seem to be mainly controlled by the surfaces which separate the different lava flows which build up the volcano. The 1, 6, 7, 8 and 9 landslides top scarp generated along with the contact between the inner border of the crater located at 2250 m and the lavas which later fill it, with the contact area being a weaker zone favourable for tension crack development. The landslides 2, 3 and 4 started at the southern bulge of the volcano, and around their top, they exhibit several open tension cracks, which were mapped by interpretation of available orthophoto maps. These landslides

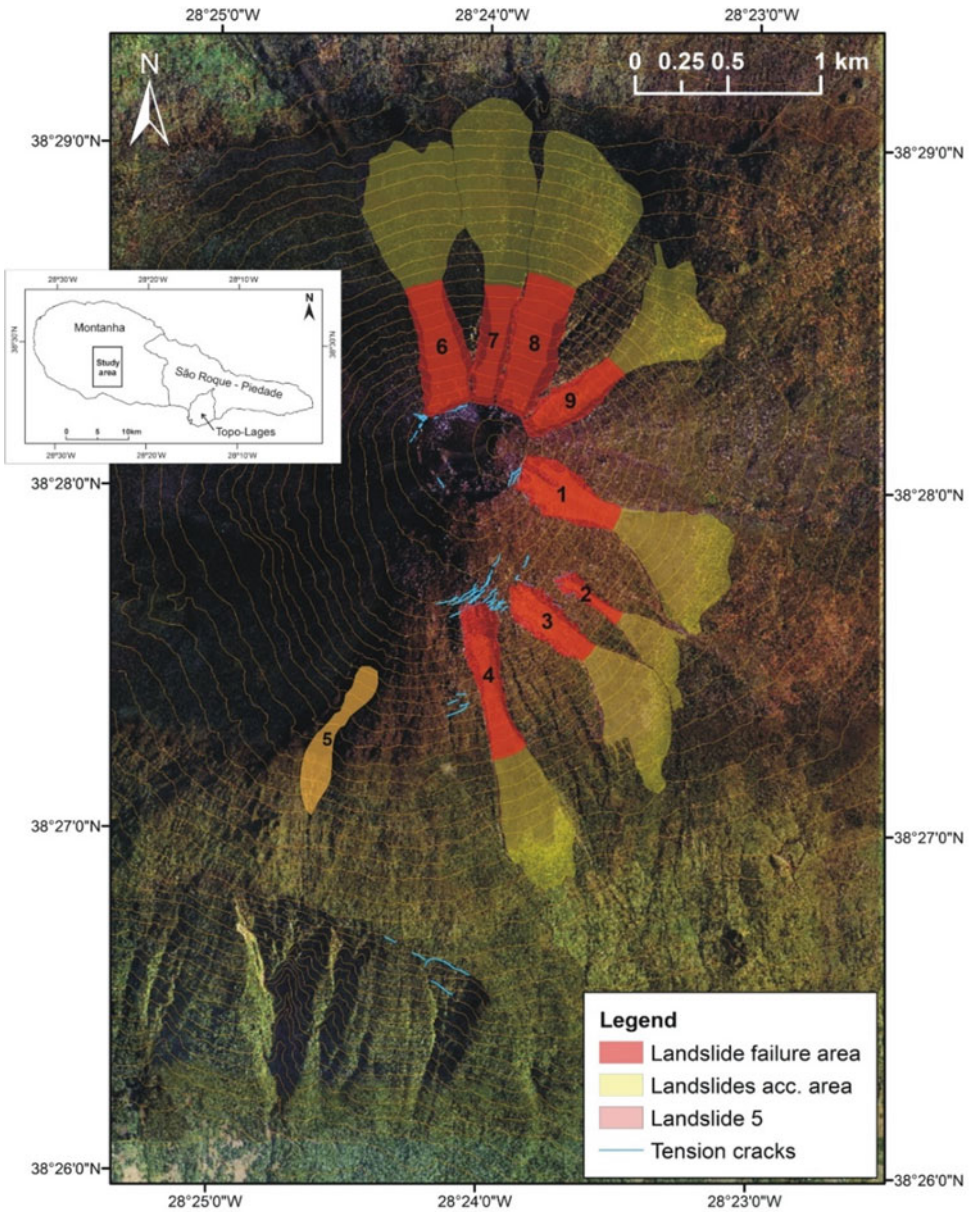

Fig. 1 Inset: Study area localization and significant geological units in Pico Island. Landslides and tension crack mapping over orthophoto map (http://wssig5.azores.gov.pt/idea/services) and contour lines (separation 50 m). The S. Caetano cliff is visible in the SSW area

Table 1 Summary data and results of the landslides studied

Landslide	Failed area (m^2)	Max. height (m)	Rupture length (m)	Slope angle (°)	Ratio depth/length	ϕ′ static c′ = 10 kPa (°)	ϕ′ ps. c′ = 10 kPa (°)	Shadow angle (°)
1	124,388	52	775	36.9	0.067	40.2	40.4	32.8
2	31,662	26	492	37.6	0.052	40.8	40.9	32.5
3	93,681	48	925	35.3	0.052	39.6	40.0	32.6
4	133,914	41	900	35.3	0.045	39.4	39.8	31.7
6	171,663	67	793	38.6	0.085	41.1	40.9	34.1
7	106,472	82	831	39.2	0.099	40.4	40.3	33.6
8	190,190	83	921	37.1	0.090	40.2	40.1	34.0
9	100,522	64	982	35.1	0.065	38.7	39.0	32.2

are relatively thin, with depth-length ratios of the failure surface lower than 0.1 (Table 1).

To enable the landslides back analysis, their middle cross-section geometry was estimated using the longitudinal profile along the deepest part of the failure surfaces and the topographic profiles drawn along the lateral margins of each failed area, based on the information of a topographic map with contour line interval of 5 m. The accuracy of the reconstructed geometry of the landslides is naturally affected by the uncertainties in the former topographic surface estimation and by the fact that part of the failure surfaces is covered by debris. However, it is felt that these uncertainties are minor compared to the thickness of the landslides, having a minor influence on the back analysis results.

The reconstructed geometry of the landslides, with a maximum depth ranging from 26 to 83 m and failure surface areas from 32×10^3 to 190×10^3 m^2, enabled a systematic back analysis made using the limit equilibrium Generalized Limit Equilibrium method with the GeoSlope SlopeW v.5 software. Considering the unavailability of water levels data, the high secondary permeability of the rock masses involved, the steep slope, the upslope limited rainwater collection area, but a very high estimated rainfall (up to 5,000 mm/year between elevations of 800–1500 m decreasing upwards to values lower than 500 mm/year (Azevedo, 2014)) an estimated high-water level located at 50% of the height of failed rock mass was considered, using the pore pressure ratio function value of ru = 0.1135, to maintain similar pore pressure conditions for all landslides. This condition is assumed to be quite extreme and exceptional and only possible with very intense and concentrated rainfall, sudden snowmelt, or a combination of the two situations.

Pseudo-static back analysis under dry conditions was also made and considering the expected maximum seismic actions in the building code in force (Eurocode 7, Portuguese National Annexes; Carvalho et al., 2001), which provided a horizontal pseudo-static coefficient of $k_h = 0.1$, equal to one half of the maximum expected acceleration, and $k_v = 0.05$, equal to one half of the horizontal coefficient, as suggested by Jibson (2011). The back analyses were made using values of effective cohesion (c′) of 0, 10, 25, 50 and 100 kPa, for a safety factor equal to 1.0, to obtain comparable values of the friction angle for each landslide and to assess the narrower range of strength parameters for all the landslides studied.

The landslides shadow angle or angle of reach was also measured from the interpreted pre-failure crest of each landslide and the distal limit of the debris cone generated by each one, which was interpreted by analysis of the contour lines of the topographic map used (contour line separation of 5 m) and of orthophoto maps. The orthophoto maps interpretation enabled the preliminary mapping of open tension cracks, mainly in the southern flank of the volcanic edifice (Fig. 1).

3 Results, Discussion and Concluding Remarks

The back analyses results (Fig. 2) indicated a narrow range of friction angles required to obtain a safety factor equal to 1 for cohesion values between c′ = 0 kPa and c′ = 25 kPa, with the narrower range corresponding to c′ = 10 kPa, with friction angles between 38.7 and 41.1° (mean value 40.1°), for wet conditions (ru = 0.1135), and similar values for the pseudo-static analysis, with c′ = 10 kPa and friction angles between 39.0 and 40.9° (mean value 40.2°). Due to the wide range of maximum depth of the interpreted failure surfaces (26–82 m, Table 1), these strength parameters seem reasonable for the preliminary long-term stability assessment for slope failures affecting the superficial parts, i.e., failures mainly controlled by separation surfaces between successive lava flows of the Pico and other volcanic edifices with similar composition and geometry.

It must be noticed that the strength data obtained in this study is much lower than the data obtained in the very

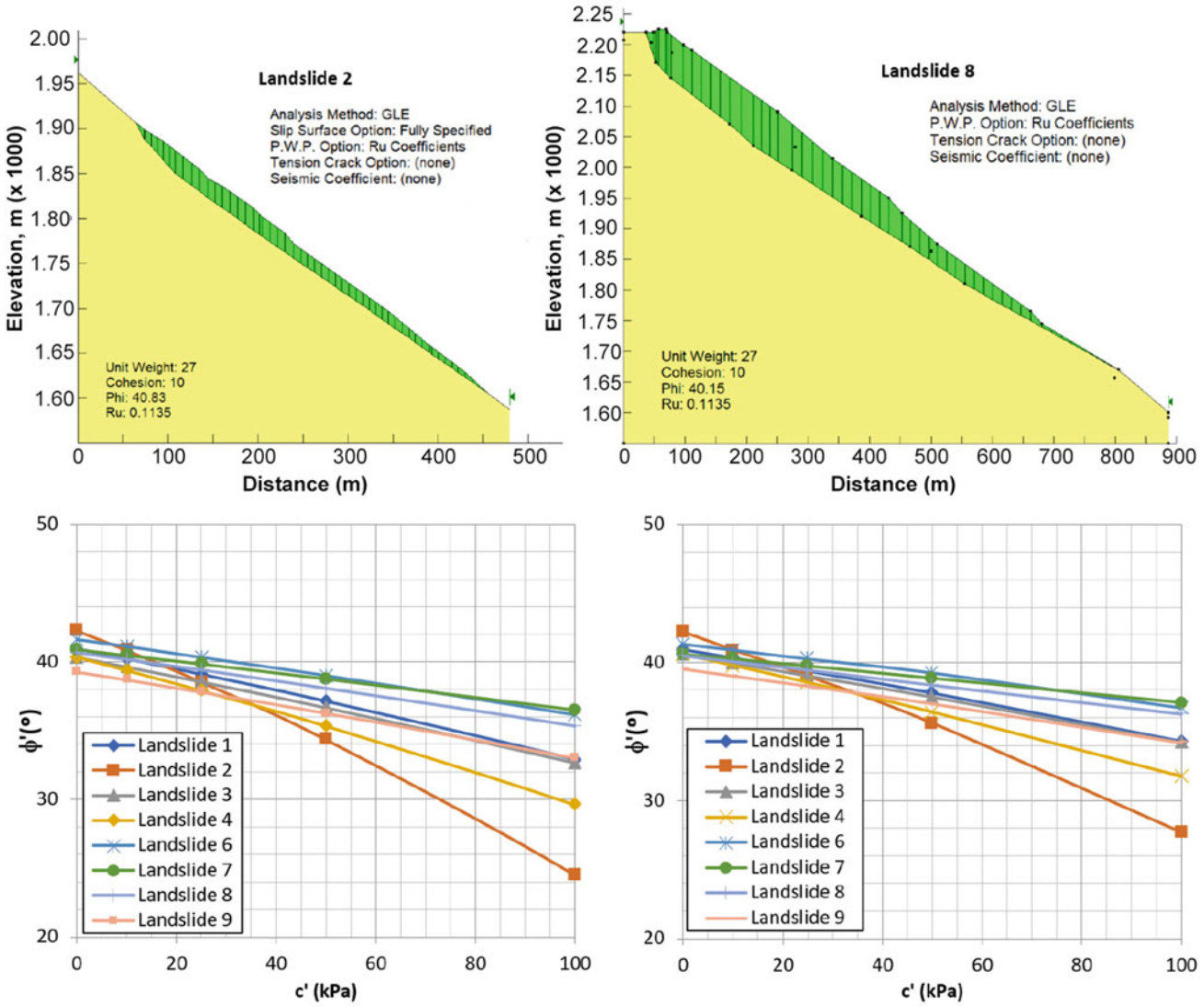

Fig. 2 Top: example profiles and back analysis results—landslides 2 (left) and 8 (right). Bottom: cohesion and friction angle required for safety factor equal to one. Left: static analysis, ru = 0.1135. Right: dry pseudo-static analysis, $k_h = 0.1$, $k_v = 0.05$

detailed studies of the Teide volcano (Tenerife) by Seisdedos et al. (2012), which were devised to assess the pre-landslide volcanic edifice models for Güímar and La Orotava mega-landslides. In fact, these authors studied the global rock mass properties for the large-scale failure of the volcanic edifice, which has a limited influence on lava flow bedding planes, which is not the case for lateral, comparatively shallow flank failures.

The landslide's shadow angle measured provided values between 31.7 and 34.1°, with a mean value of 33.0°, which do not show relations with the landslide scar elevation or the planimetric area.

Most of the Pico volcano's surrounding area is inhabited, but its southern flank is limited by the S. Caetano cliff and the village near the cliff toe. The steepest slope profiles from the volcano top to the cliff's crest reach a global slope angle of 30.4°, which is close to the landslide's shadow angle. Due to the uncertainties of the landslides shadow angle assessment, it cannot be excluded that a large landslide at the upper part of the volcano may occur, and the debris to travel down to the S. Caetano cliff crest and, with the increased downslope, the debris could strike the S Caetano village. It is also possible that a failure at the S. Caetano cliff crest can strike the locality due to the steep cliff profile and open tension cracks at the cliff crest. These preliminary results suggest that this problem requires further studies, namely installing deformation/displacement measuring systems, to prevent or minimize the possible related hazards.

Acknowledgements This work was funded by the Portuguese Fundação para a Ciência e a Tecnologia (FCT) I.P./MCTES through national funds (PIDDAC)—UIDB/50019/2020. A. Brum da Silveira and J. Madeira are acknowledged for drawing attention to the Pico volcano stability problems and providing the topographic base.

References

Azevedo, E. B. (2014). Pico Island: Climate overview. In V. H. Forjaz (Ed.), *Pico Island natural history handbook* (pp. 16–28). Observatório Vulcanológico e Geotérmico dos Açores.

Carvalho, A., Sousa, M. L., Oliveira, C. S., Campos-Costa, A., Nunes, J. C., & Forjaz, V. H. (2001). Seismic hazard for the Central Group of the Azores Islands. *Bollettino Di Geofisica Teorica Ed Applicata, 42*(1–2), 89–105.

Jibson, R. W. (2011). Methods for assessing the stability of slopes during earthquakes: A retrospective. *Engineering Geology, 122*, 43–50.

McGuire, W. J. (2006). Lateral collapse and tsunamigenic potential of marine volcanoes. *Geological Society, London, Special Publications, 269*(1), 121–140.

Nunes, J. C. (1999). *A actividade vulcânica na ilha do Pico do Plistocénico Superior ao Holocénico: mecanismo eruptivo e hazard vulcânico*. Ph.D. thesis, Universidade dos Açores, Ponta Delgada.

Seisdedos, J., Ferrer, M., & Gonzalez de Vallejo, L. (2012). Geological and geomechanical models of the pre-landslide volcanic edifice of Güímar and La Orotava mega-landslides (Tenerife). *Journal of Volcanology and Geothermal Research, 239–240*, 92–110.

Siebert, L. (1996). Hazards of large volcanic debris avalanches and associated eruptive phenomena. In R. Scarpa & R. I. Tilling (Eds.), *Monitoring and mitigation of volcano hazards* (pp. 541–572). Springer.

Thomas, M. E., Petford, N., & Bromhead, E. N. (2004). Volcanic rock-mass properties from Snowdonia and Tenerife: Implications for volcano edifice strength. *Journal of the Geological Society, 161*, 939–946.

Improving Infrastructure Management for Rockfalls During Rainfall Events

Sergio Leyva, Noelia Cruz-Pérez, Jesica Rodríguez-Martín, and Juan C. Santamarta

Abstract

Hazard refers to the probability of occurrence of a process (rockfall) with a given level of intensity or severity within a given time period and a specific area. For its evaluation, it is necessary to know the following aspects: where and when the processes occurred in the past, their intensity and magnitude, and the frequency of occurrence. The exposed elements can be people, goods, property, infrastructure, etc., which may suffer the consequences of rockfall directly or indirectly. Calculating the risk allows decisions and tailored solutions to be defined on protective measures and prioritises actions in the most at-risk sectors. Therefore, this study aims to describe the analysis of information on rainfall-induced rockfalls in Anaga, Tenerife (Canary Islands), in order to facilitate the improvement of road safety and operation in this geographical area by enabling the Road Maintenance and Conservation Services to mobilise the resources or means necessary to restore the roads to their previous state after the event/s or, where appropriate, to establish traffic limitations or restrictions to mobility.

Keywords

Vulnerability • Risk management • Hazard • Canary Islands

S. Leyva
Universidad Politécnica de Madrid, Madrid, Spain

N. Cruz-Pérez · J. C. Santamarta (✉)
Departamento de Ingeniería Agraria y del Medio Natural, Universidad de La Laguna (ULL), San Cristóbal de La Laguna, Spain
e-mail: jcsanta@ull.es

J. Rodríguez-Martín
Departamento Técnicas y Proyectos en Ingeniería y Arquitectura, Universidad de La Laguna (ULL), San Cristóbal de La Laguna, Spain

1 Introduction

Climate change favours the occurrence of natural hazards, and slope instability processes are part of these. Climate evolution may lead to changes in precipitation rates and therefore affect the incidence of instability events, both landslides and landslides since it is evident that there is an unequivocal relationship between the occurrence of both phenomena (Margottini et al., 2013).

Rockfalls are frequent in volcanic areas due to the heterogeneous composition of the rocks in these areas (Sarro et al., 2020). For this reason, a correlation between the probability of rockfalls and rainfall episodes in a rural area of the island of Tenerife, Spain, has been developed in this study.

The rural park of Anaga is a protected area of the island of Tenerife, located in the northeast of the island. Its population amounts to 2,500 people distributed in 26 different settlements. Due to its location and altitude in this island area, numerous rainfall episodes accumulated in the winter months.

This study has clear implications for management as a predictive tool in the prevention of emergencies by the Civil Protection and Emergency Services by being able to relate the expected rainfall intensity with the alert levels decreed in Tenerife by the General Directorate of Security and Emergency of the Government of the Canary Islands (pre-alert, alert and maximum alert, whose thresholds are set at 60, 100 and 180 mm in 12 h respectively). In this sense, it is essential to highlight that the current configuration of the rural park of Anaga, in terms of its connectivity, consisting of a backbone road with isolated branches to each of the population centres, implies serious mobility problems (or even isolation) in the case of partial road closures caused by rockfalls, since in most cases there are no alternative roads.

A. Malheiro et al. (eds.), *Advances in Natural Hazards and Volcanic Risks: Shaping a Sustainable Future*, Advances in Science, Technology & Innovation, https://doi.org/10.1007/978-3-031-25042-2_14

2 Methods

Two types of Events (occurrence of rockfalls) have been considered for data processing: Events and Non-Events. An Event or a Non-Event is recorded according to the following criteria:

- Event: Total number of landslides occurring on a given day. The precipitation associated with this event is the maximum precipitation recorded in "N" on previous days, including the day of the event. This criterion is because rainfall on a given day may cause a landslide on subsequent days.
- Non-Events: Total number of consecutive days without landslides. A non-event is considered to have occurred when no landslide has been recorded in N days prior to the non-event. This criterion is intended to be homogeneous with the previous definition of the event. It avoids associating precipitation with a non-event that actually causes a detachment in one of the N subsequent days. Also, in the case of a non-event, the precipitation associated with this non-event is taken as the maximum recorded in the previous "N" days, including the day of the non-event.

The starting point is a daily record of rainfall and landslides that have taken place in Anaga, Tenerife, for over 6 years. The input data must contain 5 columns with the following records:

- First column (id). Identification number of the record
- Second column (date). Date of the record
- Third column (rain). Maximum rainfall was recorded near the landslide site's meteorological station(s). This precipitation is expressed in "mm".
- Fourth column (event). This column indicates the value "1" if a landslide occurred on that date and "0" if no landslide was recorded.
- Fifth column (nevent). Number of detachments that took place that day in addition to the one indicated in the "event" column. That is, a 0 in the "nevent" column indicates that only 1 detachment was recorded that day.

Table 1 shows an example containing 18 input data records.

The calculation of the probability of an Event occurring is defined for each of the different precipitation intervals established for the area under study. The precipitation intervals taken for the study of the Anaga area are shown below: $p = 0$ mm, $0 < p <= 5$ mm, $5 < p <= 10$ mm, $10 < p <= 15$ mm, $15 < p <= 20$ mm, $20 < p <= 25$ mm, $25 < p <= 30$ mm, $30 < p <= 35$ mm, $35 < p <= 40$ mm, $40 < p <= 45$ mm, $45 < p <= 50$ mm, $50 < p <= 75$ mm, $75 < p <= 125$ mm, $p > 125$ mm.

The probability of an event occurring will be calculated for each of the precipitation intervals as:

$$\text{P.event} = (\text{Events})/(\text{Events} + \text{Non-Events}) \quad (1)$$

Table 1 Example of input data

Id	Date	Rain	Event	No. occurrences
1	01/07/2010	0.0	0	0
2	02/07/2010	16.1	0	0
3	03/07/2010	2.3	0	0
4	04/07/2010	0.0	1	0
5	05/07/2010	0.0	0	0
6	06/07/2010	15.1	0	0
7	07/07/2010	6.7	1	1
8	08/07/2010	0.0	0	0
9	09/07/2010	0.0	0	0
10	10/07/2010	0.0	0	0
11	11/07/2010	0.0	0	0
12	12/07/2010	4.1	0	0
13	13/07/2010	1.0	0	0
14	14/07/2010	18.7	1	2
15	15/07/2010	0.0	0	0
16	16/07/2010	1.1	0	0
17	17/07/2010	0.0	0	0
18	18/07/2010	7.1	1	0

The result of this calculation varies between 0 and 1, and indicates the ratio between the Events that have taken place concerning the total number of Events (Events + Non-Events). This probability ratio could estimate the likelihood of an event occurring in future situations for each precipitation interval by analysing many records.

3 Results and Discussion

The landslides of blocks and rocks are produced by the loss of stability conditions due to a series of preconditioning factors and in the presence of other external factors that trigger them. The Anaga massif is characterised by its intense relief with average slopes of 30° or even higher in large sectors, subjected to intense erosion and highly altered and weathered areas with the presence of material that looks like soil, although the structure of the original rock can be recognised. Rainfall causes the soaking or saturation of this material, which in some cases causes its instability in the following hours or days due to the action of the sun and the wind that contribute to its drying with the consequent increase of the surface tension and decrease of its apparent cohesion.

The data were processed using a Python code developed ad hoc. The final result obtained in calculating the probability of a rockfall event as a function of precipitation is shown in Fig. 1.

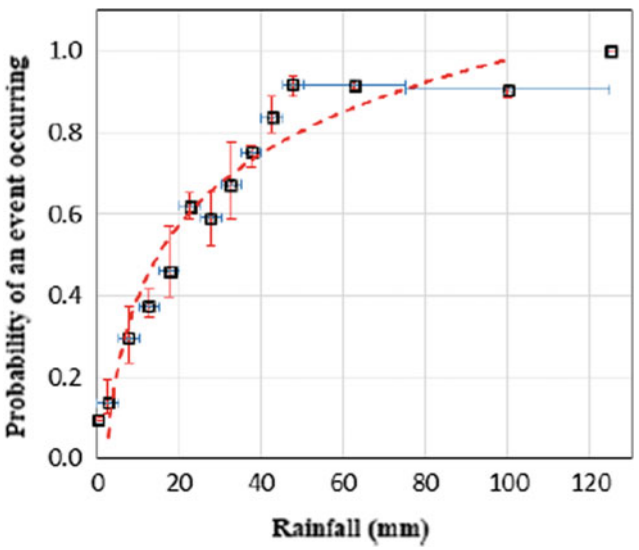

Fig. 1 Probability of a rockfall event occurring in Anaga, as a function of daily precipitation, considering N = 4, 3, 2 and 1 day. *Source* González de Vallejo et al. (2020)

The consideration of the occurrence of an Event or a Non-event is linked to a previous period of "lack" in which rainfall could have caused a landslide, or on the contrary, that level of rainfall did not cause any landslide, respectively. The Python code developed allows defining the number of days (N) before the landslide to which the maximum precipitation of the event is associated and the number of consecutive days without landslides considered Non-event. In the latter case, the maximum precipitation during those days would also be associated with it. In this way, a homogeneous criterion is sought in the definition of both Events: Event and Non-Event.

The results obtained by applying this methodology to 2,192 data with dates, precipitation levels and landslides recorded between July 1, 2010 and June 30, 2016 in the Anaga area, Tenerife, are presented in Table 2.

From the results obtained, it can be deduced that 41 Events happened without any precipitation (p = 0 mm) on the day of the detachment, nor the three previous ones. This situation represents 7% of the total events compared to 93% with some precipitation levels. With precipitation more significant than 125 mm, there are no four consecutive days without a landslide.

Calculating the mean value for all intervals, it is obtained that: (i) 39% of the maximum precipitation occurs the same day as the rockfalls event; (ii) 26% the day before, (iii) 15% two days before, and (iv) 20% on the four days before. Therefore, almost 40% of the Events are related to the maximum precipitation happening on the day of the rockfalls event.

Table 2 Anaga results for N = 4 days before, included in the event or non-event

Interval (mm)	Events	Non-events	Event + non-events	Prob. event
p = 0	41	363	404	0.101
0 < p < = 5	101	809	910	0.111
5 < p < = 10	50	164	214	0.234
10 < p < = 15	51	95	146	0.349
15 < p < = 20	31	47	78	0.397
20 < p < = 25	44	31	75	0.587
25 < p < = 30	25	18	43	0.581
30 < p < = 35	34	24	58	0.586
35 < p < = 40	25	10	35	0.714
40 < p < = 45	16	4	20	0.8
45 < p < = 50	15	1	16	0.938
50 < p < = 75	68	7	75	0.907
75 < p < = 125	31	4	35	0.886
p > 125	22	0	22	1.0

4 Concluding Remarks

Undoubtedly, a correlation can be established between heavy rainfall events in the rural area of Anaga in Tenerife and the higher probability of rockfall events. These landslides are even more critical when they affect roads and access areas since they hinder the people's daily mobility in these rural areas. Therefore, a firm strategy is needed to minimise the population's exposure and material assets to these risks in areas with volcanic terrain and heavy rainfall.

The possibility of differentiating and delimiting by road the probabilities of occurrence of events according to the expected rainfall intensity is possible, but this would require extending the study period to have a greater volume of data and information available to guarantee the method's reliability. Also, this study should not be considered a static element. Nevertheless, the validity of its conclusions should be corroborated or, if necessary, revised and updated, extending its temporal scope to the present.

Acknowledgements This work has been developed with the financial support of the Interreg Atlantic Area Programme under grant agreement No. EAPA_884/2018 (AGEO Project).

References

González de Vallejo, L. I., Hernández-Gutiérrez, L. E., Miranda, A., & Ferrer, M. (2020). Rockfall hazard assessment in volcanic regions based on ISVS and IRVS geomechanical indices. *Geosciences, 10*, 1–20.

Margottini, C., Canuti, P., & Sassa, K. (Eds.). (2013). Landslide science and practice. Proceedings of the second world landslide forum. In *Landslide science and practice: Landslide inventory and susceptibility and hazard zoning* (Vol. 1). Springer.

Sarro, R., María Mateos, R., Reichenbach, P., Aguilera, H., Riquelme, A., Hernández-Gutiérrez, L. E., Martín, A., Barra, A., Solari, L., Monserrat, O., Alvioli, M., Fernández-Merodo, J. A., López-Vinielles, J., & Herrera, G. (2020). Geotechnics for rockfall assessment in the volcanic island of Gran Canaria (Canary Islands, Spain). *Journal of Maps, 16*(2), 605–613.

Detecting Anomalies in Volcanic Ashfall Forecast During Large Volcanic Eruptions: Sakurajima Taisho Eruption Case

Haris Rahadianto, Sudip Roy, Tetsuya Takemi, Masato Iguchi, and Hirokazu Tatano

Abstract

In the form of fine ashes (i.e. ashfall), tephra affects vast, vulnerable areas with deadly consequences and long-term impacts. Moreover, both eruption scale and wind conditions exacerbate the catastrophe to a broader range. Accordingly, countries with volcanic risks have developed early warning systems to reduce the ashfall's impact when a powerful explosive eruption occurs. Such systems utilize the prediction of expected eruption coupled with the numerical weather forecast to alert the people at risk and prepare the response activities. However, abrupt weather can influence the ashfall forecast to have inaccurate warnings. Here, we evaluate the quality of the forecast results as an early warning or an evacuation policy. Using the Sakurajima Taisho eruption as a case study, we simulate a volcanic ash dispersal process with two different wind data, predictive and historical data. This study found some alarming deviations (i.e. anomalies) in the ashfall forecast under specific weather conditions. The anomalies bring errors in defining the impact areas and unforeseen damages and losses. Furthermore, this study analyses the underlying pattern that causes a disturbance in the ashfall forecast and suggests improving the forecast results to enhance decision-making during crises.

Keywords

Large volcanic eruption • Ashfall forecast • Sakurajima volcano • Anomalies

1 Introduction

Large volcanic eruptions impose catastrophic dangers to society due to disastrous impacts on various temporal and spatial scales of socio-economic systems. Of all products ejected from the volcano, ashfall (i.e. tephra in the form of very fine ashes) is the most extensive hazard, with lethal effects on human life and long-lasting disruptions in the lifeline infrastructures (Bonadonna et al., 2021). Furthermore, heavy ash fallout can enforce the wide evacuation of affected residential areas (Iguchi, 2020).

Japan may face such a catastrophe in the following decades, based on the current precursory phenomena happening in the Sakurajima volcano. Sakurajima volcano tends to have another large-scale explosive eruption similar to the Taisho eruption in 1914, following 130 years return period (Hickey et al., 2016). Therefore, the Japan Meteorological Agency (JMA) introduced a sophisticated Volcanic Ash Fall Forecast (VAFF) system to reduce the impacts of ashfall hazards. This system regularly produces an ashfall forecast on a hypothetical eruption utilizing the Grid Point Values (GPV) wind forecast data. Its forecast results provide vital information to designate a possible exposure area before eruption (Hasegawa et al., 2015). However, due to the lack of occurrences of recent large-scale explosive eruptions, the accuracy of the VAFF system still cannot be confirmed completely. Moreover, as wind conditions influence the ash dispersal proses, any extraordinary weather phenomena during the eruption will bring more severe impacts to wider locations (Macedonio et al., 2016; Poulidis et al., 2018).

Using the Sakurajima Taisho eruption as a case study, we evaluate the ash fall forecast results as an early warning or an

H. Rahadianto (✉)
Graduate School of Informatics, Kyoto University, Kyoto, Japan
e-mail: haris@imdr.dpri.kyoto-u.ac.jp

H. Rahadianto · T. Takemi · M. Iguchi
Disaster Prevention Research Institute, Kyoto University, Kyoto, Japan

S. Roy · H. Tatano
Indian Institute of Technology Roorkee, Roorkee, India

A. Malheiro et al. (eds.), *Advances in Natural Hazards and Volcanic Risks: Shaping a Sustainable Future*,
Advances in Science, Technology & Innovation, https://doi.org/10.1007/978-3-031-25042-2_15

evacuation policy and try to find the condition where it will deviate more than usual (i.e. anomalies). First, we did two ash dispersal simulations using different wind inputs with a volcanic ash transport and dispersal model (VATDM). Then, we evaluate the discrepancies between simulation results and examine the leading cause of such a disturbance in the forecast results to improve the current disaster countermeasure plans.

2 Simulation Method and Anomalies Definition

We conduct an ash dispersal simulation of the Taisho eruption (Omori, 1914; Todde et al., 2017) using the PUFF model (Searcy et al., 1998; Tanaka, 1994) with two different wind data, GPV as predictive data and JRA-55 reanalysis data as historical wind data. Here we also compare the performance of real-time wind forecast data and 24 h-prior wind forecast data. The description of the two weather datasets is available in Table 1.

The complete set of the simulation based on the fixed scenario of the Taisho eruption (VEI 4) can be seen in Table 2. The particle grain size distribution and total mass eruption agree well with the observation by Todde et al. (2017).

We then examine the differences between the two simulation results regarding the evacuation zone designation from ashfall hazards. The results from the simulation conducted on historical wind data served as ground truth. Meanwhile, other simulation results are the forecast results where the evacuation zone will be assumed in this hypothetical eruption case. Assuming all the areas of concern during a large-scale eruption (i.e. affected by ashfall under a certain damage threshold), we can assign each area inside it whether to evacuate or not. The designated evacuation zone should cover all areas determined by the ground truth (zero miss) and keep a minimum amount of areas outside it (minimum false alert). In principle, using only information from the forecast is difficult and cannot cover all those areas at risk.

A safety margin was added to ensure the evacuation zone from the ashfall forecast will always cover all critical areas at risk to alleviate this issue. Here, the evacuation zone is designated strictly following the dimension of the simulation results, which is in a $0.01° \times 0.01°$ grid (~ 1 km^2). The safety margin consists of refinement to the ashfall forecast results by adding safety boundary lines, reducing the damage threshold, and expanding the forecast area to several degrees in clockwise and counter-clockwise directions. Therefore, we can find the most optimum safety margin to be applied to all cases following:

$$\min_{\tilde{s} \in S} \sum_{n \in N} f_i(a|\tilde{s}), \tag{1}$$

subject to:

$$m_i(a|\tilde{s}) = 0, \forall n \in N \tag{2}$$

Table 1 Description of wind data sources used in this study

Parameters	GPV (Global Spectral Model)	JRA-55
Horizontal grid system	Reduced Gaussian	Reduced Gaussian
Horizontal resolution	TL959 ($\sim$20 km)	TL319 ($\sim$55 km)
Vertical levels	128 levels up to 0.01 hPa	60 levels up to 0.1 hPa
Forecast length	132 h	–
Analysis scheme	4D-Var	4D-Var

Table 2 Input values for the simulations used in this study

Parameters	Value
Total initial number of particles	5000
Simulation time (hours)	96
Time step (s)	300
Horizontal coefficient (m/s)	150
Vertical coefficient (m/s)	1.5
Particle grain size distribution (mm)	0.01–100
Particle log mean grain size (mm)	1
Particle log standard deviation (mm)	2
Mean estimated eruption mass (10^{10} kg)	1.1
Mass eruption rate	5.8×10^6–2.7×10^{10}

$$\tilde{s} = \left\{\tilde{\Gamma}, \tilde{\Delta}, \tilde{\Lambda}\right\} \tag{3}$$

where $\tilde{s}$ is the optimum set of all possible safety margins S for N number of cases. The set of safety margin $\tilde{s}$ is optimum where the ashfall forecast result a has zero miss ($m_i = 0$) and a minimum number of total false alerts (f_i). The set of safety margin $\tilde{s}$ is the combination of the length of added safety line ($\tilde{\Lambda}$), reduced damage threshold ($\tilde{\Delta}$) and degree of forecast area expansion ($\tilde{\Gamma}$). From here, we may have several optimum sets of safety margins and recommend adopting a range of values to refine the ashfall forecast results as a general set of safety margins. Then, we can define the anomalies in all the cases that cannot have zero miss ($m_i = 0$) after applying the general set of safety margin $\tilde{s}$. We then investigate the main reason behind these particular cases.

3 Results

3.1 General Set of Safety Margin

A greedy heuristic search is done for all sets of safety margins described in the earlier section. Reducing the damage threshold will bring more false alerts, although it also increases the number of zero miss cases. Meanwhile, having a more comprehensive safety line can decrease the number of people who get false alerts but keep a high zero miss case. Expanding the ashfall forecast map appeared to affect establishing an effective and efficient evacuation zone positively. Figure 1 portrays all sets of safety margins and their performance with labels inside the figure referring to a safety margin set applied to the forecast results compared against ground truth.

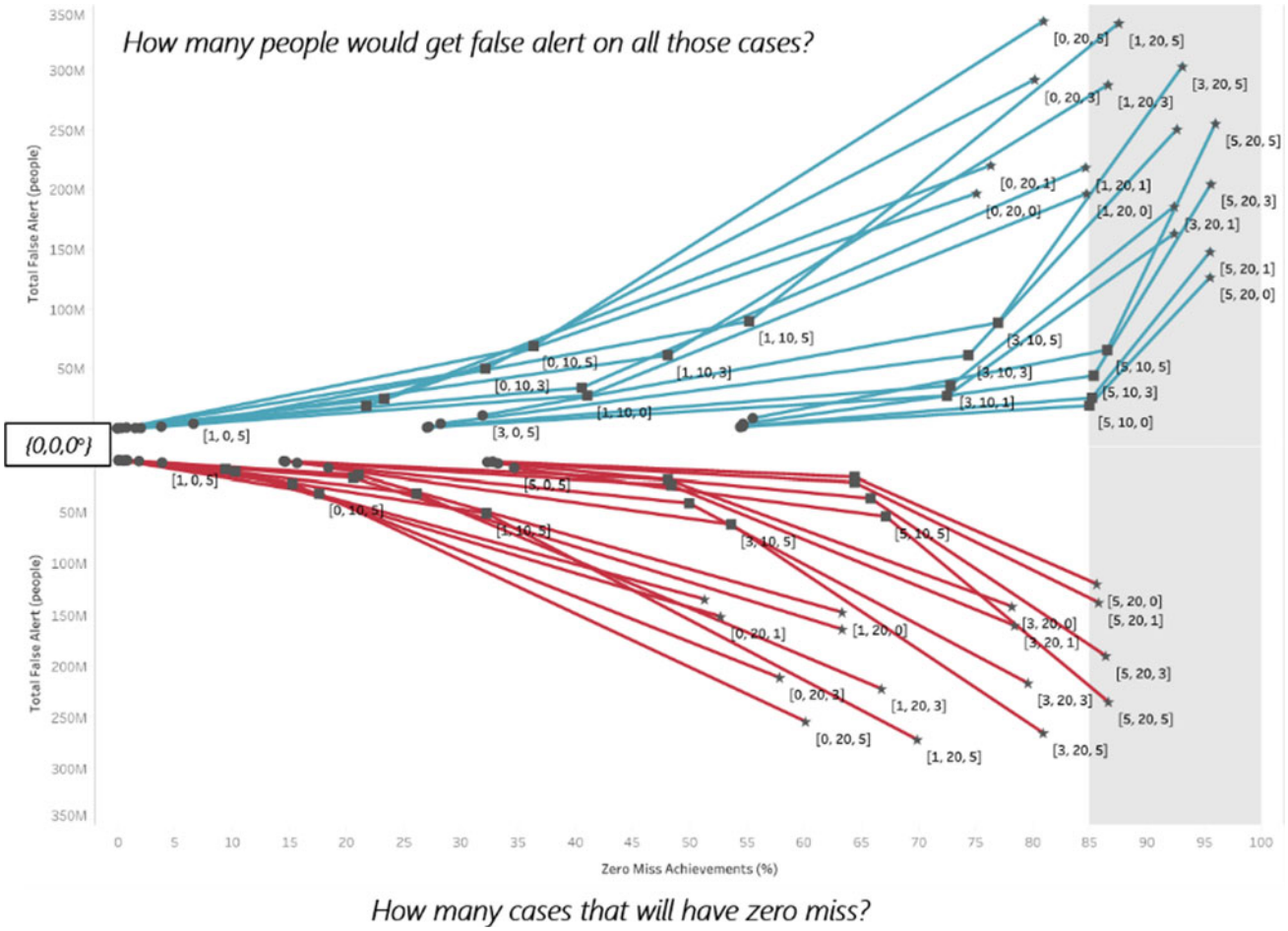

Fig. 1 The comparison of all sets of safety margin performance for real-time forecast data (blue) and 24 h prior forecast data (red) (Color figure online)

Table 3 Remained anomalies

Case	Features	Percentage of miss
Typhoons at summer	Rainfall, strong winds	27.19
Autumn rain fronts	Rainfall, thunderstorms	16.99
Heavy rain in summer	Record short-time rainfall	34.53
Exceptional high pressure in winter	Clear, sunny, slow winds	16.29

Comparing all results at once, it can be seen that the number of sets of safety margins that can achieve the high zero miss rate (>85%) is small. Furthermore, most of these sets also have varying false alerts per case. From these results, the recommendation to adopt a safety margin for deciding the evacuation zone due to ashfall during a large-scale eruption in Sakurajima can be derived. The recommended set of safety margins is adding up to a 5 km safety boundary line, using at most a 20 cm damage threshold and expanding the forecast result up to 10° in both directions, with more drastic sets of safety margins necessary to be applied on the 24 h forecast before the eruption.

3.2 Anomalies Results

Several cases did not achieve zero miss even after applying the safety margin (i.e. anomalies). The critical driver for the anomalies depends on the season, but essentially, it would occur during the condition with contrasting characteristics against the seasonal features, as shown in Table 3. Therefore, drastic and different sets of safety margins may need to be adopted when anomalies occur. For example, the measure can include a higher or different degree to expand the forecast result map, a longer safety line, and a higher reduction value for the damage threshold. However, a higher value safety margin will also return more false alerts.

4 Discussion

The complex nature of ashfall hazards depends on both the eruption magnitude and the wind condition at the time of the eruption, making it challenging to develop a complete preparation in advance (Bonadonna et al., 2021). This study found specific weather conditions when the ashfall forecast system (VAFF) will have weaker performance. Most of those cases occur due to extraordinary phenomena that bring a lot of precipitations (typhoons, heavy rains). Once we know that this condition affects the ashfall forecast results, it is critical to automatically detect such an event in advance when the eruption is expected shortly.

5 Concluding Remarks

This study confirms the performance of the ashfall forecast system for designating an evacuation zone during a large eruption event. Sets of safety margins were introduced to overcome the prediction error, and a general set was found with acceptable performance achieving a good zero miss rate by expanding the forecast result, reducing the damage threshold and adding a safety boundary line. However, even after applying the general safety margin, some anomalies were found, but those cases still did not get zero miss. One of the primary reasons is the exceptional weather phenomena with contrasting characteristics irrespective of seasonal features.

Acknowledgements The Tokio Marine Kagami Memorial Foundation supported this work.

References

Bonadonna, C., Biass, S., Menoni, S., & Gregg, C. E. (2021). Assessment of risk associated with tephra-related hazards. In P. Papale (Ed.), *Forecasting and planning for volcanic hazards, risks, and disasters* (Vol. 2, pp. 329–378). Elsevier hazards and disasters series.

Hasegawa, Y., Sugai, A., Hayashi, Y., Hayashi, Y., Saito, S., & Shimbori, T. (2015). Improvements of volcanic ash fall forecasts issued by the Japan Meteorological Agency. *Journal of Applied Volcanology, 4*(1), 2.

Hickey, J., Gottsmann, J., Nakamichi, H., & Iguchi, M. (2016). Thermomechanical controls on magma supply and volcanic deformation: Application to Aira caldera, Japan. *Scientific Reports, 6*(1), 32691.

Iguchi, M. (2020). Resilience to volcano- and landslide-related hazards. In M. Yokomatsu & S. Hochrainer-Stigler (Eds.), *Disaster risk reduction and resilience* (pp. 25–44). Disaster and risk research: GADRI book series. Springer.

Macedonio, G., Costa, A., Scollo, S., & Neri, A. (2016). Effects of eruption source parameter variation and meteorological dataset on tephra fallout hazard assessment: Example from Vesuvius (Italy). *Journal of Applied Volcanology, 5*(1), 5.

Omori, F. (1914). The Sakura-Jima eruption and earthquakes. *Bulletin of the Imperial Earthquake Investigation Committee, 8*, 1–630.

Poulidis, A. P., Phillips, J. C., Renfrew, I. A., Barclay, J., Hogg, A., Jenkins, S. F., Robertson, R., & Pyle, D. M. (2018). Meteorological

controls on local and regional volcanic ash dispersal. *Scientific Reports, 8*(1), 6873.

Searcy, C., Dean, K., & Stringer, W. (1998). PUFF: A high-resolution volcanic ash tracking model. *Journal of Volcanology and Geothermal Research, 80*(1), 1–16.

Tanaka, H. L. (1994). Development of a prediction scheme for volcanic ash fall from Redoubt volcano, Alaska. In *Proceedings of the First International Symposium on Volcanic Ash and Aviation Safety* (pp. 283–291). U.S. Geological Survey Bulletin.

Todde, A., Cioni, R., Pistolesi, M., Geshi, N., & Bonadonna, C. (2017). The 1914 Taisho eruption of Sakurajima volcano: Stratigraphy and dynamics of the largest explosive event in Japan during the twentieth century. *Bulletin of Volcanology, 79*(10), 72.

Rainfall and Its Infiltration Conditions for Landslide Occurred at Edge of Pyroclastic Flow Plateau in the Kyushu Island, Southwestern Japan

Takehiro Ohta, Jumpei Yamashita, and Yuki Sueda

Abstract

The torrential rains of July 2012 caused many landslides at the edge of the Aso pyroclastic flow plateau, consisting of the Aso-3 and the Aso-4 pyroclastic flow deposits in Kyushu Island, Japan. These landslides can be classified into two types: the caprock type, which occurred in Aso-4 areas, and the rainwater direct infiltration type, which occurred in Aso-3 areas. In both types, the landslide sliding surface is located in the lower pyroclastic fall layer of the pyroclastic flow deposit. The maximum hourly precipitation and effective precipitation with a half-life of 1.5 h control landslide occurrence and differ between landslide-prone and non-prone areas and between caprock and direct infiltration types. These parameters are larger in landslide-prone areas than in non-prone areas and are more significant in the caprock type than in the direct infiltration types. In a caprock type landslide, the effective stress in the pyroclastic fall layer estimated by theoretical calculations decreases with increased pore water pressure due to rainwater infiltration. Therefore, the landslide at the edge of the Aso pyroclastic flow plateau was caused by a decrease in effective stress in the pyroclastic fall layer.

Keywords

Pyroclastic flow plateau • Landslides • Precipitation • Infiltration • Effective stress

1 Introduction

The torrential rain in July 2012 caused many landslides in northern Kyusyu, Japan. In addition, the rains caused numerous landslides in the Aso caldera in Kumamoto Prefecture, resulting in a severe disaster. These landslides in the Aso Caldera have been studied by Kubota et al. (2012), Miyabuchi (2012), Matsushi et al. (2013), and Shimizu and Ono (2016). On the other hand, in Taketa City, Oita Prefecture, which had less precipitation than the Aso Caldera, landslides were concentrated at the edge of the Aso pyroclastic flow plateau. There is no detailed report on the landslide in Taketa City. This study aims to clarify the rainfall conditions that cause landslides at the edge of pyroclastic flow plateaus and their infiltration using rainfall data from Radar-AMeDAS (Automatic Meteorological Data Acquisition System). Radar-AMeDAS rainfall data is a 1 km mesh size time series raster data analyzed by combining weather radar and surface rain gauge data.

2 Heavy Rain in July 2012 in Kyushu

From July 11 to 14, 2012, torrential rains hit northern Kyushu. As a result, a back-building phenomenon occurred from Kumamoto City through the Aso area to the western part of Oita Prefecture, triggering a series of cumulonimbus clouds and heavy rain. Cumulative precipitation over the four days in Kumamoto, Aso, and Taketa was 367.5 mm, 816.5 mm, and 402 mm, respectively. Since the average monthly precipitation in Taketa City in July is 327.7 mm, a meteorological phenomenon that lasted only four days brought 1.2 times as much precipitation as the average monthly precipitation.

T. Ohta (✉) · J. Yamashita · Y. Sueda
Graduate School of Sciences and Technology for Innovation, Yamaguchi University, Yamaguchi, Japan
e-mail: takohta@yamaguchi-u.ac.jp

J. Yamashita
Kyushu Railway Company, Fukuoka, Japan

A. Malheiro et al. (eds.), *Advances in Natural Hazards and Volcanic Risks: Shaping a Sustainable Future*, Advances in Science, Technology & Innovation, https://doi.org/10.1007/978-3-031-25042-2_16

3 Geology of Study Area

The study area is located in the western part of Taketa City in the central part of Kyushu, 12–16 km northeast of Aso Caldera. The topography of this area is that of a pyroclastic flow plateau consisting of pyroclastic flow deposits that erupted from the Aso caldera. In this area, the Tamarai River and Takimizu River flowing from west to east have deeply eroded the plateau, forming steep slopes along the river.

The four pyroclastic flow deposits erupted from the caldera are Aso 1, -2, -3, and -4, and the pyroclastic fall layers Aso 1–2, 2–3, and 3–4 are distributed between each pyroclastic flow deposit (Ono et al., 1977). In the eastern part of the study area, Aso 2–3 pyroclastic fall layer and Aso-3 pyroclastic flow deposits are distributed on the slopes, and in the western part, Aso-3–4 pyroclastic fall layer and Aso-4 pyroclastic flow deposits are distributed on the slopes. Aso-3 flow deposits are non-welded or weak to moderately welded. Aso-4 flow deposit consists of a non-welded part and a substantial welded part, and the strong welded part forms caprock on the steep slope.

4 Method

4.1 Aerial Photointerpretation

The landslide sites and convex/concave slopes were determined by aerial photographs acquired in 2012 and 2016.

4.2 Field Survey

The detailed topography and geology around the landslide sites, i.e., slope (i), slope (ii) and slope (iii), were ascertained through field surveys. The sliding plane of each landslide was estimated from the detailed topography. On the slope of the Aso-4 area, the rock mass strength of each stratum distributed in the landslide site was measured in situ by the rock Schmidt test hammer test and/or needle penetration test.

4.3 Precipitation Analysis

Precipitation features were analyzed using the radar-AMeDAS time series raster data. The antecedent precipitation, maximum hourly precipitation, daily precipitation on July 12, cumulative precipitation, and effective precipitation with a half-life of 1.5 and 72 h were calculated for each 1 km mesh.

4.4 Calculation of Pore Water Pressure and Effective Stress at Subsurface

Most landslides are caused by changes in pore water pressure and effective stress in the subsurface ground. Imaizumi and Miyamoto (2013) proposed a theoretical calculation method for pore water pressure and effective stress in multi-layered structures due to vertical seepage flow. Since the landslide slope in Taketa City is a multi-layered structure consisting of pyroclastic flows and fall deposits, the changes in pore water pressure and effective stress of the slope under vertical seepage conditions were estimated by theoretical calculations.

5 Results and Discussion

5.1 Aerial Photointerpretation

Thirty landslides were detected in the study area by aerial photointerpretation. Six landslides were detected in the Aso-3 area and 24 in the Aso-4 area.

5.2 Landslides in Aso-3 Pyroclastic Flow Deposit Area

Aso-2–3 fall deposits and Aso-3 pyroclastic flow deposits are distributed in the lower levels of the landslide site in the Aso-3 area. Aso-2–3 fall deposit is solidified. Groundwater gushes from the boundary between the fall deposits and pyroclastic flow deposit layers. Therefore, the permeability of the fall deposits layer is estimated to be sufficiently smaller than that of the Aso-3 flow deposits. In the Aso-3 area, the landslide sliding plane is recognized at the boundary of the fall deposits and the flow deposits.

These results suggest that the landslides in the Aso-3 area were caused by vertical infiltration of rainwater from the surface of the pyroclastic flow deposits, which increased the water table in height and decreased the effective stress.

5.3 Landslides in Aso-4 Pyroclastic Flow Deposit Area

The landslide site in the Aso-4 area consists of fall deposits, pyroclastic surge deposits, non-welded pyroclastic flow deposits, and strong welded pyroclastic flow deposits from lower to upper. The fall deposits in the landslide site correspond to the upper layer of Aso-3–4 fall deposit, which is

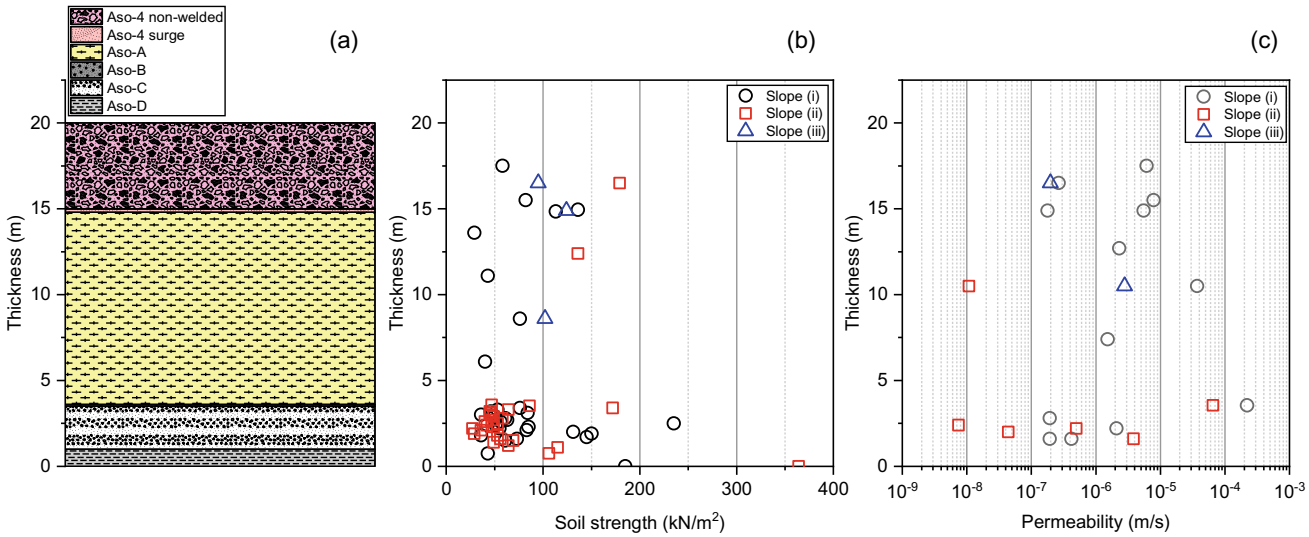

Fig. 1 Schematic geologic profile (**a**), soil strength profile (**b**), and permeability profile (**c**)

divided into three layers: lower, middle and upper layers (Ono et al., 1977). The upper layer of the Aso-3–4 pyroclastic fall deposit consists of Aso-A (yellowish-white pumice), -B (black to blackish-brown fine glassy ash), -C (alternate layers of volcanic sand, volcanic ash, and pumice), and -D (yellowish-white pumice) from the top (Ono et al., 1977), and these four layers have been identified on a landslide slope (Fig. 1a). At each site in the Aso-4 area, groundwater seepage was observed in the Aso-C layer. Therefore, pyroclastic surge deposits, non-welded pyroclastic flow deposits, and the strong welded pyroclastic flow deposits are members of the Aso-4 pyroclastic flow deposits. In the strong welded flow deposits, columnar cooling joints are developed at about 1 m interval. In the Aso-4 area, the landslide sliding surface is found between the Aso-B layer and the Aso-4 surge deposits.

Figure 1b shows the soil strength profiles of the three landslide slopes. The strength of the strong welded pyroclastic flow deposits at the top of the slope is not shown in this figure because it is more than two orders of magnitude greater than the strength of the non-welded deposits. However, each slope shows almost the same strength profile, i.e., Aso-4 non-welded flow deposits and the Aso-4 surge deposits have strengths between 100 and 200 kN/m^2, Aso-A fall deposits are mostly below 50 kN/m^2, Aso-B fall deposits have strengths between 40 and 90 kN/m^2, Aso-C fall deposits have strengths of 50–75 kN/m^2, and Aso-D has high strength of over 150 kN/m^2.

Figure 1c shows the permeability profiles of the same three landslide slopes. The permeability of Aso-4 non-welded flow deposits and Aso-4 surge deposits is 10^{-7}–10^{-5} m/s. Aso-A and -B fall deposits show higher permeability than the flow deposits in the range of 10^{-6}–10^{-4} m/s. Aso-C fall deposits have almost the same permeability as the flow deposits. Aso-D fall deposit shows low permeability of less than 10^{-9} m/s.

These results suggest that the landslides in the Aso-4 area may have been triggered by increased pore water pressure and decreased effective stress in a highly permeable zone consisting of Aso-A and -B. The increase in pore water pressure at Aso-A and -B is probably due to rainwater infiltration through the columnar joints of the strong welded pyroclastic flow deposit.

5.4 Precipitation Analysis

The study area is divided into 49 meshes (7 × 7 meshes). Each mesh is classified into the following four types: (1) 5 meshes for landslide occurrences in the Aso-3, (2) 17 meshes for landslide non-occurrences in the Aso-3, (3) 11 meshes for landslide occurrences in the Aso-4, and (4) 12 meshes for landslide non-occurrences in the Aso-4.

The average values of precipitation indices for each of the four areas are summarized in Table 1. Landslides in the Aso-3 area occurred with less precipitation than in the Aso-4 area. The ratio of landslide occurrence to non-occurrence for maximum hourly precipitation and effective precipitation with a half-life of 1.5 h is larger than that of other indices. This suggests that the landslide was effectively triggered by a short period of heavy rain.

Table 1 Average precipitation indices for each of the four types of areas

Precipitation indices	Aso-3 flow deposit area			Aso-4 flow deposit area		
	Landslides	No landslides	Ratio	Landslides	No landslides	Ratio
Maximum hourly precipitation (mm)	68.4	63.4	1.08	78.3	70.4	1.11
Cumulative precipitation (mm)	469.1	453.6	1.03	507.4	478.2	1.06
Effective precipitation with a half-life of 1.5 h (mm)	139.7	124.9	1.12	156.7	135.6	1.16

5.5 Calculation of Pore Water Pressure and Effective Stress at Subsurface

On the landslide slope in the Aso-4 area, groundwater seepage was observed in the Aso-C layer even during clear weather, indicating the existence of a steady groundwater table. Then pore water pressure and effective stress distributions on the landslide slope were calculated, assuming that the Aso-C and Aso-D layers below the groundwater table are saturated (Fig. 2b). As a result, the pore water pressure reaches a maximum of about 24 kPa at the bottom of the Aso-C layer and does not exceed the soil strength.

The landslide sliding surface was distributed between the Aso-B layer and the Aso-4 surge deposit. Therefore, in the Aso-A layer, landslides occur when the pore water pressure exceeds the ground strength. According to theoretical calculation, when the groundwater table rises to 5 m from the bottom of the Aso-A layer, the pore water pressure exceeds the strength of the lower part of the layer (Fig. 2c). This result suggests that the landslides in the Aso-4 area occurred because of the high groundwater table in the Aso-A layer due to rainwater infiltration.

6 Concluding Remarks

The landslide mechanism that occurred at the edge of the pyroclastic plateau in Kyushu during the heavy rainfall in July 2012 is discussed, and the following conclusions are drawn:

(1) The landslides are classified into the caprock type in the Aso-4 area and the direct rainwater infiltration type in the Aso-3 area;
(2) Maximum hourly precipitation and effective precipitation with a half-life of 1.5 h affected the occurrence of landslides;
(3) These precipitation indices were more significant in the caprock type than in the direct infiltration type;

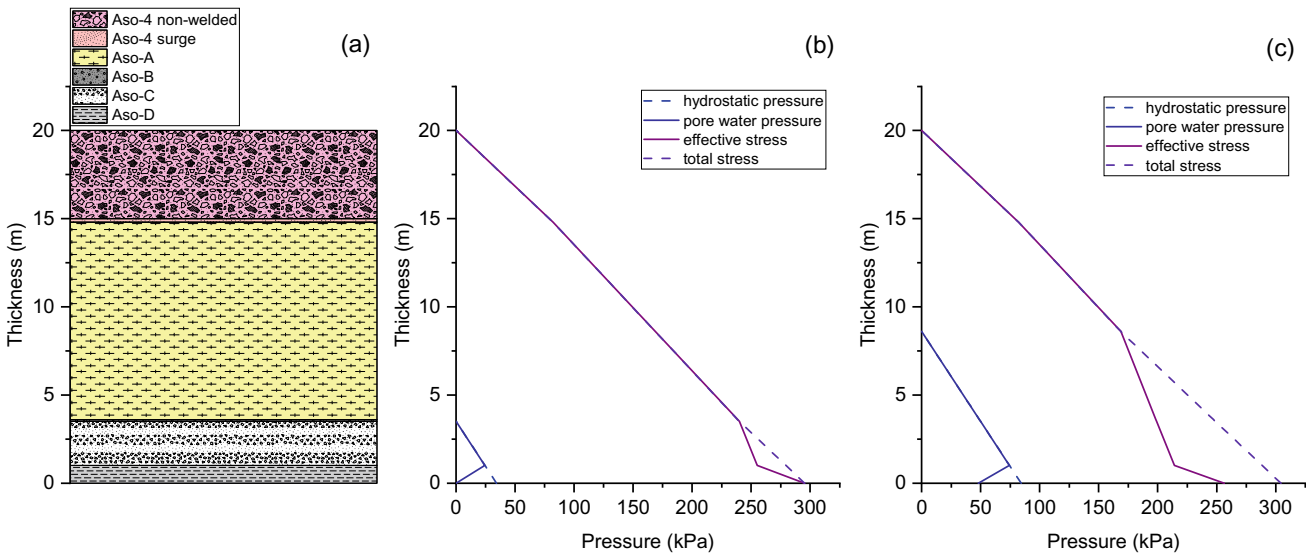

Fig. 2 Pore water pressure and effective stress profiles for the case where the groundwater table is in the Aso-C layer (**b**) and the Aso-A layer (**c**) with geologic profile (**a**)

(4) The landslide that occurred at the edge of the Aso pyroclastic flow plateau was caused by a decrease in the effective stress of the pyroclastic fall layer due to an increase in pore water pressure caused by rainwater infiltration.

References

Imaizumi, F., & Miyamoto, K. (2013). Spatial distributions of pore water pressure and effective stress in vertical seepage flow through multi-layer soil structure. *Journal of the Japan Society of Erosion Control Engineering, 65*(5), 3–10.

Kubota, T., et al. (2012). Debris disasters induced by heavy rainfall in Northern Kyushu District in July 2012. *Journal of the Japan Society of Erosion Control Engineering, 65*(4), 50–61.

Matsushi, Y., Fukuoka, H., & Furuya, G. (2013). Landslides of tephra deposits on hillslopes of the Aso caldera wall and volcanic central cones by the North-Kyushu heavy rainfall in July 2012. *Annuals of Disaster Prevention Research Institute, Kyoto University, 56B*, 237–241 (in Japanese with English abstract).

Miyabuchi, Y. (2012). Landslides triggered by the July 2012 torrential rain in Aso caldera, southwestern Japan. *Journal of Geography, 121* (6), 1073–1080 (in Japanese with English abstract).

Ono, K., Matsumoto, Y., Miyahisa, M., Teraoka, Y., & Kambe, N. (1977). Geology of the Taketa District. *Geological Survey of Japan, Japan* (in Japanese with English abstract).

Shimizu, O., & Ono, M. (2016). Relationship of tephra stratigraphy and hydraulic conductivity with slide depth in rainfall-induced shallow landslides in Aso Volcano, Japan. *Landslides, 13*, 577–582.

Infrasonic Long-Range Observations at IS42: Study Cases of Grimsvötn (Iceland), Mt. Etna and Stromboli Volcanoes (Italy)

Sandro Matos, Nicolau Wallenstein, Paola Campus, and Maurizio Ripepe

Abstract

The collaborative research UNIFI–University of the Azores (IVAR) focused on the detection and characterization of events injecting energy into the atmosphere and allowed to analyze of the Grímsvötn volcano eruptive activity (Iceland) and Mt. Etna and Stromboli volcanoes (Italy) by several Stations (among which IS42) of the CTBTO's International Monitoring System (IMS). Grímsvötn volcano, located under the Vatnajökull glacier, is the most active Icelandic volcano. The May 2011 explosive eruption broke the ice-covering and turned into sub-aerial, ejecting ash into the atmosphere and restricting flights across Northwestern Europe and the North Atlantic region. Mt. Etna, located in Sicily Island (Italy), is Europe's largest and most active volcano. It is typically effusive with explosive episodes, and lava fountaining activity has recently produced high eruptive plumes causing an impact on local air traffic and nearby airports and cities. Finally, Stromboli volcano (Italy), located in one of the Aeolian Islands (Italy) with the same name, is one of the most active volcanoes on Earth, with sustained explosive activity and permanent degassing. A strong explosive event characterized by two distinct explosions occurred on July 3rd, 2019. In this study, we describe a multiple-detections analysis of (a) the May 2011 Grímsvötn eruption as observed at IS42 and other infrasound stations and its correlations with on-site observations; (b) the Mt. Etna eruptive activity of the May–September 2011 and the 2016 eruptions, as observed at IS42 and other stations, compared with near-source observations; and (c) the Stromboli July 3rd, 2019 event detections from IS42 and other IMS infrasound stations. We relate those results with events listed in the CTBTO Reviewed Event Bulletin (REB) to evaluate the potential of the IMS network in detecting and identifying sources of volcanic activity. In the framework of earth-based volcanic monitoring techniques, infrasound is a unique technology with the potential to detect explosive eruptions at great distances. Furthermore, simultaneous infrasound recording in near- and far-field represents a substantial improvement in the characterization of explosive sources.

Keywords

IS42 • Azores • International Monitoring System (IMS) • CTBTO • Infrasound • Volcanoes • Grimsvötn • Etna • Stromboli • Detections • Bulletins

1 Introduction

IS42 is an IMS infrasound station located on Graciosa Island, the northernmost island of the Azores archipelago. The station is one of the International Monitoring System (IMS) infrasound stations of the Preparatory Commission of the Comprehensive Nuclear-Test-Ban Treaty Organization (CTBTO).

Grímsvötn volcano, a subglacial volcano, is one of Iceland's most active volcanoes located in the NE zone active rift under the Vatnajökull glacier. It has a complex of three calderas covering an area of approximately 48 km^2 at 1,725 m *asl*. In May 2011, an hydromagmatic explosive eruption extruded about 0.27 km^3 DRE (dense-rock equivalent) of basaltic magma, forming an eruptive plume that reached approximately 20 km of altitude (Hreinsdöttir et al., 2014). Preceded by an increase of seismicity and surface inflation, the May 21st to 28th, 2011 event was Grímsvötn's major eruption since 1873, with a Volcanic Explosivity

S. Matos (✉) · N. Wallenstein
Instituto de Investigação em Vulcanologia e Avaliação de Riscos (IVAR), University of the Azores, Ponta Delgada, Portugal
e-mail: sandro.b.matos@azores.gov.pt

P. Campus · M. Ripepe
Dipartimento di Scienze della Terra, Università di Firenze, Firenze, Italy

A. Malheiro et al. (eds.), *Advances in Natural Hazards and Volcanic Risks: Shaping a Sustainable Future*, Advances in Science, Technology & Innovation, https://doi.org/10.1007/978-3-031-25042-2_17

Index—VEI 4 that caused airspace closures in northern Europe due to the ash plume propagation at several flight levels.

Mt. Etna, located on Sicily Island (Italy), is a Stratovolcano with 3,340 m asl, an area of 1,190 km^2 at the base and five (5) distinct summit craters. The infrasonic activity was recorded with a small-aperture (250 m) infrasonic array of four elements (ETN), deployed at 5,500 m from the summit craters at an elevation of 2,010 m *asl* (Ulivieri et al., 2013).

Stromboli volcano (918 m *asl*) is located on a small Italian island of the same name that belongs to the Aeolian archipelago. Its persistent explosive activity and continuous degassing dating back to 3–7 AD (Rosi et al., 2000) make it likely the most famous volcano on Earth due to its impressive basaltic explosions interspersed with lava fountains (about ≈10 min) rising to 250 m (Ripepe et al., 2002). On July 3rd, 2019, a very strong explosive event (paroxysm) occurred at 14:45:43 UTC, associated with two explosions that led to a 5 km high ash column over the volcano. IS42 and various IMS infrasound stations detected this paroxysm.

Aiming to monitor nuclear test explosions, the International Data Centre (IDC) receives, processes and analyses data from the IMS stations. One of the IDC Products is the Reviewed Events Bulletin (REB). In the REB, arrivals and events from the automatic Standard Events List (SEL3) are corrected, confirmed, or deleted by expert analysts.

To verify the potentiality of the IMS infrasound stations (particularly focus on IS42) and to characterize long-distance detections of volcanic eruptions, we considered the Grímsvötn May 21st to 30th, 2011 explosive eruptions; the eruptive activity of Mt. Etna from May to August 2011 (lava fountaining) and between May 16th to 22nd, 2016; the Stromboli eruption on July 3rd, 2019 (paroxysm). Considering the source-to-station distance, it was assumed that the infrasound signals would propagate and reach the array as plane waves. Assuming an average sound speed of 343 ms^{-1}, the expected travel times were calculated, and a selected back-azimuth interval was identified.

We analyzed Mt. Etna's long-distance detections of the May–August 2011 eruptive activity and the May 2016 volcanic activity, recorded at IS17, IS26, and IS42, at distances from the source roughly between 1,200 and 4,000 km.

Long-range observations from IMS infrasound stations related to the May 2011 Grímsvötn eruption were analyzed at IS10, IS17, IS18, IS26, IS31, IS42, IS43 and IS53, respectively, at distances from the source that range roughly between 2,230 and 6,500 km. The July 3rd, 2019, Stromboli paroxysm episode was analyzed at IS26, IS37, IS42 and IS48, at distances from the source roughly between 580 and 3,680 km. For the computation of the wave parameters, we processed the raw data for the periods of all recorded eruptive activity with the interactive analysis tool, DTK-GPMCC (CEA/DASE), based on the PMCC—Progressive Multi-Channel Correlation Algorithm (Cansi, 1995) and integrated into the NDC-in-a-Box, v. 4.0 package supplied by the IDC (Table 1).

Raw data from the ETN infrasound station and IMS infrasound station records were retrieved and used for comparing far and near-field detections of Mt. Etna activity. Volcanic activity bulletins from the Laboratory of Experimental Geophysics (LGS) and National Institute of Geophysics and Volcanology (INGV) were used for validation. Long-range detections of the station IS42 (Matos et al., 2018) were correlated with near-field observations with the Icelandic Meteorological Office (IMO bulletins: the comparison was then extended to the other IMS stations in the

Table 1 IMS stations location, distances, and back-azimuths from the three volcanoes

		Grimsvötn volcano		Mt. Etna volcano		Stromboli volcano	
		(Lat, Lon) 64.4 N, 17.4 E		(Lat, Lon) 37.73 N, 15 E		(Lat, Lon) 38.79 N, 15.21 E	
Stations	Location (Lat, Lon)	Source distance (km)	Back-azimuth (°)	Source distance (km)	Back-azimuth (°)	Source distance (km)	Back-azimuth (°)
IS10	50.2 N, 96.0 W	≈4610	≈35	–	–	–	–
IS17	6.7 N, 4.9 W	≈6500	≈350	≈4000	≈27.2	–	–
IS18	76.5 N, 68.7 W	≈2230	≈105	–	–	–	–
IS26	48.9 N, 13.7 E	≈2550	≈325	≈1240	≈174	≈1130	≈176
IS31	50.4 N, 58.0 E	≈4470	≈315	–	–	–	–
IS37	69.1 N, 18.6 E	–	–	–	–	≈3380	≈185
IS42	39.0 N, 28.0 W	≈2900	≈11	≈3700	≈78.2	≈3680	≈75
IS43	56.7 N, 37.2 E	≈3000	≈310	–	–	–	–
IS48	35.6 N, 8.7 E	–	–	≈550	≈65.4	≈580	≈54
IS53	64.8 N, 147 W	≈5080	≈30	–	–	–	–

same period through the observation of detections in the expected back-azimuths and travel potentially associated to the volcanic activity. Finally, the results were compared with the REB events list to validate our analysis.

2 Results

2.1 Grímsvötn Volcano

IS42 detections of the May 21st to 28th, 2011 paroxysmal eruptive episode were selected from the period between the 21st (00:00 UTC) until 23:59 UTC of 28th, with a mean back-azimuth between 9 and 12°. We obtained 239,439 associations (pixels) with a mean frequency of 0.58 Hz, speed of 383 ms^{-1} and back-azimuth of 13.9°. We focused on the period corresponding to the beginning of the eruption that occurred in the late afternoon of the 21st and early morning of the 22nd. Five major events were detected at various IMS stations, with a minimum of 4 stations (IS18, IS42, IS10 and IS53) for the 5:49 UTC event and a maximum of 7 stations (IS18, IS26, IS42, IS43, IS31, IS53, IS17) for the 19:16 UTC episode. Mean frequencies ranged from 0.20 Hz (IS31) to 0.77 Hz (IS42), while mean speeds ranged between 330 ms^{-1} (IS43) and 377 ms^{-1} (IS43). In IS42 and for the first 4 hours, more than 50,000 pixels were grouped into 25 families with a mean back-azimuth of 16°. An average of 7 sensors was used, with a resulting strong correlation (0.728) in detection. A high detection rate was also observed for the other selected IMS stations (IS18, IS26, IS43, IS31, IS53, IS17), with maximum amplitudes ranging from 0.06 Pa (IS53) to 0.48 Pa (IS18). The maximum amplitude recorded at IS42 was 0.35 Pa.

2.2 Mt. Etna: The May–August 2011 Lava Fountaining Activity Detections

IS42 selected detections of the paroxysmal eruptive episodes were far more energetic from July 24th to 25th than on August 5th, ranging from 172 to ~33,600 pixels, respectively. The mean frequency values ranged from 0.6 Hz on July 19th and 24th to 25th, and on August 12th to 1.21 Hz on the episode of May 11th to 12th. The speed ranged between mean values of 368 ms^{-1} on August 20th and 394 ms^{-1} on the July 30th episodes. Mean back-azimuths were detected between 74.8 and 81.5° (August 5th and July 24th to 25th, respectively). A maximum amplitude of 0.07 Pa was registered from July 24th to 25th.

We present the results from IS26, which recorded the paroxysmal eruptions of: May 12th, July 9th, 19th and 24th and August 5th and 12th, with mean frequencies ranging from 0.9 Hz (July 19th) to 2.08 Hz (August 5th). The mean speed ranged from 338 ms^{-1} on July 24th to 349 ms^{-1} on August 5th. Mean back-azimuths were detected between 175.4 and 178.5°. The station IS17 recorded, for the June 19th episode, a mean frequency of 0.64 Hz, a mean speed of 350 ms^{-1}, a back-azimuth of 23.8° and a maximum amplitude of 0.02 Pa.

2.3 Mt. Etna: The May 16th–26th, 2016, Eruptive Activity

IS42 detections on the May 16th to 26th paroxysmal eruptive episode were selected between the 16th (00:00 UTC) and the 25th (23:59 UTC). Results obtained from the processed data for the 17th, 18th and 19th allowed for selection of ~39,000 pixels, corresponding to 158 families with a mean frequency of 1.09 Hz, speed of 350 ms^{-1}, and back-azimuth of 79.81°. Raw data from IS26 was used with results obtained for days 17th, 18th, 19th and 21st. Mean frequencies range from 0.7 to 1.40 Hz, speeds between 332 and 343 ms^{-1}, back-azimuths from 174.5 to 177.5°, and maximum amplitudes from 0.01 to 0.05 Pa, with IS42 recording a maximum amplitude of 0.03 Pa.

2.4 Stromboli Results

Data from July 3rd, 2019, events were retrieved from various IMS stations (IS26, IS37, IS42 and IS48) at source-to-receiver distances that range roughly between 580 km (IS48) and 3,680 km (IS42), and back-azimuths from 54° (IS48) to 185° (IS37), with mean frequencies from 0.72 Hz (I26DE) to 1.97 Hz (IS48), mean speed between 337 ms^{-1} (IS37) and 367 ms^{-1} (IS48). Maximum amplitudes varied from 1.87 Pa (IS48) to 0.004 Pa (IS37). For IS42, a back-azimuth of 74°, mean frequency of 1.07 Hz, speed of 367 ms^{-1} and maximum amplitude of 0.13 Pa were retrieved.

3 Discussion

On Grímsvötn volcano, from May 21st to 28th, 2011 activity, 18 distinct periods of activity were analyzed. Most events (11) corresponded to 61% of all detections and occurred within the first two days after the eruption, while the others were distributed from May 23rd to the 25th. The detections at IS42 of the first period contained many pixels (more than 90% of the total) grouped in 30 families. The strong correlation obtained in the pixels detection shows that we were in the presence of stable families, indicating well-defined different source characteristics. Furthermore, the high number of detections retrieved from all the other selected IMS stations and present also in the IDC REB correlates well with

the locally observed explosive intensity associated with the beginning of the subaerial eruption (IMO bulletins).

For Mt. Etna, in the period from May to August 2011, it was observed that detections coincident with locally registered Strombolian phases episodes, the number of families, which represented the diversity of source characteristics, varied from a minimum of 2, in the activity of July 19th, to a maximum of 54 in the activity of August 20th. Similar frequencies and maximum amplitudes were observed for Strombolian and lava fountaining phases. However, the Strombolian phases were associated with higher trace velocities and several pixel detections: this correlated well with more explosive episodes, except for the events on May 12th and July 25th, where more complex source characteristics were inferred from the retrieved number of families. In the July 19th lava fountaining, the high number of detections registered showed the considerable strength of the event: INGV and UNIFI bulletins reported that lava fountains rose to heights ranging from 250 to 2,000 m. The July 19th and 25th events registered a higher number of detections compared to August, as correlated with the local observations. It was also verified that no detections were associated at IS42 with the Strombolian phase of July 30th. Comparing the results of the IMS stations and ETN, it was verified that most of the detection periods were related to moderate or high-intensity IP (Infrasonic parameter) values (LGS bulletins). Compared with the Reviewed Event Bulletin (REB), events registered on July 19th and 25th were consistent with the detections on the ETN array and most certainly were associated with the eruptive activity.

As for the Mt. Etna eruptive activity between May 16th and 22nd, 2016, three distinct periods of detections were analyzed and correlated with ETN array detections: the comparison revealed the existence of several clusters of detections that could be associated with the significant increases in the IP during the alert phases, between May 17th and 19th. According to the LGS and INGV bulletins, those clusters could be related to changes in the type of activity, such as explosions and pulsating lava fountaining. However, some detections recorded at IS42 did not satisfy the required parameters (e.g. trace velocities or frequency) to be compared with the ETN records, bulletins and REB events.

It was also possible to locate the July 3rd, 2019, paroxysm event at Stromboli volcano with an uncertainty ellipse centred at about 55 km WSW from its ground truth source. This was accomplished by working only with raw data from the IMS infrasound stations and processing the selected signal arrivals with the Event location tool (Geotool). The results obtained were in line with the events presented in the IDC REB.

4 Concluding Remarks

In general, depending on the type of event, e.g. Strombolian activity, lava fountaining or major eruptions, the detection capability of the IS42 station and other IMS infrasound stations depends on the wave's energy (amplitude) and the minimum number of sensors used. It was observed that when the average number of used sensors is less than 4, and in the presence of low-energy acoustic signals, the results obtained show a reduced number of detections. In the same way, it was observed that the presence of stable families of detections with high levels of consistency associated with a strong correlation of signals allowed to characterize and better constrain different source characteristics.

The results confirmed that it is possible to detect and locate long-range explosive volcanic eruptions with IMS infrasound stations and the good detection capabilities of station IS42, even considering that it is located on a North Atlantic oceanic island.

References

Cansi, Y. (1995). An automatic seismic event processing for detection and location: The PMCC method. *Geophysical Research Letters, 22*, 1021–1024.

Hreinsdóttir, S., Sigmundsson, F., Roberts, M. J., Björnsson, H., Grapenthin, R., Arason, P., Árnadóttir, T., Hólmjárn, J., Geirsson, H., Bennett, R. A., Gudmundsson, M. T., Oddsson, B., Ófeigsson, B. G., Villemin, T., Jonsson, T. H., Sturkell, E. C., Höskuldsson, Á., Larsen, G., Thordarson, T., & Óladóttir, B. A. (2014). Volcanic plume height correlated with magma-pressure change at Grímsvötn Volcano, Iceland. *Nature Geoscience, 7*, 214–218.

Icelandic Meteorological Office. (2011). *Eruption has started in Grímsvötn*. Retrieved May 5, 2021.

LGS—Laboratory of Experimental Geophysics—Dipartimento di Scienze della Terra/Centro di Competenza Protezione Civile—Universitá Degli Studi Firenze bulletins and personnel communications.

Matos, S., Wallenstein, N., Marchetti, E., & Ripepe, M. (2018). 2011 Grímsvötn (Iceland) and 2016 Etna (Italy) volcanic activity: Long-range infrasound observations at IS42, Azores, North-Atlantic. In *EGU General Assembly 2018*, Vienna, Austria.

National Institute of Geophysics and Volcanology—Sezione di Catania—Osservatorio Etneo. Retrieved September 14, 2021, from www.ct.ingv.it.

Ripepe, M., Harris, A., & Carniel, R. (2002). Thermal, seismic and infrasonic evidences of variable degassing rates at Stromboli volcano. *Journal of Volcanology and Geothermal Research, 118* (3–4), 285–297.

Rosi, M., Bertagnini, A., & Landi, P. (2000). Onset of the persistent activity at Stromboli Volcano (Italy). *Bulletin of Volcanology, 62*, 294–300.

Ulivieri, G., Ripepe, M., & Marchetti, E. (2013). Infrasound reveals transition to oscillatory discharge regime during lava fountaining: Implication for early warning. *Geophysical Research Letters, 40*, 3008–3013. https://doi.org/10.1002/grl.50592.

Volcanic Island Drainage Divide Migration: Implications for Land Planning (Assomada Plateau, Santiago, Cape Verde)

Rui Fernandes, José Teixeira, Alberto Gomes, and Martin Stokes

Abstract

Volcanic landscapes during island formation are due to lava flows and their accumulation processes. However, erosive processes dominate landscape reshaping during periods of volcanic inactivity, posing unique and crucial land-use planning challenges. In the North Atlantic Ocean, the Cape Verde archipelago is an excellent area for assessing the implications of erosive processes on the definition of land planning strategies. Accordingly, this study focuses on the extensive Assomada Plateau (municipality of Santa Catarina), located on Santiago Island. The research uses the geomorphological index Chi (χ) to evaluate directional erosional trends of the drainage divides and relates them with the present and future (master plan) of urban occupation. This study aims to define problematic areas where it is expected that the erosion from drainage divide migration will likely cause severe problems for human occupation. For the Assomada settlements, the master plan establishes the consolidation of the existing urban area and expansion of its periphery close to the southern plateau edge. Furthermore, asymmetric Chi value patterns reveal areas of intense erosion from the movement of the drainage divide to the North and West. Watercourses have already eroded the plateau base, with erosion branching off in three directions. As a result, several cliff edge buildings are at risk, and any further expansion in these areas is questionable.

Keywords

Volcanic island erosion • Chi index • Land planning • Cape Verde

1 Introduction

In volcanic island settings, erosive processes are essential in landscape reshaping through periods of volcanic inactivity (Salvany et al., 2012), posing unique and crucial land-use planning challenges. Thus, erosive processes can adversely affect the resident population, infrastructures, and living conditions on volcanic islands. Consequently, populations and built areas exposed to such processes present a significant challenge to urban planning in these environments (Fernandes, 2021).

In the last two decades, geomorphometry has remarkably developed in quantifying, modelling, and analysing erosive processes acting on the Earth's surface (Anbazhagan et al., 2011). Using modern geomorphometric indices can contribute significantly to understanding geomorphological processes (Hengl & Reuter, 2008). For example, the integral method (Chi—χ) index is a recent method developed to calculate the channel steepness (Royden et al., 2000; Perron & Royden, 2012), with the resulting χ values being used to estimate stream power values or predict the migration of watershed boundaries, i.e., the mobility of the drainage divides (Willett et al., 2014).

This research uses the geomorphological index χ to evaluate erosion trends of the drainage divides and relates them with the present and future (master plan) urban occupation areas in the Assomada Plateau, located on Santiago

R. Fernandes
Department of Geography, University of Porto, Porto, Portugal
e-mail: ruimoraisfernandes@gmail.com

J. Teixeira (✉) · A. Gomes
Centre of Studies in Geography and Spatial Planning (CEGOT-FLUP), Department of Geography, University of Porto, Porto, Portugal
e-mail: jateixeira@letras.up.pt

A. Gomes
e-mail: atgomes@letras.up.pt

M. Stokes
School of Geography, Earth and Environmental Sciences, University of Plymouth, Plymouth, UK
e-mail: M.Stokes@plymouth.ac.uk

A. Malheiro et al. (eds.), *Advances in Natural Hazards and Volcanic Risks: Shaping a Sustainable Future*, Advances in Science, Technology & Innovation, https://doi.org/10.1007/978-3-031-25042-2_18

Island, Cape Verde. The aim is to define problematic sectors where it is expected that the erosion from drainage divide migration will cause severe problems for human occupation.

2 Local Setting

The Cape Verde archipelago comprises ten major and several minor islands in the North Atlantic Ocean. They are approximately 600 km off the coast of Senegal and 1400 km from the mid-Atlantic rift (Fig. 1). They result from hotspot activity generally known as the Cape Verde Rise (Ramalho, 2011). The islands are disposed in an arc-like shape and are generally grouped into either the Windward or Leeward Islands. Santiago Island is the fourtholdest island, with its geological formations dating from around 11 Ma (Ramalho, 2011). This research is focused on the Assomada Plateau of Santiago Island. The plateau surface comprises the Assomada Formation, a wide, horizontally layered, resistant basaltic lava flow sequence superimposed onto older and less resistant volcanic formations.

The archipelago presents a semi-arid climate characterised by torrential precipitation events that occur in short, highly concentrated downpours, unevenly distributed in time and space (e.g., Duarte & Romeiras, 2009; Ramalho, 2011). This precipitation pattern, associated with lithological heterogeneities and differential weathering, has a significant erosional impact, driving deep incisions into the volcanic edifice relief (Mannaerts & Gabriels, 2000; Ramalho, 2011).

3 Materials and Methods

The initial assessment of the geological/geomorphological context of the study area was done using hypsometry (with slope and local topography) and geological data. This characterisation allowed the definition of the geomorphological units to be analysed using the geomorphological index (Fig. 2). Accordingly, the integral index method (Chi—χ) was calculated using the methodology proposed by Royden et al. (2000), Sorby and England (2004), and Perron and Royden (2013) to predict the migration of the drainage

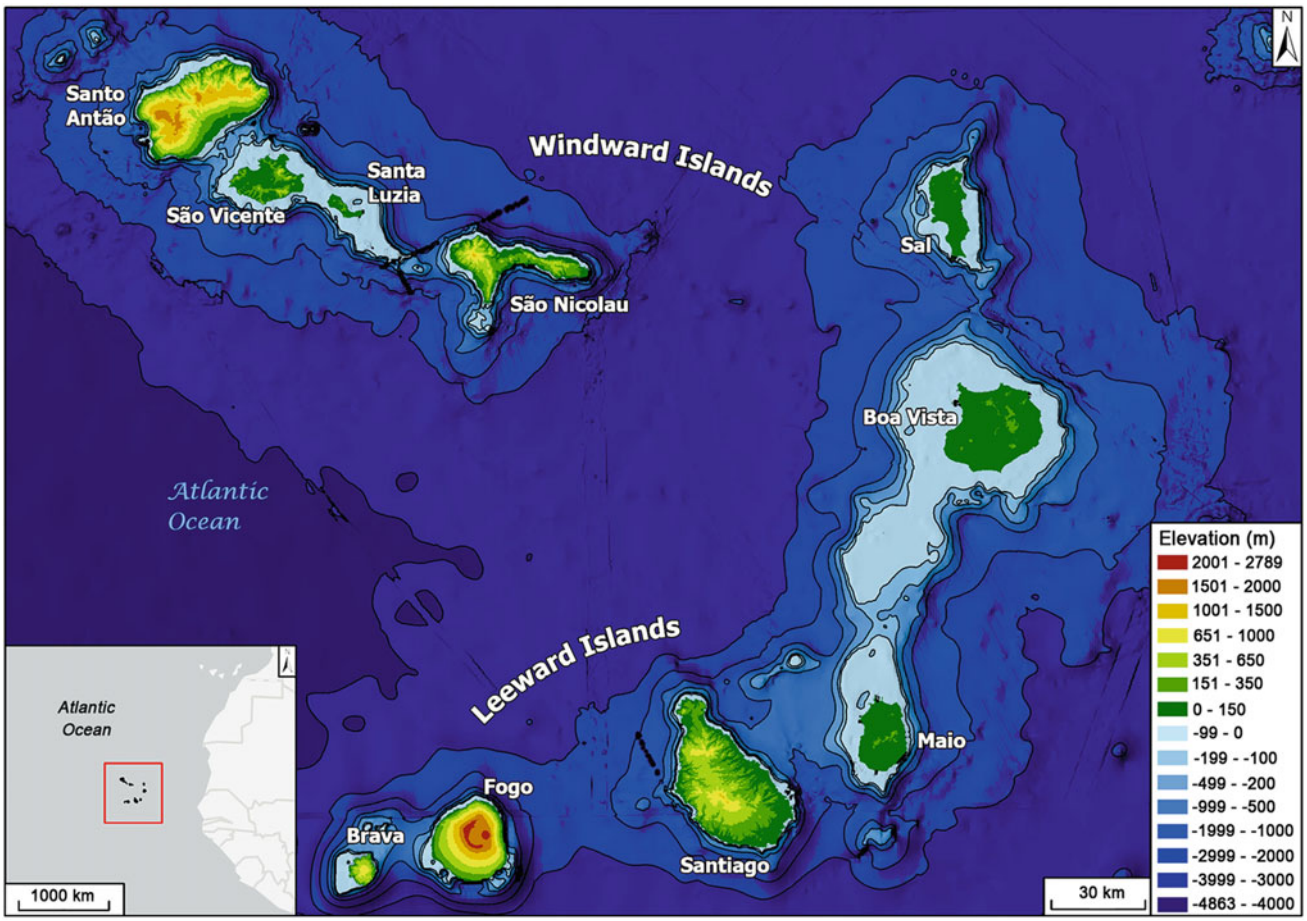

Fig. 1 Location of Santiago Island in the Cape Verde Archipelago

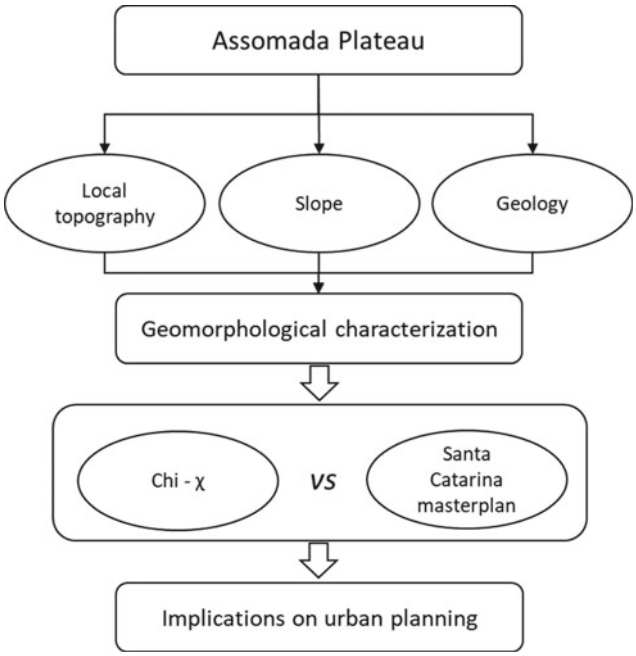

Fig. 2 The methodological approach of this study

basin limits around the Assomada Plateau. The results were then cross-checked with the Santa Catarina master plan to assert if the municipality plans, especially those implying urban expansion/consolidation, are aware of the migratory geomorphological processes.

The Chi—χ index was calculated in MathWorks' MATLAB. The index was calculated from a Digital Elevation Model (DEM) obtained from the Direcção Geral do Ordenamento do Território e Desenvolvimento Urbano of Cape Verde (DGOTDU) cartography and NASADEM Global Digital Elevation Model, including modernisation and reprocessing of the SRTM data. The free and open-source app TopoToolbox (https://topotoolbox.wordpress.com/) was used for all processing in the MATLAB environment.

χ can predict drainage basin migration (Willett et al., 2014). When considering the channels along each side of a drainage divide, the one with the highest χ value will be the victim relative to the one with the lowest χ value. The divide should accordingly move in the victim's direction until a steady state is reached (Fig. 3a). Similar χ values indicate a stable divide (Fig. 3b).

4 Results and Discussion

Santa Catarina Municipality comprises the western and central areas of Santiago Island. It is primarily a rural municipality, and the dominant economic activities are agriculture, fishing, and livestock production (JC&S & MLTM, 2010; Fernandes, 2011). Around 40% of the population of Santa Catarina lives in Assomada City. The city is positioned on the top of the Assomada Plateau.

The Assomada Plateau (Fig. 4) is part of one of the seven geomorphological units of the island, namely the Santa Catarina Highlands. This plateau extends westward, cut by numerous streams, culminating in an extremely narrow strip. The average altitude of the Assomada Plateau is around 525 m, descending westward. Streams penetrate deep into the municipality in the west, leaving some plateaus in between. To the north of the Assomada Plateau, two further extensive plateaus are found at slightly lower altitudes (Fig. 4): Fundura (440 m) and Boa Entrada (458 m).

The Assomada Plateau is suffering erosion by the Ribeira das Águas Belas stream to the South, and Ribeira da Boa Entrada to the North. The three plateaus could be considered part of an ancient plateau, with a total area of 56 km^2 (Fernandes, 2021). The current area of the plateaus is around 33 km^2, representing a loss of over 40%. These erosional processes occurred after the creation of the Assomada Formation. This volcanic formation is relatively recent in geological time, which denotes the speed of this erosional process.

The calculated Chi values were used to predict the erosion direction. As expected, the cliff to the east is more erosionally active than the flat plateau top, causing the streams on that slope to be the aggressors. The victims are the streams at the top of the plateau. The south of the Assomada Plateau has the most significant Chi anomalies in the area, where the Ribeira Mato Gegê is pushing the divide north at the expense of the streams at the top.

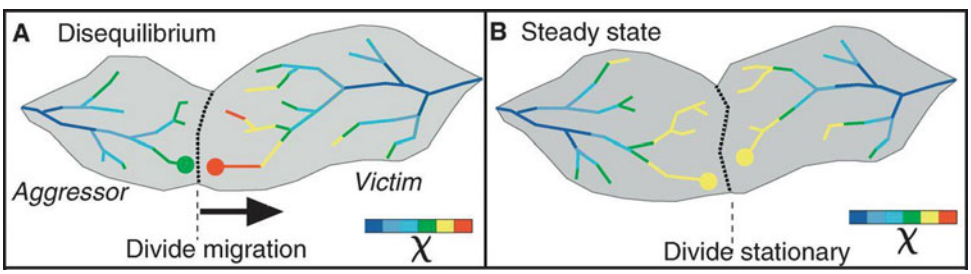

Fig. 3 Chi relationships between rivers that share a drainage divide (adapted from Willett et al., 2014)

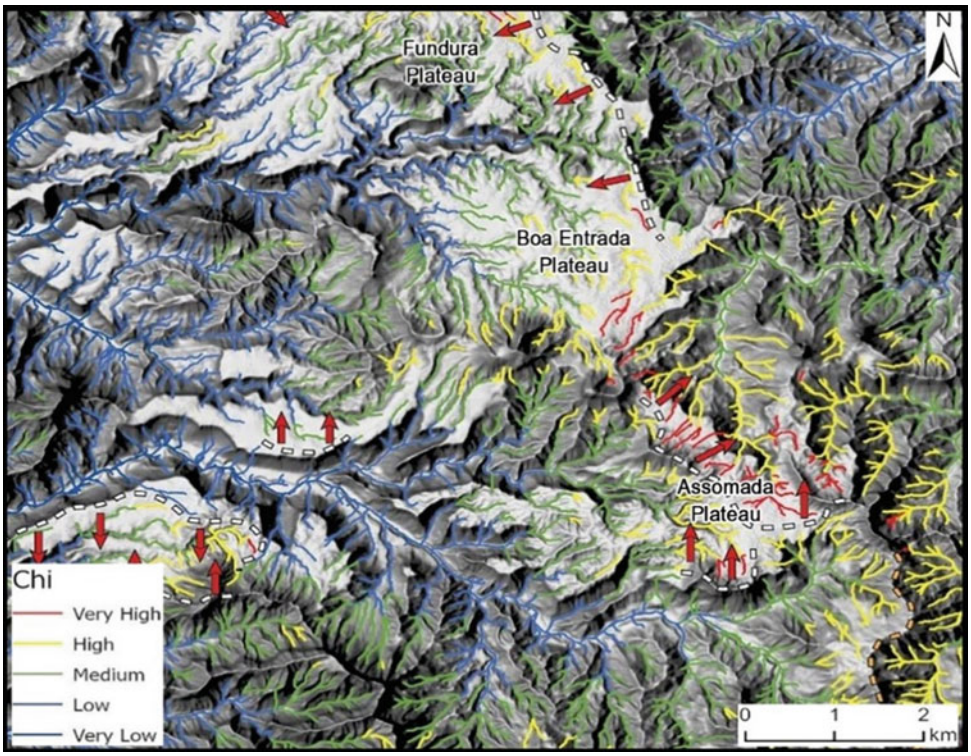

Fig. 4 Chi values and estimated drainage divide migration trends on the Assomada, Boa Entrada and Fundura plateaus

Fig. 5 Houses on the plateau's edge in southeastern Assomada city. Fonte Lima is visible in the foreground, in the valley

However, the expansion of the city periphery is problematic regarding the calculated Chi values and erosion trends. The Assomada Plateau is being threatened to its south by the Ribeira das Águas Bela's catchment streams, and the buildings are perched on the plateau's edge (Fig. 5). The southern area sits on the resistant Assomada Formation. The drainage network has already eaten through the plateau's base and branched in three distinct directions. Several buildings on the cliff's edge are at risk, and any further expansion in this area is ill-advised.

This urban consolidation will lead to more areas of impermeable soil. This consolidation will cause fewer infiltration rates and more runoff (Hiscock, 2014). More runoff will inevitably lead to higher erosion rates on the slopes, accelerating the process. The erosional processes will be a recurring problem with the consolidation of urbanised areas on the plateaus.

5 Concluding Remarks

The Santa Catarina Plateau does not appear to be an extremely complex zone, geomorphologically speaking. It is essentially a basalt lava flow cover, capping two formations of the island-building stage. The lower formations are more weathered and therefore less resistant. This configuration

gives us the present morphology, where the drainage network carves out the lower formations. Losing its support, the Assomada Formation begins to collapse.

This area presents a significant challenge in terms of urban planning. The steep slopes separating the top of the plateaus from the valleys creates significant problems, such as the gradual loss of area at the top of the plateau due to erosive processes. This is especially pertinent along the immediate edges of the plateaus, as they will be the first areas to collapse. Constructions in these areas are at an increased risk of suffering damage or even being destroyed in more extreme cases. From a geomorphological perspective, suitable areas to build in are the central portions of the plateaus, away from the cliff.

The importance and strength of the erosive process in the region cannot be overlooked. Therefore, it is considered it a significant oversight that Santa Catarina's master plan does not have sufficient consideration of the risks associated with the geomorphological processes occurring on the area.

References

Anbazhagan, S., Subramanian, S. K., & Yang, X. (Eds.). (2011). *Geoinformatics in applied geomorphology*. CRC Press.

Duarte, M. C., & Romeiras, M. M. (2009). Cape Verde Islands. In R. G. Gillespie & D. A. Clague (Eds.), *Encyclopedia of Islands* (pp. 143–148). University of California Press.

Fernandes, N. F. (2011). *Evolução Urbana e Planeamento Urbano da Cidade de Assomada (Cabo Verde)*. M.Sc. dissertation, University of Coimbra, Coimbra.

Fernandes, R. (2021). *Erosive stage of the Cape Verde Islands: Implications in urban planning*. M.Sc. dissertation, University of Porto, Porto.

Hengl, T., & Reuter, H. I. (Eds.). (2008). *Geomorphometry: Concepts, software, applications. Developments in soil science* (Vol. 33). Elsevier.

Hiscock, K. M., & Bense, V. (2014). *Hydrogeology: Principles and practice* (2nd ed.). Willey Blackwell.

JC&S & MLTM. (2010). *Anteprojeto do plano diretor municipal de Santa Catarina*. JC&S Arquitetos Associados and MLTM Arquitetura e Urbanismo. Retrieved from https://sites.google.com/site/cmscurbanismo/planos-projectos-obras/planos/pmot/pdm-santa-catarina. Last accessed February 2022.

Mannaerts, C. M., & Gabriels, D. (2000). Rainfall erosivity in Cape Verde. *Soil and Tillage Research, 55*(3–4), 207–212.

Perron, J. T., & Royden, L. (2013). An integral approach to bedrock river profile analysis. *Earth Surface Processes and Landforms, 38* (6), 570–576.

Ramalho, R. A. (2011). *Building the Cape Verde Islands*. Springer theses. Springer Berlin, Heidelberg.

Royden, L. H., Clark, M. K., & Whipple, K. X. (2000). Evolution of river elevation profiles by bedrock incision: Analytical solutions for transient river profiles related to changing uplift and precipitation rates. *EOS, Transactions of the AGU, 81*(48).

Salvany, T., Lahitte, P., Nativel, P., & Gillot, P. Y. (2012). Geomorphic evolution of the Piton des Neiges volcano (Réunion Island, Indian Ocean): Competition between volcanic construction and erosion since 1.4 Ma. *Geomorphology, 136*(1), 132–147.

Sorby, A. P., & England, P. C. (2004). Critical assessment of quantitative geomorphology in the footwall of active normal faults, Basin and Range province, western USA. *EOS, Transactions of the American Geophysical Union, 85*.

Willett, S. D., McCoy, S. W., Perron, J. T., Goren, L., & Chen, C. Y. (2014). Dynamic reorganisation of river basins. *Science, 343*(6175).

Does the Updating of Landslides Inventories Have a Relevant Impact on the Landslide Susceptibility Assessment?

Raquel Melo, Sérgio C. Oliveira, Ricardo A. C. Garcia, and José Luís Zêzere

Abstract

Landslide inventories are essential for developing an accurate susceptibility assessment. However, the complete and systematic updating of these inventories is a time-consuming and challenging task. Therefore, we aimed to verify if the temporal updating of historical inventories improves the susceptibility models and if the size of the study area plays a relevant role in the decision to update or not landslide inventories. To answer these questions, the work was carried out in two study areas with different sizes but with a similar geomorphological context. The landslide susceptibility modelling, developed using the Information Value method, was performed for distinct types of landslides and using three landslide inventories: one with landslides that occurred before 2012; a second with landslides that occurred during the event of 2010; and a third with landslides that occurred up to 2019. The results indicate no improvement or only a residual enhancement in the susceptibility models' predictive capacity, regardless of the type of landslide or the study area's size.

Keywords

Landslides • Inventories completeness • Susceptibility assessment • Predictive capacity

1 Introduction

Landslides have been studied for at least three decades in the northern surroundings of the Lisbon district, which have resulted in systematically updated inventories (e.g., Ferreira et al., 1987, Zêzere et al., 1999, 2004, 2008, Oliveira, 2012, Oliveira et al., 2015, 2017, Melo et al., 2019). These inventories have been often developed based on orthophoto map interpretation, identification of morphological patterns from digital topography and field surveying.

Landslide inventories usually integrate the landslide typology, its spatial configuration and date of occurrence if known. Therefore, the inventories are used as baseline information for developing studies focused on landslides' susceptibility, hazard, and risk assessment. An accepted assumption by the scientific community is that future slope instability is more prone to occur in similar conditions to those that generated instability in the past (Samia et al., 2017). Hence, it is assumed that landslides do not occur randomly since they result from the interaction between physical processes and mechanical laws that determine slope stability. Therefore, it is reasonable to question when inventories should be updated for a certain study area in this context. Thus, the present work intends to answer two questions: (1) does the temporal updating of historical landslide inventories provide a considerable improvement in the landslide susceptibility (LS) models, or is there a limit beyond which this improvement becomes residual? (2) does the study area's size play a relevant role in updating or not the landslide inventories? In order to try to answer these questions, the present work was developed for two study areas with different sizes but similar geomorphological backgrounds: the GPR basin (≈111 km^2) and the SSA basin (43 km^2).

R. Melo · S. C. Oliveira (✉) · R. A. C. Garcia · J. L. Zêzere
Centre of Geographical Studies, Institute of Geography and Spatial Planning, University of Lisbon, Lisbon, Portugal
e-mail: cruzdeoliveira@campus.ul.pt

R. Melo
School of Science and Technology, University of Évora, Évora, Portugal

S. C. Oliveira · R. A. C. Garcia · J. L. Zêzere
Associated Laboratory TERRA, Lisbon, Portugal

A. Malheiro et al. (eds.), *Advances in Natural Hazards and Volcanic Risks: Shaping a Sustainable Future*, Advances in Science, Technology & Innovation, https://doi.org/10.1007/978-3-031-25042-2_19

Table 1 Number of landslides used for training and validation in each landslide susceptibility (LS) model developed for GPR and SSA river basins

		Model A (DS)	Model A (SR)	Model A (ST)	Model B (DS)	Model B (SR)	Model B (ST)
GPR	Training	369	221	138	520	279	146
	Validation	55	74	33	55	74	33
SSA	Training	N/a	N/a	64	N/a	N/a	144
	Validation	N/a	N/a	17	N/a	N/a	17

2 Study Areas and Landslide Inventories

The GPR and the SSA are river basins located in the northern surroundings of Lisbon´s district, Portugal. Both areas are mainly composed of lithological units of sedimentary nature, with a predominance of clays and marls from the Jurassic period (Melo et al., 2019; Oliveira et al., 2015). The slope angle is gentle to moderate in both study areas, with values below 15º in 88% of GPR and 82% of SSA river basins. The elevation ranges between 5 and 440 m in the former study area and between 0 and 377 m in the latter.

The climate is the Mediterranean, and the rainfall regime varies between intense and short-duration episodes of precipitation and prolongated periods of precipitation or drought (Zêzere et al., 2008).

Three landslides inventories were constructed for GPR and SSA study areas: inventory #1, with landslides that occurred before 2012; inventory #2, with landslides that occurred during the event of 2010; and inventory #3, with landslides that occurred up to 2019. The landslides that occurred in the seasonal 2010 event (inventory #2) were excluded from inventory #1 and #3. The landslide magnitude distribution (landslide area frequency) of inventory #2 is similar to the historical landslide inventory and therefore used in an independent way to validate the susceptibility models. Furthermore, for GPR, the following landslide types were individualized: deep-seated (D.S.), shallow rotational (S.R.) and shallow translational (S.T.) slides; whereas in SSA, only shallow translational slides were inventoried. Overall, considering the three inventories and all the landslide types, 1107 landslides were identified in GPR and 161 shallow translational slides in SSA.

3 Methods

The LS assessment, considering the completeness of the inventories and the size of the areas under study, was developed for GPR and SSA through the following steps: (1) construction of Model A, by using inventory #1 for training and inventory #2 for validation; (2) construction of Model B, by using the inventories #1 and #3 for training and the inventory #2 for validation. A total of six models, considering all landslide types (D.S., S.R. and S.T.), were developed for GPR and two models for SSA (Table 1).

The LS models were computed using a data-driven method: the Information Value (IV), developed by Yin and Yan (1988). The independent validation of models A and B was carried out using landslide inventory #2 and by computing the ROC curves and the calculation of the Area Under the ROC curve (AUROC).

4 Results and Discussion

According to the completeness of landslide inventories (models A and B), the six LS models developed for the GPR basin and the type of landslides (D.S., S.R. and S.T.) can be seen in Fig. 1. The validation of these models is presented in Fig. 2. The validation of the models for GPR shows no difference regarding the AUROC values for the D.S. landslides (AUROC = 0.74 in models A and B) and for the S.T. slides (AUROC = 0.94 in models A and B), which means no enhancement in the predictive capability of the models developed with the updated inventory. However, regarding the S.R. slides, we estimated a difference of 0.01 in the AUROC values (0.69 for Model A and 0.70 for Model B), which indicates a slight improvement in the predictive capacity of the susceptibility model developed with the updated inventory (Model B).

Regarding the SSA study area, the results for the two susceptibility models developed for S.T. slides and according to the completeness of landslide inventories (models A and B) can be seen in Fig. 3 and the validation of these models in Fig. 4.

The SSA study area (43 km^2) has less than half of the extent of the GPR basin (111 km^2), allowing to conduct this research in an area of a different size. The validation of the susceptibility models developed in SSA for S.T. slides indicates that the updated inventory provided only a residual improvement in the model's predictive capacity, translating into a difference of 0.01 in AUROC values (0.88 for Model A and 0.89 for Model B).

The results obtained are in line with those observed in recent studies (e.g. Ghosh et al., 2020, Ozturk et al., 2021),

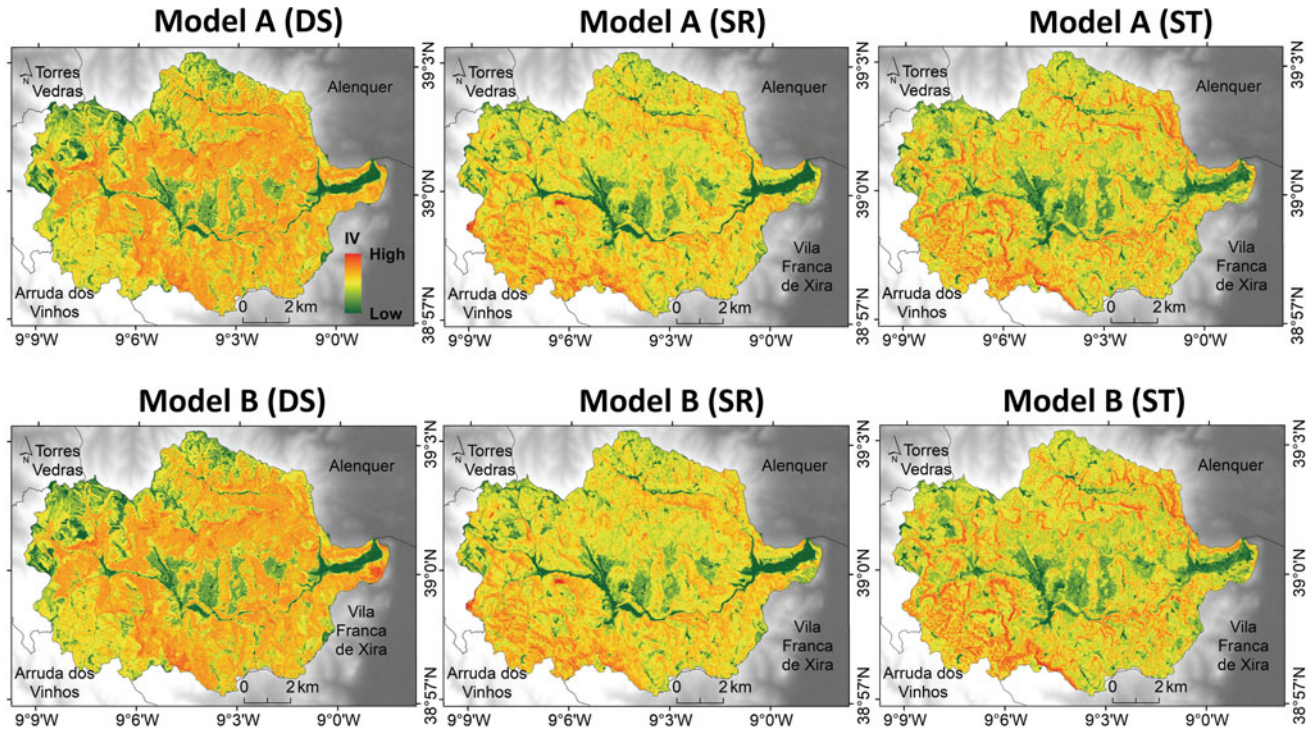

Fig. 1 Landslide susceptibility (LS) models for GPR basin

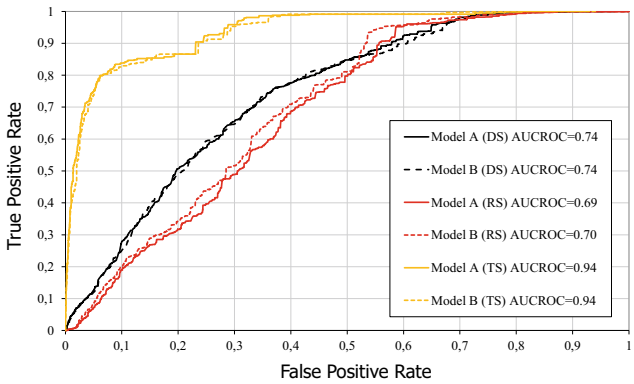

Fig. 2 Validation of landslide susceptibility (LS) models for GPR basin

where the authors verified that the accuracy of the models only slightly increased even with the temporal updating of the landslide inventories. Furthermore, the authors highlighted that the inventory completeness regarding the landslide spatial distribution might not be relevant for improving the robustness of the LS model.

5 Concluding Remarks

The research intended to determine if (1) the temporal updating of historical landslide inventories resulted in an improvement of the landslide susceptibility (LS) assessment and (2) if the size of the study area was a relevant factor to be considered for the updating of the landslide inventories.

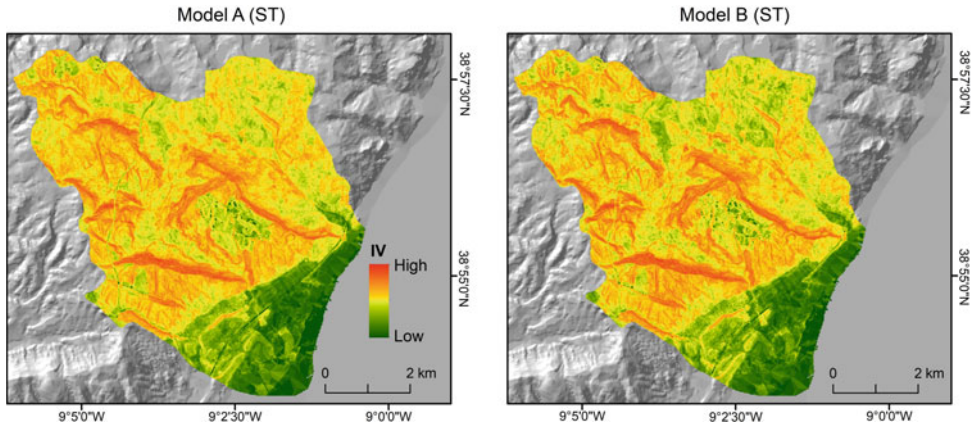

Fig. 3 Landslide susceptibility (LS) models for SSA basin

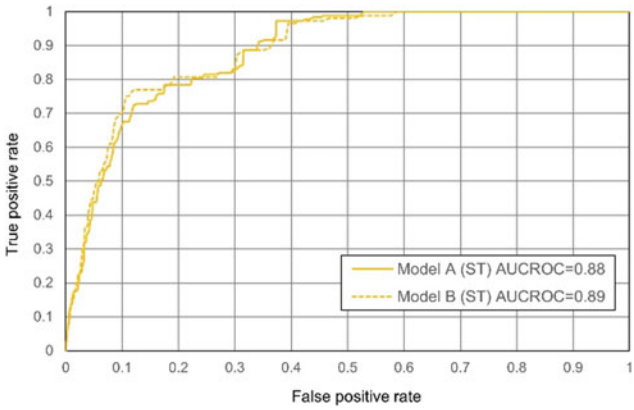

Fig. 4 Validation of landslide susceptibility (LS) models for SSA basin

However, the results indicated no improvement or only a residual improvement in the LS models' predictive capability, regardless of the type of landslide or the size of the river basin, which indicates in general terms that both hypotheses were not confirmed. Nevertheless, it is highlighted that the predictive capacity of these LS models can be improved by increasing the quality of the cartographic base data that spatially represents the predisposing factors, such as a high detailed lithological map. Therefore, future research should be considered for this purpose.

Acknowledgements This work is funded by FCT—Portuguese Foundation for Science and Technology, I.P., through the project BeSafeSlide—Landslide Early Warning soft technology prototype to improve community resilience and adaptation to environmental change (PTDC/GES-AMB/30052/2017) and by the Research Unit UIDB/00295/2020 and UIDP/00295/2020. Ricardo A.C. Garcia's collaboration was supported by the RISKCoast Interreg Sudoe project (SOE3/P4/E0868).

References

Ferreira, A. B., Zêzere, J. L., & Rodrigues, M. L. (1987). Instabilité des versants dans la région au Nord de Lisbonne. *Essai De Cartographie Géomorphologique. Finisterra, 22*(43), 227–246.

Ghosh, T., Bhowmik, S., Jaiswal, P., Ghosh, S., & Kumar, D. (2020). Generating substantially complete landslide inventory using multiple data sources: A case study in Northwest Himalayas, India. *Journal of the Geological Society of India, 95*(1), 45–58.

Melo, R., Zêzere, J. L., Rocha, J., & Oliveira, S. C. (2019). Combining data-driven models to assess susceptibility of shallow slides failure and run-out. *Landslides, 16*, 2259–2276.

Oliveira, S. C., Zêzere, J. L., Catalão, J., & Nico, G. (2015). The contribution of PSInSAR interferometry to landslide hazard in weak rock-dominated areas. *Landslides, 12*, 703–719.

Oliveira, S. C., Zêzere, J. L., Lajas, S., & Melo, R. (2017). Combination of statistical and physically based methods to assess shallow slide susceptibility at the basin scale. *Natural Hazards and Earth Systems Sciences, 17*, 1091–1109.

Oliveira, S. C. (2012). Incidência espacial e temporal da instabilidade gemorfológica na bacia do rio Grande da Pipa (Arruda dos Vinhos). Instituto de Geografia e Ordenamento do Território, Universidade de Lisboa, Lisboa (Ph.D. thesis).

Ozturk, U., Pittore, M., Behling, R., Roessner, S., Andreani, L., & Korup, O. (2021). How robust are landslide susceptibility estimates? *Landslides, 18*(2), 681–695.

Samia, J., Temme, A., Bregt, A., Wallinga, J., Guzzetti, F., Ardizzone, F., & Rossi, M. (2017). Do landslides follow landslides? Insights in path dependency from a multi-temporal landslide inventory. *Landslides, 14*(2), 547–558.

Yin, K., & Yan, T. (1988). Statistical prediction models for slope instability of metamorphosed rocks. In Bonnard, C, (Ed.), *Landslides: Proceedings of the Fifth International Symposium on Landslides. International Symposium on Landslides, Lausanne* (Vol. 3, pp. 1269–1272).

Zêzere, J. L., Ferreira, A. B., & Rodrigues, M. L. (1999). The role of conditioning and triggering factors in the occurrence of landslides: A case study in the area north of Lisbon (Portugal). *Geomorphology, 30*, 133–146.

Zêzere, J. L., Reis, E., Garcia, R., Oliveira, S., Rodrigues, M. L., Vieira, G., & Ferreira, A. B. (2004). Integration of spatial and temporal data for the definition of different landslide hazard scenarios in the area north of Lisbon (Portugal). *Natural Hazards and Earth Systems Sciences, 4*(1), 133–146.

Zêzere, J. L., Trigo, R. M., Fragoso, M., Oliveira, S. C., & Garcia, R. A. C. (2008). Rainfall-triggered landslides in the Lisbon region over 2006 and relationships with North Atlantic oscillation. *Natural Hazards and Earth Systems Sciences, 8*, 483–499.

From Geological to Lithological Maps—Exploring Differential Erosion to Improve Lithological Information for Landslide Susceptibility Assessment

Sérgio C. Oliveira, Raquel Melo, Fernando Marques, Rute Fonseca, Rita Pimenta, and José Luís Zêzere

Abstract

For landslide susceptibility assessment, lithology information is often extrapolated from official geological maps, which do not allow a direct spatial transformation into a detailed lithological map. To overcome this limitation, a study was made for the Grande da Pipa River basin, Portugal, to detail the existing geological maps, keeping the units' age sequence but separating the main lithological types. In addition, it explored supplementary cartographic information (e.g., slope angle) to infer the boundaries of lithological units using differential erosion and associated morphological interpretation criteria. Finally, the lithological map produced was compared with the official geological map using sensitive analysis and different partitions of a historical landslide inventory. The results consistently record improved predictive capacity for landslide susceptibility if more detailed lithological maps are used instead of the commonly available geological maps.

Keywords

Geological map • Lithological map • Cartographic information • Susceptibility • Landslides

1 Introduction

Independently of the geomorphological characteristics of a study area, lithology is a major predisposing factor that controls the spatial occurrence of different types of landslides. For landslide susceptibility assessment, lithological information is often extrapolated from the geological formations (GF) identified in official geological maps, being the map scales are usually 1:50,000 or 1:25,000. Although supported by field surveying, photointerpretation, stratigraphic and structural characterization and laboratory studies and laboratory analysis of rock and soil samples, these geological maps do not allow a direct spatial transformation into a detailed lithological map. As a rule, the age of each lithological unit (LU) is the essential agglutinating criterion to define the extension of each GF in these maps. To overcome this limitation, a new approach is proposed for the Grande da Pipa River (GPR) basin, Portugal, to detail the existing official geological maps, keeping the different geological formations stratigraphically grouped but spatially differentiating the main lithological types within. In addition, the work explores ancillary cartographic information (e.g., slope maps) to infer the limit of the different lithological units with different geomechanical characteristics, considering differential erosion processes and associated morphological interpretation criteria. As research hypotheses, we assume that: (i) this approach is particularly efficient for geological formations characterized by intercalation of soft rocks (e.g., clay, marl) with harder rocks (e.g., sandstone, limestone); (ii) the lithological map is more suitable for assessing landslide susceptibility than commonly available geological maps.

S. C. Oliveira (✉) · R. Melo · J. L. Zêzere
Centre of Geographical Studies, Institute of Geography and Spatial Planning (IGOT), University of Lisbon, Lisbon, Portugal
e-mail: cruzdeoliveira@campus.ul.pt

S. C. Oliveira · J. L. Zêzere
Associated Laboratory TERRA, Lisbon, Portugal

R. Melo
School of Science and Technology, University of Évora, Évora, Portugal

F. Marques
Faculty of Sciences, Department of Geology, University of Lisbon, Instituto Dom Luiz, Lisbon, Portugal

R. Fonseca
Faculty of Sciences, Department of Geology, University of Lisbon, Lisbon, Portugal

R. Pimenta
GEOCORE – Consultores de Geologia, Ambiente e SIG, Oeiras, Portugal

A. Malheiro et al. (eds.), *Advances in Natural Hazards and Volcanic Risks: Shaping a Sustainable Future*,
Advances in Science, Technology & Innovation, https://doi.org/10.1007/978-3-031-25042-2_20

2 Study Area and Materials

The GPR basin (110.6 km^2) is located in the north of the Lisbon region, Portugal. Elevation ranges from 440 m (west) to 5 m (east), close to the Tagus river alluvial plain. In the study area, eleven geological formations (GF) were mapped (Fig. 1A). The intercalation of Upper Jurassic limestones, marls, clays and sandstones (Zbyszewski & Assunção 1965; Kullberg et al., 2006) is predominant in almost 96% of the study area and constitutes four main geological formations, where most of the landslides occur (Oliveira et al., 2015): GF5—limestones, marls, 150 m to 250 m, 5.8%; GF6—mudstones, sandstones, marls, and limestones, 65 m to 130 m, 16.1%; GF7—coral limestones, but also marls, marly limestone, compact sandstone, 30 m to 80 m, 16%; and GF8—marls, clays and sandstones complex, 800 m, 57.8%. Slope angle (Fig. 1B) was obtained from a digital elevation model (DEM) resulting from topographic data (1:10,000 scale). The slope angle in the GPR basin is gentle to moderate (slope < 15° in 87.5% of the study area). Lastly, a landslide inventory is available (Fig. 1C) containing more than 1400 landslides (Oliveira et al., 2015) classified according to the Cruden and Varnes (1996) classification scheme.

3 Methods

The approach used to test our research hypotheses encompasses two distinct steps: (i) exploring differential erosion and auxiliary information (slope angle) to map different lithological units; (ii) comparing the contribution of GF and LU maps for susceptibility to different landslide types through validation using sensitivity analysis.

3.1 Lithological Units Mapping

The construction of a detailed lithological map from existing geological maps, keeping the different units stratigraphically grouped but spatially differentiating the main lithological types, is explored in this work and is supported by exploring ancillary information, mainly a slope angle map. Additionally, available orthophotomaps and 1:15,000 scale aerial photographs are also used to validate the new lithological limits by exploring, for example, the presence of rill and gully phenomena generated by runoff, allowing better definition of permeable and impermeable lithological unit boundaries. To infer differential erosion, the slope angle map was explored considering an analogous interpretation process such as the ones associated with a photography construction (photo negative/photo positive), in which for a negative photographic film (image), the lightest areas of an object look darkest, and the darkest areas look lightest. The relationship between slope angle and differential erosion to identify lithological units and map their limits is explored similarly. Two interpretation rules are defined:

(i) Negative perspective—the sharp transition between two lithological units is made without a clear sign in the slope angle map, even in the steepest slope sectors associated with limestone rock walls. In this case (Fig. 2A), the tops and spurs related to the presence of resistant lithologies (structural control) appear associated with flat or gentle slope angles; and soft lithological units are characterized by moderate slope angles (the steepest areas in the context <25º). The vertical limestone rock walls. Generally, 10–20 m high are not appropriately represented in the slope angle map due to the topographic map resolution (1:10 000, 5 m contour

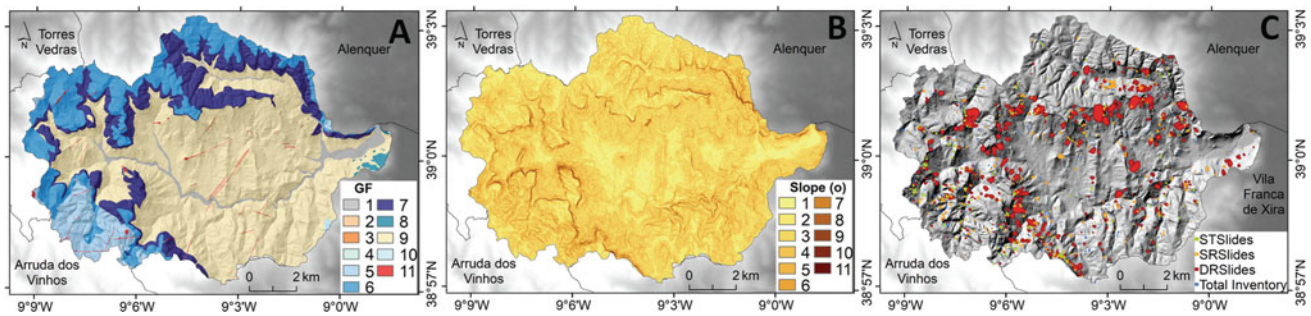

Fig. 1 Grande da Pipa River (GPR) basin: geological (GF) map (**A**), slope map (**B**) and landslide inventory map (**C**): STSlides (shallow translational slide), SRSlides (shallow rotational slide), DRSlides (Deep-seated rotational slide)

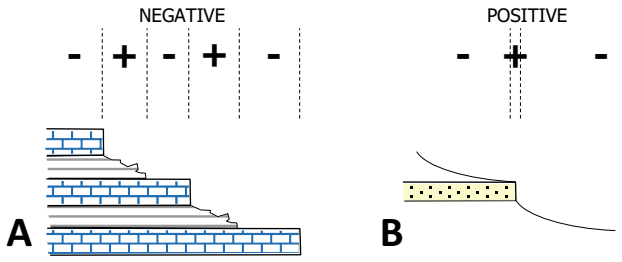

Fig. 2 Interpretation rules to identify lithological units from slope angle and differential erosion relationship: negative and positive perspectives

interval). This is observable for thicker lithological units;

(ii) Positive perspective—the presence of narrow lanes with the highest slope values. These are interpreted as more resistant lithological units. Usually, they correspond to thin sandstone or limestone layers inside thick clay and marl lithological units in the study area. The result is a small topographic step and a near-horizontal spur on gentle to moderate slopes (Fig. 2B).

The official geological map overlapped with the classified slope angle map to map the lithological unit limits. Iteratively it was verified that a slope class limit of 20º allowed the best separation between soft (<20º) and resistant (>20º) lithologies (thicker layers) and that a slope class between 20º to 25º allows the best identification of thin resistant layers intercalated in soft lithologies. Lastly, the lithological map was confronted with previous lithological/lithostratigraphic maps produced for different test sites, which were validated with fieldwork in the following GPR sub-basins: Laje and Salema (Pimenta, 2011), Monfalim and Louriceira (Lajas, 2016; Oliveira et al., 2017), Quintas (Fonseca, 2020).

3.2 Assessment of the Geological and Lithological Maps Predictive Capacity

In the first step, the Favorability Function (Chung and Fabbri 2003) was computed to compare the relationships between independent geological/lithological map classes and dependent landslide inventory maps. In practice, it expresses the conditional probability of finding a landslide in each class of a variable and can be assumed as a susceptibility indicator (Zêzere et al. 2004). Four different partitions of the historical landslide inventory map for the GPR basin were considered as dependent variables (Oliveira et al., 2015): Inv. #1—total landslide inventory (1434 landslides); Inv. #2—424 deep-seated rotational slides; Inv. #3—382 shallow rotational slides; and Inv. #4—169 shallow translational slides. The landslides that occurred on man-made cut and fill slopes were not used in the analysis. In the second step, the Information Value (IV) bivariate statistical method (Yin & Yan, 1988) was applied for computing the overall landslide susceptibility capacity of both geological (GF) and lithological (LU) maps used as the only landslide predisposing factor. Eight susceptibility models were computed according to the modelling strategy defined in Table 1. The validation of these susceptibility maps was carried out by computing the corresponding Receiver Operating Characteristic (ROC) curves and the estimation of the Area Under the ROC curve (AUROC). Only the model adjustment to the landslide inventories is considered since the same landslide inventories were used to train and validate the susceptibility maps.

4 Results and Discussion

The lithological map produced for the GPR basin (Fig. 3A) contains17 lithological units and is an increment of the lithological differentiation in the study area, starting from the 11 geological formations identified in the official map (Fig. 1A). The limits of the new lithological units inferred from the slope angle map show a reasonable fit to the detailed lithological maps developed independently for different sub-basins in the RGP basin (Fonseca, 2020; Lajas, 2016; Pimenta, 2011). Small limits adjustments were made based on aerial photointerpretation. The IV scores were computed for the GPR basin, expressing which predisposing factor classes conditioned more the occurrence of a certain landslide type. The overall sensitive validation (model adjustment) of both GF and LU maps using the landslide inventory partitions #1 to #4 are shown in Fig. 3B. The validation (model adjustment) of the GF and LU susceptibility models for the GPR basin shows significative

Table 1 Training/validation strategy for the landslide susceptibility models based on geological (GF) and lithological (LU) maps

		Independent predisposing factors	
		GF	LU
Dependent variable	Inv. #1	Model A1	Model A2
	Inv. #2	Model B1	Model B2
	Inv. #3	Model C1	Model C2
	Inv. #4	Model D1	Model D2

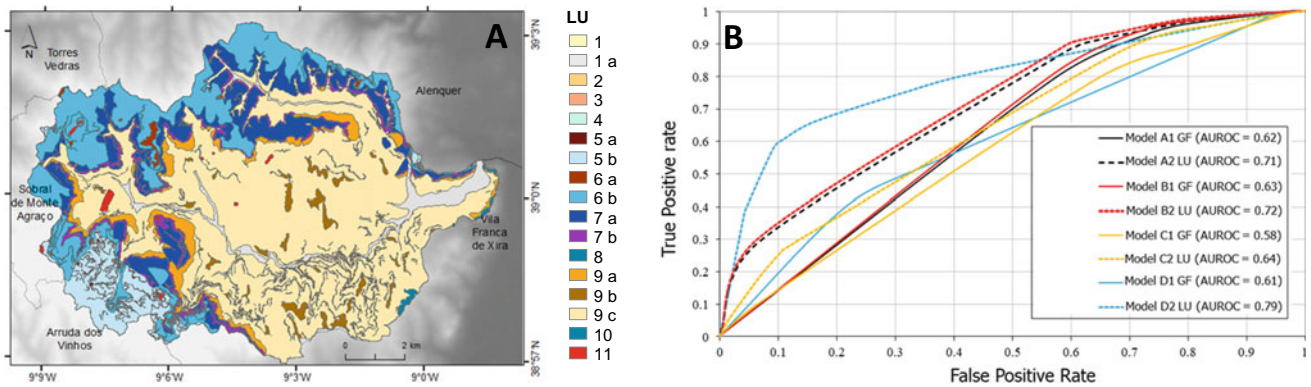

Fig. 3 Lithological (LU) map for the Grande da Pipa River basin (**A**): 1a) alluvium incipient deposits, (1) alluvium, (2) limestone intercalations, (3) conglomerates, sandstones, mudstones, (4) sandstones, marls, limestones; (5a) sandstones/limestones, (5b) marls; (6a) sandstones/limestones; (6b) clays/marls; (7a) limestones; (7b) marls, (8) limestones, (9a) slope deposits, (9b) sandstones, (9c) clays and marls, (10) conglomerates, (11) dykes and magmatic intrusions; (**B**) Validation of landslide susceptibility models for GPR basin

difference expressed by the AUROC values obtained for the four landslide inventories used as dependent variables (Fig. 3B), where models built with the LU map consistently show better results. AUROC differences between GF and LU susceptibility models range from 0.06 (Models D1-D2), 0.09 (Models A1-A2 and B1-B2) to 0.18 (Models D1-D2), which quantitatively reinforces the predictive capacity of the susceptibility models when a more detailed lithological map is used.

5 Concluding Remarks

The present work explores ancillary cartographic information of a slope angle map to infer the position and limit of the different lithological units, starting from preexisting official geological maps, considering their association to differential erosion processes, and using morphological interpretation criteria. The results consistently record improved predictive capacity for landslide susceptibility if more detailed lithological maps are used instead of the commonly available geological maps. Although it is presented as a practical lithological mapping approach, it is necessary to establish relationships between slope angle and soft/resistant lithologies and establish adequate interpretation criteria adjusted to the morphological and geological contexts. This work highlights how important can be the improvement of a predisposing factor map (geology/lithology) in landslide susceptibility assessment and encourages future research to improve the base maps used as landslide predisposing factors.

Acknowledgements This work is funded by FCT—Portuguese Foundation for Science and Technology, I.P., through the project BeSafeSlide—Landslide Early Warning soft technology prototype to improve community resilience and adaptation to environmental change (PTDC/GES-AMB/30052/2017) and through national funds (PIDDAC) by the Research Units UIDB/00295/2020, UIDP/00295/2020 and FCT-UIB/50019/2020-IDL.

References

Cruden, D. M., & Varnes, D. J. (1996). Landslide types and processes. In A. K. Turner, & R. L. Schuster (Eds.), *Landslides investigation and mitigation. Transportation research board. National Academic Press, Washington DC, Special Report* (Vol. 247, pp. 36–75).

Fonseca, R. (2020). Determinação da suscetibilidade à ocorrência de instabilidades em vertente à escala regional com métodos de base física. Faculdade de Ciências, Universidade de Lisboa, Lisboa (MSc Dissertation).

Henriques, C., Zêzere, J. L., & Marques, F. (2015). The role of the lithological setting on the landslide pattern and distribution. *Engineering Geology, 189*, 17–31.

Kullberg, J. C., Rocha, R. B., Soares, A. F., Rey, J., Terrinha, P., Callapez, P., & Martins, L. (2006). A Bacia Lusitaniana: Estratigrafia, Paleogeografia e Tectónica. In R. Dias, A. Araújo, P. Terrinha, J.C. Kullberg (Eds.), *Geologia de Portugal no contexto da Ibéria. Universidade de Évora* (pp. 317–368).

Lajas, S. M. A. (2016). Integração de métodos estatístico e determinístico para a avaliação da suscetibilidade a deslizamentos superficiais. IGOT, Universidade de Lisboa, Lisboa (MSc Dissertation).

Oliveira, S. C., Zêzere, J. L., Catalão, J., & Nico, G. (2015). The contribution of PSInSAR interferometry to landslide hazard in weak rock-dominated areas. *Landslides, 12*, 703–719.

Oliveira, S. C., Zêzere, J. L., Lajas, S., & Melo, R. (2017). Combination of statistical and physically based methods to assess

shallow slide susceptibility at the basin scale. *Natural Hazards and Earth Systems Sciences, 17*, 1091–1109.

Pimenta, R. S. G. G. (2011). Avaliação da suscetibilidade à ocorrência de movimentos de vertente com métodos de base física. Faculdade de Ciências, Universidade de Lisboa, Lisboa (MSc Dissertation).

Yin, K., & Yan, T. (1988). Statistical prediction models for slope instability of metamorphosed rocks. In C. Bonnard (Ed.), *Landslides: Proceedings of the Fifth International Symposium on Landslides, International Symposium on Landslides, Lausanne* (Vol. 3, pp. 1269–1272).

Zbyszewski, G., & Assunção, C. T. (1965). Notícia explicativa da folha 30-D (Alenquer). Carta Geológica de Portugal (1:50 000). Serviços Geológicos de Portugal, Lisboa.

Road Network Exposure to Deep-Seated and Shallow Slides at the Basin-Scale (Grande da Pipa River Basin, Portugal)

Igor Branco, Sérgio C. Oliveira, and Raquel Melo

Abstract

Landslides are well-known for their destructive capacity; however, risk only exists if an interaction with people, activities, structures and infrastructures occurs. When landslides affect roads and potential human losses, both road damage and road disruption can cause significant economic losses. Therefore, in the framework of spatial planning, civil protection, emergency and risk management and the evaluation of road network landslide exposure is necessary. The primary goal of this work is to assess the present road network exposure to deep-seated and shallow slides at the Grande da Pipa River basin (North of Lisbon region, Portugal), an area naturally prone to geomorphological hazards. Our approach to assessing road network exposure is sustained by two different dataset inputs: (i) three landslide susceptibility maps and (ii) one road network map. The susceptibility to landslides, computed with the Information Value method and validated with success and prediction rate curves, as well as with the estimation of the area under the curves, was individually assessed for deep-seated rotational, shallow rotational and shallow translational slides. The road network exposure to each landslide type resulted from the intersection between the two top landslide susceptibility classes and the classified road network according to its rank, allowing the critical road sections to be identified. The road network is mainly exposed to deep-seated rotational slides. However, the other landslide types can also disrupt the road functionality and affect residents and economic activities.

Keywords

Deep-seated and shallow slides • Road network • Susceptibility • Exposure • Basin-scale

1 Introduction

Risk, as considered by the conceptual model of risk, equals the crossing of a hazard with the value of the elements at risk through their vulnerability (Zêzere et al., 2008). Identifying each of these components is very important to the risk analysis. However, identifying elements at risk is possibly the most crucial step in risk assessment (Zêzere et al., 2008). The area north of Lisbon is one of Portugal's most critical landslide-prone areas, and landslides have been responsible for road damage in the last decades (Zêzere et al., 2007). When landslides affect roads and potential human losses, both road damage and road disruption can cause significant economic losses. The primary objective of this research is to evaluate the present road network exposure to landslides (REL) and to identify critical road sections (CRS) at the Grande da Pipa River (GPR) basin (North of Lisbon, Portugal), an area naturally prone to geomorphological hazards (Oliveira et al., 2015), represented in Fig. 1.

2 Materials and Methods

Our approach to assessing REL is sustained by two different dataset inputs: (i) three landslide susceptibility maps and (ii) one road network map. Three slide inventories and seven predisposing factors were applied to assess the susceptibility to landslides.

I. Branco
Centre for Social Studies, University of Coimbra, Coimbra, Portugal

S. C. Oliveira (✉) · R. Melo
Centre of Geographical Studies, Institute of Geography and Spatial Planning (IGOT), University of Lisbon, Lisbon, Portugal
e-mail: cruzdeoliveira@campus.ul.pt

R. Melo
Department of Geosciences, School of Science and Technology, University of Évora, Évora, Portugal

S. C. Oliveira
Associated Laboratory TERRA, Lisbon, Portugal

A. Malheiro et al. (eds.), *Advances in Natural Hazards and Volcanic Risks: Shaping a Sustainable Future*, Advances in Science, Technology & Innovation, https://doi.org/10.1007/978-3-031-25042-2_21

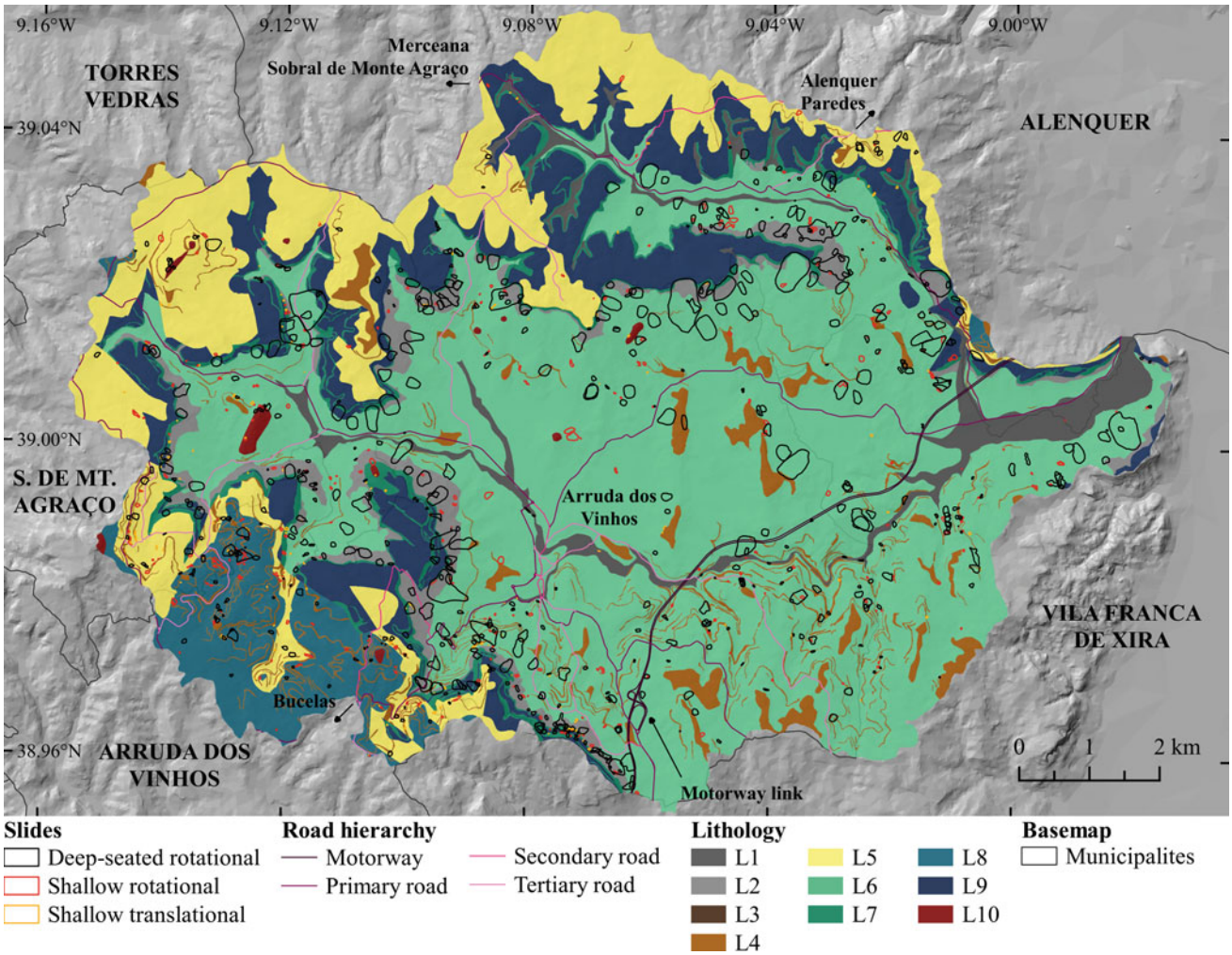

Fig. 1 Grande da Pipa River basin. Slides' distribution can be seen, as well as the road network hierarchy and lithology, organized by lithological type. L1—Alluvium, L2—Slope deposits, L3—Conglomerates, sandstones, and mudstones, L4—Sandstones, L5—Mudstones, sandstones, marls, and limestones, L6—Marls and mudstones, L7—Marls, L8—Limestones and marls, L9—Limestones, and L10—Igneous intrusive rocks

2.1 Susceptibility Assessment

The landslide susceptibility was individually assessed for each one of the three landslide types that most frequently occur in Portugal's most important landslide-prone areas: deep-seated rotational (DR), shallow rotational (SR), and shallow translational (ST) slides. The data required for this step included three landslide inventories (Oliveira et al., 2015), one for each landslide type (DR, SR and ST), and seven independent predisposing factors (slope, aspect, plan curvature, Topographic Position Index, Slope Over Area Ratio, soil thickness, lithology), selected due to their acknowledged importance for the constrain of landslide activity in GPR basin (Oliveira et al., 2015). Concerning the landslide susceptibility processing, the inventories for each type of landslide were randomly partitioned into a 70–30% ratio, where 70% of the landslides were used for training and 30% to validate the modelling results. For the statistical relationship assessment between each type of landslide and the dataset of predisposing factors, we used the Information Value (IV) method, a bivariate statistical and Bayesian approach that quantifies, in scores, the landslide susceptibility for every single class of any given predisposing factor (Yin & Yan, 1988). The scores can be estimated by the following formula (Yin & Yan, 1988):

$$li = \ln \frac{SI/NI}{S/N} \quad (1)$$

in which li is the IV of the Xi factor, SI is the amount of unstable map area units (cells with a resolution of 5 m) with episodes of slope failure and the occurrence of the Xi factor, NI is the amount of map area units with the Xi factor, S is the amount of unstable map area units with episodes of slope

failure, and N is the amount of map area units. Due to the logarithmic normalization, the IV cannot be assessed when $SI = 0$; in these cases, we assume the IV as the decimal below the lowest IV value. Positive values demonstrate that there is an association between the class of the predisposing factor and the occurrence of landslides. The higher the value, the stronger the relationship. Negative values indicate that the class of the predisposing factor has less influence on the phenomenon's occurrence (Piedade et al., 2011). The susceptibility value for each map area unit corresponds to the total IV, determined by the expression hereinbelow (Yin & Yan, 1988):

$$lj = \sum_{i=1}^{n} Xjili \quad (2)$$

where lj is the final IV for each map area unit, n is the amount of conditioning factors, and Xji is equal to 1 or 0, depending on the factor's existence or absence in the j map area unit, respectively.

Both landslide susceptibility training performance and independent prediction capacity were computed with success and prediction rate curves, respectively, and with the estimation of the area under the curves (AUC). Regarding the classification for each landslide susceptibility map, it was defined that each class must cumulatively validate, respectively, 50% (very high), 70% (high), 85% (moderate), 95% (low) and 100% (very low) of the landslide area from the validation group (e.g. 70% of the landslides from the validation group are included in the very high and high susceptibility classes).

2.2 Road Network Exposure

The road network was extracted from OpenStreetMap, downloaded at the Geofabrik server (https://download.geofabrik.de/europe/portugal.html), and ranked in four main categories: motorways (21.5 km), primary/national roads (51.4 km), secondary/municipal roads (8.6 km) and tertiary/rural roads (36 km). The motorway's viaduct sections were not considered for road network exposure to shallow rotational and translational slides, as we do not expect shallow slides to damage the pillars that support those motorway's viaduct sections.

The road network exposure to landslides (REL) relative to each landslide type (REL-DR, REL-SR and REL-ST) results from the intersection between the two top landslide susceptibility classes (high and very high) and the different road categories. Therefore, every road section has a susceptibility value attached. Road sections that intersect with high and very high susceptibility areas are classified as exposed (value 1) and the remaining road sections as not exposed (value 0). Furthermore, we summed the three binary REL maps and classified the roads assigned with value 3 (indicating exposure to all slide types simultaneously) as critical road sections (CRS). This set of methods allowed us to identify the roadways which we consider a priority from an emergency and risk management perspective.

3 Results and Discussion

3.1 Susceptibility Assessment

The IV scores show that the areas with the ideal conditions for the occurrence of DR, SR, and ST slides at the GPR basin are generally located on moderate (>10° in the case of DR) to steep (>25°) concave slopes, covered by poorly developed soils (0.5 to 1.5 m thick), and characterized by medium to high Slope Over Area Ratio indexes, which indicates the potential to accumulate water. Nevertheless, DR slides tend to occur on L2 and L6 units, while SR and ST slide occurs on L5, L6 and L8 layers (Fig. 1). The success and prediction AUC's resulted in the following values: 0.80 (DR), 0.76 (SR) and 0.88 (ST) by the former and 0.76 (DR), 0.73 (SR) and 0.84 (ST) by the latter. After the classification, it was ascertained that the high and very high susceptible classes cover 30% (DR), 34% (SR) and 23% (ST) of the GPR basin and are mainly located at the L6 complex, on slopes distinguished by a moderate slope angle (DR), and at the hilly southwestern side of the basin (SR and ST), as shown in Fig. 2.

3.2 Road Network Exposure

Considering the total length of the road network, 29%, 27% and 25% are exposed to DR, SR, and ST slides, respectively. These sections are mainly located (i) on the south side of the basin, from Arruda dos Vinhos village to Vila Franca de Xira municipality; (ii) on the southwestern side of Arruda dos Vinhos municipality; (iii) at the northeast side of the basin, where the road network heads straight to the north and to Alenquer municipality; (iv) and at the west side of the basin, from central Arruda dos Vinhos municipality to Sobral de Monte Agraço municipality (Fig. 2).

About the road network exposure to deep-seated rotational slides (REL-DR), these sections are mostly located along primary roads (16.4 km; 48%), tertiary roads (8.1 km;

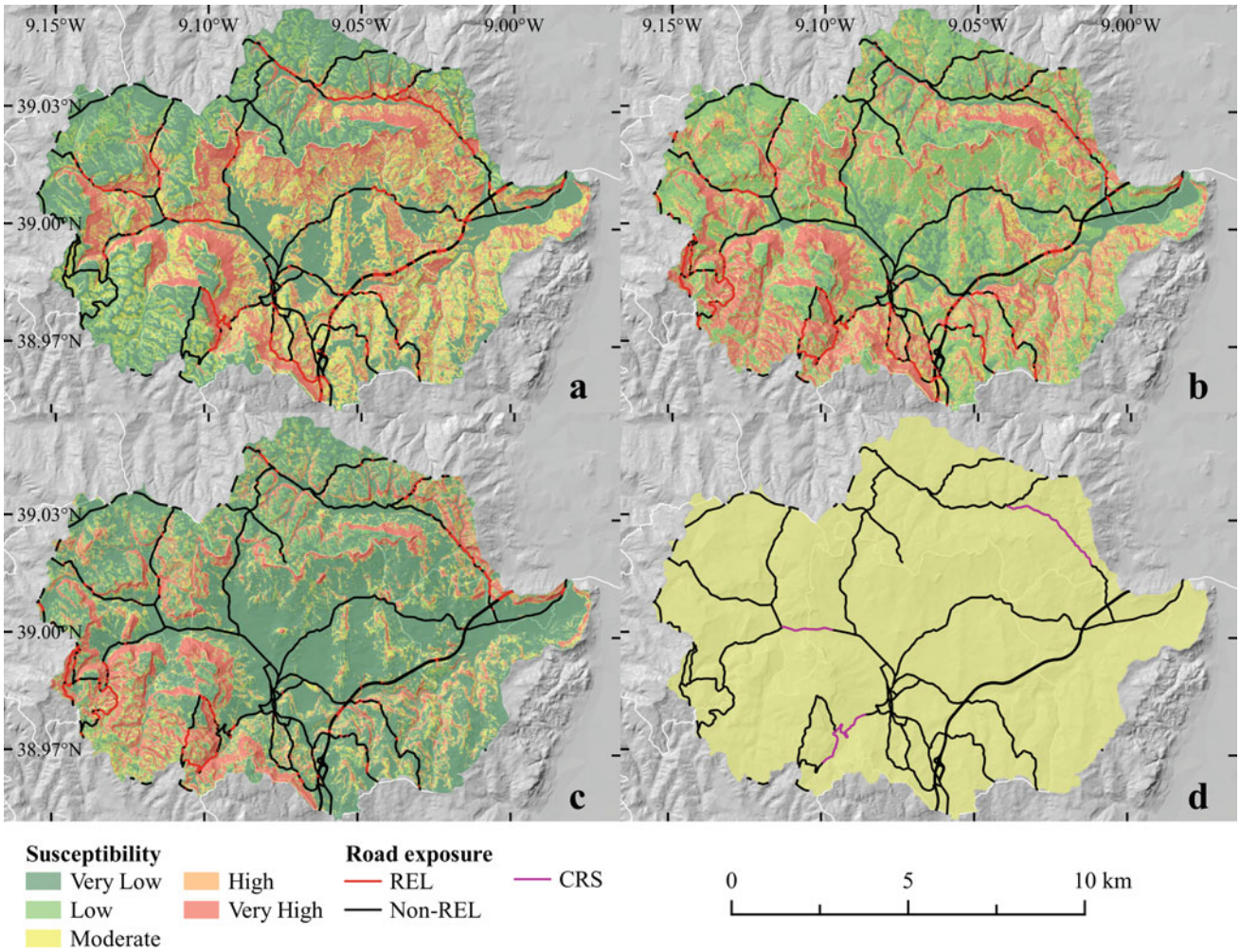

Fig. 2 Grande da Pipa River basin landslide susceptibility (green-yellow–red palette) and road network exposure (red lines) to DR slides (**a**), SR slides (**b**), and ST slides (**c**). Critical road sections (CRS) are highlighted in purple at **d**

24%) and the motorway (8.2 km; 24%), and include the unique section that links all the road network in the basin to the motorway (Figs. 1 and 2).

The road network is also highly exposed to SR slides. These sections are found along primary roads (13.6 km; 45%) and tertiary roads (10.8 km; 36%). Regarding the ST slides, the road network is less exposed than REL-DR or REL-SR, but some sections also should receive attention, mainly along primary roads (8.5 km; 48%) and tertiary roads (5.6 km; 32%). The critical road sections (CRS) are located at the (i) northeast side of the basin, (ii) south side of the basin and (iii) between the west side and the centre side of the basin. These CRS are important means of communication, not only because they establish the connection between the north and south sides of the basin to its centre, as well as to its most crucial settlement (Arruda dos Vinhos), but also by providing connection to other municipalities' settlements (Alenquer, Sobral de Monte Agraço, Bucelas).

4 Concluding Remarks

The primary goal of this research was to assess the road network exposure to landslides at the basin-scale. First, the landslide susceptibility was assessed for three different slide typologies: deep-seated rotational, shallow rotational and shallow translational slides. The most susceptible areas are mainly found at the L2 and L6 units, on slopes distinguished by a moderate slope angle. Then, the road network exposure to landslides (REL) was assessed by intersecting each

model's two highest landslide susceptibility classes with the road network. The road network is highly affected by all landslide types, mainly by deep-seated rotational slides. These sections are located at the basin's south, northeast, and west sides, linking the basin's centre and the Arruda dos Vinhos village with the neighbouring municipalities. Finally, the critical road sections (CRS) were also assessed considering the sum of the three REL maps. The selected three CRS represent the sections that should receive more attention from an emergence and risk management perspective.

Acknowledgements We would like to thank the BeSafeSlide project team for all its contributions to this research. This research was supported by national grants through FCT (Foundation for Science and Technology, I. P.), under the framework of the project BeSafeSlide—Landslide early warning soft technology prototype to improve community resilience and adaptation to environmental change (PTDC/GES-AMB/30052/2017) and by the Research Unit UIDB/00295/2020 and UIDP/00295/2020.

References

Oliveira, S. C., Zêzere, J. L., Catalão, J., & Nico, G. (2015). The contribution of PSInSAR interferometry to landslide hazard in weak rocks dominated areas. *Landslides, 12*(4), 703–719.

Piedade, A., Zêzere, J. L., Garcia, R. A. C., & Oliveira, S. C. (2011). Modelos de susceptibilidade a deslizamentos superficiais translacionais na Região a Norte de Lisboa. *Finisterra, 46*(91), 9–26.

Yin, K., & Yan, T. (1988). Statistical prediction models for slope instability of metamorphosed rocks. In C. Bonnard (Ed.), *Landslides: Proceedings of the Fifth International Symposium on Landslides*, *International Symposium on Landslides, Lausanne* (Vol. 3, pp. 1269–1272).

Zêzere, J. L., Garcia, R. A. C., Oliveira, S. C., & Reis, E. (2008). Probabilistic landslide risk analysis considering direct costs in the area north of Lisbon (Portugal). *Geomorphology, 94*, 467–495.

Zêzere, J. L., Oliveira, S. C., Garcia, R. A. C., & Reis, E. (2007). Landslide risk analysis in the area North of Lisbon (Portugal): Evaluation of direct and indirect costs resulting from a motorway disruption by slope movements. *Landslides, 4*(2), 123–136.

The Functional Schematisation of the City as a Model for Anticipating Post-event Scenarios for Volcanic Hazards

Rafael Ramírez Eudave and Tiago Miguel Ferreira

Abstract

Risk analysis requires the accurate characterisation of the hazardous events and their possible effects on the exposed elements. As demonstrated in recent events, volcanic activity may inflict several perturbations in urban functions, even compromising emergency-response actions. Thus, it is of the utmost interest to have holistic approaches that consider the city through its components for assembling feasible scenarios and performing mitigation strategies based on the system's critical vulnerabilities. Failure Tree, Event Tree and Failure Mode and Event analysis are presented in this article as suitable approaches for conducting vulnerability-oriented research by using the village of San Pedro Tlalmimilulpan (México), in the context of the Popocatepetl volcano, as a case study. As demonstrated herein, these approaches facilitate the schematisation of the city based on the functions and infrastructures that, for a specific event scenario, are identified as critical for supporting sheltering and evacuation activities using such a traffic-light alert system. These analyses, supported by the existence of Risk Maps, reveal a series of proactive actions that would mitigate the adverse consequences of volcanic events. Furthermore, it is possible to find some highlights for designing a more efficient evacuation plan based on the most likely failures when analysing the singularities and location of a determinate village. The schematisation of urban functions in failure and event-based trees permitted identifying critical components of Tlalmimilulpan towards volcanic hazards, which may support the production of straightforward policies for risk mitigation and management in similar urban areas.

Keywords

Evacuation • Scenarios • FTA • ETA • FMEA

1 Introduction

Risk management demands a robust conceptual framework. International standard ISO 31000 (International Organization for Standardization 2006) proposes a generalised definition of risk understood as the effect of uncertainty on achieving the objectives of an organisation. Although "organisation" is not a common word for referring to human settlements, the logic behind this definition of risk is completely suitable when observing urban entities as functional schemes. Furthermore, the physical configuration of cities is often a material result of a series of functions and interdependencies (Ramírez Eudave & Ferreira, 2021a). Thus, it becomes convenient to assess the effects of perturbing events, such as volcanic activity, based on the effects that may cause on the functions of human settlements. Although damage and loss-based analysis are common strategies for assessing risk in this context, a functional schematisation at a local level would help design emergency response strategies. The present work discusses the potential suitability and opportunities of function-based modelling of human settlements towards volcanic activity.

2 Human Settlements as Functional Networks

A function-based analysis of the urban environment departs from encoding some capacities and limits states of its infrastructures and networks, namely regarding the sustainability of functions towards a sudden diminution of supplies (such as water, electricity, etc.) or physical perturbations (such as the interruption of roads). The analysis depends on

R. Ramírez Eudave (✉)
Departamento de Engenharia Civil, Universidade do Minho, ISISE, Guimarães, Portugal
e-mail: r.92@outlook.es

T. M. Ferreira
College of Arts, Technology and Environment, School of Engineering, University of the West of England, Bristol, UK

A. Malheiro et al. (eds.), *Advances in Natural Hazards and Volcanic Risks: Shaping a Sustainable Future*, Advances in Science, Technology & Innovation, https://doi.org/10.1007/978-3-031-25042-2_22

a hazard-based framework in which the conditions imposed by the disruptive event are qualitative and/or quantitative described.

2.1 Methodology

A representative hazard assessment framework (that of the Mexican Volcanic Traffic Light Alert—VTLAS) has been used to categorise the city's potential disruptions due to volcanic activity. Then, the analysis of the city must be consistent with the hazard indicators. The work of Guzman (2020) illustrates a generic approach for organisations (that of SWOT: strengths, Weaknesses, Opportunities and Threats) for characterising historical cities. This approach is performed to assess the historic city's sustainability due to numerous sources of pressure, considering natural events. Another approach (Vehbi & Hoskara, 2009) suggests identifying representative indicators corresponding to causal events and their expected outcomes of interest for a determined context. This approach is conveniently suitable for event-based analysis, where indicators and descriptors are tailored to specific functions, performance, and perturbation. Therefore, the analysis primarily departs from the knowledge of the conditions in which functions can be sustained and the confrontation against the agents and/or components related to a determined hazard. This work suggests the use of Failure Mode and Event Analysis (FMEA) as well as Failure and Event Tree Analysis (FTA and ETA) for this purpose.

2.2 Exposure-Based Assessments: The Mexican Alert System

Mexican experience with volcanic alert systems is primarily developed in the context of the Popocatepetl volcano, located in the centre of the country, ca. 60 km away from Mexico City. The existence of densely populated cities in the surrounding area promoted the design and implementation of an Early Warning System (EWS) based on a colour code. This Volcanic Traffic Light Alert—VTLAS ("Semáforo de Alerta Volcánica", in Spanish) is intended to provide an easy and straightforward synthesis for the public, facilitating preparedness against eruptive scenarios (De la Cruz-Reyna & Tilling, 2008). This system establishes thresholds and scenarios for seven phases associated with three levels: Green I and II; Yellow I, II and III; and Red I and II. The description of each phase summarises a series of expected sub-events, such as seismic activity, fumaroles, ejection of materials, etc.

The VTLAS approach, together with the maps contained in the Mexican National Atlas of Risks, facilitates framing the occurrence of certain phenomena in a given place or region during a specific phase associated with a VTLAS colour. Given the description of events, it is feasible to identify the elements exposed according to the information in the public Geographical Information System, that of the Mexican National Map (INEGI—Instituto Nacional de Estadística y Geografía, 2020). This cartography includes some relevant territorial features, such as roads, infrastructure related to health, education and emergency services, etc. The susceptibility of these elements toward determinate volcanic phenomena will be further assessed.

2.3 San Pedro Tlalmimilulpan in the Context of Volcanic Hazards

San Pedro Tlalmimilupan (1637 habitants in 2019) is a settlement of the municipality of Tetela del Volcán, state of Morelos, México. It is located 16 km away from Popocatepetl. The present paper is aimed to assess the functions of this settlement in the context of evacuation activities when the VTLAS alert raises Red phase I or Red phase II levels, corresponding to a Vulcanic Explosivity Index value higher than 3.

The settlement was spotted in each one of the hazard maps of the Mexican National Atlas Risk, revealing how exposed the settlement is to the following specific hazards: tephra, projectiles, pyroclastic density currents, lahar (or mudflows), lava flows and debris avalanches. Each map represents a series of rings centred on the volcanic cone, identifying a progressive series of exposure levels. The ring corresponding defines the relative exposure to San Pedro Tlalmimilulpan (y) in the context of the total of rings considered (x) (Table 1).

This assessment permitted identifying the more likely hazards to induce perturbations in the system. The specific incidence of these hazards is complementary to the identification and detailed analysis of the sensitivities that the components of the city have. As discussed in the next section, this task can be performed using different approaches, including the Failure Mode and Effect Analysis.

2.4 Results: A Functional Schematisation of San Pedro Tlalmimilulpan Towards Volcanic Events.

The Failure Mode and Effect Analysis (FMEA) is aimed to characterise a system by subdividing it into components (Alizadeh et al., 2015). Each component is further assessed on its description, function, interaction, performance requirements, potential failure modes (and the corresponding root causes and effects), means or methods of detection and mitigating measures (Table 2). Based on the hazards that are

Table 1 Relative exposure to hazard

Hazard	Relative exposure of San Pedro Tlalmimilupan (*y*/*x*)	Hazard	Relative exposure of San Pedro Tlalmimilupan (*y*/*x*)
Tephra	2/3	Lahar or mudflows	1/4
Projectiles	0	Lava flows	0
Pyroclastic density currents	¼	Debris avalanches	1

Table 2 Summary of the FMEA analysis for the components of the settlement

Hazard	Summary
Roads	Can be interrupted by structural collapses (i.e., accumulation of debris) or thick tephra layers, compromising evacuation and/or transporting supplies
Vehicles	Private vehicles are the only motorised mean of evacuation. A census, periodical check of vehicles and emergency gas supply would be needed to maximise their use during an emergency
Public Address service	Based on loudspeakers is the most robust way of informative diffusion in the surrounding area. However, it may fail due to lack of energy, compromising the organisation and emergency response
Provisional shelter	Safe places offer food, clean water, beds and medical materials during an emergency. It is subjected to overpopulation or limitations if the available resources are insufficient
Electrical emergency supply	It gives redundancy to the municipal infrastructure by using backup plants. However, it may be compromised in case of mechanical failure and/or lack of petrol
Clean water supply	Reservoirs for guaranteeing a minimum supply during an emergency. It can be compromised if wells and deposits are not correctly isolated. Very sensitive to contamination due to ashes

more likely to occur in San Pedro Tlalmimilulpan and the actions recommended on the VTLAS system, the FMEA approach for this settlement is focused on the eventual need for evacuation.

The systems identified during the FMEA stage are valid for assessing events that may cause or have origin in a determined failure of the system. The Failure and Event Tree Analysis are schematic representations of conditions. FTA is a pre-event assessment of multiple chained facts that result in a determinate failure of the system (Fig. 1). It is possible to start with a determinate failure for assessing a series of post-event scenarios (ETA) to calculate potential outcomes, namely related to probabilities of loss or damage (Fig. 2). Both assessments can be combined (Ramírez Eudave & Ferreira, 2021b) to establish the events/conditions and their relations (logical operators).

3 Discussion

The joint use of FMEA, FTA and ETA analysis permitted concluding that the probability of short-term losses and damages in San Pedro Tlalmimilulpan during volcanic activity is low. Nevertheless, there is a series of realistic sources of thread for performing the evacuation of the settlement, which may lead to mid and long-term losses and damages. A very critical aspect is the rapidness of reaction, conditioned by the success of Public Address systems, usability conditions of the roads and the number of available vehicles. In addition, it is critical to have sheltering capacities for supporting acceptable conditions and services for the population if evacuation is delayed.

It is convenient to note that safety conditions during all stages of evacuation are conditioned to external events that

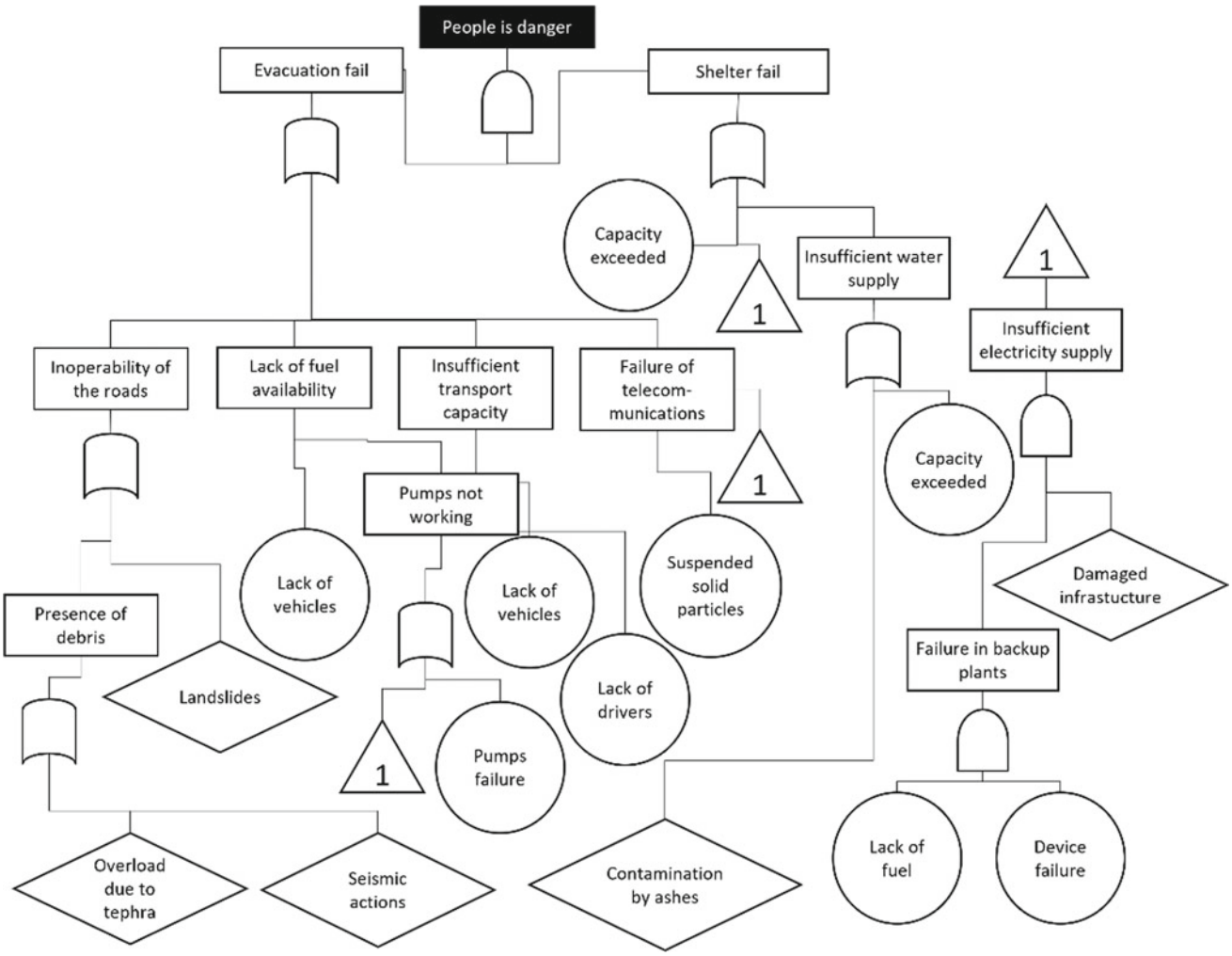

Fig. 1 Failure more analysis considering the series of events that may put people in danger

are not easily predictable, such as landslides. However, most threat triggers can be minimised by the mean of permanent inspections.

4 Concluding Remarks

To systematise a human settlement as a functional organisation helps recognise potential damage and loss scenarios toward volcanic events. This can be done using FMEA, FTA and ETA analysis and hazard-based maps, for example. These approaches contextualise sensitive aspects of the settlement that may receive attention for mitigating damages and losses. The robustness of emergency planning and early response can be modelled in these schemes to test how different series of events can trigger dangerous situations and how a series of conditions shape the event and post-event scenarios. It is convenient to note that some components, circumstances and conditions deserve specific detailed assessments given their complexity. Nevertheless, this approach is compatible with enlarged analysis that may become a more robust and enlargeable analysis tool for risk assessment and management.

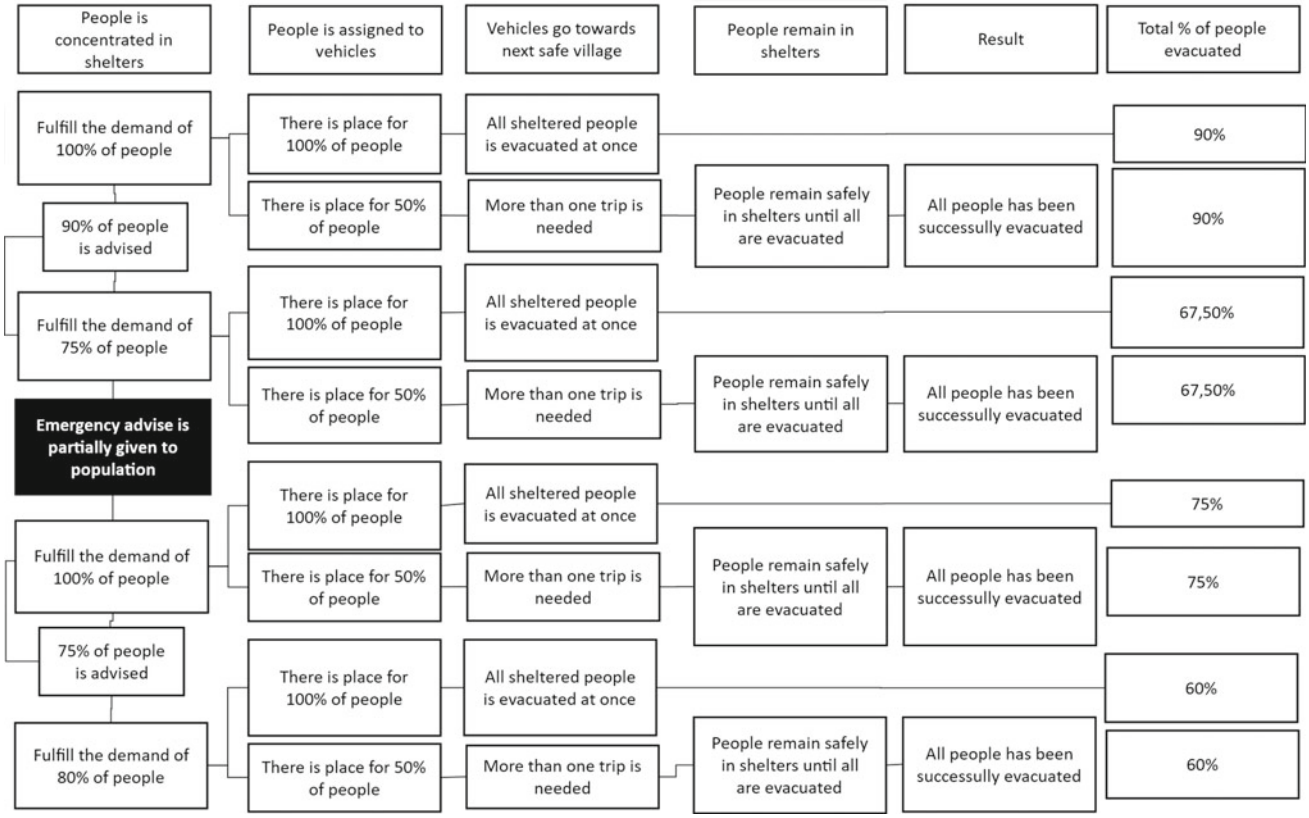

Fig. 2 Even tree analysis of the events that are likely to compromise the success of evacuation once the emergency advice is given

Acknowledgements This research was funded by the Portuguese Foundation for Science and Technology (FCT) through the grant number PD/BD/150385/2019. This work was partly financed by FCT/MCTES through national funds (PIDDAC) under the R&D Unit Institute for Sustainability and Innovation in Structural Engineering (ISISE), underreference UIDB/04029/2020.

References

Alizadeh, S. S., Rasoulzadeh, Y., Moshashaie, P., & Varmazyar, S. (2015). Failure modes and effects analysis (FMEA) technique: A literature review. Scientific Journal of Review. https://doi.org/10.14196/sjr.v4i1.1805

De la Cruz-Reyna, S., & Tilling, R. I. (2008). Scientific and public responses to the ongoing volcanic crisis at Popocatépetl Volcano, Mexico: Importance of an effective hazards-warning system. *Journal of Volcanology and Geothermal Research, 170*, 121–134. https://doi.org/10.1016/j.jvolgeores.2007.09.002

Guzman, P. (2020). Assessing the sustainable development of the historic urban landscape through local indicators. Lessons from a Mexican World Heritage City. *Journal of Cultural Heritage, 46*, 320–327. https://doi.org/10.1016/j.culher.2020.06.017

INEGI - Instituto Nacional de Estadística y Geografía. (2020). Mapa Digital de México. Retrieved 26 October, 2020, from http://gaia.inegi.org.mx/mdm6/.

International Organization for Standardization. (2006). ISO 31000 Risk management — Principles and guidelines. 61010-1 © Iec2001 2006:13.

Ramírez Eudave, R., & Ferreira, T. M. (2021a) Characterisation of the historic urban landscape through the aristotelian four causes: Towards comprehensive GIS databases. Remote Sens, *13*, 1879. https://doi.org/10.3390/rs13101879.

Ramírez Eudave, R., & Ferreira, T. M. (2021b). Towards a semi-quantitative approach for assessing evacuation scenarios in the context of Popocatépetl Volcano, México—The case of San Pedro Tlalmimilulpan. *GeoHazards, 2*, 1–16. https://doi.org/10.3390/geohazards2010001.

Vehbi, B. O., & Hoskara, ŞÖ. (2009). A model for measuring the sustainability level of historic urban quarters. *European Planning Studies, 17*, 715–739. https://doi.org/10.1080/09654310902778201

Multi-Hazard and Multi-vulnerability Analysis in Historical Urban Areas: Challenges and Opportunities

Chiara Arrighi, Marco Tanganelli, Vieri Cardinali, Maria Teresa Cristofaro, Antonino Maria Marra, Fabio Castelli, and Mario De Stefano

Abstract

Natural hazards increasingly threaten urban areas, and single-risk analyses performed within different methodological frameworks are often not comparable with each other and pose some difficulties for decision-makers. This work highlights the challenges and opportunities of multi-hazard and multi-vulnerability assessment in historical urban areas with a multi-disciplinary approach. Two hazards, i.e., seismic and flood, are included in a multi-risk workflow based on common exposure, vulnerability, and risk metrics. The city center of Florence (Italy) is selected to demonstrate the methodology. The application suggests that estimating direct physical damages for earthquakes and floods requires a different characterisation of exposure and vulnerability parameters. The results show significant differences in the spatial distribution of multi-risk, mostly depending on the evolution of the constructive typologies from the Middle Ages to the XX century and the anthropic alteration of terrain morphology.

Keywords

Multi-risk • GIS mapping • Floods • Earthquakes • Damage curves

1 Introduction

Natural hazards cause adverse consequences on human health and urban environments. In 2021, natural events caused overall losses of US$ 280bn and 9200 fatalities (Munich, 2022). Cities and metropolitan areas concentrate high exposure values and population density and are thus particularly important to study. Most risk assessments are carried out for single hazards (Blyth et al., 2020; Garrote et al., 2020). However, some works evaluate multiple exposures to hazards or produce multi-hazard qualitative indicators (Rahmati et al., 2019). The aims of this work are (i) to highlight key challenges for multi-hazard, multi-vulnerability risk assessments, (ii) to present a multi-risk workflow for buildings to overcome these challenges and provide a scientific basis for informed decision making, and (iii) to understand how the historical evolution of urban stock affects multi-risk. The application of the method is carried out in the most ancient portion of Florence (Italy), a UNESCO World Heritage site since 1982.

2 Materials and Methods

2.1 Challenges for Multi-risk Assessment

Multi-risk assessment requires a multi-hazard and a multi-vulnerability analysis, which considers the damage caused by different physical processes. Multi-risk is the sum of multiple damages, accounting for hazard-specific vulnerability, weighted by their annual exceedance probability in any given year, i.e., the average annual loss (AAL) (Arrighi et al., 2022). Thus, the information on hazard, exposure and vulnerability should be collected and used in a consistent path to be merged into a single multi-risk metric. Seismic and flood risk analyses are characterised by several methodological differences, namely (i) the spatial resolution of hazard information, (ii) the

C. Arrighi (✉) · A. M. Marra · F. Castelli
Department of Civil and Environmental Engineering, University of Florence, Florence, Italy
e-mail: chiara.arrighi@unifi.it

M. Tanganelli · V. Cardinali · M. T. Cristofaro · M. De Stefano
Department of Architecture, University of Florence, Florence, Italy

A. Malheiro et al. (eds.), *Advances in Natural Hazards and Volcanic Risks: Shaping a Sustainable Future*, Advances in Science, Technology & Innovation, https://doi.org/10.1007/978-3-031-25042-2_23

vertical distribution of exposure, and (iii) the vulnerability mechanisms. However, the spatial distribution of the seismic hazard can also be quite homogeneous for wide areas when seismic micro-zonation is available.

On the contrary, flood depths may vary significantly from building to building according to terrain elevations. The vertical exposure distribution includes the whole building above the ground for earthquakes and only the basement and lower floors for floodings. Assessing vulnerability and potential losses have reached a different state of the art for floods and earthquakes. In flood, if significant solid transport and other associated phenomena, such as scour or local erosion, are neglected, buildings rarely collapse or suffer structural damages. However, they often require a renovation, i.e., cleaning, replacing plastering, etc. Widely adopted flood vulnerability models assign expected relative damage to flood depth, accounting for limited structural losses (Molinari et al., 2021). In the case of earthquakes, structural damages occur frequently, constructive typologies and materials play a more crucial role, and the physical effects of seismic acceleration on a single building can be explicitly modelled (D'Altri et al., 2020). The above methodological differences require a multi-disciplinary approach to align methods, data resolution and output resolution and construct a consistent multi-risk workflow.

2.2 A Multi-risk Assessment Workflow

The multi-risk method here introduced is based on constructing a GIS database where the information on multi-hazard, multi-exposure and multi-vulnerability and other attribute data (e.g., period of construction, market values etc.) are consistently stored. Spatial correlation and joint probability analysis of the main multi-risk components are part of the method (Fig. 1). Multi-hazard information, i.e., average flood depths and seismic intensity for assigned probabilistic scenarios, are assigned to the same cartographic building data. The multi-exposure analysis considers the basement and ground floor for floods and all the floors above ground for seismic hazards, and the same footprint area and market value. Hazard-specific vulnerability functions are used (Molinari et al., 2021; Lagomarsino & Giovinazzi, 2006) to determine the physical damage concerning the corresponding exposure and calculate monetary losses for each probabilistic scenario.

The construction of the loss-frequency curve allows the calculation of single and multi-risk in the study area, expressed as €/year. Furthermore, the flood damage model has been validated through comparisons with flood scenarios in other Italian contexts, while the seismic recovery costs have been validated from the L'Aquila earthquake costs (Cosenza et al., 2018). Further details on the multi-risk method and joint probability analysis can be found in Arrighi et al. (2022).

2.3 Study Area

The study area (ca. 0.3 km^2) is the core of Florence (Italy) inside the town walls erected in 1172 (Fig. 2). The study area includes the old Roman *castrum* and a buffer area with successive urbanisation. Masonry structures, erected over Roman foundations, dominate the area characterised by three main demolitions and reconstructions that occurred in the Middle Ages, then in 1865 when Florence was temporarily the Capital of Italy and finally after WWII. The most recent buildings are reinforced concrete structures. Cultural heritage buildings, such as the cathedral and other monuments, are excluded from the analysis because their value and structural complexity does not allow a generalisation as the other buildings.

3 Application and Results

Physical and monetary damages in the study area are driven by multi-exposure. In fact, for floods, exposure is limited to basements in the westernmost part of the study area due to low water depth. In the easternmost part also, the ground floors are exposed. High-probability floods do not affect the study area, which starts to be exposed for a 1-in-100 year event. For earthquakes, the seismic exposure points out significant values. The constructions' significant dimensions denounce major values in the XIX century area.

Nonetheless, other high-exposed structures are pointed out in the Medieval area due to slender tower-houses. The physical damage is diffused along the entire area since different parameters increase and decrease the vulnerability of different structures. Table 1 summarises flood and seismic impacts for high-, medium- and low-probability scenarios. The average multi-risk on the building footprint is 23 €/m^2 mostly due to the seismic contribution. The most ancient constructions, e.g., tower houses, show very high multi-risk values (Fig. 2). Multi-risk calculated in the area is 3.15 M€/year, of which 2.64 M€/year is of seismic risk and 0.51 M€/year is of flood risk. If the three historical portions of territory in the study area are separately analysed, it can be noticed that the most ancient area (in orange in Fig. 2) has the highest multi-risk (17€/m^2), followed by the district built-in 1860–1945 (12 €/m^2).

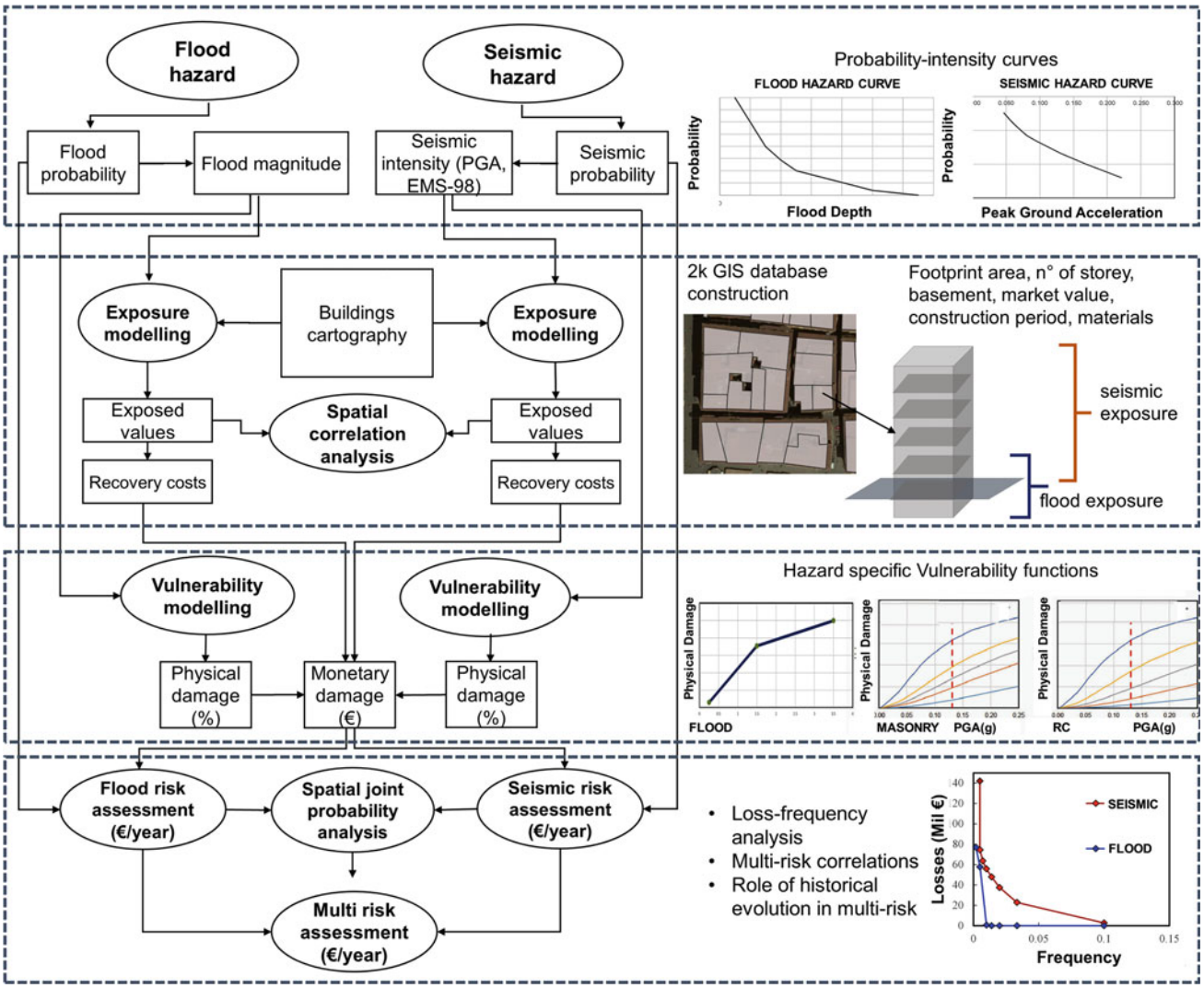

Fig. 1 Multi-risk methodological workflow including hazard, exposure vulnerability and risk analysis (left flow chart) and application (right) (modified from Arrighi et al., 2022)

4 Discussion

The procedure results point out significant outcomes in a multi-risk perspective, namely on how the historical evolution of the city centre shaped multi-risk components. The identified historical cluster influences the multi-risk response of the area as the alteration in the city layout alters the two risks reciprocally. For example, flood hazard has been reduced in the 1860–1945 area because of (i) the demolition of ancient buildings has increased terrain elevation, and (ii) roads have been widened. The seismic risk is widely diffused along with the different areas. However, the vulnerability is reduced for the 1860–1945 cluster. The high exposure of the assets majorly drives the risk results. In the post-1945 buildings, demolitions and construction materials have reduced flood exposure and seismic vulnerability, respectively. The most ancient portion of the city centre has the highest multi-risk evaluated on the territory's surface due to the high building density and building types typical of the Middle ages. This result supports identifying and prioritising mitigation policies with a multi-risk perspective. Although frequently adopted mitigation measures, such as dry flood-proofing or steel tie rods, do not produce benefits for multiple hazards, the multi-risk information allows selecting hazard-specific strategies that do not aggravate other hazards. For instance, a flood risk specialist would recommend moving flood-vulnerable contents, e.g. archive documents,

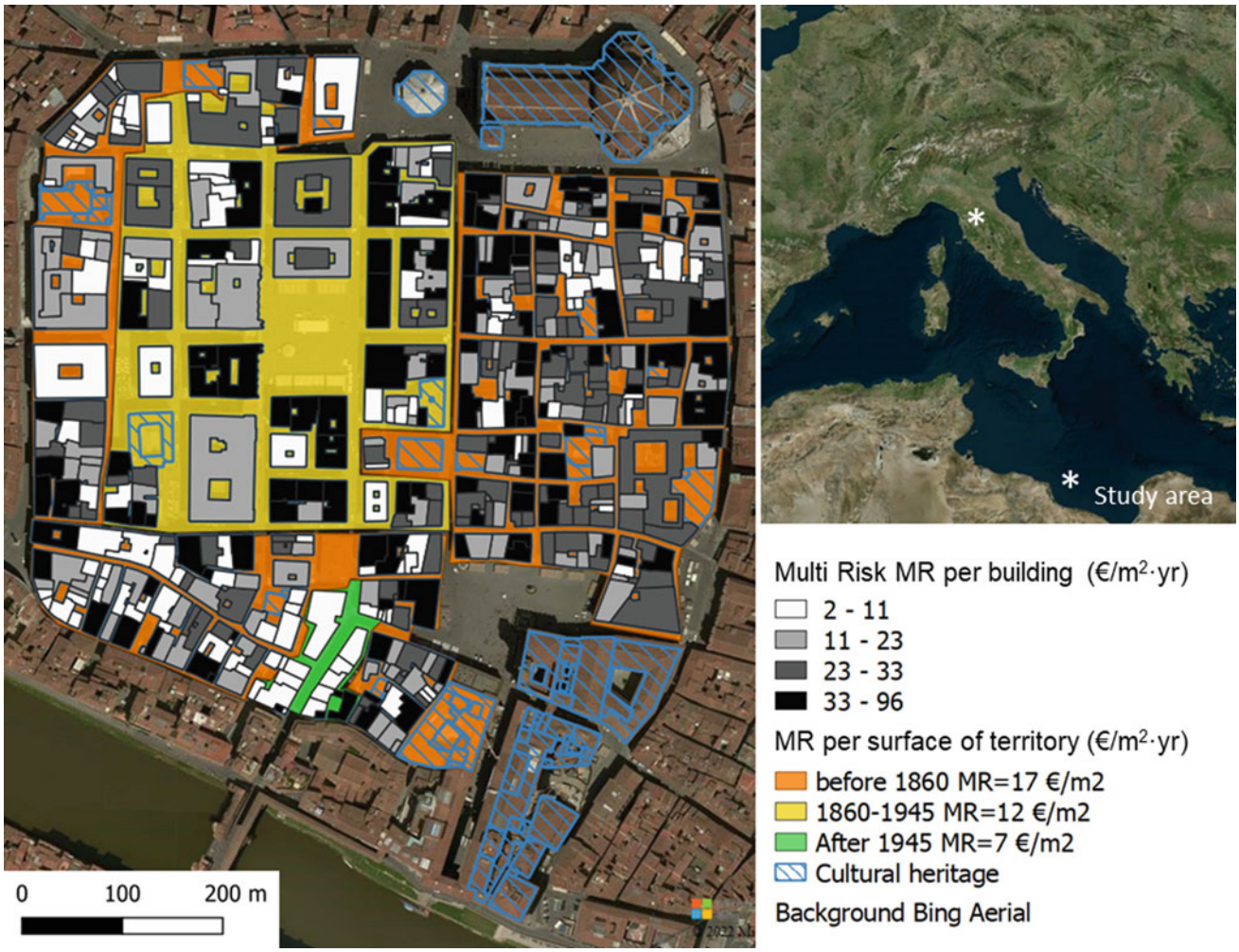

Fig. 2 Single-building and territorial multi-risk assessment for the investigated area

Table 1 Multi-hazard scenario losses for different probabilistic scenarios

Event probability (return period)	Floods [M€]	Earthquake [M€]
High (10–50)	0.00	2.75–37.53
Medium (75–100)	0–0.73	47.89–55.89
Low (200–500)	57.72–76.87	74–47-142.01

to upper floors with detrimental effects on seismic risk, where significant masses at the top levels are deleterious. A seismic risk specialist would recommend installing contour mouns or base isolators to prevent overturning of artworks, but this would prevent the fast displacement of artworks in case of a flood warning. A multi-risk analysis is thus an opportunity to integrate and harmonise risk mitigation strategies to make future cities more resilient.

5 Concluding Remarks

The multi-risk assessment of urban areas represents an open issue in contemporary societies. Interdisciplinary approaches involving experts can suggest further insights useful for urban stock management. This work presents a multi-risk workflow dealing with seismic and flood hazards. Although

targeted at evaluating historical contexts, it can be adapted for many worldwide realities and extended to other types of hazards. Further research should explore hazard interactions and compound and cascade events.

Acknowledgements The Italian Ministry of Education, University and Research is acknowledged for supporting the research within the PRIN funding programme 2015 WELAX9.

References

Arrighi, C., Tanganelli, M., Cristofaro, M. T., Cardinali, V., Marra, A. M., Castelli, F., & De Stefano, M. (2022). Multi risk assessment in a historical city. *Natural Hazards*. https://doi.org/10.1007/s11069-021-05125-6

Blyth, A., Di Napoli, B., Parisse, F., Namourah, Z., Anglade, E., Giatreli, A.-M., Rodrigues, H., & Ferreira, T. M. (2020). Assessment and mitigation of seismic risk at the urban scale: An application to the historic city center of Leiria, Portugal. *Bulletin of Earthquake Engineering, 18*, 2607–2634. https://doi.org/10.1007/s10518-020-00795-2.

Cosenza, E., Del Vecchio, C., Di Ludovico, M., Dolce, M., Moroni, C., Prota, A., & Renzi, E. (2018). The Italian guidelines for seismic risk classification of constructions: Technical principles and validation. *Bull Earthquake Engineering, 16*, 5905–5935. https://doi.org/10.1007/s10518-018-0431-8

D'Altri, A. M., Sarhosis, V., Milani, G., Rots, J., Cattari, S., Lagomarsino, S., Sacco, E., Tralli, A., Castellazzi, G., & Miranda, S. (2020). Modeling strategies for the computational analysis of unreinforced masonry structures: Review and classification. *Archives Computational Methods in Engineering, 27*, 1153–1185. https://doi.org/10.1007/s11831-019-09351-x

Garrote, J., Diez-Herrero, A., Escudero, C., & Garcia, I. (2020). A framework proposal for regional-scale flood-risk assessment of cultural heritage sites and application to the Castile and León region. *Water, 12*, 329.

Lagomarsino, S., & Giovinazzi, S. (2006). Macroseismic and mechanical models for the vulnerability assessment of current buildings. *Bulletin of Earthquake Engineering, 4*(4), 445–463. https://doi.org/10.1007/s10518-006-9024-z

Molinari, D., Scorzini, A. R., Arrighi, C., Carisi, F., Castelli, F., Domeneghetti, A., Gallazzi, A., Galliani, M., Grelot, F., Kellermann, P., Kreibich, H. G. M., Moimann, M., Natho, S., Richert, C., Schroeter, K., Thieken, A., Zischg, A. P., & Ballio, F. (2020). Are flood damage models converging to "reality"? Lessons learnt from a blind test. *Natural Hazards and Earth Systems Sciences, 20*, 2997–3017. https://doi.org/10.5194/nhess-20-2997-2020

Munich, R. E. (2020). The 2019 natural catastrophe year at a glance. Retrieved from 10 December, 2020, from https://www.munichre.com/en/company/media-relations/media-information-and-corporate-news/media-information/2020/causing-billions-in-losses-dominate-nat-cat-picture-2019.html.

Rahmati, O., Yousefi, S., Kalantari, Z., Uuemaa, E., Teimurian, T., Keesstra, S., et al. (2019). Multi-hazard exposure mapping using machine learning techniques: A case study from Iran. *Remote Sens, 11*, 1–20. https://doi.org/10.3390/rs11161943.

Multi-scale Characterization of Flood Risk Components: A Case Study at the Municipal Level

Pedro Pinto Santos, Susana Pereira, Tiago Miguel Ferreira, Maria Xofi, José Carlos Domingues, Carolina Pais, Sérgio Cruz Oliveira, Ricardo A. C. Garcia, Eusébio Reis, José Luís Zêzere, and Paulo B. Lourenço

Abstract

Floods are complex processes that combine local and global factors, causing recurrent and significant human and material losses worldwide. The presented research consists of a multi-scale flood risk assessment process based on data sources collected at distinct scales, expressing hazard, exposure and physical vulnerability of buildings. Detailed Census-derived parameters are essential in representing exposure and vulnerability, while flood hazard is quantified from geomorphologically validated susceptibility maps combined with historical data that characterize events' magnitude and frequency. The results allow a cross-scale analysis of risk, from the building to the municipality level, by identifying exposed populations, buildings, and physical vulnerability. The Lisbon Metropolitan Area is a highly contrasting territory regarding flood risk: some areas are susceptible to slow-onset floods in extensive floodplains but with low exposure, while densely urbanized areas are susceptible to flash floods in small watersheds. While the building level assessment is valuable for local civil protection and urban planning, municipal-level indices provide a comparable inter-municipal perspective of flood risk.

P. P. Santos (✉) · S. Pereira · C. Pais · S. C. Oliveira · R. A. C. Garcia · E. Reis · J. L. Zêzere
Centre for Geographical Studies, Institute of Geography and Spatial Planning, University of Lisbon, Lisbon, Portugal
e-mail: pmpsantos@campus.ul.pt

P. P. Santos · S. Pereira · S. C. Oliveira · R. A. C. Garcia · E. Reis · J. L. Zêzere
Associated Laboratory TERRA, University of Lisbon, Lisbon, Portugal

T. M. Ferreira · M. Xofi · J. C. Domingues · P. B. Lourenço
Institute for Sustainability and Innovation in Structural Engineering, Department of Civil Engineering, University of Minho, Guimarães, Portugal

T. M. Ferreira
Department of Geography and Environmental Management, University of the West of England, Bristol, UK

Keywords

Flood • Hazard • Exposure • Vulnerability • Multi-scale

1 Introduction

Globally, floods are the most recurrent natural hazard, ranked among the natural processes with the highest social and economic impact. Along with highly recurrent processes with moderate losses, low probability flood events with significant human, environmental, and economic impacts are observed worldwide, whether in developed or developing countries. Despite the increasing research on the drivers of flood-related disasters, flooding is one of the most complex processes to model due to the wide range of variables necessary to describe flood scenarios (UNDRR, 2020) accurately. This work describes a flood risk assessment process that combines data from detailed to municipal-level scales, expressing hazard, exposure, and vulnerability. For this exploratory research, the selected case study is the Lisbon Metropolitan Area (LMA), a Portuguese NUT III administrative region composed of 18 municipalities with 2.8 million inhabitants and around 3000 km^2.

2 Data and Methods

Input data with high resolution—expressing historical occurrences, flood susceptibility and buildings' vulnerability, for example—is processed to reach a lower-scale expression of risk at the municipal level. Flood hazard is evaluated using five parameters: maximum event recorded (H1), which represents the maximum historical flood event registered in the last 150 years considering the DISASTER database (Zêzere et al., 2014); frequent flood event (H2), representing the total amount of events recorded in the database, and occurred in a given municipality

A. Malheiro et al. (eds.), *Advances in Natural Hazards and Volcanic Risks: Shaping a Sustainable Future*, Advances in Science, Technology & Innovation, https://doi.org/10.1007/978-3-031-25042-2_24

independently of the degree of loss (very often, the cumulative effects of a frequent event can be more impacting in the long term than low probability/high consequence events); annual exceedance probability of the maximum event recorded in the entire LMA (H3); annual exceedance probability of the frequent events in the LMA (H4); and spatial scale of the assessment, which measures the impact scale of the hazard within the entire unit of analysis (H5). Data sources express both the susceptibility, magnitude and recurrence of floods. All five parameters are represented at the municipal level. A weighted mean valuing H5 with 40% of the weight and assigning 15% to the remaining four parameters was calculated and normalized by the min–max method to the range [0, 1].

The exposure module identifies and characterizes the exposed elements in each municipality, focusing on the residential buildings (approx. 450,000 points of the BGE—Georeferenced Buildings Database and resident population from BGRI—Geographic Base for Information Referencing, both obtained from Statistics Portugal). First, the dasymetric distribution of the resident population by buildings with a total or partial residential function was performed (Garcia et al., 2015). Then, the refinement of exposure to flooding was done by quantifying the number of buildings and respective resident populations within flood susceptible areas (the same ones used to define the flood hazard parameter H5). The vulnerability module focuses on the characteristics of residential buildings. The assessment of their physical vulnerability (PV) to flooding takes into account the period of construction (P1), the number of storeys (P2), material of the external cladding (P3), the material of structural system (P4), soil/lithological substrate (P5), building exposure (P6) and building condition (P7) (see Fig. 1). Each parameter is then evaluated using four vulnerability classes A to D, where A represents the least vulnerable condition, and D represents the most vulnerable one. The classes and weights are based on expert opinion and dedicated literature, namely Kappes et al. (2012), Agliata et al. (2021), D'Ayala et al. (2020) and Ferreira and Santos (2020).

Finally, a weighted risk index is calculated (Eq. 1), which adopts the exponentiation followed in the EU/Joint Research Centre INFORM risk index, although applied to distinct risk components than those used in that global index:

$$Flood\ risk = H^{1/3} * E^{1/3} * PV^{1/3} \quad (1)$$

3 Results

Flood hazard in the LMA is conditioned by the Tagus river floodplain, the Tagus estuary and the small watersheds that drain to the Tagus, directly to the Atlantic ocean or the municipalities outside the LMA. The maximum flood event (H1) in each municipality differs, although two events stand out: the flash floods of November 1967 and November 1983, which impacted the municipalities of V.F. Xira, Loures, Odivelas and Oeiras (Fig. 2). Adding to these municipalities,

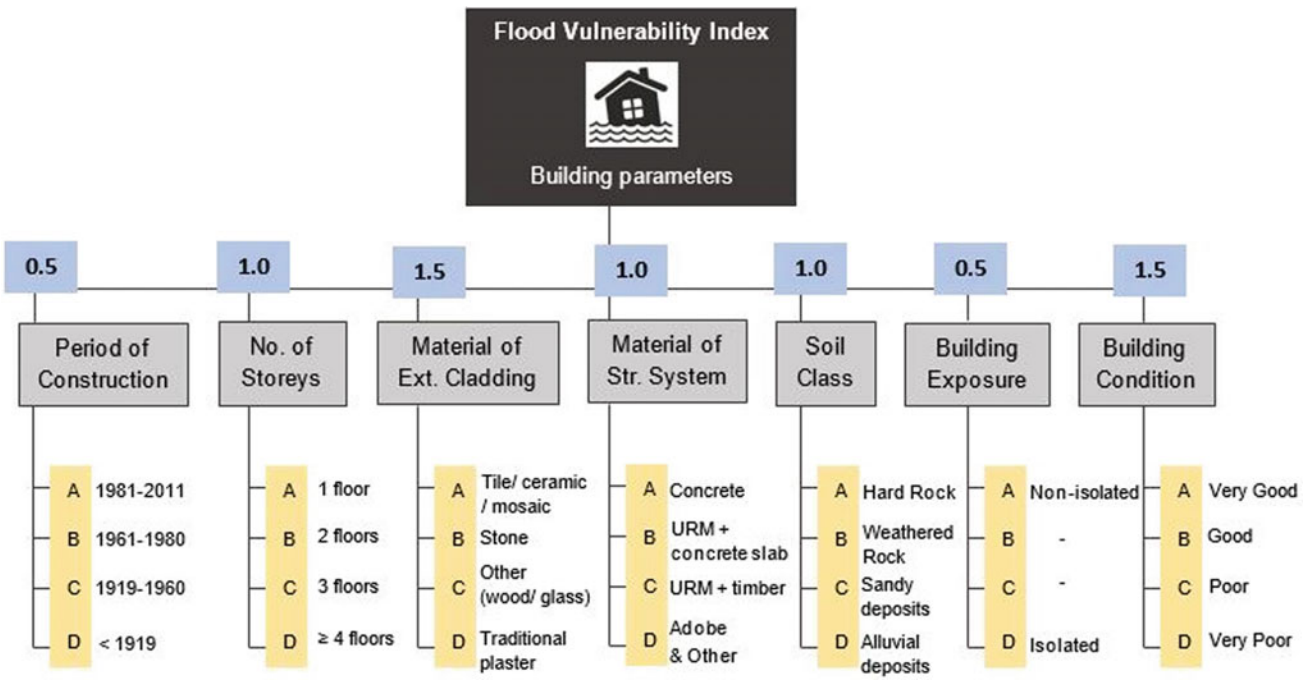

Fig. 1 Parameters, properties and respective weights used to assess buildings' physical vulnerability to flooding

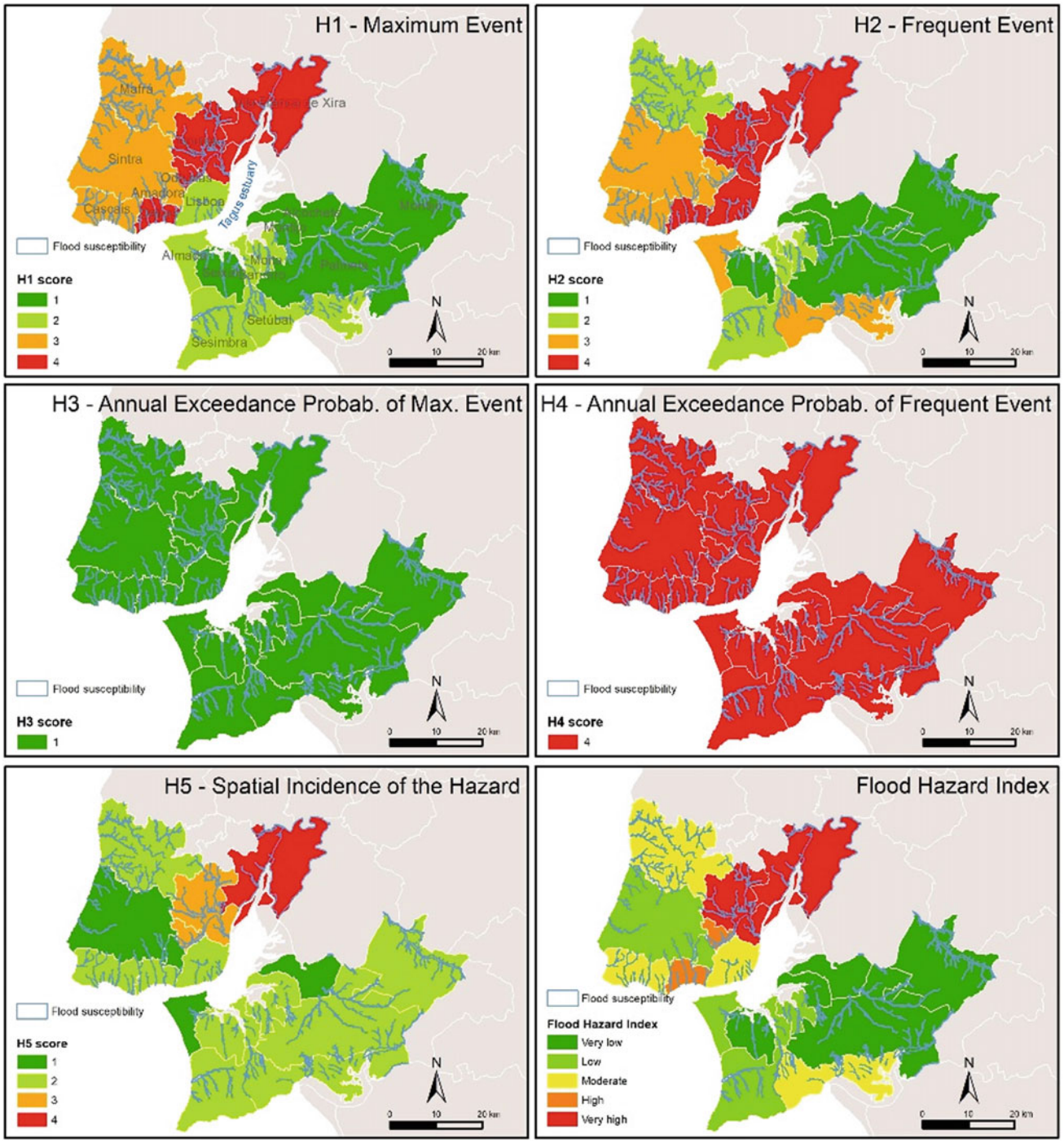

Fig. 2 Flood hazard parameters and index in the Lisbon Metropolitan Area at the municipal level

the higher scores concerning the frequent events (H2) include the district capitals of Lisbon and Setúbal, as well as Almada and Mafra. Parameter H3 assumes the major of the maximum events could have affected the 18 municipalities evenly. For this reason, an equal score was assigned to all municipalities with a low probability event (Loat & Petrascheck, 1997). The same principle was applied to the probability of the frequent event in parameter H4. Finally, H5 highlights the municipalities of V.F. Xira, Odivelas, and Loures due to the highest proportion of flood-susceptible areas in the corresponding territory (60.4, 11.5 and 11.1%, respectively). These four municipalities and Oeiras are characterized by a very high and high flood hazard (Fig. 2) due to a high spatial propensity and historical record of floods, either with a high magnitude or a high degree of loss. Exposure is higher in the most urbanized municipalities, and

Table 1 Population and buildings' exposure and physical vulnerability

Municipality	No. Bldg	No. Inhab	Mean PV	Inhabitant per building condition (parameter P7)			
				Very poor	Poor	Good	Very good
Alcochete	12	24	0.38	0	3	11	10
Almada	194	888	0.33	0	9	146	733
Amadora	28	226	0.23	7	0	29	190
Barreiro	46	190	0.41	11	6	62	111
Cascais	779	3304	0.30	67	46	1028	2163
Lisbon	1813	17,675	0.50	1062	922	6050	9641
Loures	991	3503	0.31	88	123	832	2460
Mafra	255	523	0.33	14	4	145	360
Moita	124	235	0.30	14	3	90	128
Montijo	39	66	0.35	2	2	30	32
Odivelas	1314	13,419	0.40	88	281	5508	7542
Oeiras	340	2726	0.39	25	82	589	2030
Palmela	336	876	0.31	7	4	128	737
Seixal	532	4691	0.37	15	77	941	3658
Sesimbra	5	4	0.25	0	0	0	4
Setúbal	1781	14,485	0.44	191	754	4623	8917
Sintra	577	5311	0.36	19	107	1479	3706
V. F. Xira	1035	4515	0.38	17	203	1335	2960
Sum (*Mean*)	10,201	72,661	*0.35*	1627	2626	23,026	45,382

it is linked to the occupation of the small streams and valley floors, particularly in Lisbon, Odivelas and Setúbal (Table 1). Globally, 2.5% of the LMA residents live in flood susceptible areas. When exposure is combined with the physical vulnerability of buildings, it becomes more evident where the most critical contexts for potential flood losses are located. The mean PV in the AML is 0.35, with maximum average values of 0.50 in Lisbon and 0.44 in Setúbal. Nevertheless, a detailed analysis of PV needs to consider each parameter individually; this is because, for example, the general condition of the buildings (Table 1) —as it was recorded in the Census—may not be concerning, but other parameters like lithological substrate, the material of the external cladding and structural system do act as stronger drivers of physical vulnerability.

When analyzing the hazard and risk index, mapped respectively in Figs. 2 and 3, it is interesting to see that when PV is included in the analysis, it changes considerably the results obtained for the hazard alone. This is very clear for the municipality of Setúbal, which stands out strikingly in the risk map in Fig. 3, but not in the hazard maps provided in Fig. 2. Analyzing the proportion of the risk index explained by the hazard score represents less than ¼ of the final risk index, while exposure (in brown) and vulnerability (in violet) represent the vast proportion of the risk components. It should be highlighted that E and PV accounted only with flood susceptible areas. In the opposite case, the municipality of Loures, previously assigned a very high hazard Index, drops to an intermediate position in the risk index. This is explained by the proportionally low contribution of exposure and physical vulnerability of buildings.

4 Concluding Remarks

By taking into account the data from the BGE and the BGRI, crossed with a precise assessment of susceptibility based on geomorphological criteria, the analysis carried out makes it possible to locate precisely where the buildings susceptible to flooding are, to know their main physical characteristics and to estimate their resident population. For a lower scale of inter-municipal strategic decisions, such data was processed to obtain municipal-level risk indices, which may conceal critical local hotspots. Inter-municipal risk management policies should not be restricted to the sole focus on emergency and civil protection, as cross-sectoral and comprehensive responses to disaster risk reduction include social, environmental, urban planning, mobility and land use management policies.

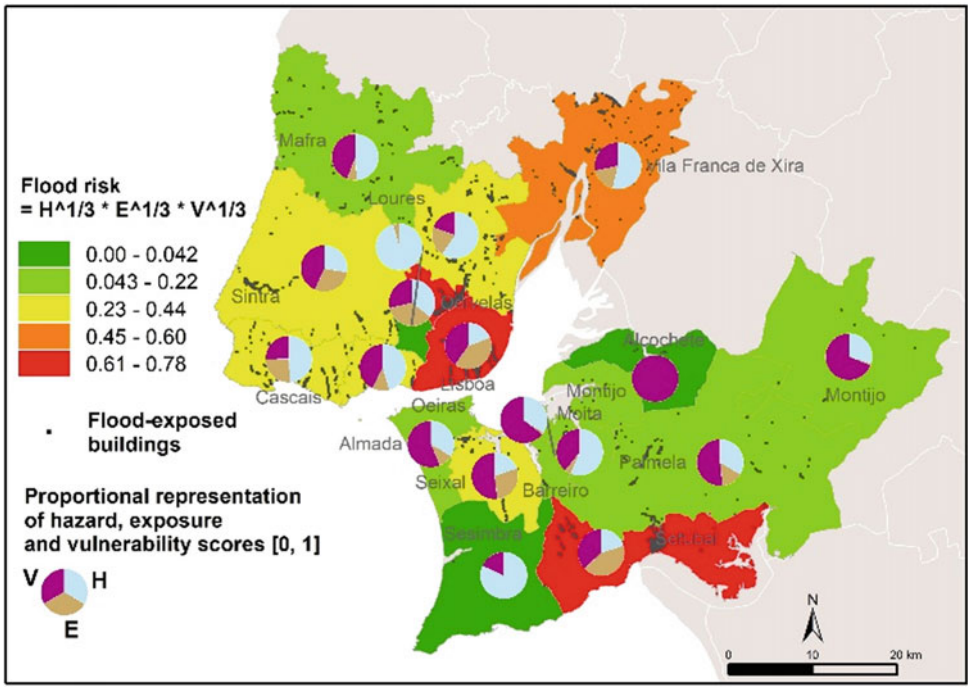

Fig. 3 Flood risk index as an expression of flood susceptibility, buildings' and population's exposure, and buildings' physical vulnerability at the municipal level in the LMA

Acknowledgements The MIT-Portugal project MIT-RSC—Multi-risk Interactions Towards Resilient and Sustainable Cities (MIT-EXPL/CS/0018/2019) is financed by the Portuguese Foundation for Science and Technology (FCT). RISKCOAST is funded by the Interreg Sudoe Programme (SOE3/P4/E0868). Pedro Pinto Santos is financed through FCT under the contract CEECIND/00268/2017.

References

Agliata, R., Bortone, A., & Mollo, L. (2021). Indicator-based approach for the assessment of intrinsic physical vulnerability of the built environment to hydro-meteorological hazards: Review of indicators and example of parameters selection for a sample area. *International Journal of Disaster Risk Reduction, 58*, 102199.

D'Ayala, D., Wang, K., Yan, Y., Smith, H., Massam, A., Filipova, V., & Pereira, J. J. (2020). Flood vulnerability and risk assessment of urban traditional buildings in a heritage district of Kuala Lumpur, Malaysia. *Natural Hazards and Earth System Science, 20*(8), 2221–2241.

Ferreira, T. M., & Santos, P. P. (2020). An integrated approach for assessing flood risk in historic city centres. *Water, 12*(6), 1648.

Garcia, R. A. C., Oliveira, S. C., & Zêzere, J. L. (2016). Assessing population exposure for landslide risk analysis using dasymetric cartography. *Natural Hazards Earth System Sciences, 12*, 2769–2782.

Kappes, M. S., Papathoma-Köhle, M., & Keiler, M. (2012). Assessing physical vulnerability for multi-hazards using an indicator-based methodology. *Applied Geography, 32*(2), 577–590.

Loat, R., & Petrascheck, A. (1997). Prise en compte des dangers dus aux crues dans le cadre des activités de l'aménagement du territoire. Office fédéral de l'économie des eaux (OFEE), Office fédéral de l'aménagement du territoire (OFAT), Office fédéral de l'environnement, des forêts et du paysage (OFEFP), Bern, Switzerland.

UNDRR. (2020). Global Assessment Report on Disaster Risk Reduction 2019. United Nations Office for Disaster Risk Reduction, Geneva, Switzerland

Zêzere, J. L., Pereira, S., Tavares, A. O., Bateira, C., Trigo, R. M., Quaresma, I., Santos, P. P., Santos, M., & Verde, J. (2014). DISASTER: A GIS database on hydro-geomorphologic disasters in Portugal. *Natural Hazards, 72*(2), 503–532.

Sustainable Earth Systems, Hazards, and Climate Change

Study, Definition and Application of General Alert and Alarm Criteria for Road Geotechnical Structures in the Operation and Maintenance Phase

José Sousa, Pedro Varela, Sara Sanches, Adriana Neves, and Alexandra Ferreira

Abstract

The main purpose of this paper is to present the study, definition and application of general alert and alarm criteria to road geotechnical structures during the operation and maintenance phase. This work results from the need to apply global alert and alarm criteria to all the geotechnical structures of ASCENDI IGI. In the group of structures analysed, the following typologies of structures emerged: (i) Embankment slopes, (ii) Excavation slopes, (iii) Anchored walls, (iv) Reinforced Concrete walls, (v) Reinforced Earth walls, and (vi) Gabion walls. This document presents the monitoring and instrumentation methods implemented at ASCENDI. The general alert and alarm criteria were defined to support the interpretation of the installed instrumentation, particularly at the level of variations of displacements, deformations and loads. The definition of these criteria considers the type of structure (rigid or flexible), geometric characteristics, and material characteristics (geological and geotechnical). Since climate change is one of the greatest environmental threats of the twenty-first century, with profound consequences for various areas of society, this work intends to constitute an alternative approach to increase the resilience of geotechnical structures to natural hazards.

Keywords

Alert and alarm criteria • Natural hazards • Geotechnical structures • Instrumentation

1 Introduction

The implementation of an observation and auscultation plan, which includes a set of instruments and monitoring devices for measurement of variables, should be planned and developed during the design and construction phase and must have continuity with the operation phase of the structure. Furthermore, this observation project/plan must be a document that the designer must develop and deliver to the company responsible for the work during the operation phase (Ferreira, 2015a, 2015b).

In Ascendi I.G.I., a significant number of instrumented walls and slopes were developed and implemented an annual observation and auscultation plan for the operation phase of the structures, considering the lack of observation plans for this stage. However, the main missing elements are the alert and alarm levels that allow the verification of the safety and condition of the structure (Ferreira, 2015a, 2015b).

In order to address this shortcoming and improve the interpretation of the results obtained from the instrumentation readings, general alert and alarm criteria were studied, developed and applied for different types of geotechnical structures present in the Ascendi I.G.I. network. This work also relied on two Portuguese consultants (Alexandre Pinto, JSJ, and Eduardo M. Fernandes, Geovia).

2 Definition and Application of General Alert and Alarm Criteria

Along with Portugal's road network, several geotechnical structures have installed instrumentation and no specific Instrumentation and Observation Plan. The absence of criteria that allow the interpretation of the auscultation campaigns makes it challenging to analyse the stability of the structures correctly.

Aiming to overcome this drawback, generalist alert and alarm criteria are studied and defined to support the

J. Sousa (✉) · P. Varela · S. Sanches · A. Neves · A. Ferreira
ASCENDI IGI, Edifício Litografia Lusitana, Praça Mouzinho de Albuquerque, Porto, Portugal
e-mail: jrsousa@ascendi.pt

A. Malheiro et al. (eds.), *Advances in Natural Hazards and Volcanic Risks: Shaping a Sustainable Future*,
Advances in Science, Technology & Innovation, https://doi.org/10.1007/978-3-031-25042-2_25

interpretation of the readings from instrumentation (e.g., Lienhart et al., 2018; Sabatini et al., 1997).

The alert and alarm criteria and the measures to be applied in case these values are exceeded require a risk analysis and should be defined by the project entity since they are the expert ones with the best knowledge of the structure.

These values should be defined taking into account the individual characteristics of each project, such as: (i)—Type of structure developed and its characteristics (materials used, geometric characteristics, surface coating, among others), (ii)—Characteristics of the earth to be supported, (iii)—Geographical location and climatic characteristics, (iv)—Requests to which the structure is subjected and (v)—Surroundings of the structure (existence of neighbouring buildings, traffic circulation, among others).

It should be noted that the alert and alarm levels presented in this document must only be applied to walls and slopes which do not have an Instrumentation and Observation Plan or do not present alert and alarm levels defined for the operational phase of the structure. Their criteria must be applied to the walls and slopes that already have an instrumentation and observation plan.

During the initial phase of the study of the alert and alarm levels, different types of infrastructures that compose the Ascendi I.G.I. road network were defined to determine specific levels for each one. From this evaluation, were identified the following types of slopes and walls: (i) Embankment slopes, (ii) Excavation slopes, (iii) Anchored walls, (iv) Reinforced Concrete walls, (v) Reinforced Earth walls, and (vi) Gabion walls. Therefore, this document presents only the criteria for anchored walls and embankment slopes.

Whenever the project does not include a specific plan for geotechnical infrastructure, general criteria are proposed for horizontal and vertical displacements in retaining structures, measured by topographical targets (total reflection prisms), inclinometers (ABS gutters) and load variation in anchors measured by load cells. Table 1 presents the alert and alarm criteria defined for anchored walls.

Based on the alert and alarm criteria proposed for walls and slopes, a methodology was developed and presented to improve the evaluation and analysis of the data related to the horizontal and vertical displacements measured by topographic targets. The methodology proposed consists of developing a graphic for each structure typology, showing on the X-axis the horizontal displacements and on the Y-axis the vertical displacements, allowing: (I)—to correlate the two displacements and (II)—to observe all the available information in a single graphic.

The previous table (Table 1) shows that the criteria for calculating the alert and alarm levels depend on height (H). Due to this fact, it was unsuitable to represent walls with different heights on a single graph since walls with different heights have different alert and alarm criteria. In order to overcome this constraint, the displacements represented in the graphs will be divided by H (height of the wall); in this way, it is possible to represent in a single graph all the walls of the same typology.

After the horizontal and vertical displacements measured by topographic targets are applied to the criteria presented above, the representation of the results of the readings is performed as follows: (i) on the horizontal axis; the $\delta H/H$ will be represented; (ii) on the vertical axis the $\delta V/H$ will be represented.

In order to improve the analysis of the results obtained, the alert and alarm levels and the readings obtained will be presented as a percentage. Figure 1 shows the percentages of horizontal and vertical displacements to the height of the

Table 1 Alert and alarm criteria for Anchored Walls (adapted from Sousa, 2020)

Level	Criteria for Anchored Walls		
	Topography/Inclinometers (Top. and Inclin.)		Load Cells
	$H \leq 10$ m	$H > 10$ m	
1 (Stable)	$\delta_H < {}^{H}/_{500}$ $\delta_V < {}^{H}/_{1000}$	$\delta_H < \left(\frac{10}{500}\right) + \left(\frac{H-10}{2\times 500}\right)$ $\delta_V < \left(\frac{10}{1000}\right) + \left(\frac{H-10}{2\times 1000}\right)$	$\Delta P < \pm 20\%$
2 (Alert)	${}^{H}/_{250} > \delta_H > {}^{H}/_{500}$ ${}^{H}/_{500} > \delta_V > {}^{H}/_{1000}$	$\left(\frac{10}{250}\right) + \left(\frac{H-10}{2\times 250}\right) > \delta_H > \left(\frac{10}{500}\right) + \left(\frac{H-10}{2\times 500}\right)$ $\left(\frac{10}{500}\right) + \left(\frac{H-10}{2\times 500}\right) > \delta_V > \left(\frac{10}{1000}\right) + \left(\frac{H-10}{2\times 1000}\right)$	$\pm 30\% > \Delta P > \pm 20\%$
3 (Alarm)	$\delta_H > {}^{H}/_{250}$ $\delta_V > {}^{H}/_{500}$	$\delta_H > \left(\frac{10}{250}\right) + \left(\frac{H-10}{2\times 250}\right)$ $\delta_V > \left(\frac{10}{500}\right) + \left(\frac{H-10}{2\times 500}\right)$	$\Delta P > \pm 30\%$

δ_H, δ_V—horizontal and vertical displacements, respectively [mm]

ΔP—variation of the final ground anchor load [%]

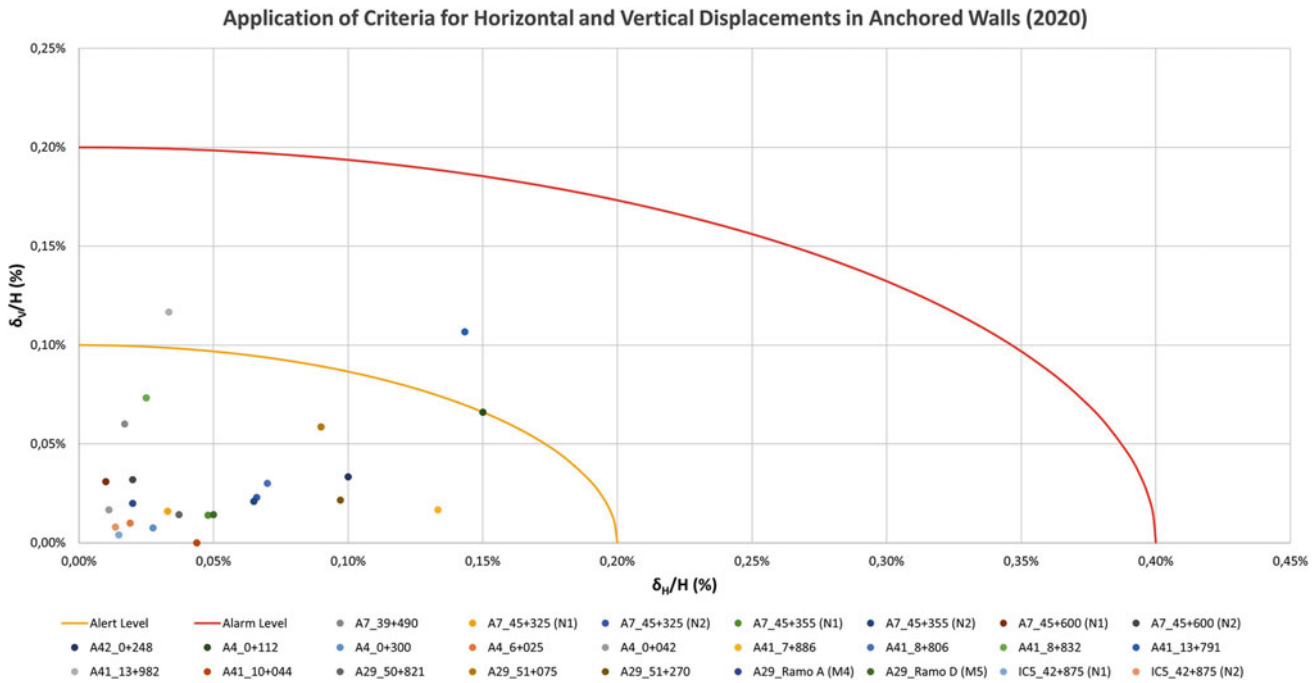

Fig. 1 Application of criteria for horizontal and vertical displacements in walls (2020)

wall for anchored walls (Table 1), and as shown in the graph, only three walls are at the alert level.

Regarding the slopes is possible to use laser scanning technology, or equivalent, for geometric mapping. However, in more straightforward situations, the slope can be monitored using topographic targets and/or full reflection prisms (Intrieri et al., 2012; Slob et al., 2007). Table 2 proposes general criteria for the control of embankment slope displacements, the opening of cracks/scars, as well as the control of deformation rates (Δδ).

Conversely to walls, the alert and alarm levels applied to slopes do not rely on their height, so the displacements are not presented as a percentage in the graph.

Figure 2 demonstrates the application of the criteria for Embankment Slopes present in Table 2, and as shown in the graph, there is no slope at the alert level.

The ellipse equations were adopted for the representation of the criteria. This decision was based on the fact that initially, the alert and alarm levels proposed for the horizontal and vertical displacements were studied to be applied and analysed individually. Considering the several analyses, it was concluded that the ellipse is the equation that reveals itself as the most adjusted to the compatibility criteria of the displacements in both directions.

The answer to the interpretation of the alert and alarm levels of infrastructure monitoring is reflected in the subsequent actions described in Table 3.

Table 2 Alert and alarm criteria for embankment slopes (adapted from Sousa, 2020)

Level	Criteria for Embankment Slopes		
	Top./Inclin.	Cracks/Scars	Deformation Rates (Top./Inclin.)
1 (Stable)	$\delta_H < 40\ mm$ $\delta_V < 15\ mm$	$\Delta_{mm} < 40\ mm$	$\Delta\delta_H < 1.5\ mm/day$ $\Delta\delta_V < 0.5\ mm/day$
2 (Alert)	$80\ mm > \delta_H > 40\ mm$ $30\ mm > \delta_V > 15\ mm$	$80\ mm > \Delta_{mm} > 40\ mm$	$3.0\ mm/day > \Delta\delta_H > 1.5\ mm/day$ $1.0\ mm/day > \Delta\delta_V > 0.5\ mm/day$
3 (Alarm)	$\delta_H > 80\ mm$ $\delta_V > 30\ mm$	$\Delta_{mm} > 80\ mm$	$\Delta\delta_H > 3.0\ mm/day$ $\Delta\delta_V > 1.0\ mm/day$

δ_H, δ_V—horizontal and vertical displacements, respectively [mm]

Δ_{mm}—opening of cracks/scars [mm]

Δδ—deformation rate of excavation and backfill slopes [mm/day]

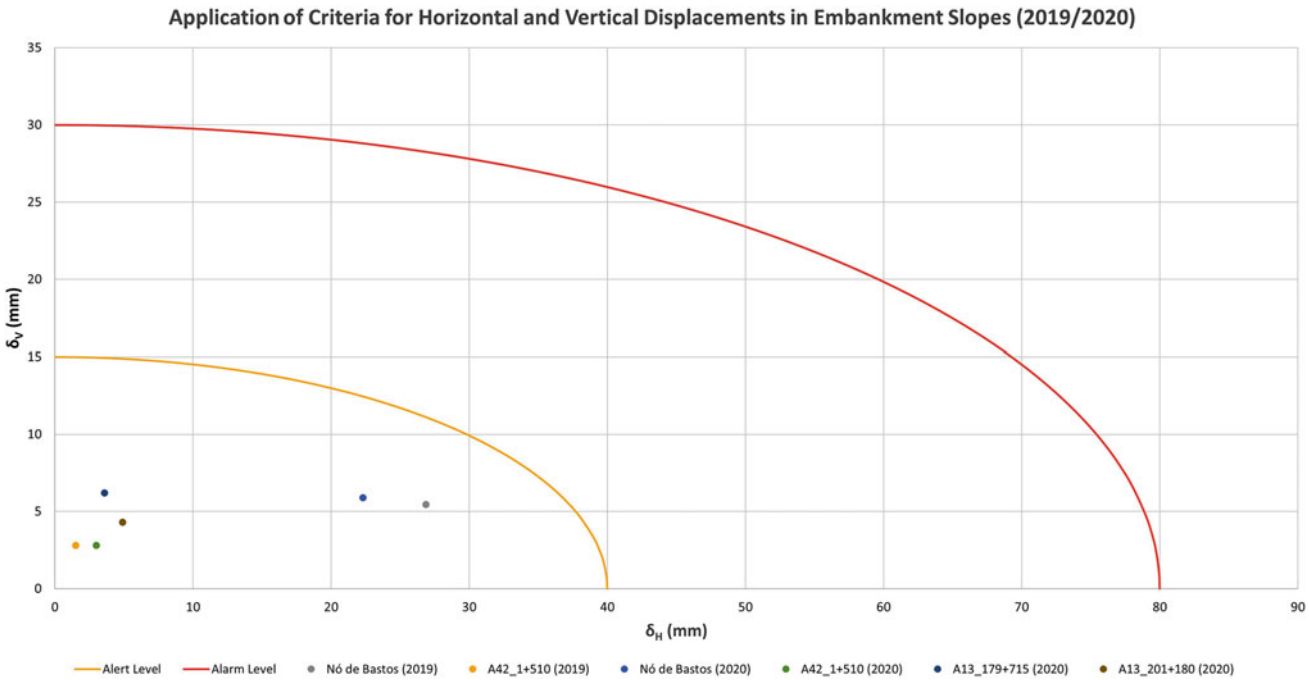

Fig. 2 Application of criteria for horizontal and vertical displacements in embankment slopes (2019/2020)

Table 3 Definition of actions according to the levels obtained (adapted from Sousa, 2020)

Level	Action
1 (Stable)	Stable;
2 (Alert)	Communication to the entities involved, reinforced monitoring, verification of readings, preparation of an action plan;
3 (Alarm)	Communication to the entities involved, verification of readings, increase the frequency of readings and application of immediate safety measures.

3 Concluding Remarks

Safety, sustainability, and resilience are fundamental factors in engineering works, which, after planning and design, must be subject to an observation and auscultation plan, with the following objectives: (I) Ensure the safety of road users and (II) Avoid the evolution of Damages/Pathologies in the infrastructures that imply higher costs during their period of operation. Otherwise, as all geotechnical structures are subject to actions, they may suffer instability processes that may ultimately lead to their rupture. With the application of these criteria, the main intention is to avoid such situations, intervening in advance or promptly before the occurrence or development of instabilization situations, reducing the costs of maintenance and/or conservation to be carried out to restore the structure's adequate level of safety.

These general criteria were also applied to geotechnical structures that already had these criteria defined throughout the study. The comparison of the application of the two, and considering that the proposed criteria are general, validated that the proposed criteria are more conservative.

Since climate change is one of the greatest environmental threats of the twenty-first century, with profound consequences for various areas of society, this study was developed to increase the resilience of geotechnical structures to natural hazards.

References

Ferreira, A., Neves, A., & Sanches, S. (2015a). *Inspeção visual de muros e taludes*. ASCENDI, Porto.

Ferreira, A., Neves, A., & Sanches, S. (2015b). Sustims—muros & taludes. In *9º Congresso Rodoviário Português* (pp. 1–10). http://crp.pt/docs/A54S222-9CRP_Artigo_147.pdf.

Intrieri, E., Gigli, G., Mugnai, F., Fanti, R., & Casagli, N. (2012). Design and implementation of a landslide early warning system. *Engineering Geology, 147–148*, 124–136.

Lienhart, W., Monsberger, C. M., Kalenjuk, S., & Woschitz, H. (2018). High resolution monitoring of retaining walls with distributed fibre optic sensors and mobile mapping systems. In *Proceedings of the 7th Asia-Pacific Workshop on Structural Health Monitoring, APWSHM* (pp. 79–87).

Sabatini, P. J., Elias, V., Schmertmann, R., & Bonaparte, R. (1997). Geotechnical engineering circular no. 2: earth retaining systems. Federal Highway Administration, Report, FHWA-SA-96-038.

Slob, S., Hack, H. R., Feng, Q., Röshoff, K., & Turner, A. K. (2007). Fracture mapping using 3D laser scanning techniques. In L Ribeiro e Sousa, C Olalla, & N Grossmann (Eds.), *Proceedings of the 11th Congress of the International Society for Rock Mechanics, Lisbon* (pp. 299–302). Taylor & Francis.

Sousa, J. R. (2020). Estudo e definição de critérios gerais de alerta e de alarme para muros de suporte e taludes rodoviários na sua fase de exploração: casos de estudo. Instituto Superior de Engenharia do Porto, Porto (MSc Dissertation). http://hdl.handle.net/10400.22/16927.

The Effectiveness of Post-Wildfire Slope Stabilization Measures: A Case Study in Oliveira Do Hospital

Luis Araújo Santos, Paulo Coelho, and António Correia

Abstract

The wildfires of the 15th of October 2017 consumed more than 190,000 hectares in central Portugal. Oliveira do Hospital stands out among the most battered regions, where 43,191 hectares of forest were lost. In the aftermath of this natural disaster, several interventions aiming at stabilizing unstable slopes were conducted in different regions of the council, namely along the road which connects Penalva de Alva to Oliveira do Hospital. These works consisted of temporary barriers along the upstream slope of the road. Due to three consecutive storms in 2019, several slope instability phenomena were recorded near the study area. Despite some minor surface landslides, almost all the instability events affected slopes that had not been intervened after the 2017 wildfires. The stabilized slopes showed a better response due to the non-degradation of the mechanical characteristics of the soils and the roots system. The conclusions are then discussed concerning the behaviour of volcanic soils and the potential effects of wildfires on slopes in regions having these materials.

Keywords

Wildfires • Storms • Slope instability • Slope stabilization • Soils

L. Araújo Santos (✉) · P. Coelho
CITTA—Research Centre for Territory, Transport and Environment, Coimbra, Portugal
e-mail: lmsantos@isec.pt

L. Araújo Santos · A. Correia
Coimbra Institute of Engineering, Polytechnic Institute of Coimbra, Coimbra, Portugal

P. Coelho
Department of Civil Engineering, University of Coimbra, Coimbra, Portugal

1 Introduction

2017 to 2019 were dramatic years from the wildfire's perspective in mainland Portugal, mainly in the central region, 2017 being the deadliest in Portugal's history, with a total number of deaths and injured people over 100 and 300, respectively. This year, 6.1% of Portugal's mainland burned (Podlaha et al., 2018), with 47% of the burned area resulting from wildfires between the 14th and 16th of October. During this period, 207,948 ha of vegetation was burned, 80,610 ha of which were concentrated in the City Council of Oliveira do Hospital, in the central Portugal region (ICNF, 2017a). 2017 wildfires cannot be dissociated from the meteorological conditions observed during that year. Indeed, this year has been classified as one of the driest and warmest years (IPMA, 2017). According to these authors, in October 2017, there were temperature deviations greater than 4 ºC compared to the average for this time of the year, having been classified as the hottest month in more than eight decades. In addition, 99% of the territory was in meteorological drought due to the lack of precipitation.

The spring of 2018, on the contrary, was classified as the third rainiest spring in the last 90 years (IPMA, 2018). In the study area, in March, the total precipitation exceeded 400% of March's monthly average, reaching values of 500 mm. April was also a rainy month. Between 150 and 200 mm of total precipitation in the study area exceeded April's average by 25% (IPMA, 2018). Although 2019 was one of the hottest years in Europe, the temperatures in Portugal were mild. However, the lack of rain leads to a meteorological drought across Portugal's mainland (IPMA, 2019). The severe weather events only occurred in December, between the 15th and 22nd, when three consecutive storms ravaged Portugal. This week, more than 200 mm of total precipitation was registered in the study area and nearby areas. It rained 1.5 times more than the winter average (IPMA, 2019).

As a result of the severe events briefly described above, in an area where, before 2017, only two references to slope

A. Malheiro et al. (eds.), *Advances in Natural Hazards and Volcanic Risks: Shaping a Sustainable Future*, Advances in Science, Technology & Innovation, https://doi.org/10.1007/978-3-031-25042-2_26

instabilities were found in a local newspaper, and dozens of slope instability events were recorded in recent years. Several occurred along Municipal Road M514, crossing the study area (Araújo Santos et al., 2020). According to these authors, more than EUR 450,000 were spent by the municipality of Oliveira do Hospital to recover the M514 road and the surrounding slopes.

2 Materials and Methods

2.1 Case Study

The case study is located at 40º 20′14.27″ N and 7º 49′30.44″ W Greenwich, 285 above the sea level. These coordinates refer to the intersection between municipal roads M514 and M506, which connect the city of Oliveira do Hospital—and the settlements of São Giao—SG and Penalva de Alva—PA (Araújo Santos et al., 2020). According to these authors, the slopes studied face mostly south along M506 (direction of OH), M514 (direction of PA) and M514 (direction of SG). In this area, slopes present an average inclination of 30º. At the surface, according to Lourenço et al. (2012), soils are classified as Umbric leptosol, being characterized as predominantly shallow and stony soils.

2.2 Methodology

The analysis of the effectiveness of the slope stabilization measures is based on fieldwork by collecting evidence of the performance of such measures and by comparing the slope response to all the severe events previously described. This collection is an ongoing project, with the first evidence collected in May 2018 and the last in September 2021. Whenever possible, photographic recording and information collection is done shortly after severe meteorological events, as happened in winter 2020, when the fieldwork was carried out a few days after the passage of storm Fabien. This continuous evaluation of site condition is essential since, according to Schmidt et al. (2001), roots' contribution to soil cohesion may take 8–12 years to reach its minimum value after the tree dies. During this time, slope instability phenomena may occur.

3 Continuous Assessment of the Efficacy of the Adopted Solutions

After the October 2017 wildfires, the Portuguese Institution for Nature and Forest Conservation has identified several emergency interventions and the stabilization of slopes in Oliveira do Hospital. Neighbouring or nearby councils represented about 45% of the funds applied to these measures (ICNF, 2017b). Along the slopes in the case study, the adopted stabilization technique was a temporary barrier to erosion control. These structures, installed to facilitate infiltration and accumulate sediments and reduce their movements on burned slopes (Ferreira et al., 2010), are made of burned tree logs (Fig. 1a) and smaller trunks and burned branches (Fig. 1b). Although these techniques are not primarily intended to enhance land cover, it should be noted that local flora grew up quickly, enabling an environmental integration of the installed structures (see Fig. 1c, d).

These interventions took place along the slopes of the road infrastructures that connect OH and PA (municipal roads M506 and M514). From the intersection that serves as a geographical reference for the case study, no stabilization works were conducted along the slopes that develop to the northeast, in the direction of SG. It is essential to mention that the adopted solutions were not applied on both slopes of the roads. From the intersection mentioned above to OH and PA, solely the righter slopes suffered interventions. Leaving untouched the lefter slopes and those that develop to the northeast was not the best choice. Indeed, after the December 2019 storms, most of the registered instability phenomena occurred on these slopes. Dozens of surface and shallow landslides occurred along these roads, but the most significant instability affected the stability of the road towards SG, and the competent authorities had to interrupt the traffic on this section of M514. As shown in Fig. 2a, the landslide on the slope below the road required reprofiling works on the slope and the construction of a hydraulic passage.

Later, during the 2021 winter, more landslides and rockfalls were registered along the same road. Amongst several less significant occurrences, two of which are illustrated in Fig. 2b, forced the deconstruction of the unstable areas of the slope and cleaning works, conditioning, again, the road traffic towards SG. It should also be noted that, although no significant consequences have been observed yet, longitudinal cracks and soil subsidence are observable in the downstream ditch of the municipal road M514 (towards SG), which are precursor signs of more severe problems if extreme weather events as those of 2019 occur.

Towards the southwest, along the municipal roads which connect OH and PA (M514 and M506), no relevant occurrences were registered. All the events boil down to surface landslides that required only cleaning works of the road and removal of bigger particles from the ditches.

4 Learning Outcomes for Volcanic Soils

Although only 1% of the Earth's surface consists of volcanic soils, they affect a significant part of its population. There are three significant areas of volcanic soils in the world, and the

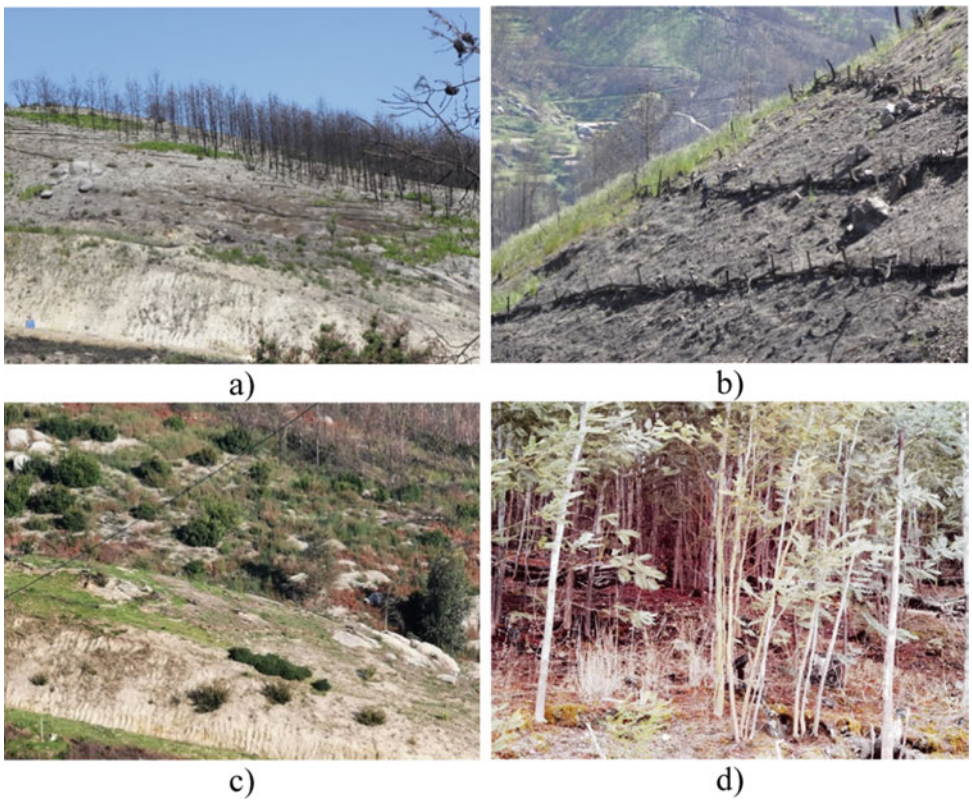

Fig. 1 Temporary barriers applied along the case study slopes: **a** barriers made of tree logs in 2018 (M506); **b** barriers made of burned branches in 2018 (M514); **c** integration of barriers made of tree logs in 2020 (M506); **d** detail of barriers made of burned branches in 2020 (M514)

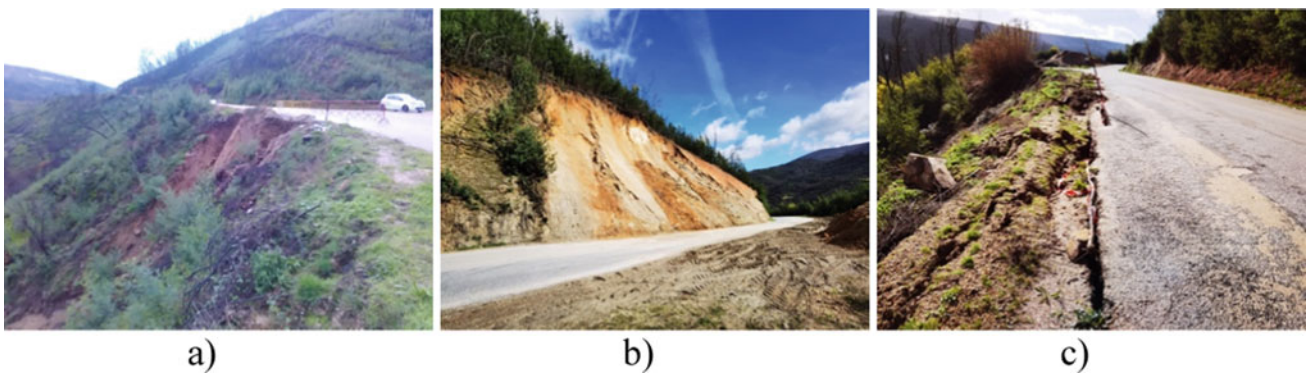

Fig. 2 Instability phenomena registered on the slopes in the direction of São Gião (M506): **a** downstream slope during 2020 winter; **b** upstream slope during winter 2021; **c** downstream slope during winter 2021

Azores, the Canary Islands, and many islands of the West Indies that belong to the so-called equatorial Atlantic region. A detailed description of these soils' chemical and physical properties does not fall within the scope of this communication. However, it is worth mentioning that some of their key features are the low unit weight, lower than 9.0 kN/m^3, and excellent drainage properties. The conjunction of these properties makes volcanic soils excellent mediums for planting roots where they can extend relatively free up to 6 m depth. A last interesting feature is that these soils may lose water irreversibly: once they dry out, they cannot rehydrate (Neall, 2009). According to this author, these soils are particularly vulnerable to extreme rainfall events, and massive landslide failures may occur, a problem that will undoubtedly be exacerbated by the effects of wildfires in the driest regions.

Azores archipelago is located in a triple junction of tectonic plates, which causes frequent seismic and volcanic events. Still, landslides are the most common geological hazard, commonly triggered by extreme rainfall episodes, causing severe infrastructure damages (Silva et al., 2018). For example, on S. Miguel Island, between 2005 and 2016, 442 shallow landslides were triggered by rainfall (Gordo et al., 2019). According to Wallenstein (1999), volcanic soils on this island are characterized by low cohesion and shear resistance angle values.

These soils' agricultural and economic values do not make them suitable areas for forestry. However, based on the previous information, namely on S. Miguel Island, the possible consequences of forest fires on these soils, followed by rainfall events, are predictable. This problem is even more severe in other volcanic islands with driest climates, namely when extreme rainfall events occur. Since the shear strength parameters of these soils are low, the contribution of root systems to the overall shear resistance is significant. Depending on the severity of the fire, roots will slowly die, and the surplus resistance they provide to volcanic soil disappears, increasing its susceptibility to suffering landslides. In such a situation, and given the effectiveness of the adopted measures in Oliveira do Hospital after the 2017 wildfires, the inclusion of temporary barriers would probably be an adequate stabilization measure.

5 Concluding Remarks

Wildfire's dramatic consequences are not limited to the short term. Due to land cover changes, extreme rainfall events may trigger landslides during the following years, depending on the fire severity and vegetation resilience, namely the roots systems. Temporary barriers made of tree logs and trim branches proved an adequate stabilization measure along the municipal roads M506 and M514 in Oliveira do Hospital to prevent such hazards. Indeed, after this stabilization, storm-induced slope instabilities, some of them significant, only affected unprotected slopes.

The outcomes of the continuous follow-up of slope movements in the presented case study may be relevant if similar hazards occur in weaker soils, such as volcanic soils. The intrinsic characteristics of such soils make them prone to landslides during extreme rainfall events. Moreover, if soils and roots are affected by wildfires, which may occur in the driest climates or due to climatic variability, the consequences would be even more severe. Therefore, to avoid or mitigate the effects of landslides, temporary barriers can be considered stabilization measures to promote soil infiltration and the establishment of vegetation, whose roots will contribute to a crucial increase in the resistance of volcanic soils.

References

Araújo Santos, L. M., Correia, A. J. P. M., & Coelho, P. A. L. F. (2020). Post-wildfire slope stability effects and mitigation: A case study from hilly terrains with unmanaged forest. *SN Applied Sciences, 2*, 1883. https://doi.org/10.1007/s42452-020-03660-8.

Ferreira, A. D., Prats, S., Carvalho, T., Silva, J. S., Pinheiro, A. Q., & Coelho, C. (2010). Soil and water conservation strategies and techniques after fires. In F. Moreira, F. X. Catry, J. S. Silva, & F. C. Rego (Eds.), *Ecologia do fogo e gestão de áreas ardidas* (pp. 229–252). ISA Press. (in Portuguese).

Gordo, C., Zêzere, J. L., & Marques, R. (2019). Landslide susceptibility assessment at the basins scale for rainfall- and earthquake- triggered shallow slides. *Geosciences, 9*, 268.

ICNF. (2017a). 10th Interim rural fire report 2017a. Instituto da Conservação da Natureza e das Florestas, Lisboa (Portugal) (in Portuguese).

ICNF. (2017b). Identification sheet of needs for post-fire emergency stabilization interventions_REE Seixo da Beira e Troviscal. Instituto da Conservação da Natureza e das Florestas, Lisboa (Portugal) (in Portuguese).

IPMA. (2017). 2017 Annual Climate Bulletin for Portugal Mainland. Instituto Português do Mar e da Atmosfera, Lisboa (Portugal) (in Portuguese).

IPMA. (2018). 2018 Annual Climate Bulletin for Portugal Mainland. Instituto Português do Mar e da Atmosfera, Lisboa (Portugal) (in Portuguese).

IPMA. (2019). 2019 Annual Climate Bulletin for Portugal Mainland. Instituto Português do Mar e da Atmosfera, Lisboa (Portugal) (in Portuguese).

Lourenço, L., Nunes, A. N., Bento-Gonçalves, A. J., & Vieira, A. (2012). Soil erosion after wildfires in Portugal: What happens when heavy rainfall occur? In D. Godone & S. Stanchi (Eds.), *Research on soil erosion*. InTech. https://doi.org/10.5772/50447.

Neall, V. (2009). Volcanic soils. In W. H. Verheye (Ed.), *Encyclopedia of land use, land cover and soil sciences part 2* (Vol. VII, pp. 23–45), Oxford: EOLSS Publishers, UNESCO

Podlaha, A., Bowen, S., & Lõric, M. (2018). *Weather, climate & catastrophe insight. 2017 Annual Report.* Aon Benfield, London, UK.

Schmidt, K. M., Roering, J. J., Stock, J. D., Dietrich, W. E., Montgomery, R. R., & Schaub, T. (2001). The variability of root cohesion as an influence on shallow landslides susceptibility in the Oregon Coast Range. *Canadian Geotechnical Journal, 38*, 995–1024. https://doi.org/10.1139/t01-031.

Silva, R. F., Marques, R., & Gaspar, J. L. (2018). Implications of landslides typology and predisposing factor combinations for probabilistic landslide susceptibility models: A case study in Ladejo parish (Flores Island, Azores—Portugal). *Geosciences, 8*, 153.

Wallenstein, N. (1999). Study of the recent eruptive history and eruptive behaviour of the Fogo volcano (S. Miguel Azores). Preliminary Hazard Assessment. University of Azores, Ponta Delgada, Ph.D. Thesis, (in Portuguese).

Methodologies for Mapping in Large Rock Excavations in Hazardous Geotechnical Contexts

Cláudio Santa, Helder I. Chaminé, and Isabel Fernandes

Abstract

This work intends to summarise the principles of geotechnical mapping as one of the fundamental elements in diverse applications, emphasising its use in underground works. This activity is generally integrated into the construction and extractive industry projects and is often the starting point for dimensioning and layout design. Developed and applied by geo-professionals with well-established and systematized techniques, with the support of new technologies and tools, while never leaving aside old and always reliable tools derived from geological mapping as the compass and geological hammer, geotechnical mapping has undergone several developments. As a result, it is increasingly recognised as part of major projects. Its application in underground works is a key part of their development, whether in the on-site investigations, design development, and excavations monitoring.

Keywords

Mapping • GIS-based tools • Engineering geology • Geotechnics • Geomaterials

C. Santa (✉) · I. Fernandes
Department of Geology, IDL—Instituto Dom Luiz, Faculty of Sciences, University of Lisbon, Lisbon, Portugal
e-mail: claudio_santa@hotmail.com

C. Santa · H. I. Chaminé
Department of Geotechnical Engineering, Laboratory of Cartography and Applied Geology (LABCARGA), School of Engineering (ISEP), Polytechnic of Porto, Porto, Portugal

C. Santa
EPOS—Empresa Portuguesa de Obras Subterrâneas SA, Oeiras, Portugal

H. I. Chaminé
Centre GeoBioTec|UA, Aveiro, Portugal

1 Introduction

Engineering geological mapping and geotechnical mapping are fundamental tools for different applications, such as civil and mining engineering projects and works, environmental management, land use and planning. Engineering geology surveys focus on fieldwork data on rock-mass evaluation in geotechnical practice. The lessons learned in engineering projects highlight the importance of engineering geology and geomechanics data accuracy in rock mass description and assessment (e.g., Chaminé et al., 2013, 2021; De Freitas, 2009; González de Vallejo & Ferrer, 2011; Rocha, 2013).

A comprehensive study and characterisation of the ground conditions are significant for any economic feasibility study. A rigorous and demanding study estimates operating costs in the different stages and engineering activities (excavations, foundations, support, etc.). In contrast, the lack of a rigorous study or geological engineering characterisation easily results in budget slippages caused by geotechnical issues (González de Vallejo & Ferrer, 2011). The thoughts of William Smith (1769–1839) are still topical: "The theory of geology is in the possession of one class of men, the practice in another" (Winchester, 2009). Therefore, it is vital to investigate the ground conditions for engineering purposes with an integrative approach and design with geohazards (González de Vallejo, 2012).

2 Engineering Geological Mapping: A Brief Outline

In current days, engineering geology mapping is a fundamental tool in engineering practice and professional geology. For example, Zuquette and Gandolfi (2004) pointed out that engineering maps containing important geological information were produced to implement civil works. One of the first works in the arising of geotechnical mapping was presented in 1902 when the United States Geological Survey

A. Malheiro et al. (eds.), *Advances in Natural Hazards and Volcanic Risks: Shaping a Sustainable Future*, Advances in Science, Technology & Innovation, https://doi.org/10.1007/978-3-031-25042-2_27

published an applied geological report for urban planning purposes in New York City, combining 1400 boreholes and geological features. Langen presented insightful sketches and maps of Europe during the International Construction Exhibition in Leipzig, Germany (1913). These documents consisted of plans set for the development projects of some German cities, which were intended to define, through colours and symbols, the geological bedrock, flood areas, water table variation and the areas of exploitation of materials for civil construction.[1]

Since the well-defined engineering geological map concept in practice by IAEG–CEGM (1976) until the vital importance of mapping standards and geotechnical models in current days pointed out by several authors (e.g., Chacón et al., 2006; Culshaw, 2018; Davis, 2021; De Freitas, 2021; Dearman, 1991; Fookes et al., 2015; González de Vallejo & Ferrer, 2011; Griffiths, 2001, 2002, 2014; Hutchinson, 2001; Norbury, 2017, 2021; Parry et al., 2014; Zuquette & Gandolfi, 2004, and references therein), this science developed dramatically.

IAEG–CEGM (1976) outlined an engineering geological map as: "(…) a type of geological map which provided a generalized representation of all those components of a geological environment of significance in land-use planning, and in design, construction and maintenance as applied to civil and mining engineering". González de Vallejo and Ferrer (2011) underline that topical issue: "engineering geological maps represent comprehensive geological and geotechnical information for land use and planning, construction and maintenance of engineering infrastructures". In addition, it provides reliable data on the ground parameters to evaluate its behaviour and foresee geotechnical issues or hazards.

Consequently, mapping is essential in on-site investigations, design, and modelling studies (e.g., Chaminé et al., 2016, 2021; González de Vallejo & Ferrer, 2011; Griffiths, 2001, 2014; Oliveira, 1975, 1977, 1987; Parry et al., 2014). The review of methods and techniques for geological mapping for rock engineering purposes or geotechnical surveys can be complemented by reading the works of Terzaghi (1965), Varnes (1974), Goodman (1976), Oliveira (1977, 1978), Priest (1993), Hudson and Cosgrove (1997), Price (2009), Hencher (2012), Chaminé et al., (2013, 2021), and Cosgrove and Hudson (2016).

In geotechnical practice, engineering geology mapping is crucial in applied geosciences, geotechnical engineering, environmental geotechnics and natural hazards. Therefore, it is an integral part of any large-scale project in preliminary and on-site investigations and during the design and project phases.

[1] Details in: https://langen.ykom.de/serverlocal/diys_static/langen.html (accessed in January 2021).

3 Rock Surveys: Methodologies and Techniques

The rock mass quality is decisive in adequate ground stability support design for tunnels or underground excavation. Therefore, structural geology knowledge is vital to describe the rock mass fissured media, mainly through detailed geotechnical surveys (Fig. 1). The best approach is collecting in-situ data and a comprehensive interpretation based on representative surveys backed by laboratory and field-testing techniques (e.g., ISRM, 1978, 1981, 2007, 2015; GSE, 1995; CFCFF, 1996; NAP, 2020). So, studying the rock mass and intact rock allows its description, classification, and evaluation in engineering practice (e.g., Norbury, 2020; Zhang, 2017). Finally, the standards and codes related to the ground investigations must be followed (Norbury, 2017).

Rock survey sampling along a scanline is an objective approach to the systematic record of joints, fractures, fissures, faults, veins, and geological contacts (details in Chaminé et al., 2015; Mahé et al., 2015; Peacock, 2006; Priest, 1993, 2004; Santa et al., 2019; Watkins et al., 2015; Zeeb et al., 2013). Nevertheless, some practices should be guaranteed to avoid systematic or random errors in collecting geostructural data. Therefore, it is essential to set up a thorough, unbiased sampling methodology (e.g., Terzaghi, 1965, ISRM 1981, Priest, 1993, 2004, Hudson & Cosgrove, 1997, Peacock, 2006, Chaminé et al., 2015, Mahé et al., 2015, Watkins et al., 2015, and references therein).

The scanline surveys are suitable for mapping rock exposures, describing and evaluating the discontinuities network, and collecting geotechnical parameters (e.g., ISRM, 1978, 1981; CFCFF, 1996; ASTM D4879-08, 2008; NAP, 2020). Defining the rock mass's strength, deformability, and permeability is essential. Several authors (e.g., Culshaw, 2018; Giordan et al., 2020; Monsalve et al., 2019; Russell & Stacey, 2019) underline the extensive use of digital mapping, particularly GIS-based and geomatic techniques. So, it is more usual to combine data from digital photogrammetry, unmanned aircraft vehicles (UAV), high-resolution global positioning systems (GPS), 3D laser scanner technologies, as well as geovisualisation techniques, geo-database systems, and GIS and BIM-based mapping.

The method of mapping presentation depends essentially on purpose, which can be more descriptive or schematic. Also, it depends on the project requests and the geostructure to be characterised. Figure 2 shows engineering geology mapping in diverse geotechnical contexts and rock engineering works (e.g., underground rock excavation faces, rock slopes or rock foundation slab base, wall of an underground cavern, and a planimetric representation of a tunnel). Although the representation procedure may vary, information must be included in any engineering geology mapping,

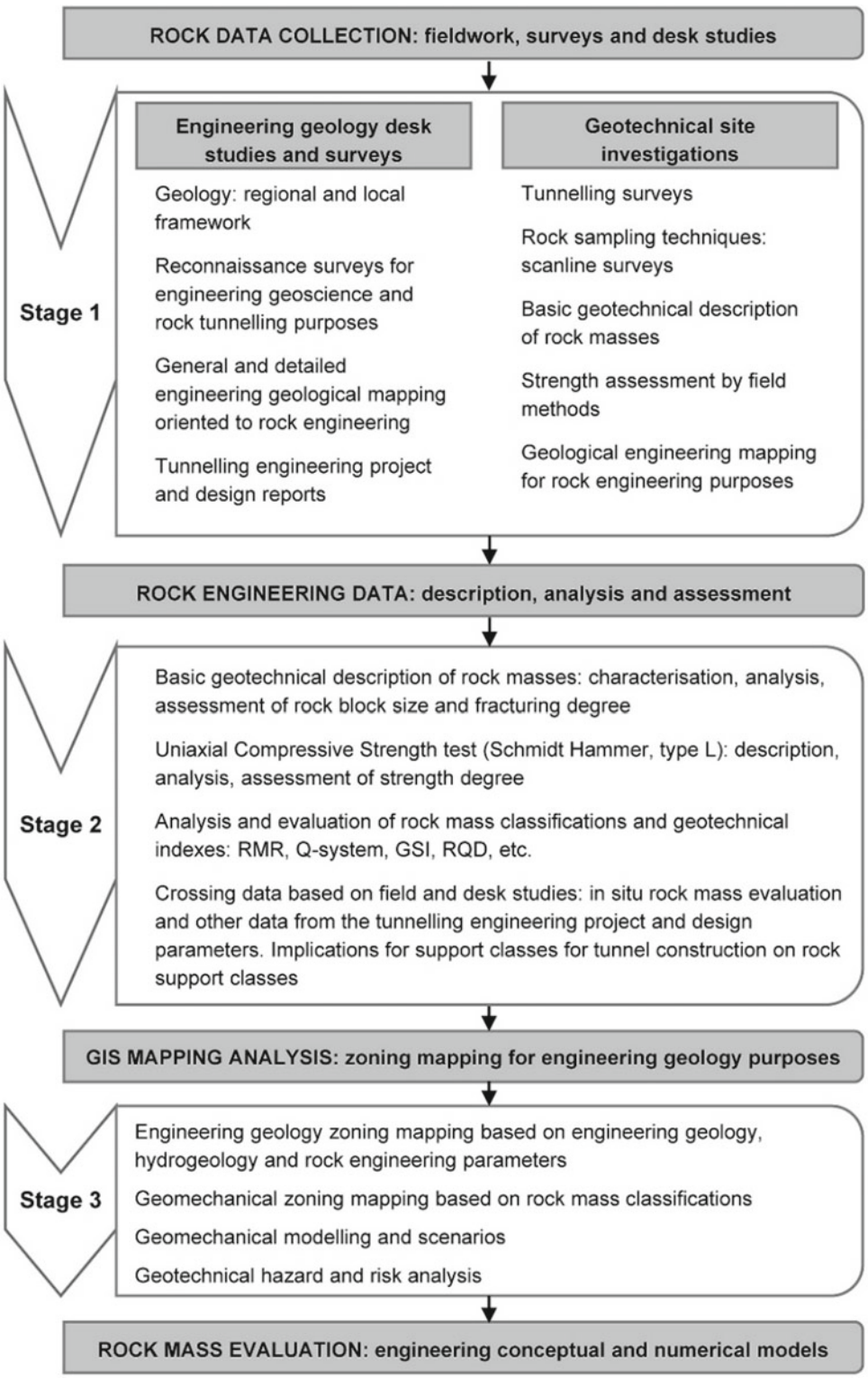

Fig. 1 Schematic flowchart of the on-site investigation methodology for rock mass evaluation for tunnels or underground excavations (adapted from Santa et al., 2019)

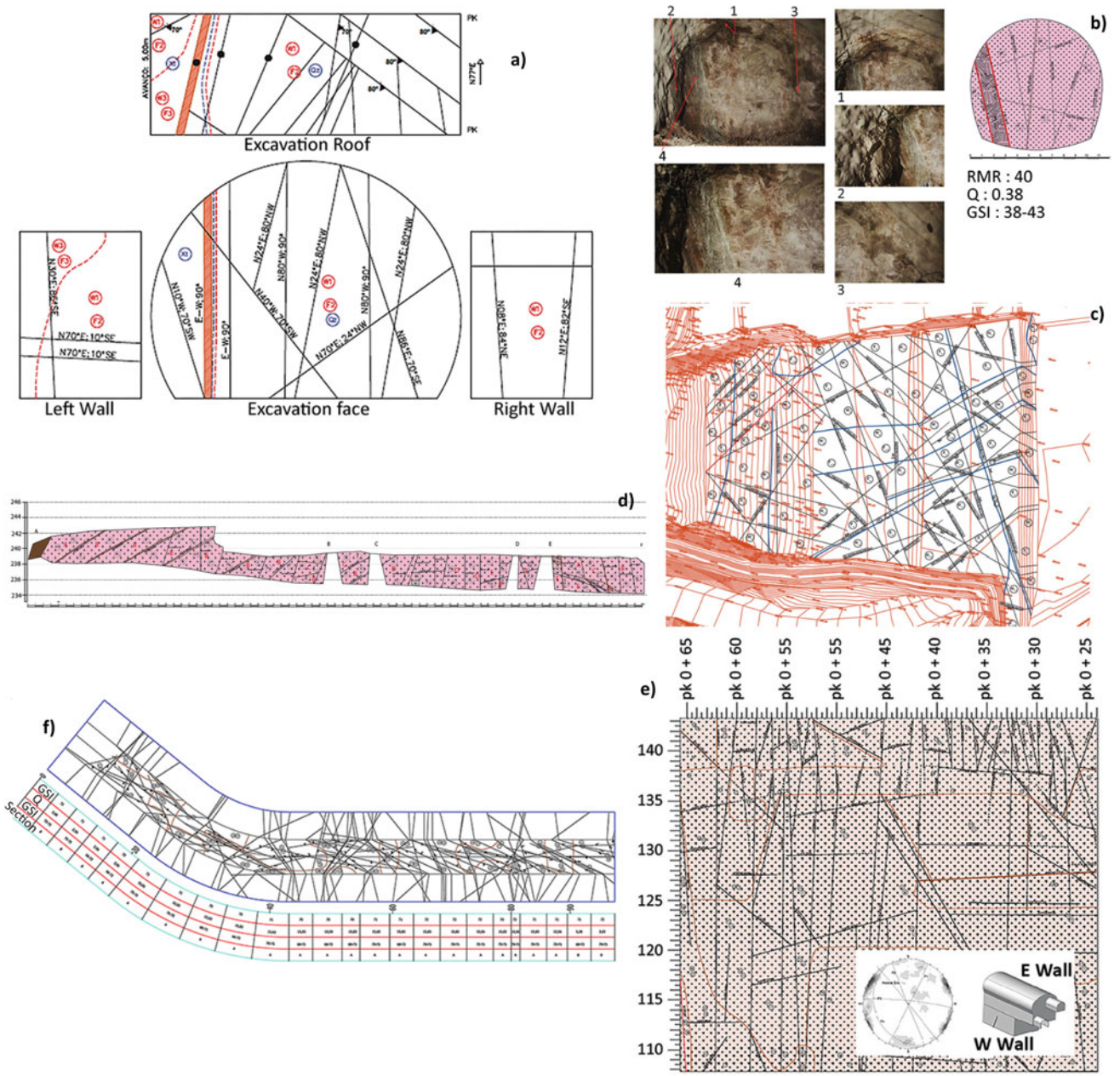

Fig. 2 Examples of engineering geology mapping in diverse geotechnical contexts and rock engineering works in mainland Portugal. **a** mapping of an underground excavation face with tunnel mapping of roof and walls; **b** mapping of a tunnel face with the photographic record; **c** mapping of the base for the foundation slab; **d** mapping of a rock slope; **e** mapping of an underground cavern wall; **f** mapping of a tunnel combining geostructure and planimetric background

such as lithological heterogeneity and structure, the description of the degree of weathering and fracturing, and the discontinuities characterisation presence of water and strength grade evaluation.

4 Concluding Remarks

Engineering geology mapping must be systematised to minimise errors, flaws, and uncertainties. Currently, several techniques are available to support the characterisation of the rock masses, including in the geotechnical hazard framework. The vital issue is accurately describing and evaluating the geological, geotechnical, and geomechanical parameters following the standards and codes (IAEG, ISRM, ASTM, and EuroCodes). Therefore, engineering geology mapping is valuable and reliable in characterising and evaluating the rock masses. Consequently, engineering geology mapping plays a role in decision-making, but understanding that geological media presents spatial variability and inherent heterogeneity. Griffiths (2004) stated: "Without doubt, field mapping of engineering geology and geomorphology has proved to be an extremely cost-effective investigative tool for all aspects of ground engineering".

Acknowledgements LABCARGA|ISEP re-equipment program (IPP-ISEP| PAD'2007/08) and Centre GeoBioTec| UA (UID/GEO/04035/2020) supported HIC. This work was funded by the Portuguese Fundação para a Ciência e a Tecnologia (FCT) I.P./MCTES through national funds (PIDDAC)—UIDB/50019/2020. We thank L. Freitas (LABCARGA|ISEP) for helping with the final editing of the figures.

References

ASTM D4879-08. (2008). Standard guide for geotechnical mapping of large underground openings in rock. ASTM International, West Conshohocken, PA.

CFCFF – Committee on Fracture Characterization and Fluid Flow, (1996). *Rock fractures and fluid flow: Contemporary understanding and applications*. National Academy Press, Washington DC.

Chacón, J., Irigaray, C., Fernández, T., & El Hamdouni, R. (2006). Engineering geology maps: Landslides and geographical information systems. *Bulletin of Engineering Geology and Environment, 65*(4), 341–411.

Chaminé, H. I., Afonso, M. J., Ramos, L., & Pinheiro, R. (2015). Scanline sampling techniques for rock engineering surveys: insights from intrinsic geologic variability and uncertainty. In D. Giordan, K. Thuro, C. Carranza-Torres, F. Wu, P. Marinos, & C. Delgado (Eds.), *Engineering geology for society and territory—Applied geology for major engineering projects* (vol. 6, pp. 357–361). IAEG, Springer.

Chaminé, H. I., Afonso, M. J., Teixeira, J., Ramos, L., Fonseca, L., Pinheiro, R., & Galiza, A. C. (2013). Using engineering geosciences mapping and GIS-based tools for georesources management: Lessons learned from rock quarrying. *European Geologist Journal, 36*, 27–33.

Chaminé, H. I., Afonso, M. J., Trigo, J. F., Freitas, L., Ramos, L., & Carvalho, J. M. (2021). Site appraisal in fractured rock media: Coupling engineering geological mapping and geotechnical modelling. *European Geologist Journal, 51*, 31–38.

Chaminé, H. I., Teixeira, J., Freitas, L., Pires, A., Silva, R. S., Pinho, T., Monteiro, R., Costa, A. L., Abreu, T., Trigo, J. F., Afonso, M. J., & Carvalho, J. M. (2016). From engineering geosciences mapping towards sustainable urban planning. *European Geologist Journal, 41*, 16–25.

Cosgrove, J. W., & Hudson, J. A. (2016). *Structural geology and rock engineering*. Imperial College Press.

Culshaw, M. G. (2018). Engineering geological maps. In P.T. Bobrowsky & B. Marker (Eds.), *Encyclopedia of engineering geology. Encyclopedia of earth sciences series* (pp. 265–377). Springer.

Davis, J. A. (2021). Geotechnical baseline reports: Ground models you can just make up? *Quarterly Journal of Engineering Geology and Hydrogeology, 54*(2). https://doi.org/10.1144/qjegh2020-019.

De Freitas, M. H. (2009). Geology: Its principles, practice and potential for geotechnics. *Quarterly Journal of Engineering Geology and Hydrogeology, 42*, 397–441.

De Freitas, M. H. (2021). Future developments for ground models. *Quarterly Journal of Engineering Geology and Hydrogeology, 54*(2), 2020–2034.

Dearman, W. R. (1991). *Engineering geological mapping*. Butterworth-Heinemann.

Fookes, P., Pettifer, G., & Waltham, T. (2015). *Geomodels in engineering geology: An introduction*. Whittles Publishing.

Giordan, D., Adams, M., Aicardi, I., Alicandro, M., Allasia, P., Baldo, M., De Berardinis, P., Dominici, D., Godone, D., Hobbs, P., Lechner, V., Niedzielski, T., Piras, M., Rotilio, M., Salvini, R., Segor, V., Sotier, B., & Troilo, F. (2020). The use of unmanned aerial vehicles (UAVs) for engineering geology applications. *Bulletin of Engineering Geology and the Environment, 79*(7), 3437–3481.

González de Vallejo, L. I. (2012). Design with geohazards: An integrated approach from engineering geological methods. *Soils Rocks International Journal of Geotechnical and Geoenvironmental Engineering, 35*(1), 1–28.

González de Vallejo, L. I., & Ferrer, M. (2011). *Geological engineering*. CRC Press.

Goodman, R. E. (1976). *Methods of geological engineering in discontinuous rocks*. West Publishing Company.

Griffiths, J. S. (2001). Engineering geological mapping. In J.S. Griffiths & D. Circus (Eds.), *Land surface evaluation for engineering practice*, Geological Society. *Engineering Geology Special Publications, 18*(1), 39–42.

Griffiths, J. S. (2002). Mapping in engineering geology. *Key issues in earth sciences* (vol. 1), The Geological Society of London.

Griffiths, J. S. (2014). Feet on the ground: Engineering geology past, present and future. *Quarterly Journal of Engineering Geology and Hydrogeology, 47*(2), 116–143.

GSE – Geological Society Engineering Group Working Party Report. (1995). The description and classification of weathered rocks for engineering purposes. *Quarterly Journal of Engineering Geology and Hydrogeology, 28*(3), 207–242.

Hencher, S. (2012). *Practical engineering geology*. Spon Press, Taylor & Francis Group.

Hudson, J. A., & Cosgrove, J. W. (1997). Integrated structural geology and engineering rock mechanics approach to site characterization. *International Journal of Rock Mechanics and Mining Sciences and Geomechanic Abstract, 34*(3/4), 136.1–136.15.

Hutchinson, J. N. (2001). Reading the ground: Morphology and geology in site appraisal. *Quarterly Journal of Engineering Geology and Hydrogeology, 34*, 7–50.

IAEG–CEGM. (1976). Engineering geological maps: A guide to their preparation. Earth Sciences Series No. 15, Commission on Engineering Geological Maps of the International Association of Engineering Geology, IAEG-CEGM, The UNESCO Press, Paris.

ISRM – International Society for Rock Mechanics. (1978). Suggested methods for the quantitative description of discontinuities in rock masses. *International Journal of Rock Mechanics and Mining Sciences and Geomechanic Abstract, 15*(6), 319–368.

ISRM—International Society for Rock Mechanics. (1981). Basic geotechnical description of rock masses. *International Journal of Rock Mechanics and Mining Sciences and Geomechanic Abstract, 18*, 85–110.

ISRM—International Society for Rock Mechanics. (2007). The complete ISRM suggested methods for characterization, testing and monitoring: 1974–2006. In R. Ulusay & J.A. Hudson (Eds.), *Suggested methods prepared by the commission on testing methods*. ISRM.

ISRM—International Society for Rock Mechanics. (2015). The ISRM suggested methods for rock characterization, testing and monitoring: 2007–2014. In R. Ulusay (Ed.), *Suggested methods prepared by the commission on testing methods, ISRM*. Springer.

Mahé, S., Gasc-Barbier, M., & Soliva, R. (2015). Joint set intensity estimation: Comparison between investigation modes. *Bulletin of Engineering Geology and the Environment, 74*(1), 171–180.

Monsalve, J., Baggett, J., Bishop, R., & Ripepi, N. (2019). Application of laser scanning for rock mass characterization and discrete fracture network generation in an underground limestone mine. *International Journal of Mining Science and Technology, 29*(1), 131–137.

NAP – National Academies of Sciences, Engineering, and Medicine,. (2020). *Characterization, modeling, monitoring, and remediation of fractured rock*. The National Academies Press.

Norbury, D. (2017). Standards and quality in ground investigation; squaring the circle. *Quarterly Journal of Engineering Geology and Hydrogeology, 50*(3), 212–230.

Norbury, D. (2021). Ground models: A brief overview. *Quarterly Journal of Engineering Geology and Hydrogeology, 54*(2). https://doi.org/10.1144/qjegh2020-018.

Norbury, D. N. (2020). *Soil and rock description in engineering practice* (3rd Rev. edn.). Whittles Publishing.

Oliveira, R. (1975). Underground constructions: Engineering geological investigations and in situ testing. *Memórias LNEC, Lisbon, 467*, 1–13.

Oliveira, R. (1977). Cartografia geológica de túneis. *Memórias LNEC, Lisbon, 489*, 1–12.

Oliveira, R. (1987). Engineering geological investigations of rock masses for civil engineering projects and mining operations. *Memórias LNEC, Lisbon, 693*, 1–28.

Parry, S., Baynes, F. J., Culshaw, M. G., Eggers, M., Keaton, J. F., Lentfer, K., Novotny, J., & Paul, D. (2014). Engineering geological models: An introduction: IAEG commission 25. *Bulletin of the International Association for Engineering Geology and the Environment, 73*, 689–706.

Peacock, D. C. (2006). Predicting variability in joint frequencies from boreholes. *Journal of Structural Geology, 28*(2), 353–361.

Price, D. G. (2009). *Engineering geology: Principles and practice*. Springer Verlag.

Priest, S. D. (1993). *Discontinuity analysis for rock engineering*. Chapman and Hall.

Priest, S. D. (2004). Determination of discontinuity size distributions from scanline data. *Rock Mechanics and Rock Engineering, 37*(5), 347–368.

Rocha, M. (2013). Mecânica das Rochas. Edição no âmbito das comemorações do centenário do nascimento do Engenheiro Manuel Rocha—1913–2013. Laboratório Nacional de Engenharia Civil, LNEC, Lisboa

Russell, T. M., & Stacey, T. R. (2019). Using laser scanner face mapping to improve geotechnical data confidence at Sishen mine. *Journal of Southern African Institute of Mining and Metallurgy, 119*(1), 11–20.

Santa, C., Gonçalves, L., & Chaminé, H. I. (2019). Comparative study of GSI chart versions in a heterogeneous rock mass media (Marão tunnel, north Portugal): A reliable index in geotechnical surveys and rock engineering design. *Bulletin of Engineering Geology and the Environment, 78*, 5889–5903.

Terzaghi, R. D. (1965). Sources of errors in joint surveys. *Géotechnique, 15*, 287–304.

Varnes, D. J. (1974). *The logic of geological maps, with reference to their interpretation and use for engineering purposes*. U.S. Geological Survey Professional Paper 837, USGS, Washington.

Watkins, H., Bond, C. E., Healy, D., & Butler, R. W. H. (2015). Appraisal of fracture sampling methods and a new workflow to characterise heterogeneous fracture networks at outcrop. *Journal of Structural Geology, 72*, 67–82.

Winchester, S. (2009). *The map that changed the world: William Smith and the birth of modern geology*. Harper Perennial.

Zeeb, C., Gomez-Rivas, E., Bons, P. D., & Blum, O. (2013). Evaluation of sampling methods for fracture network characterization using outcrops. *AAPG Bulletin, 97*(9), 1545–1566.

Zhang, L. (2017). *Engineering properties of rocks* (2nd ed.). Elsevier.

Zuquette, L., & Gandolfi, N. (2004). *Cartografia geotécnica*. Oficina de Textos.

Dimension Stone Quarries Risk Assessment Estremoz Marbles

Luís Lopes, Ruben Martins, António Pinho, Isabel Duarte, and Paula Faria

Abstract

For centuries, dimension stone marble exploitation from the Estremoz Anticline, south Portugal, leads to a peculiar landscape consisting of hundreds of deep open-pit quarries. In the 80s of the last century, more than 180 quarries operate side-by-side simultaneously. The struggle for interesting outcrops, in addition to private property that legally characterises the mineral masses in Portugal, led to a situation where the quarries very close to each other developed into a well and independently. As the quarries reached greater depths, in several cases over 100 m, issues related to the slope stability became more evident and dangerous. It took an accident that caused 5 deaths due to a slope collapse that destroyed a municipal road for public entities to pay more attention to this issue. Within the scope of the Intervention Plan in Quarries Under Critical Situations (2019–2021), approved at the meeting of the Council of Ministers on February 7 (RCM 50/2019), the University of Évora carried out 34 slope stability studies in approximately 40 exploitation cavities for ornamental marble. This work summarises the identified main situations and the measures recommended for their mitigation.

Keywords

Dimension stone • Quarry • Risk assessment • Estremoz • Marbles

L. Lopes (✉) · R. Martins · A. Pinho · I. Duarte · P. Faria
Departamento de Geociências, Universidade de Évora, Évora, Portugal
e-mail: lopes@uevora.pt

L. Lopes
Instituto de Ciências da Terra, Pólo de Évora, Évora, Portugal

A. Pinho · I. Duarte · P. Faria
Centro GeoBioTec|UA, Aveiro, Portugal

1 Introduction

The Estremoz Anticline corresponds to a substantially elliptical shape NNW-SSE macrostructure, individualised in the Estremoz—Barrancos sector of the Ossa—Morena Zone tectonostratigraphic unit, belonging to the Iberian Peninsula Variscan orogen. The pre-Silurian stratigraphic sequence of the Estremoz Anticline includes: (1) Ediacaran greywackes, shales and black cherts (Mares Formation- Série Negra Succession), which crop out in two separate elongated ribbons in the core of the Estremoz Anticline; (2) Cambrian arkosic sandstones at the base (which unconformably overlie the Série Negra rocks), and dolomitic limestones (∼400 m) towards the top (Dolomitic Formation); (3) a silica-rich (quartz and iron-rich) layer atop the dolomitic marbles; (4) thick-bedded Cambrian–Ordovician (?) marbles (70–100 m) with interbedded basalts, rhyolites and shales (Volcano–Sedimentary Complex of Estremoz, which includes the Estremoz marbles) (Pereira et al., 2012).

Numerous bibliographical references corroborate the existence of extractive activity since around 370 B.C. (Cabral et al., 2001). However, it was not until the 1970s that the exploitation of marbles in the anticline reached an industrial dimension worthy of the name.

The social and economic conditions that underpinned the expansion of the marble industry in the Estremoz Anticline, essentially from the 1970s onwards, conditioned the location and progress of mining in these quarries. However, because of the lack of a global strategic vision right from the start, there was no real planning of the territory, which is the main reason for the risk situations identified in the quarries of the Estremoz Anticline.

About thirty years later, a captive area for marble was defined, and from then on, the PROZOM (Regional Planning for the Marble Zone) was recognised in the Diário da República (Resolution of the Council of Ministers 93/2002, May 5, 2002), followed by the Thematic Cartography of the Estremoz Anticline (Vintém et al., 2003). Later, five UNORs

A. Malheiro et al. (eds.), *Advances in Natural Hazards and Volcanic Risks: Shaping a Sustainable Future*,
Advances in Science, Technology & Innovation, https://doi.org/10.1007/978-3-031-25042-2_28

(Regional Areas of Territorial Planning, Carvalho et al., 2008) were defined, where the base geological cartography was published on a large scale (1:2,000).

Added to this superficial knowledge is a series of deep drillings with core recovery (some more than 400 m deep) carried out by government entities and many other exploration drillings to aid exploration carried out by companies.

The Estremoz Anticline, and the five planning areas that constitute the main quarry centres, are among the places in Portugal where there is more detailed geological and structural knowledge that must be leveraged for integrated exploitation plans where, firstly, workers' safety conditions are ensured, but also where access to mineral masses takes place on broad fronts, allowing for more rational exploitation with higher yields.

By the 1970s, the international marble market was until then entirely dominated by Italian companies based in Tuscany (Carrara—Massa). In the search for differentiated and alternative materials to those also marketed since the Roman Period, these companies rediscovered the famous pink marbles in the Alentejo's marbles, with or without stripes and veins, meaning the textural chromatic complement they are looking for. Some Italian businessmen even ended up settling in the region, acquiring quarries, and importing equipment and tools that, in a way, boosted the sector in the region. In addition, authentic Portuguese ex libris, the varieties Rosa Portogallo and Rosa Aurora, gained recognition in the most prestigious fairs until now. In this way, foreign interest in a product that was just around the corner motivated local rural workers who saw in this industry an opportunity to improve their lives.

Small companies of three or four men rented compressed air compressors that allowed them to use compressed air hammers that made it easier for them to "pull out of the ground" commercially sized blocks sold at a very good price. Otherwise, they would only be equipped with rudimentary tools such as shovels, pickaxes, hammers, mallets, steel wedges, manual jacks, steel cables, etc. with whom the whole process was arduous and time-consuming. In addition to half a dozen companies long-established in the region, these enterprising men will boost the marble as an ornamental stone industry in what would later be known as the "Marble Triangle" (Estremoz-Borba-Vila Viçosa). The considerable number of existing exploration and prospecting cavities in the region (more than 500) and the simultaneous number of quarries in activity at the end of the 1980s (226 of the 366 quarries of ornamental rocks in Portugal belonged to the Estremoz Anticline) (Quintas, 2021) is therefore partially explained within this historical framework. Despite the publication in 1972 (Gonçalves, 1972) of a 1:25,000 scale map focusing on the potential existence of marble as an ornamental stone, this was entirely ignored by those whose belief was based on empirical knowledge of Nature that often did not work. Despite this, some have been successful, and these are in 2022, the owners of some of the most dynamic companies in the region. However, they now recognise the importance of geology and geological engineering as crucial to quarry development and workers' safety and, therefore, to the economic feasibility of the company.

2 Methodology

The studies focused on the preliminary characterisation of the quarries from a geotechnical point of view to identify potential situations of instability and propose measures, if necessary, in a subsequent execution project, which will solve the identified situations without compromising the future of exploitations.

Not only were the technical constraints of the project considered, but also all the situations that could make it possible to eliminate hazards and risks, namely issues related to land use planning (location of roads, paths, etc.) and the history and development holdings (past and future perspectives). Therefore, the studies elaboration was developed according to the following methodology:

- Collection of bibliographic information of interest for the framework of the quarry;
- A brief overview of the quarry's history;
- Geological survey (fieldwork);
- Analysis and treatment of all information;
- Identification and assessment of geotechnical risks;
- Proposal of measures and work to be carried out.

Regarding the physical and mechanical characterisation of the marbles of the Estremoz Anticline, the values expressed in Table 1 were considered (Casal Moura et al., 2007). These results also serve as a reference for geotechnical applications.

The rock masses were classified according to the Basic Geotechnical Description (BGD) of the International Society for Rock Mechanics (ISRM, 1981) regarding the weathering state and the rock mass's discontinuities. The geotechnical properties of Portuguese marbles and the values obtained by Silva (2002) for the Lagoa Nucleus (UNOR4) were used as references (Table 2).

In each quarry, a fieldwork campaign was carried out based on visual inspection of the slopes of cavities and heaps, photographic records of critical situations, structural and hydrogeological data collection, and characterisation of lithologies and their state of alteration. This preliminary analysis identified the most evident critical situations, where preventive and/or corrective measures are presented and

Table 1 Physical and mechanical characteristics of the Estremoz Anticline marbles. Mean values for 36 samples (Casal Moura et al. 2007)

		Máx.	Mín.
Compressive strength	(MPa)	108,56	59,04
Compressive strength after freezing test	(MPa)	103,66	67,18
Mechanical strength to bending	(MPa)	29,52	14,51
Dry density	(kg/m^3)	2726	2703
Absorption of water at atmospheric pressure	(% height)	0,11	0,03
Open porosity	(% volume)	0,32	0,05
Dilation coefficient	(×10–6 °C)	16,3	5,4
Wear resistance	(mm)	3,8	1,4
Shock resistance	(mm)	70–75	45

Table 2 Geotechnical properties of marbles from Lagoa area, Estremoz Anticline (Silva, 2002)

Lithology	E(GPa)	ɣ	σ_c(MPa)	σ_t(MPa)	c(MPa)	ϕ(°)
Cream marble without stripes	66	0.222	94	10.4	13.1	50
Cream marble with stripes	57	0.39	61	9.0	10	48
Grey marble with stripes	59	0.38	64	9.0	19	47

E(GPa) Young's modulus; σ_t (MPa) Tensile strength; ɣ Poisson´s ratio; c (MPa) Cohesion; σ_c (MPa) Uniaxial compressive strength; ϕ (°) Friction angle

justified, and the need for detailed and in-depth studies at a later stage provided in the schedule delivered to each company.

3 Results

The most critical situations detected were related to built structures' instability in the vicinity of the cuts, some even showing tensile cracks indicative of recent movements and very likely collapse in the short term of these structures. In addition, some Derrick cranes even had to be removed because they did not have fixing bases in good condition. Also, in most of the analysed cases, poor sanitation was found at the top of the slopes, with probable and/or effective fall of soil and rocks into the cavity.

The most superficial geotechnical horizon of the rock/mass, along the entire perimeter of the cavities, is frequently altered ($W_{4\text{-}5}$) and moderately fractured (F_3). Karstification can go beyond 5 m, with residual soil filling ("*terra rossa*"), favouring material slides (rock blocks and soils), from the top of the slope to the cavity interior.

The slope stability structural analysis was carried out by Stereograph free software. All slopes were considered individually in each cavity, and the existing equilibrium conditions were determined. In the case of slopes cut into rock masses with competent rock, if there is mass instability, this will necessarily be related to the discontinuities that occur, which correspond to the fracturing of the massif.

In the study of the slope's potential instability, the methodology of Hoek and Bray (1981) was considered, having resorted to the Markland method (Markland, 1972), considering the refinement introduced by Hocking to this method (Hocking, 1976), in the distinction between the type of planar failure and the type of failure wedge rupture. Regarding analysing the potential instability through toppling failure, the conditions proposed by Goodman and Bray (1976) were used. In the stability evaluation, the friction angle value of 30° was considered for the most open fractures and filled with terra rossa. This situation corresponds to the characteristics of the more open fractures that exist at the most superficial level of the quarries.

The wedge failure will most likely occur from the analysis carried out. This situation is predictable due to a late stress field of regional expression, with maximum compression tilting around 30°, which originates oblique conjugate fractures concerning the vertical slopes of the cavities. Although the late stress fields are well known, it should be noted that the local geological conditions at the quarry's scale define the orientation of the present discontinuities. For example, the existence of a dolerite dyke, metavolcanic rocks and dark shales interbedded in the marbles, among other factors, will determine the geometry and density of the discontinuities that occur in each quarry. As a result, planar rupture situations are frequent. On the other hand, toppling failure was only occasionally observed in the field, although the probability of occurrence was detected in the stereograms analysis.

4 Concluding Remarks

From the analysis carried out, it is concluded that most risk situations can be mitigated or even eliminated if future mining plans include several adjacent licenses. In this way, unnecessary defence zones are eliminated, recovering that volume for commercial purposes while substantially improving the safety conditions of workers.

As expected, since confined stress intensely increases, it was found that fracture density decreases at depth, and the existing discontinuities also tend to be more closed. On the other hand, the connectivity between fractures is low, which explains that despite the large extension of the slopes, only one accident occurred on November 19, 2018, at EM 255 in Borba, which caused 5 victims. However, three more cases are known in 40 years, fortunately without victims.

A very conservative assessment of the existing raw material in the anticline (Lopes and Martins, 2015) indicates that even the highest annual production rates were ever achieved. Therefore, enough quality marble will be for another 550 years of uninterrupted mining. However, for this to happen, it must be changed, both in exploitation methods, aiming at optimising mining and mitigating the risks associated with it and the business model and organisation of the companies.

Acknowledgements The work was supported by the Portuguese Foundation for Science and Technology (FCT) project UIDB/04683/2020—ICT (Institute of Earth Sciences).

References

Cabral, J., Maciel, J., Lopes, L., Lopes, J., Marques, A., Mustra, C., Freitas, M., & Carreira, P. (2001). Petrographic and isotopic characterisation of marble from the Estremoz Anticline: Its application in identifying the sources of Roman works of art. *Journal of Iberian Archeology, 3*, 121–128.

Carvalho, J., Vintém, C., Henriques, P., Falé, P., Luís, G., Midões, C., Antunes, C., Dili, A., Saúde, J., Bonito, N., & Sobreiro, S. (2008). *Cartografia temática do anticlinal - Zona dos Mármores, Cevalor & INETI.*

Casal Moura, A., Carvalho, C., Almeida, I., Saúde, J., Farinha Ramos, J., Augusto, J., Rodrigues, J., Carvalho, J., Martins, L., Matos, M. J., Machado, M., Sobreiro, M., Peres, M., Martins, N., Bonito, N., Henriques, P., & Sobreiro, S. (2007). *Mármores e calcários ornamentais de Portugal*. INETI.

Gonçalves, F. (1972). Observações sobre o anticlinório de Estremoz: Alguns aspectos geológico-económicos dos mármores. *Estudos, Notas e Trabalhos Serviço de Fomento Mineiro, 22*(1–2), 121–132.

Goodman, R. E., & Bray, J. (1976). Toppling of rock slopes. *ASCE, Proceedings Specialty Conference on Rock Engineering for Foundations and Slopes, Boulder, CO, 2*, 201–234.

Hocking, G. (1976). A method for distinguishing between single and double plane sliding of tetrahedral wedges. *International Journal of Rock Mechanics and Mining Sciences, 13*, 225–226.

Hoek, E., & Bray, J. (1981). *Rock slope engineering* (3rd edn.). Institute Mining and Metallurgy.

ISRM. International Society for Rock Mechanics (1981). Basic geotechnical description of rock masses. *International Journal of Rock Mechanics and Mining Science and Geomechanics Abstract, 18*, 85–110.

Lopes, L., & Martins, R. (2015). Global heritage stone: Estremoz marbles, Portugal. In D. Pereira, B.R. Marker, S. Kramar, B. J. Cooper, B.E. Schouenborg (Eds.), *Global heritage stone: Towards international recognition of building and ornamental stones* (vol. 407, pp. 57–74). Geological Society of London, Special Publications.

Markland, J. T. (1972). A useful technique for estimating the stability of rock slopes when the rigid wedge sliding type of failure is expected. *Imperial College Rock Mechanics Research Report, 19*, 1–10.

Pereira, M., Solá, R., Chichorro, M., Lopes, L., Gerdes, A., & Silva, J. (2012). North-Gondwana assembly, break-up and paleogeography: U-Pb isotope evidence from detrital and igneous zircons of Ediacaran and Cambrian rocks of SW Iberia. *Gondwana Research, 22*(3–4), 866–881.

Quintas, A. (2021). Os Mármores do Alentejo. História, património e valorização cultural (1850–2020). Universidade de Évora, Évora (Ph.D. Thesis).

Silva, M. (2002). Zonamento das propriedades geotécnicas dos mármores portugueses. In *Actas do 8º Congresso Nacional de Geotecnia, Lisboa*.

Vintém, C., Henriques, P., Falé, P., Luís, G., Midões, C., Antunes, C., Dili, A., Carvalho, J., Saúde, J., Bonito, N., & Sobreiro, S. (2003). *Cartografia temática do anticlinal como instrumento de ordenamento do território e apoio à indústria extractiva*. Relatório Final do Projecto. Instituto Geológico e Mineiro e Cevalor, Lisboa.

Rock Cut-Slope Quarry Assessment (NW Portugal): A Preliminary Hazard Assessment

Luís Ramos, Ana Mendes, José Filinto Trigo, Fernando Pedro Figueiredo, Liliana Freitas, Maria José Afonso, and Helder I. Chaminé

Abstract

To safeguard the operations in rock quarrying, it is required to evaluate slope stability hazards systematically. This work investigates the slope stability in a rock quarry in NW Portugal and demonstrates the significance of geological, geotechnical, and geomechanical in situ investigations. The rock mass is a monzogranite, medium-grained, two-mica, essentially biotitic, predominantly fresh to slightly weathered (W_{1-2}) to moderately weathered (W_3), and highly fractured. The geomechanical classifications and geotechnical indexes RMR, GSI, SMR, SQR, and Q-Slope allowed five geomechanical zones. Globally, the Southern part of the quarry has a fair to very good quality and the Northern part has a poor to fair quality. Three cut-slopes were studied in the Northern part of the quarry, which was considered unstable to partially stable. Several potential failures may occur, namely wedge slides and toppling failures. The application of the RHRSm2 system and the SQI permitted the classification of the cut-slopes with a high to very high-risk level and an urgent to very urgent intervention. RocFall and Swedge Rocscience software were used to model block fall in different areas and potential rock failures.

L. Ramos · A. Mendes · J. F. Trigo · L. Freitas · M. J. Afonso (✉) · H. I. Chaminé
Laboratory of Cartography and Applied Geology (LABCARGA), School of Engineering (ISEP), Polytechnic of Porto, Porto, Portugal
e-mail: mja@isep.ipp.pt

J. F. Trigo
Division for Construction Studies (NEC), School of Engineering (ISEP), Polytechnic of Porto, Porto, Portugal

F. P. Figueiredo
Geosciences Centre and Department of Earth Sciences, Faculty of Sciences and Technology, University of Coimbra, Coimbra, Portugal

L. Freitas · M. J. Afonso · H. I. Chaminé
Centre GeoBioTEc, UA, Aveiro, Portugal

Keywords

Cut-slope • Quarry • Slope stability • Hazard assessment

1 Introduction

The hazard assessment of rock slopes is a vital issue for risk analysis in quarries. The geomechanical characteristics of rock masses, the geometrical parameters of slopes, and external factors, like precipitation and blasting, are among the most critical parameters that can lead to rock slope failures (e.g., Wyllie & Mah, 2004).

In Northern Portugal, rockfalls are a common rock slope instability (Trigo et al., 2020). This work assesses the stability of several cut-slopes in a granitic quarry, where there is a history of frequent falling blocks with different shapes and dimensions.

2 The Curviã Rock Quarry

The rock cut-slopes are in the Curviã quarry (Joane, V. N. Famalicão, NW Portugal; see Fig. 1). The geological unit that outcrops in the study area is a monzogranite, medium-grained, with a porphyric tendency, two-mica, essentially biotitic (Montenegro de Andrade et al., 1986). The rock mass is predominantly fresh to slightly weathered (W_{1-2}) to moderately weathered (W_3) and highly fractured.

In the first stage, this work involved a geological, geomorphological, and hydrological description of the area and, later, geotechnical and geomechanical in situ surveys and investigations. Next, the scanline surveys were used to study the free rock mass surfaces (ISRM, 2007). Then, the geostructural data were analysed with Dips (Rocscience software). Also, the weathering grade and rock strength were evaluated considering the ISRM (2007) recommendations. Finally, all the information was collected in a geodatabase,

A. Malheiro et al. (eds.), *Advances in Natural Hazards and Volcanic Risks: Shaping a Sustainable Future*, Advances in Science, Technology & Innovation, https://doi.org/10.1007/978-3-031-25042-2_29

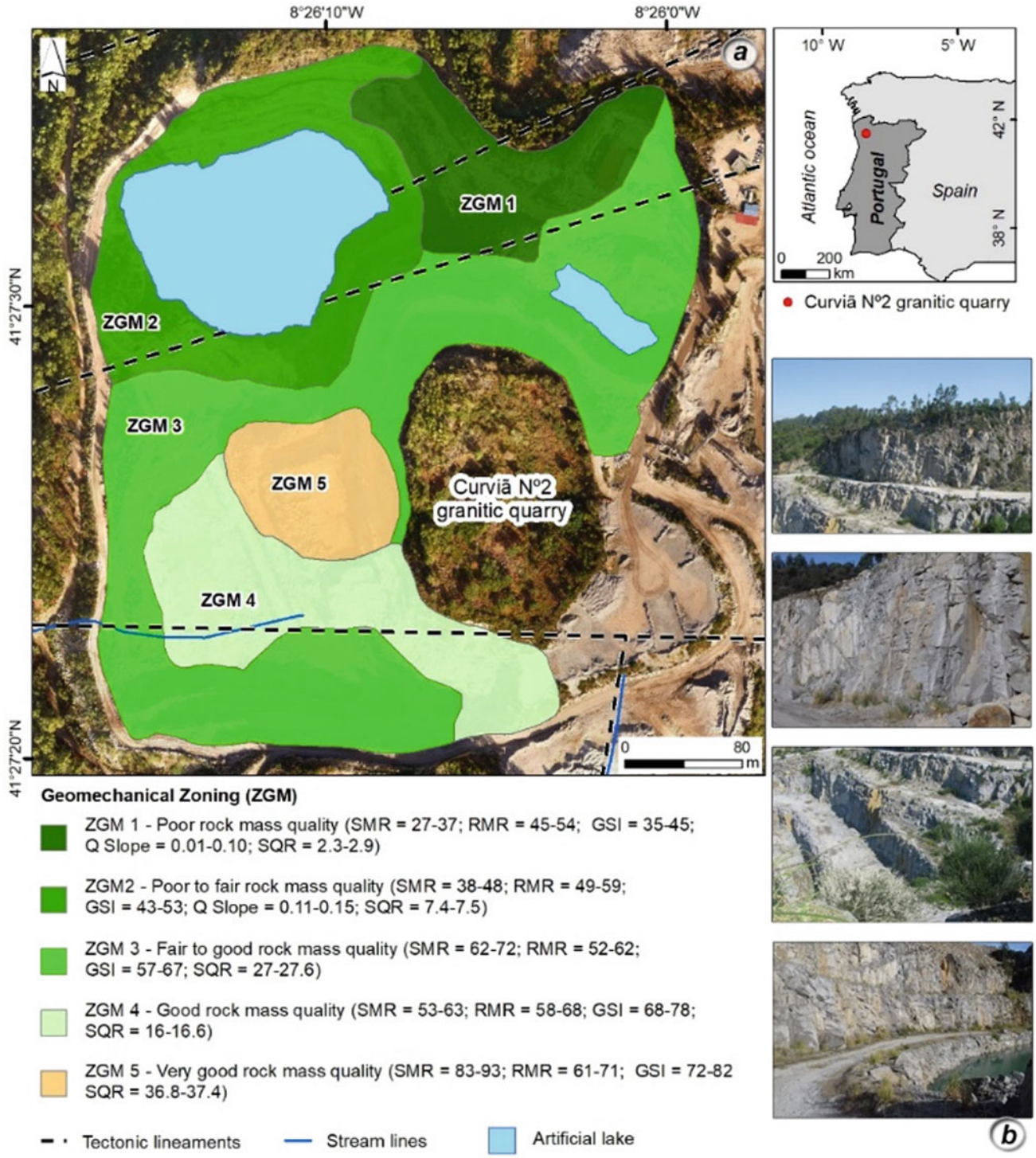

Fig. 1 Curviã quarry. **a** Geomechanical zoning; **b** several aspects of the benches and cut-slopes

and geotechnical and geomechanical zoning mapping was performed.

To assess the rock mass quality was used rock mass classifications and geotechnical indexes, such as: Rock Mass Rating (Bieniawski, 1989); Geological Strength Index (Hoek et al., 2013); Q-system (Barton et al., 1974; NGI, 2015); Slope Mass Rating (Romana, 1985); Slope Quality Rating (Fereidooni et al., 2015) and Q-Slope (Barton & Bar, 2015). Moreover, SMR, SQR, and Q-Slope, the Markland Test (Wyllie & Mah, 2004), and the Eurocode 7 (NP EN 1997-1, 2010) were applied for the stability analysis. The susceptibility and level of geotechnical risk were evaluated using the

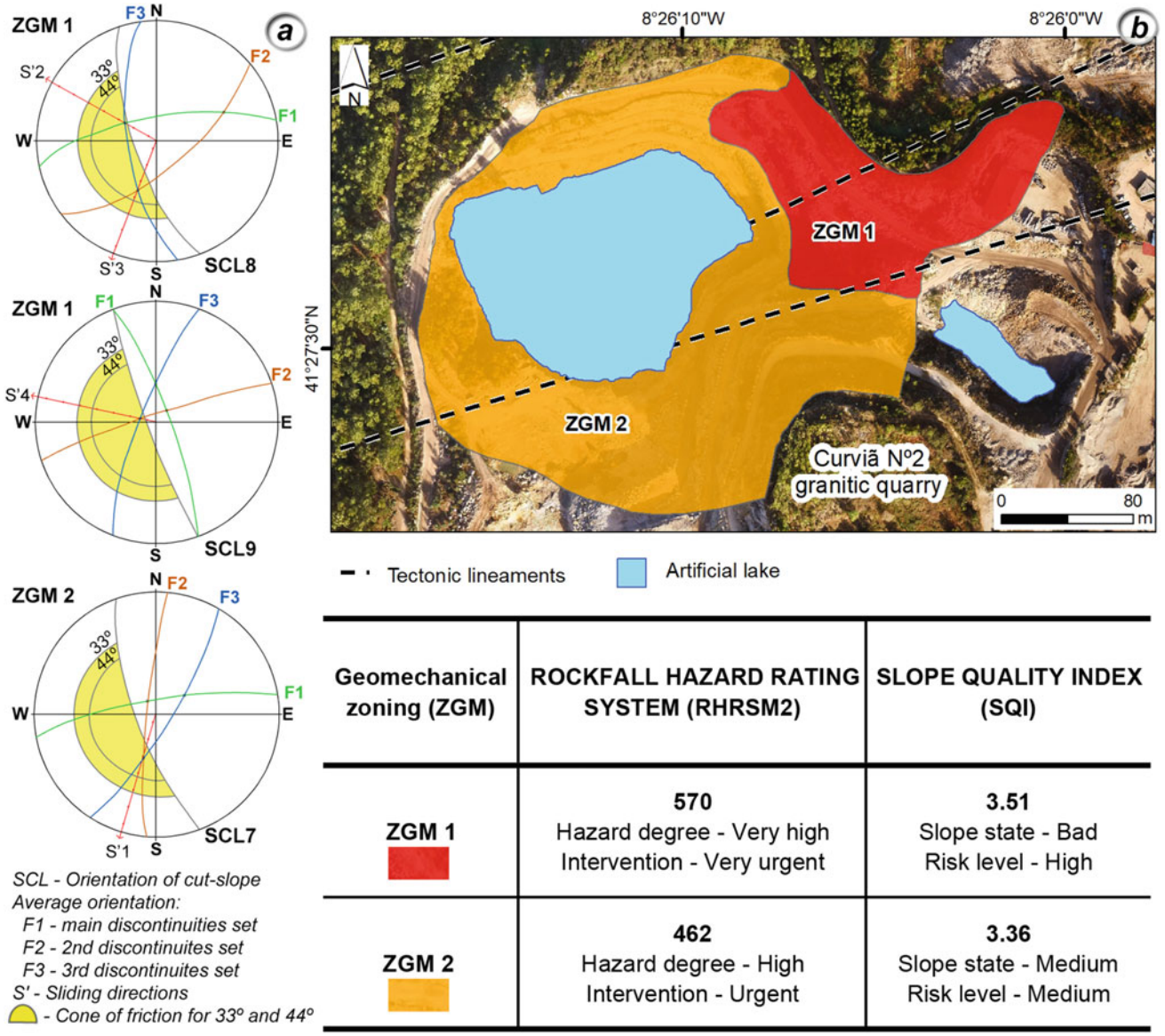

Geomechanical zoning (ZGM)	ROCKFALL HAZARD RATING SYSTEM (RHRSM2)	SLOPE QUALITY INDEX (SQI)
ZGM 1	**570** Hazard degree - Very high Intervention - Very urgent	**3.51** Slope state - Bad Risk level - High
ZGM 2	**462** Hazard degree - High Intervention - Urgent	**3.36** Slope state - Medium Risk level - Medium

Fig. 2 Stability analysis of the cut-slopes of zones ZGM1 and ZGM2. **a** Markland diagrams; **b** rockfall hazard and slope quality mapping

RHRSm2 system and an updated version of the Slope Quality Index (Pinheiro et al., 2015). Rockfall modelling and potential rock failures were developed with RocFall and Swedge software (Rocscience).

The integrated analysis of the various rock mass classifications shows a rock mass of fair to very good quality in the Southern part of the quarry (ZGM3, ZGM4, and ZGM5), while in the Northern part, the rock mass is of poor to fair quality (ZGM1 and ZGM2), (Fig. 1).

The three studied cut-slopes are in the geomechanical zones ZGM1 (2) and ZGM2 (1). Their orientation is NNW-SSE, with steep angles (75º–85º).

Considering the SMR values and the classes established by Romana (1985), zone ZGM1 is considered unstable, while zone ZGM2 is partially stable. To emphasise the proposals of stability and failure types of Romana (1985), the cut-slopes were characterised based on the Markland Test (Fig. 2a). In zone ZGM1, several potential failures may occur, namely wedge slides, with effective sliding directions towards SW and NW, and toppling failures. Moreover, in zone ZGM2 wedge failures may occur, with active sliding directions towards SW.

The analysis of the rockfall hazard (RHRSm2) and the cut-slopes quality (SQI) allowed us to distinguish the zones ZGM1 and ZGM2 (Fig. 2b). The slope state is less good in zone ZGM1, with a higher risk level and rockfall hazard. Therefore, in this zone, immediate intervention of the slopes is required.

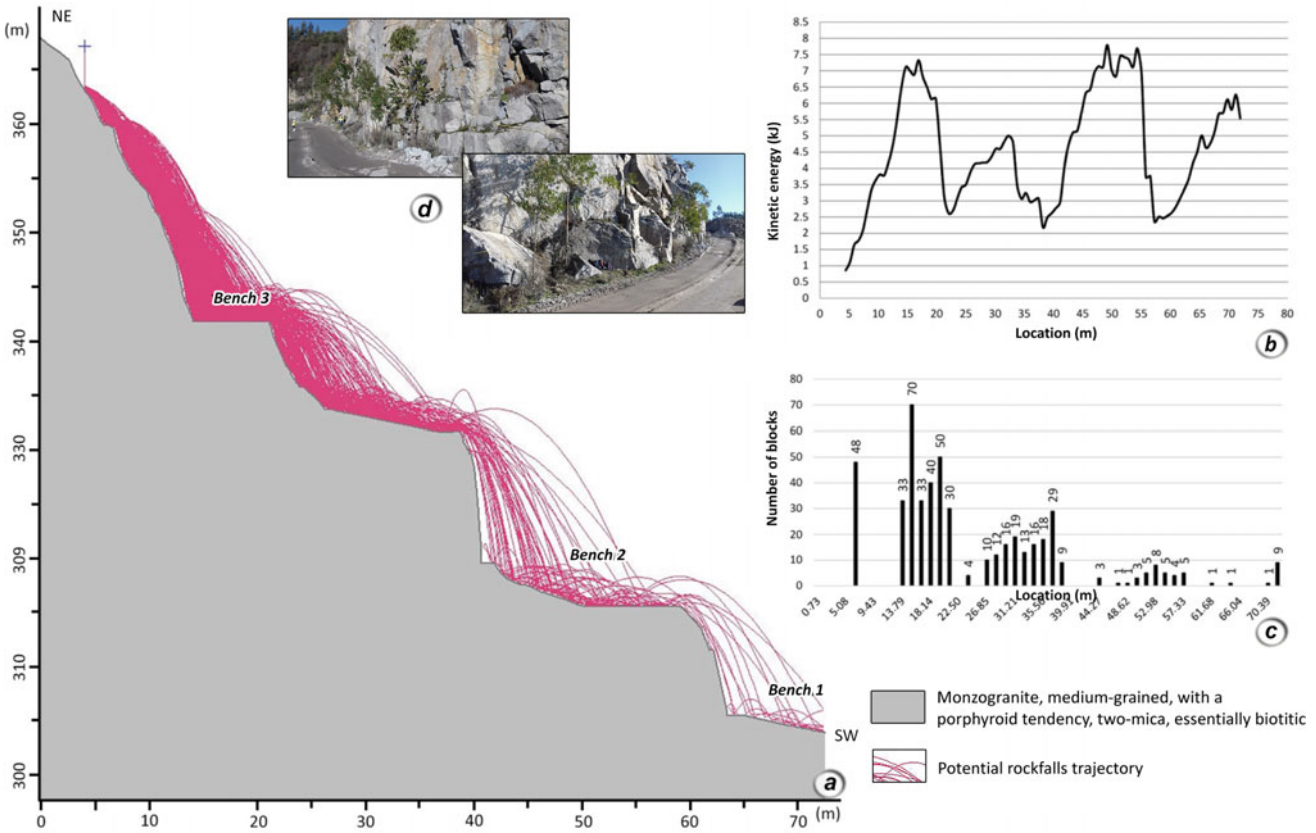

Fig. 3 Geotechnical modelling of rockfalls from profile 6; **a** Topographic profile and potential rockfalls trajectory; **b** relation between maximum total kinetic energy (kJ) and location (m); **c** relation between the number of blocks and location (m); **d** general aspects of bench 3

The geotechnical modelling of rockfall was analysed in zone ZGM1, applying the RocFall software. To illustrate this, profile 6 was selected (Fig. 3). Profile 6 has an extension of 73 m and a difference in elevation of 63 m (Fig. 3a). If the rockfall takes place in bench 3, the maximum kinetic energy generated is 7.79 kJ at 51 m (Fig. 3b), and the blocks are quite distant from each other, whereas 70 blocks are deposited at 15 m (Fig. 3c), and the mass of each block is approximately 40 kg.

3 Concluding Remarks

The hazard assessment of cut-slopes is a crucial element of quarry risk management. Since quarries get deeper over time and the cut-slopes angle becomes steeper, the regular check of benches and haul roads will permit the identification of small-scale rock failures that might reveal larger-scale ground instabilities. This assessment can be done with engineering geology surveys, hazard assessment maps and geotechnical modelling.

Acknowledgements Labcarga|ISEP re-equipment program (IPP-ISEP|PAD'2007/08), Centre GeoBioTec|UA (UID/GEO/04035/2020) and CGEO (UIDB/00073/2020) supported this study.

References

Barton, N., & Bar, N. (2015). Introducing the Q-slope method and its intended use within civil and mining engineering projects. In W. Schubert & A. Kluckner (Eds.), *Future development of rock mechanics, Proceedings of the ISRM regional symposium Eurock 2015 & 64th Geomechanics colloquium, Salzburg, Austria* (pp. 157–162).

Barton, N., Lien, R., & Lunde, J. (1974). Engineering classification of rock masses for the design of tunnel support. *Rock Mechanics, 6*(4), 189–239.

Bieniawski, Z. T. (1989). *Engineering rock mass classifications*. Wiley.

Fereidooni, D., Khanlari, G. R., & Heidari, M. (2015). Assessment of a modified rock mass classification system for rock slope stability analysis in the Q-system. *Earth Sciences Research Journal, 19*(2), 147–152.

Hoek, E., Carter, T. G., & Diederichs, M. S. (2013). Quantification of the geological strength index chart. In *Proceedings of the Geomechanics Symposium, 47th US Rock Mechanics, San Francisco, CA, ARMA13-672* (pp. 1–8).

ISRM—International Society for Rock Mechanics (2007). The complete ISRM suggested methods for characterisation, testing and monitoring: 1974–2006. In R. Ulusay & J.A. Hudson (Eds.), *Suggested methods prepared by the commission on testing methods, ISRM*. Ankara.

Montenegro de Andrade, M., Noronha, F., & Rocha, A. (1986). *Carta Geológica de Portugal, folha 9B−Guimarães, escala 1:50000*. Serviços Geológicos de Portugal.

NGI. (2015). *Using the Q-system: Rock mass classification and support design*. NGI handbook.

Pinheiro, M., Sanches, S., Miranda, T., Neves, A., Tinoco, J., Ferreira, A., & Correia, A. G. (2015). A new empirical system for rock slope stability analysis in exploitation stage. *International Journal of Rock Mechanics and Mining Sciences, 76*, 182–191.

Romana, M. (1985). New adjustment rating for application of the Bieniawski classification to slopes. In *Proceedings international symposium rock mechanics mining and civil works* (pp. 59–63). ISRM.

Trigo, J. F., Pacheco, C., Fernandes, J., Ferraz, P., Sousa, J., Machado, R., Duarte, S., Mendes, A., Freitas, L., Teixeira, J., Ramos, L., Afonso, M. J., & Chaminé, H. I. (2020). Geotechnical hazards in rocky slopes (Northern Portugal): focused on methodology. In F. Fernandes, A. Malheiro, H.I. Chaminé (Eds.), *Advances in natural hazards and hydrological risks: Meeting the challenge, Proceedings of the 2nd international workshop on natural hazards (NATHAZ'19), Pico Island—Azores 2019* (pp. 69–73). ASTI Springer, Cham.

Wyllie, D. C., & Mah, C. W. (2004). *Rock slope engineering: Civil and mining* (4th ed.). Spon Press.

Monitoring System Implemented to Evaluate the Kinematics of an Instability Zone at Flores Island

F. Marques, L. Moniz, P. Amaral, A. Malheiro, and A. Santos

Abstract

Taking into account its geology, morphology and hydrology, the island of Flores (Azores archipelago) is susceptible to the occurrence of slow slope movements. These situations of instability have been more studied in the last 20 years. Following the studies, it has been found that these instability phenomena are increased when the weather conditions are more adverse, particularly regarding the duration and intensity of rainfall. The study presented in this document concerns two localities on Flores Island: Lajedo and Fajãzinha. The monitoring systems (vibrating wire and Casagrande piezometers, inclinometers, rain gauge station and total robotic station) were installed in two mass movements, and their results are presented. This work aims to determine alert and alarm thresholds based on the amount of precipitation and the water level variation in possible fault surfaces.

Keywords

Monitoring • Landslides • Risk management • Flores Island

1 Introduction

Despite the geodynamic setting of the Azores archipelago (Miranda et al., 2015; Searle, 1980), precipitation is the main trigger of instabilities occurring in the Azores islands (Amaral et al., 2009; Marques et al., 2015). The excess water causes a decrease in shear forces due to the reduction of apparent cohesion and/or the increment of the positive water pressure along the rupture surface (Malet, 2005, Amaral, 2010). To support efficient land-use planning, studies have been developed to determine the relationships between water level and displacement velocities that occur in mass movements, particularly in translational and rotational movements (Malet, 2005).

This study includes two situations of geomorphological instability on the island of Flores (Lajedo and Fajãzinha), where the kinematic behaviour is slow to very slow, presenting a deep fault surface. Furthermore, the mass movements where the monitoring equipment was installed put the building, support services and streets of the parishes mentioned above at risk.

2 Case Study

The sites where the monitoring equipment was installed are located in the parishes of Lajedo and Fajãzinha, on the island of Flores. This island belongs to the western group of the Azores archipelago (Fig. 1).

2.1 Test Site #1 (Lajedo)

The last year 2010 (in December), during heavy rainfall, several landslides occurred, affecting many infrastructures in the parish of Lajedo, southwest of Flores Island. In Fig. 2, the three main instabilities observed in that parish are identified, as well as the location of the areas where monitoring equipment was implemented.

This work analyzed the most conditioning geomorphological instability, site #L2 (Fig. 2). This instability consists of a complex movement of the deep earthflow type. This site presents an average gradient of 18º. Sometimes variations in the slope can be observed that correspond to small scarps of the unstabilized terrain.

F. Marques (✉) · L. Moniz · P. Amaral · A. Malheiro
Regional Laboratory of Civil Engineering, LREC, Ponta Delgada, Azores, Portugal
e-mail: Filipe.MP.Marques@azores.gov.pt

A. Santos
Regional Department for the Environment, Ponta Delgada, Azores, Portugal

A. Malheiro et al. (eds.), *Advances in Natural Hazards and Volcanic Risks: Shaping a Sustainable Future*, Advances in Science, Technology & Innovation, https://doi.org/10.1007/978-3-031-25042-2_30

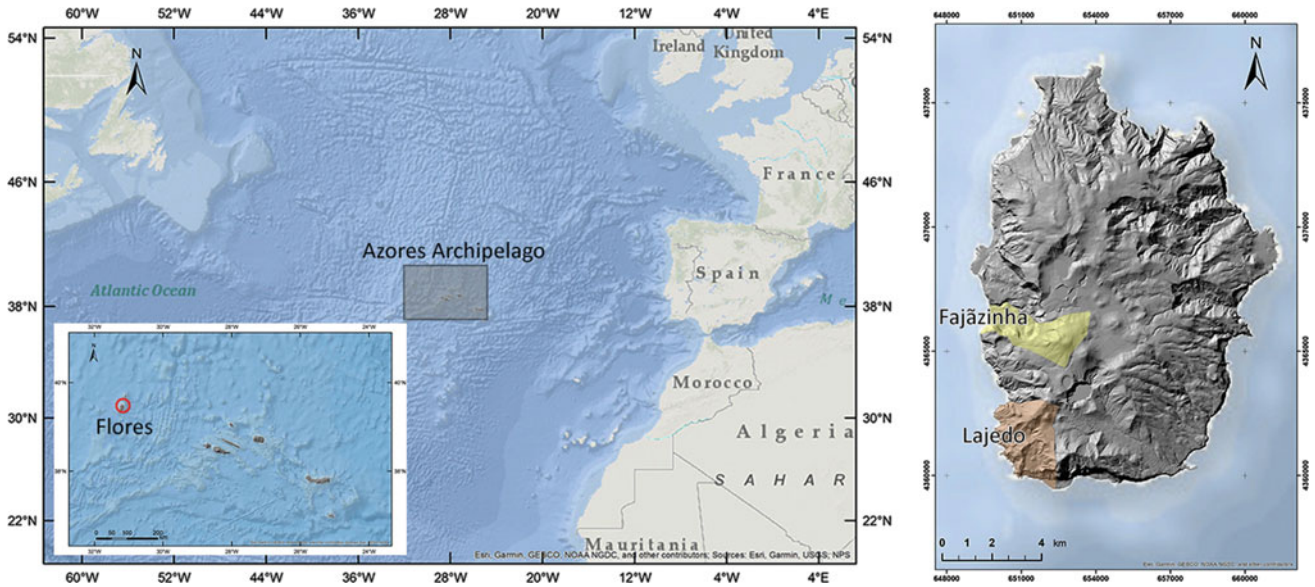

Fig. 1 Location of the parishes of Lajedo and Fajazinha sites

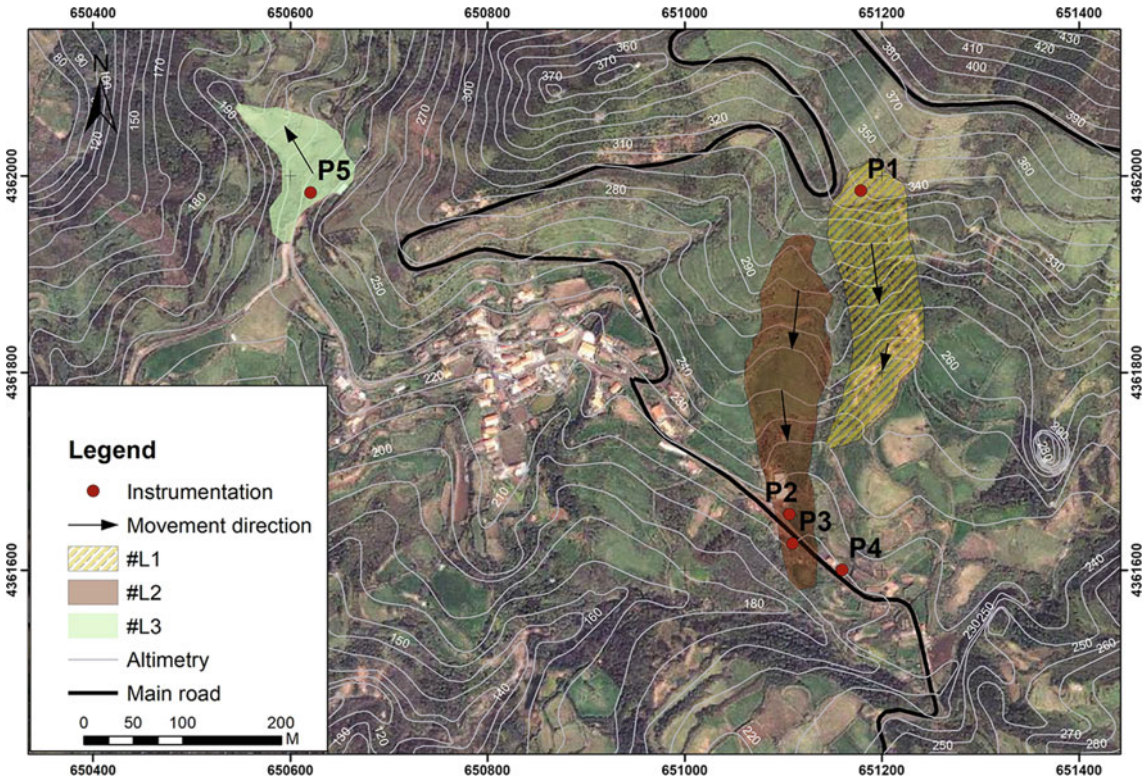

Fig. 2 Mapping of the three landslides and location of installed equipment

2.2 Test Site #2 (Fajãzinha)

Fajãzinha parish develops over a vast colluvial platform whose slope varies between seven and twenty degrees. Slopes delimit this platform with heights occasionally greater than two hundred meters and sub-vertical slopes. In the field survey, several indications of mass movements in the area were identified, such as concave and convex shapes, secondary scars, etc. Furthermore, the analysis of kinematic activity for the hydrological year 2012–2013 allowed the

Fig. 3 Pathologies verified: **a** in housing; **b** streets

identification of recent geomorphological activity visible on roads and houses (for example, cracks in the ground—Fig. 3b, diagonal and longitudinal cracks in the walls of houses, Fig. 3a). This instability phenomenon consists of a complex mass movement with a deep fault surface. In the coastal zone, it is possible to observe the foot of the geomorphological instability, the material's geological nature and several springs' existence.

3 Implementation of Monitoring Equipment and Presentation of Results

3.1 Lajedo

The fieldwork started with installing different hydrological and geotechnical monitoring equipment in the three locations identified in Fig. 2. As mentioned above, this work will only refer to the monitoring network and the respective results of location # L2. At this location, three inclinometers, two Casagrande piezometers, two vibrating wire piezometers and a rainfall station were installed.

In Fig. 4a, it is possible to observe the water level variation measured by a vibrating wire piezometer installed in #L2 and the accumulated daily precipitation. For example, between 18-11-2016 and 31-03-2019, it is possible to see that the water level was at a reduced depth, ranging between 1.0 and 1.6 m.

Figure 4b presents the most significant measurements performed on the P2i inclinometer during the observation above period. The analysis of the results allowed us to identify two active failure zones, one at a depth of about 4.5 m (first active zone—Fig. 4b) and another at about 10.5 m (second active zone—Fig. 4b). These failure zones have different displacement rates, the maximum recorded value being 13.8 mm, which corresponds to an average speed of 5.7 mm/year. Based on the classification by Cruden & Varnes (1996), it is an extremely slow movement.

In addition, it was also possible to verify that the instability in location #L2 is reactivated in the rainy seasons

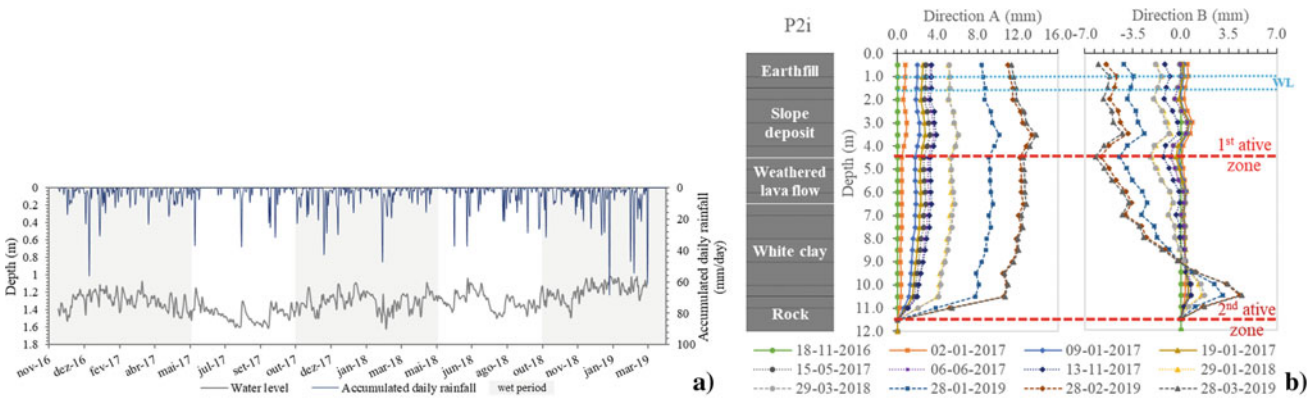

Fig. 4 **a** fluctuation of water level on P2p1 and daily rainfall; **b** inclinometer readings on P2i (18-11-2016 to 31-03-2019)

(October to May), slowing down its movement in the dry seasons (June to September).

3.2 Fajãzinha

In the case of Fajãzinha, the monitoring system implemented makes it possible to assess the surface deformation of the terrain using a Leica TM50 total station of 0.5" (0.15 mgon). The use of this type of equipment implies the use of three components (Table 1) (Afeni & Cawood, 2013).

Figure 5 shows the spatial distribution of the 34 monitoring points installed in November 2017.

The data presented in this study relate to the period between 01-01-2018 and 30-06-2020 and comprise 47 data acquisition campaigns (≈2/month) whose objective is to evaluate the development of displacements on the topographic surface.

Figure 5a represents the variation of the measured surface displacements for all control marks. In order to understand the movements in planimetric, average displacement vectors obtained in the campaigns of 30-06-2020 are projected in Fig. 5b to give a global picture of deformation rates. It was found that the reference marks (installed outside the unstable zone) did not register significant variations, with the observed fluctuations being due to seasonal and daily factors. On the other hand, the remaining marks showed a record within the tolerance range, with small variations until December 2018. However, after this period and until March 2019, a significant increase in displacement variations occurred, suggesting the monitored system's reactivation due to the amount of precipitation (Amaral et al., 2020). As a result, the slope distance rate increases rapidly by almost 40 mm in some points, while others are located outside the landslide zone maintained without displacement.

Figure 5a shows the daily rainfall registered by the meteorological station of Terreiros, which is located about 1 km from Fajãzinha. From these data, it can be seen that December 2018 and January and February 2019 showed high precipitation values (with an accumulated of 620 mm, in which only on three different days precipitation values between 50 and 75 mm were recorded) compared to the hydrological year 2017/2018, in which cumulative annual precipitation of around 1150 mm was recorded. Thus, a reactivation of the instability under study affected Fajãzinha in these three months.

In the monitoring period in question, values in the range of -37 ± 12 mm for E, 12 ± 5 mm for N, and -16 ± 11 mm for Z were recorded concerning the mean displacement. The planimetric displacement orientation is compatible with the terrain movement's main direction towards the west. The observed records for displacement allow defining an evolutionary process since January 2018 in which the average annual planimetric velocity is 15 ± 5 mm/year.

4 Concluding Remarks

Due to the type and dimension of instability events, implementing engineering techniques to reduce the risk is not feasible, given the high cost that these techniques usually present and the high environmental impact they often require. Thus, it is essential to use monitoring methods to monitor and evaluate the state of instability situations.

The Fajãzinha landslide affects a significant part of the urban centre of this parish. Lajedo parish is affected by some landslides. However, the #L2 study case, which presented more activity until now, crosses an important municipal road that connects the parish centre to some dispersal houses and agricultural services.

The results obtained from the monitoring system implemented in the parish of Lajedo allowed the conclusion that there is an almost immediate response to intense precipitation episodes. In addition, it was also observed the increase in displacements with the periods of higher precipitation. So, it is observed that the landslide process shows dynamic and intermittent behaviour regarding its state of activity.

It should be noted that the results presented correspond to the initial phase of the monitoring process in the parishes of Lajedo and Fajãzinha, having already been possible to obtain some conclusions. It is intended to continue to perform these measurements over time better to understand the kinematic behaviour in the face of precipitation. However, the current

Table 1 Components of the monitoring system

Components	Description	Monitoring network
1	A reference network materialized with prisms fixed in a stable position, visible from the instrument	4 reference points (Ci/PRi)
2	One or more base stations established on the stable ground at locations from which the landscape surface is visible	2 base stations (PEi)
3	A group of control prisms at the unstable zone	30 control points (Ci)

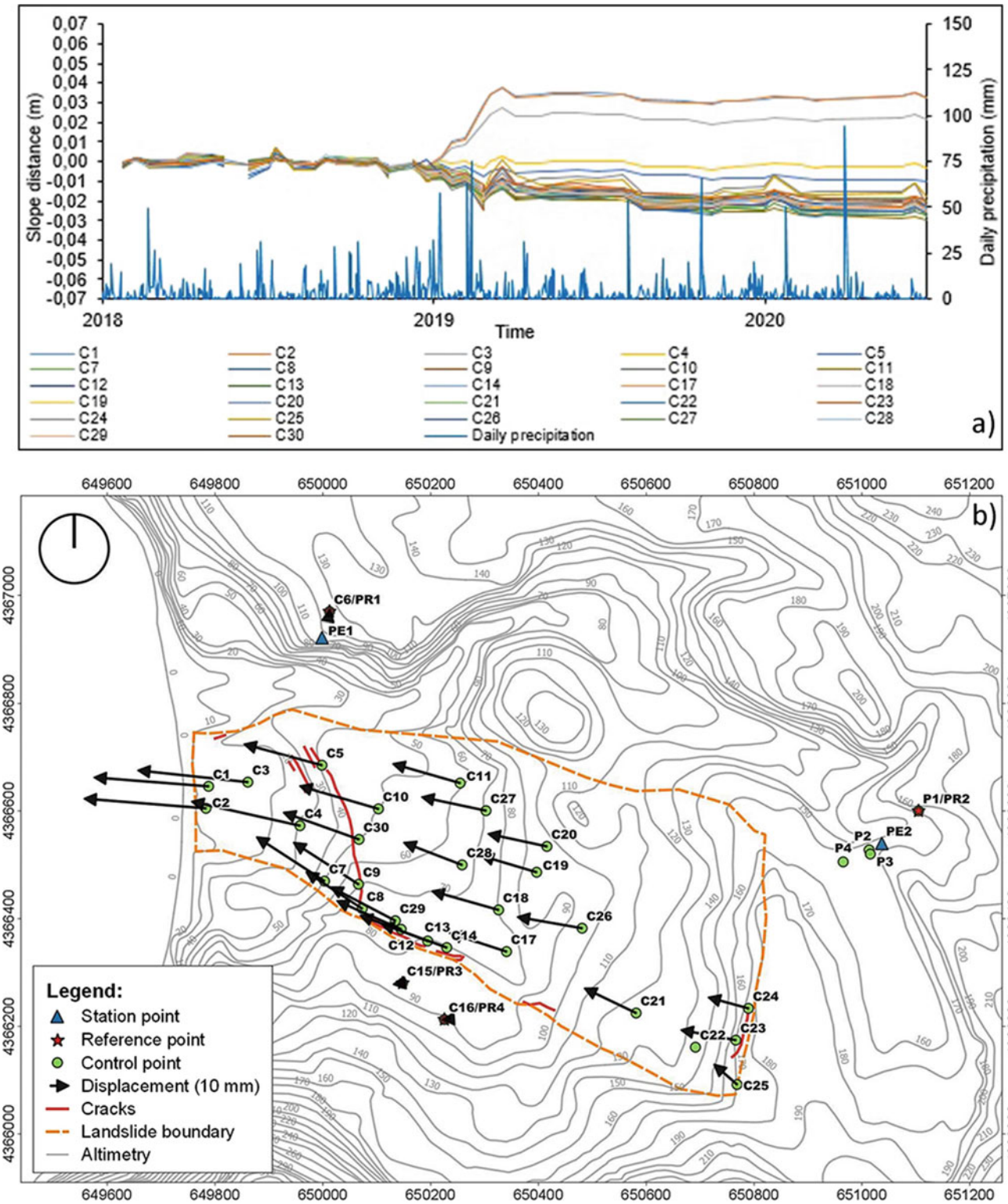

Fig. 5 **a** Variation on slope distance for all targets (base station PE1) with daily precipitation; **b** monitoring network with the kinematics movement

monitoring programme must complement other real-time and high-frequency time acquisition devices for both cases. In both landslides, reactivations occur after a peak of high-intensity rain, usually when it exceeds 50 mm/day. However, these peaks are preceded by periods of low intensity and continuous precipitation over time.

In future works, statistical analysis as cross-correlation techniques of displacements and rainfall, with more data, will be developed to establish correlations in order to identify and quantify the relationship between a rainfall peak and slope movement peak, providing early warning for the occurrence of future events represented by typical values of displacement rates.

References

Afeni, T. B., & Cawood, F. T. (2013). Slope monitoring using total station: What are the challenges and how should these be mitigated? *South African Journal of Geomatics, 2*, 41–53.

Amaral, P. (2010). Caracterização geotécnica e hidrológica de depósitos vulcânicos: Modelação a estabilidade de taludes no concelho da Povoação (Ilha de S. Miguel, Açores). Universidade dos Açores, Ponta Delgada (Ph.D. Thesis).

Amaral, P., Malheiro, A., Marques, F., Moniz, L., Furtado, S., & Loura, N. (2020). The use of total station for monitoring mass movements: application to Fajãzinha landslide at Flores Island (Azores Archipelago). In F. Fernandes, A. Malheiro, H.I. Chaminé (Eds.), *Advances in natural hazards and hydrological risks: Meeting the challenge, Proceedings of the 2nd international workshop on natural hazards (NATHAZ'19), Pico Island—Azores 2019* (pp. 59–62). ASTI Springer Series, Cham.

Amaral, P., Marques, R., Zêzere, J.L., Queiroz, G., & Marques, F. (2009). Distributed transient modelling of rainfall triggered shallow landslides for susceptibility assessment in Ribeira Quente valley (S. Miguel, Azores). In *Landslide Processes, from geomorphological mapping to dynamic modelling, Strasbourg, France 6–7 February 2009* (pp. 29–94). Strasbourg, CERG.

Cruden, D. M., & Varnes, D. J. (1996). Landslide types and processes. Transportation Research Board, U.S. *National Academy of Sciences, Special Report, 247*, 36–75.

Malet, J.-P., van Asch, T. H. W. J., van Beek, R., & Maquaire, O. (2005). Forecasting the behaviour of complex landslides with a spatially distributed hydrological model. *Natural Hazards and Earth System Sciences, 5*, 71–85.

Marques, R., Amaral, P., Araújo, I., Gaspar, J. L., & Zêzere, J. L. (2015). Landslides in S. Miguel Island (Azores): Susceptibility analysis and validation of rupture zones using a bivariate GIS-based statistical approach. In J.L. Gaspar, J.E. Guest, A.M. Duncan, F.J.A. Barriga, & D.K. Chester (Eds.), *Volcanic geology of São Miguel island (Azores Archipelago)* (vol. 44, pp. 167–184). Geological Society, London.

Miranda, J. M., Luis, J. F., Lourenço, N., & Fernandes, R. M. S. (2015). The structure of the Azores Triple Junction: implications for São Miguel Island. In J.L. Gaspar, J.E. Guest, A.M. Duncan, F.J.A., & D.K. Chester (Eds.), *Volcanic geology of São Miguel island (Azores Archipelago)* (vol. 44, pp. 5–13). Geological Society, London.

Searle, R. (1980). Tectonic pattern of the Azores spreading centre and triple junction. *Earth and Planetary Science Letters, 51*, 415–434.

Geotechnics, Georesources and Natural Hazards: Impacts in Marine Technology and Oceanic Engineering

Ana Pires and Helder I. Chaminé

Abstract

This essay addresses the importance of geotechnics and marine georesources in developing technologies. The study proposes a coastal and marine geoengineering approach that focuses on five domains (5G's): georesources, geology, geotechnics, geomechanics and geotechnologies. These domains are considered in several engineering projects related to coastal, hydraulic, marine, and maritime applications. The reality of a world in rapid, continuous evolution has put into perspective a multidisciplinary approach combining different practices and coastal strategies. That is the main driving force that should be considered when dealing with geoengineering projects in general. Moreover, geological resources and the potential exploitation of mineral and rock raw materials boost innovative techniques and upscaling geo-robotic systems. Finally, the essay unravels new trends in challenging and extreme environments and natural hazards, highlighting emerging fields such as deep-sea mining, geo-exploration, offshore, coastal, harbour and marine geotechnics.

Keywords

Multidisciplinary • Geotechnologies • Geoengineering • Marine technology

1 Introduction and Background

"We know that when we protect our oceans, we are protecting our future" (Clinton, 2011). The quote refers to challenging questions regarding anthropic actions and ecosystem balance. These thoughts and reflections at that time underline the current "United Nations Sustainable Development Goals",[1] in particular: "Goal 9—Industry, Innovation, and Infrastructure"; "Goal 13—Climate Action"; "Goal 14—Life Bellow Water"; "Goal 15—Life on Land"; and, also to "Goal 4—Quality education". Trenberth and Stepaniak (2004) raised a central question regarding the ocean covers nearly 71% of the Earth's surface: "why does the current society not have this ability?".

The coastal adaptations have gained interest in the last years. As such, they have long been essential foci of human settlement (Bailey, 2004; Bicho et al., 2011). The artistic view could also highlight that adaptation is a coastal evolution tool (e.g., Amorim et al., 2019; McInnes, 2008, and references therein). However, the impetuousness of humankind and climate change create severe pressures on coastal regions (Dupray & Simm, 2008). Therefore, it is essential to relate the concept with the development of geotechnologies. That approach highlights the necessity to create bridges between Research, Industry and Society (Fig. 1) to safeguard a sustainable design with nature and geohazards (González de Vallejo, 2012; McHarg, 1992).

A. Pires (✉)
Centre for Robotics and Autonomous Systems (CRAS|INESC TEC), Porto, Portugal
e-mail: ana.c.pires@inesctec.pt

Laboratory of Autonomous Systems, School of Engineering (ISEP), Polytechnic of Porto, Porto, Portugal

A. Pires · H. I. Chaminé
Laboratory of Cartography and Applied Geology (LABCARGA), Department of Geotechnical Engineering, School of Engineering (ISEP), Polytechnic of Porto, Porto, Portugal

H. I. Chaminé
Centre GeoBioTec|UA, University of Aveiro, Aveiro, Portugal

[1] "https://www.un.org/sustainabledevelopment/sustainable-development-goals/".

A. Malheiro et al. (eds.), *Advances in Natural Hazards and Volcanic Risks: Shaping a Sustainable Future*, Advances in Science, Technology & Innovation, https://doi.org/10.1007/978-3-031-25042-2_31

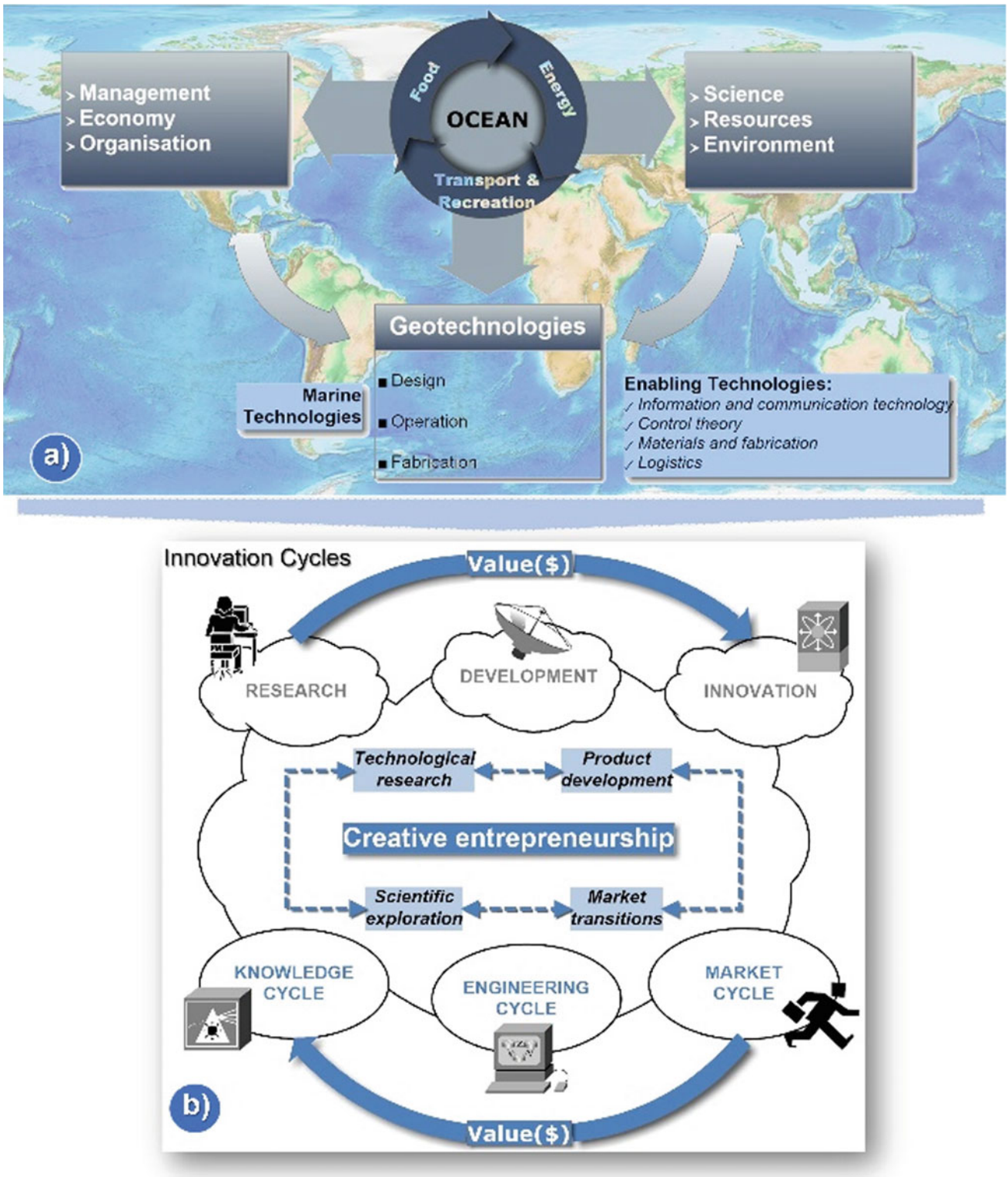

Fig. 1 **a** Knowledge-based maritime cluster and marine activities; **b** conceptual flowchart based on creative entrepreneurship model (adapted from Berkhout, 2000; Berkhout & van der Duin, 2007; Pires, 2015)

2 The Coastal Strategy: A Geoengineering Approach

The importance of studying different maritime environments is featured in this research. This work was supported by previous investigations involving several scientific fields, networks and interdisciplinary integrative fields (details in Chaminé et al., 2016; Pérez-Alberti et al., 2019; Pires et al., 2014, 2016). Figure 2 identifies the 5Gs that are the driving force of this approach.

The contribution of cross-cutting fields and the new trends and challenges displayed in Fig. 2, together with the 5Gs, contribute to balanced coastal management and territory planning. That joint work foresees three dimensions: land, coast, and ocean. A coastal geoengineering concept is proposed, considering a holistic perspective. This strategy is the "missing" piece of the puzzle that "forces" somehow all the fields to cooperate and interconnect with each other. The so-called geoengineering field is an emerging, unifying and eclectic domain (CERF, 1994; Manoliu & Radulescu, 2008; McCabe et al., 2012; Chaminé et al., 2013).

3 New Trends and Challenges: Are We Really Getting There?

As stated before, the challenges ahead of us are immense. Researchers must push science, engineering, and technology limits daily, developing innovative solutions and facing extreme environments. The emerging fields and new trends considered in current days are: Oceanic and Sea Engineering; Marine and Underwater Technologies; Deep-Sea Mining; Offshore Geotechnics; Harbour, Marine and Coastal Geotechnics. These are emerging fields involving real projects that support the importance of the coastal geoengineering approach presented herein. The holistic perspective, integrating different geotechnologies and methodologies, and combining several fields, stresses this essay's focus. Are we getting there? Are we getting there? We believe that the answer is visible, for example, in two European projects like "¡VAMOS!"—"Viable and Alternative Mine Operating System", or UNEXMIN—"An Autonomous Underwater Explorer for Flooded Mines". These projects involve multidisciplinary teams and a geotechnological approach to exploring deep-sea mining and flooded mines (Bakker et al., 2017; Lopes et al., 2017). Offshore geotechnics or transportation geotechnics related to harbour, marine and coastal geotechnics is a unique field that is increasingly developing, showing a wide field of applications in engineering the sea and coastal areas (e.g. CIRIA, CUR & CETMEF, 2007; Chaney & Almagor, 2015; Pires et al., 2016). We have no doubts that we are getting there, facing new challenges in the future, and constantly evolving, exploring, and discovering. But always in a balanced design with nature, climate variability and societal pressures.

4 Concluding Remarks

The main remarks are: (i) the research proposes a holistic vision for projects related to oceanic engineering, including the coastal areas; (ii) shows the importance of transdisciplinary and multidisciplinary teams; (iii) the development of technologies should also integrate the "5Gs" as the driving force in the maritime engineering projects; (iv) the coastal geoengineering concept can help to support coastal management decisions and territory planning strategies. Finally, this essay proposes a particular approach for future projects related to geo-marine technologies in a balanced design with nature, climate, geohazards, and society.

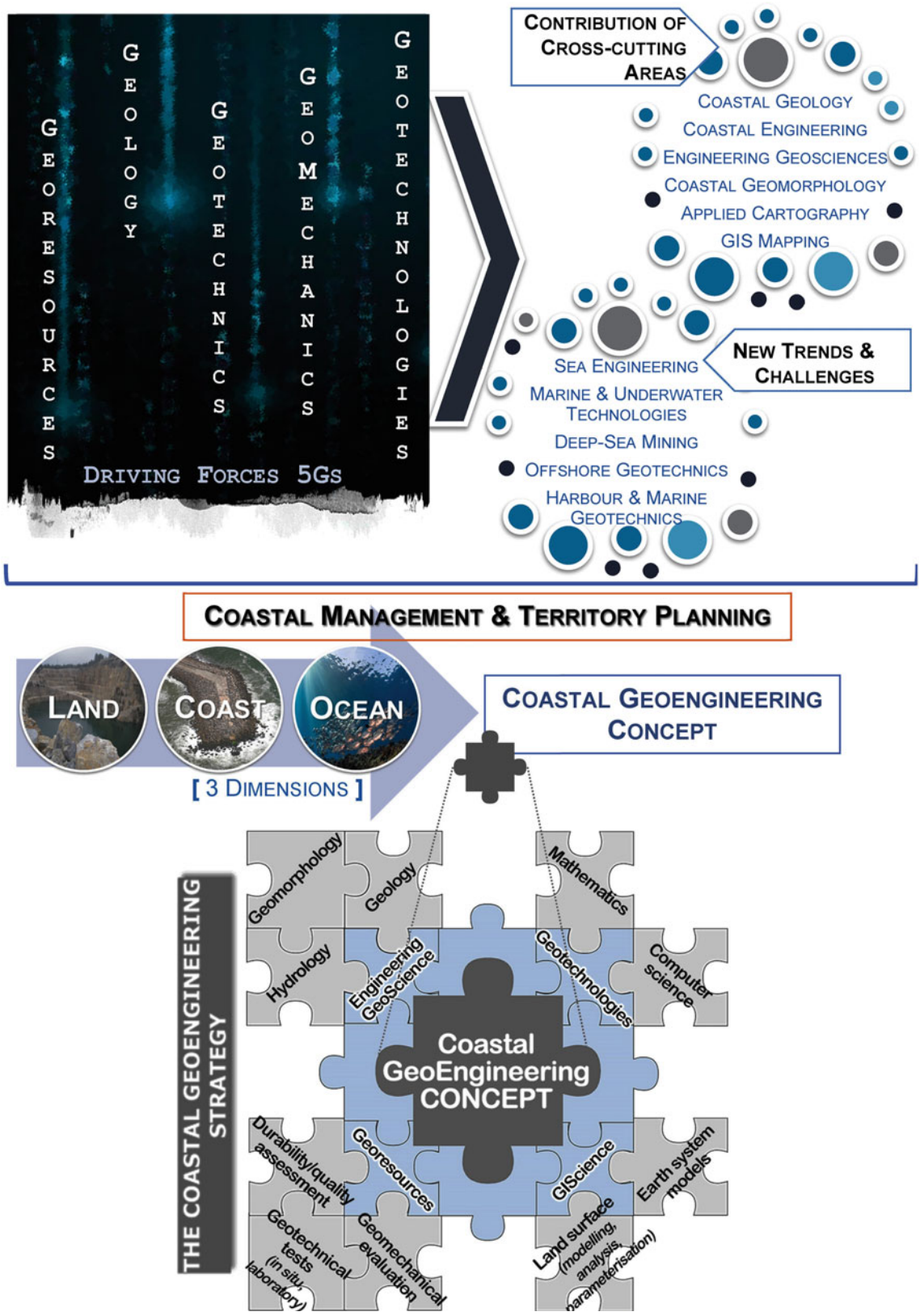

Fig. 2 The coastal geoengineering matrix categorises the Gs for research development (adapted from Pires, 2015)

Acknowledgements The work was supported by the Portuguese Foundation for Science and Technology, FCT (SFRH/BD/43175/2008, CEECIND/00835/2018) to AP and by project UIDB/50014/2020. HIC was supported by LABCARGA|ISEP re-equipment program (IPP-ISEP| PAD'2007/08) and Centre GeoBioTec|UA (UID/GEO/04035/2020). Our thanks for the topical discussions in last 17 years, particularly, with F. Rocha (Portugal), C. Bernardes (Portugal), A. Pérez-Alberti (Spain), T. Abreu (Portugal), A. Gomes (Portugal), J.S. Griffiths (UK), L. Gómez-Pujol (Spain), A. Trenhaile (Canada), L.S. Dupray (France), J. Simm (UK), L. González de Vallejo (Spain), F. Piqueiro (Portugal), H. Lopes (Portugal), F. Santiago Miranda (Portugal), E. Brògueira Dias (Portugal), A. Pinto (Portugal), A. Gómez-Pazo (Spain), J.C. Amorim (Portugal), and R. McInnes (UK).

References

Amorim, J. C., Pires, A., & Chaminé, H. I. (2019). Pictorial catalogue: art as a tool in coastal evolution. A brief history of Portuguese coastal art: Insights through science and technology. Viaggiatori Journal, Ebook Volume 1 (Monografie), Naples. http://www.viaggiatorijournal.com/cms/cms_files/20190107011256_zzno.pdf

Bailey, G. N. (2004). World prehistory from the margins: The role of coastlines in human evolution. *Journal of Interdisciplinary Studies of Historical and Archaeology, 1*(1), 39–50.

Bakker, E., Žibret, G., & Rainbird, J. (2017). The ¡VAMOS! sustainable underwater mining solution. *European Geologist Journal, 44*, 59–62.

Berkhout, A. J. (2000). *The dynamic role of knowledge in innovation: An integrated framework of cyclic networks for the assessment of technological change and sustainable growth*. Delft University Press.

Berkhout, A. J., & van der Duin, P. A. (2007). New ways of innovation: An application of the cyclic innovation model to the mobile telecom industry. *International Journal of Technology Management, 40*(4), 294–309.

Bicho, N. F., Haws, J. A., & Davis, L. (Eds.). (2011). *Trekking the shore: Changing coastlines and the antiquity of coastal settlement*. Series Interdisciplinary Contributions to Archaeology. Springer Science + Business Media.

CERF—Civil Engineering Research Foundation. (1994). Geoengineering: A vision for the 21st Century. CERF Report #94-5020, Civil Engineering Research Foundation, Washington DC, USA.

Chaminé, H. I., Afonso, M. J., Teixeira, J., Ramos, L., Fonseca, L., Pinheiro, R., & Galiza, A. C. (2013). Using engineering geosciences mapping and GIS-based tools for georesources management: Lessons learned from rock quarrying. *European Geologist Journal, 36*, 27–33.

Chaminé, H. I., Teixeira, J., Freitas, L., Pires, A., Silva, R. S., Pinho, T., Monteiro, R., Costa, A. L., Abreu, T., Trigo, J. F., Afonso, M. J., & Carvalho, J. M. (2016). From engineering geosciences mapping towards sustainable urban planning. *European Geologist Journal, 41*, 16–25.

Chaney, R. C., & Almagor, G. (2015). *Seafloor processes and geotechnology*. CRC Press, Taylor & Francis Group, Boca Raton.

CIRIA, CUR, CETMEF. (2007). *The rock manual: The use of rock in hydraulic engineering*, 2nd edn., C683, CIRIA—Centre for Civil Engineering Research, London, UK.

Clinton, W. J. (2011). Public papers of the presidents of the United States—William J. Clinton (2000–2001, Book III) 3. United States National Archives and Reco, USA.

Dupray, S., & Simm, J. (2008). Climate change materials and materials use. *The Edge, The Magazine of Coastnet, Coastal Industry* (pp. 14–15).

González de Vallejo, L. I. (2012). Design with geohazards: An integrated approach from engineering geological methods. *Soils and Rocks, International Journal of Geotechnical and Geoenvironmental Engineering, 35*(1), 1–28.

Lopes, L., Zajzon, N., Henley, S., Vörös, C., Martins, A., & Almeida, J. M. (2017). UNEXMIN: A new concept to sustainably obtain geological information from flooded mines. *European Geologist Journal, 44*, 54–57.

Manoliu, I., & Radulescu, N. (Eds.). (2008). *Education and training in geoengineering sciences: Soil mechanics and geotechnical engineering, engineering geology, rock mechanics*. Routledge.

McCabe, B., Pantazidou, M., & Phillips, D. (Eds.). (2012). *Shaking the foundations of geoengineering education*. CRC Press.

McHarg, I. L. (1992). *Design with nature*. 25th-anniversary edition, Wiley series in sustainable design, Wiley.

McInnes, R. (2008). *Art as a tool in support of the understanding of coastal change*. The Crown Estate.

Pérez-Alberti, A., Pires, A., & Chaminé, H. I. (2019). Shoreline and coastal terrain mapping. In C.W. Finkl & C. Makowski (Eds.), *Encyclopedia of coastal science* (2nd edn., pp. 1558–1571) Springer Nature.

Pires A (2015) Integrated coastal geoengineering approach for maritime environments. University Aveiro, Aveiro (Ph.D. Thesis) URI. http://hdl.handle.net/10773/15484

Pires, A., Chaminé, H. I., Piqueiro, F., Pérez-Alberti, A., & Rocha, F. (2016). Combining coastal geoscience mapping and photogrammetric surveying in maritime environments (Northwestern Iberian Peninsula): Focus on methodology. *Environmental Earth Sciences, 75*, 196.

Pires, A., Chaminé, H. I., Piqueiro, F., & Rocha, F. (2014). Coastal geoengineering techniques for the assessment of rock armour structures. *Marine Georesources and Geotechnology, 32*(2), 155–178.

Trenberth, K. E., & Stepaniak, D. P. (2004). The flow of energy through the earth's climate system. *Quarterly Journal of the Royal Meteorological Society, 130*(B-603), 2677–2701.

Analysis of Morphological Changes at Aveiro Coast (NW Portugal) Between 2012 and 2018

Tiago Abreu, Paulo A. Silva, Paulo Baptista, Cristina Bernardes, Sandra Fernández-Fernández, Caroline Ferreira, and Ángela Fontán-Bouzas

Abstract

Repetitive data collection is imperative regarding accurate coastal monitoring and appropriate coastal management strategies design. This study analyses high-resolution topo-bathymetric data gathered at Aveiro coast (NW Portugal) between 2012 and 2018. Using Geographic Information System techniques, the beach response and the sediment budget evolution are assessed for both emerged and submerged areas, evidencing places where coastal erosion and accretion occur. The methodology includes creating digital terrain models to compute the volume differences for this period and estimate the sediment budgets. The results are discussed in anthropic activities such as dredging and artificial nourishment operations in this littoral region. An overall erosion tendency is observed on the emerged beach, which seems to be compensated with beach nourishment interventions. However, the submerged beach also reveals a general erosive tendency at the inlet, and, among other factors, it seems to be affected by dredging operations and the southwest extension of the north pier.

Keywords

Artificial nourishments • Coastal zone management • Dredging operations • Morphodynamics

1 Introduction

Field data-based information on coastal dynamics is highly relevant for coastal managers in the present context of climate changes (e.g., Bonaldo et al., 2019). The impacts of sea-level rise and possible modifications in the frequency and intensity of coastal storms entail that coastal managers need to implement efficient solutions for increasing coastal resilience, namely, reprofiling the beach to restore the sediment balance and provide space for natural beach dynamics.

Data-based methods and repetitive data collection help document morphological changes in different spatiotemporal scales (Mendes et al., 2021). High-resolution surveys provide meaningful results, but, as it turns out, data is not always available in the needed quantity or quality. For example, the Aveiro coast (NW Portugal), exposed to highly energetic waves from the North Atlantic Ocean, has experienced an intense retreat in the last 50 years (Lira et al., 2016; Luijendijk et al., 2018).

The main aim of this study is to analyse the emerged and submerged beach morphological evolution of the coastal stretch in the south of Aveiro lagoon entrance between 2012 and 2018 through a set of high-resolution topo-bathymetric data using Geographic Information System (GIS) techniques. The methodology includes creating digital elevation models (DEM) to compute volume differences between surveys and estimate the sedimentary budget of this study area, evidencing places where coastal erosion and accretion occur. It is noted that, along this coastal stretch, jetties and groins were built to protect it from shoreline retreat and to ensure safe transport conditions in navigation channels at the harbour entrance. The beach response and the sediment

T. Abreu (✉)
Department of Civil Engineering, School of Engineering (ISEP), Polytechnic of Porto, Porto, Portugal
e-mail: taa@isep.ipp.pt

T. Abreu · P. A. Silva · P. Baptista · C. Bernardes · S. Fernández-Fernández · C. Ferreira · Á. Fontán-Bouzas
CESAM-Centre for Environment and Marine Studies, University of Aveiro, Aveiro, Portugal

P. A. Silva · C. Ferreira
Department of Physics, University of Aveiro, Aveiro, Portugal

P. Baptista · C. Bernardes
Department of Geosciences, University of Aveiro, Aveiro, Portugal

Á. Fontán-Bouzas
Centro de Investigación Mariña (CIM), University of Vigo, GEOMA, Vigo, Spain

A. Malheiro et al. (eds.), *Advances in Natural Hazards and Volcanic Risks: Shaping a Sustainable Future*, Advances in Science, Technology & Innovation, https://doi.org/10.1007/978-3-031-25042-2_32

budget evolution are assessed for this period. The results are analysed by considering the anthropic activities such as dredging, artificial nourishment operations and the extension of the north jetty of the harbour in 2013, whose effects overlap the beach's natural morphological variations.

2 Data and Methods

2.1 Topographic and Bathymetric Data

The physiography of Aveiro's lagoon inlet and adjacent areas results from the coastal system's response to successive interferences and, in particular, to the subsequent actions of the extension of the northern jetty, the last performed in 2013 to protect the entrance to the lagoon. Therefore, to analyse the recent evolution of Aveiro's lagoon inlet, morphological characterisation of this area is carried out for the period between 2012 and 2018, including the adjacent southern coastal stretch (Barra-Vagueira) of about 9 km in length (Fig. 1). The topographic and bathymetric data comes from different sources (Aveiro Harbor Authority and the University of Aveiro). In addition, it has been referenced to the ETRS89 / Portugal TM06 coordinate system and the mean sea level (MSL).

The topographic data of the emerged beach were acquired with the INSHORE system (Baptista et al., 2011) once a year between 2013 and 2018 (Oct-13, Feb-2014, Oct-2015, Jan-2016, Oct-2017 and Jan-18). Furthermore, regarding the submerged beach, bathymetric data were also obtained using the INSHORE system adapted for boat (laser replaced by single beam echosounder) in the years 2012 (Feb), 2013 (Mar), 2015 (Feb) and 2016 (Oct).

2.2 Digital Elevation Models

The acquired topographic and bathymetric survey data were used to create the DEMs with a geographic information system software (QGIS, version 3.10). The DEMs were obtained separately for the emerged and submerged beach areas, and, therefore, the morphological evolution involving the computation of sediment balances was assessed individually. For example, Fig. 1b illustrates the first bathymetric survey performed in February 2012 and Fig. 1c shows the last topographic survey performed in January 2018. Beach elevations range from −30 m to 9.5 m (MSL).

Sometimes the DEM obtained covers slightly different areas. The area must overlap to obtain topo-bathymetric differences between consecutive surveys. Therefore, the areas and volumes of accretion (sediment gain) and erosion (sediment loss) computed in this work report overlapping areas. This is particularly relevant because bathymetric data cover various areas, unlike the emerging beach zone. Consequently, the volumetric computations can only report to the inlet section (orange polygon in Fig. 1b) and not the southern coastal stretch. In addition, to compare the results over time, due to different time intervals between data

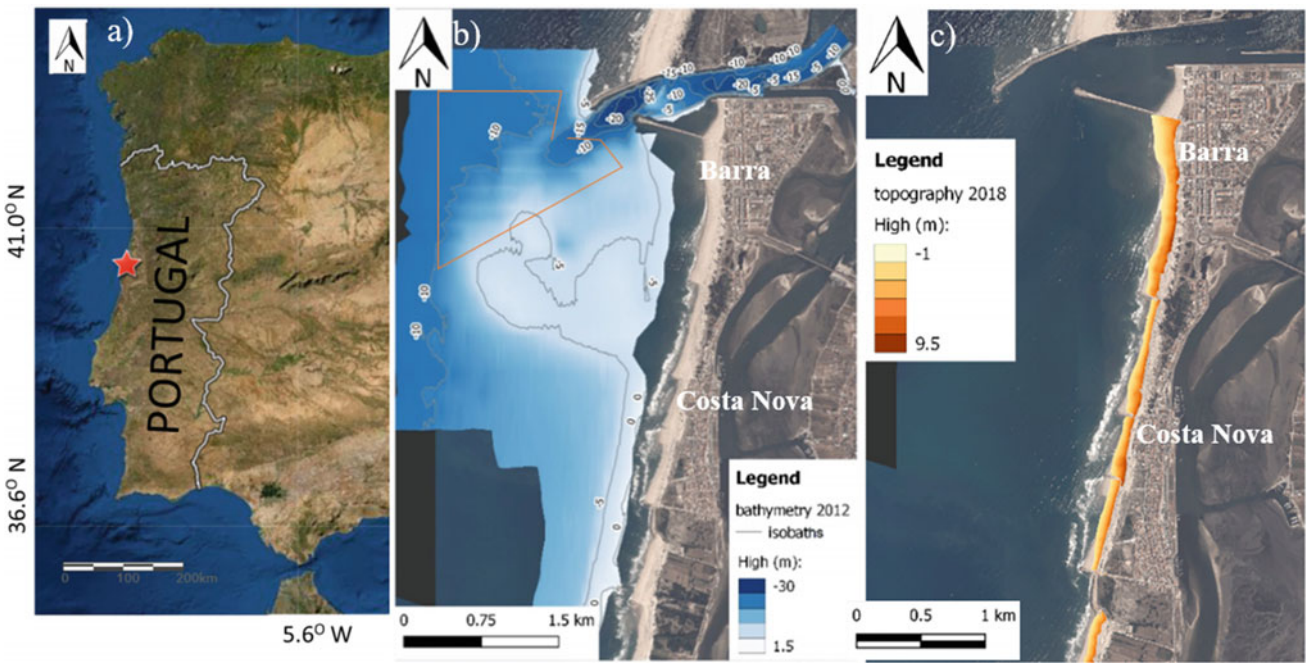

Fig. 1 **a** Study site location, **b** Bathymetry (February 2012) and **c** topography (January 2018) of the study area

acquisition, the outcomes were normalised by time in months, i.e., the sediment balances in m^3/m^2/month are obtained through Eq. (1):

$$\text{Sediment balance} = \frac{\text{Accretion volume} - \text{Erosion volume}}{(\text{Accretion area} + \text{Erosion area}) \times \text{Time}} \quad (1)$$

3 Results

3.1 Emerged Beach

The calculated erosion, accretion and sediment balance volumes, normalised by area and time, between topographic surveys between 2012 and 2018 are presented in Fig. 2. Seasonal variability is observed between winters and summers, leading to more significant erosion and accretion.

The sediment balance was negative in 2013–2014, 2015–2016 and 2017–2018, with values of about −0.21, −0.10 and −0.20 m^3/m^2/month, respectively. Notably, in the 2013–2014 and 2017–2018 periods, it was found that the rates of sediment accumulation were significantly lower than the erosion rates, giving rise to negative sediment balances, i.e., there was a greater volume of sediment erosion than accretion, which may indicate a retreat of the coastline in those periods as observed by Fernandéz-Fernandéz et al. (2019).

In contrast to the previous periods, in 2014–2015 and 2016–2017, the accretion rates were slightly more significant than the erosion rate, and the sediment balance was positive, with values of about 0.06 and 0.03 m^3/m^2/month.

3.2 Submerged Beach

Figure 3 presents the normalised volume values of erosion, accretion and sediment balance between bathymetric surveys carried out between 2012 and 2016.

The sediment balance at the inlet was negative in 2012–2014 and 2014–2015, with values of about −0.017 and −0.006 m^3/m^2/month, respectively. In 2015–2016, the accretion rate was slightly higher than the erosion rate, and the sediment balance was positive at about 0.003 m^3/m^2/month.

To analyse bathymetric data and interpret the sediment balances, it might be necessary to consider dredging interventions at the inlet and deposition of the dredged material.

4 Discussion

The most prolonged interval between topographic field surveys is 20 months, while the shortest is three months. The 2014–2015 and 2016–2017 periods show positive sediment balances (0.06 and 0.03 m^3/m^2/month, respectively). The positive balance means an average increase in the elevation of the emerged beach during these months. However, in the periods 2013–2014, 2015–2016 and 2017–2018, the sediment balances presented are negative, reflecting a reduction of sediments and, consequently, the elevation of the emerged beach. It is also noticed that these periods comprise only three or four winter months. Additionally, beach nourishment operations were carried out during some of the analysed periods, increasing its volume. These interventions took place in 2014 in Praia da Barra with a volume of 220,000 m^3 and a backshore feeding in 2016 in the Costa Nova–Mira sector (south of the study area) with a volume of 1,000,053 m^3 (Pinto et al., 2020).

Concerning the submerged beach, the dredged volumes need to be considered in the analysis and this information was made available by Aveiro Harbor Authority. The sediment balance shows two periods with markedly negative sediment balance: 2012/2014 and 2014/2015. The volumes dredged at the inlet in these periods were about 1,350,633 m^3 and 358,934 m^3. In 2015/2016, when a positive sediment balance was seen, the dredging volume was

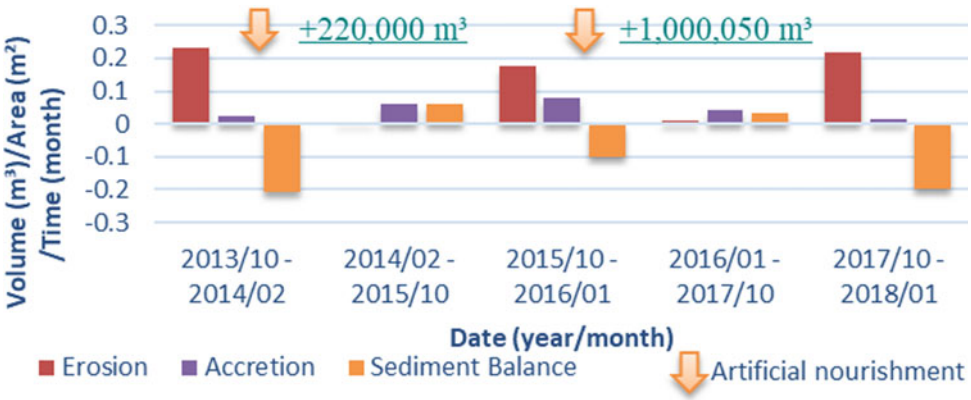

Fig. 2 Normalised sediment balance (accretion-erosion) between Aveiro's southern jetty and Vagueira for the subaerial beach

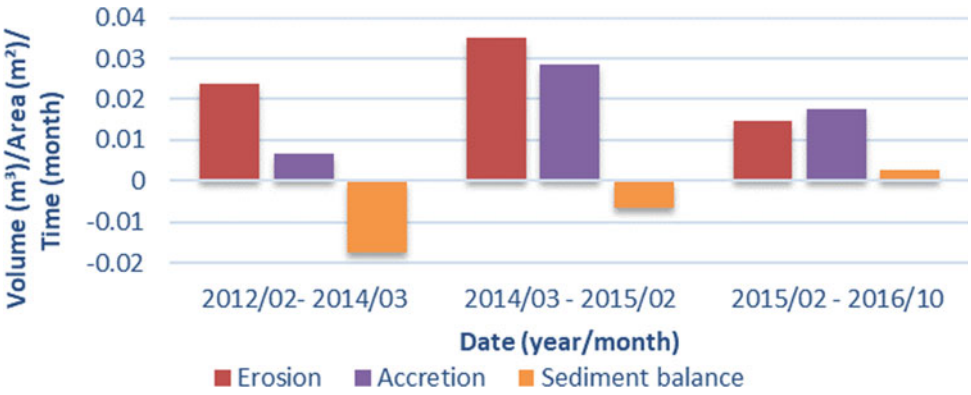

Fig. 3 Normalised sediment balance (accretion-erosion) at Aveiro's inlet

small. It should be noted that from 2013 onwards (end of the jetty's extension interventions), the sediment accretion is progressively lower, and the dredged values also tend to be lower.

It is intended to investigate morphology relationships with storm sequencing in the future. It is recognised that wave conditions continuously influence beach changes, and attention should be given to individual storm events or storm clusters. For example, recall the very well-documented energetic winter of 2013/2014 that strongly affected the equilibrium of beaches and integrated this analysis period (e.g., Dodet et al., 2019). Such results should also be confronted with interventions made on the beach, taking the information concerning the deposition of sand dredged on the beach.

5 Concluding Remarks

The morphological evolution of the emerged and submerged beach at Aveiro coast (NW Portugal) is analysed using high-resolution topo-bathymetric data gathered between 2012 and 2018.

An overall tendency of erosion is observed over time on the emerged beach. Still, monitoring also suggests that a contrary and positive effect can be associated with beach nourishment interventions that were carried out.

The bathymetric data also reveals a general erosive tendency on the submerged beach near the inlet, which is more accentuated during periods with more dredging operations. In addition, the southwest extension of the north jetty concluded in 2013 seems to have modified the ebb flow in that direction, resulting in the interruption of sediment accumulation in the inlet zone.

The dynamic interaction between natural and anthropogenic processes affects this littoral region, and this kind of study provides valuable knowledge to design appropriate coastal management strategies.

Acknowledgements This research was made under the scope of "Estudo de Viabilidade da Transposição Aluvionar das Barras de Aveiro e da Figueira da Foz", supported by the Portuguese Environment Agency (APA), the project SandTrack (PTDC/CTA-GEO/31779/2017) funded by FEDER, through COMPETE2020 - Programa Operacional Competitivida-de e Internacionalização (POCI), and by national funds (OE), through FCT/MCTES for the financial support to CESAM (UIDP/50017/2020 + UIDB/50017/2020 + LA/P/0094/2020).

References

Baptista, P., Cunha, T., & Bernardes, C. (2011). The validation analysis of the INSHORE system: A precise and efficient coastal survey system. *Environmental Monitoring and Assessment, 179*(1–4), 589–604.

Bonaldo, D., Antonioli, F., Archetti, R., Bezzi, A., Correggiari, A., et al. (2019). Integrating multidisciplinary instruments for assessing coastal vulnerability to erosion and sea-level rise: Lessons and challenges from the Adriatic Sea, Italy. *Journal of Coastal Conservation, 23*, 19–37.

Dodet, G., Castelle, B., Masselink, G., Scott, T., Davidson, M., Floc'h, F., Jackson, D., & Suanez, S. (2019). Beach recovery from extreme storm activity during the 2013–14 winter along the Atlantic coast of Europe. *Earth Surface Processes and Landforms, 44*, 393–401.

Fernandéz-Fernandéz, S., Baptista, P., Bernardes, C., Silva, P., Fontán-Bouzas, Á., Lópes-Olmedilla, L., & Ferreira, C. (2019). Variação da linha de costa em praias arenosas: Aveiro (Portugal). In: *IX Congresso sobre Planeamento e Gestão das Zonas Costeiras dos Países de Expressão Portuguesa, Lisboa, Portugal.*

Lira, C. P., Silva, A. N., Taborda, R., & Andrade, C. F. (2016). Coastline evolution of Portuguese low-lying sandy coast in the last 50 years: An integrated approach. *Earth System Science Data, 8*, 265–278.

Luijendijk, A., Hagenaars, G., Ranasinghe, R., Baart, F., Donchysts, G., & Aarninkhof, S. (2018). The state of the World's Beaches. *Scientific Reports, 8*, 6641.

Mendes, D., Pais-Barbosa, J., Baptista, P., Silva, P. A., Bernardes, C., & Pinto, C. (2021). Beach response to a shoreface nourishment (Aveiro, Portugal). *Journal of Marine Science and Engineering, 9*(10), 1112.

Pinto, C. A., Silveira, T., & Teixeira, S. (2020). Beach nourishment practice in mainland Portugal (1950–2017): Overview and retrospective. *Ocean and Coastal Management, 192*, 105211.

Equilibrium Beach Profile: La Garrofera Beach Case Study

Tiago Abreu, Maria de Fátima Silva, Luís Vasconcelos, and Sheila Torres-Toran

Abstract

The constructive and destructive forces acting on a beach profile influence the beach cross-shore profile. For an equilibrium profile, the response to wave forcing should result in a constant shape depending on incident waves or sediment characteristics. A panoply of formulations can be found to represent this equilibrium beach profile in both tidal and non-tidal beaches and the presence or absence of longshore bars. The main objective of this work is to verify if some easy-to-apply and straightforward models can provide an excellent fit for the cross-shore profile of La Garrofera beach, located in the Mediterranean Sea at Valencia (Spain). Beach characterization is made in terms of its morphology, nature of the soil and sediment characteristics, and wave regime. Three models are tested against bathymetric field data, showing reasonable predictions of the measured beach cross-shore profile. Furthermore, they all correctly predict the expected concave-up form characteristically found on wave-dominated beaches.

Keywords

Coastal management • Cross-shore profile • Equilibrium profile • Beach morphodynamics

T. Abreu (✉) · M. de Fátima Silva
Civil Engineering Department, School of Engineering (ISEP), Polytechnic of Porto, Porto, Portugal
e-mail: taa@isep.ipp.pt

T. Abreu
CESAM–Centre for Environmental and Marine Studies, University of Aveiro, Aveiro, Portugal

L. Vasconcelos
Civil Engineering Department, Polytechnic Institute of Viseu (ESTGV-IPV), Viseu, Portugal

S. Torres-Toran
Universitat Politècnica de València, Valencia, Spain

1 Introduction

The use of sandy coasts for tourist activities grew significantly in the last decades of the last century, becoming one of the most important economic activities of many Mediterranean regions. The strong demand for sea views and proximity to beaches resulted in new urban areas accommodating growing populations, and the coastal area has lost its natural setting (e.g., Garcia & Llorens, 2020). These urban areas may have significant negative impacts on coastal environments, aggravated by the impacts of climate change, such as erosion, flooding and sea-level rise.

The erosive processes entail social and economic issues associated with coastal property losses, including damage to nearshore infrastructures and assets. Various defence strategies can be adopted to maintain the beaches, including artificial nourishment interventions and other experimental solutions that help to reduce coastal erosion. The importance of studying equilibrium beach profiles is directly connected with the management and nourishment of beaches. Still, the equilibrium beach profile is never reached due to the constant changes in the sea state, and, consequently, the sediments on the beach are moving at all times. Therefore, coastal monitoring is a fundamental tool for assessing any adopted strategy's effectiveness and supporting management and decision-making initiatives.

This work aims to study La Garrofera beach, located in Valencia (Spain), more specifically in the south of Valencia's harbour, in terms of its equilibrium state. The beach is placed in La Albufera Natural Park and is a privileged spot in the shelter of the dunes. Characterization of the beach is made, providing information on its morphology, nature and sediment grain size and wave regime. Particular attention is given to the beach cross-shore profile, using three different models: Dean (1977), Bernabeu et al. (2002) and Yu & Slinn (2003).

A. Malheiro et al. (eds.), *Advances in Natural Hazards and Volcanic Risks: Shaping a Sustainable Future*, Advances in Science, Technology & Innovation, https://doi.org/10.1007/978-3-031-25042-2_33

2 Data and Methods

2.1 Study Site Characterization

La Garrofera beach is a Mediterranean sandy beach found in the natural Park of L'Albufera in the east of Spain. Located between two of the most important beaches in Valencia, called El Saler and La Dehesa, La Garrofera beach counts 2650 m in length and 35 m wide, being orientated NNW-SSE (Fig. 1).

The bathymetry of the beach was provided by Direccion General de Sostenibilidad de la Costa y el Mar (DGCM), belonging to the Spanish Secretariat of State of the Environment, and it shows a seafloor composed of sand with contour lines approximately parallel to the shoreline, denoting longshore uniformity (Fig. 1). The beach comprises a sandy coast and soft seabeds, where the sediments are cumulated. The composition of the beach consists mainly of uniform sand, presenting a median grain size of $d_{50} = 0.27 \pm 0.4$ mm. At deeper locations, the bottom is more irregular due to rocky outcrops.

During the last years, no appreciable changes were observed on the shore, but the reduced size of the beach reveals its vulnerability to erosion processes. One recognizes that the Port of Valencia influences sediment transport in this particular case. Since it was built, the natural longshore sediment transport was interrupted, and the beaches located in the south, such as La Garrofera beach, do not have sediment contributions coming from the north, suffering coastal erosion. On the other hand, this erosion is also affected by reducing sediment transport from Turia's River to the coast, resulting from river regulation works.

According to the information gathered on the Puertos del Estado website (www.puertos.es), Valencia's coastal buoy (Boya Costera de Valencia I) shows a wave regime essentially characterized by significant wave heights between [0, 0.5] m, with relative frequencies close to 55% and between [0.5, 1] m, with relative frequencies of 34%. A more significant dispersion can be observed for the wave peak period. The values range between 1.5 and 13 s. Most of the data (61.2%) are concentrated within [3.5, 6.5] s. The dominant directions of propagating waves result essentially from the first and second quadrants. It can be observed that swells from the first quadrant occur more frequently, presenting a NE direction. The second quadrant waves exhibit lower frequencies with a SE direction.

2.2 Beach Cross-Shore Profiles

Bruun (1954) introduced the concept of an equilibrium beach profile from field studies of beach profiles on the coasts of Denmark and California. The author noticed that the cross-shore profiles fit curved and concave shapes very well. Dean (1977) further examined this concept, proposing the generalized power law for each profile:

$$Z = Ax^m \tag{1}$$

where z represents the depth of the profile below the mean water level, x is the distance to the shoreline, and the parameters A and m are empirical coefficients based on representative profiles. For example, Dean (1991) proposed a mean value for m equal to 2/3 and established an empirical correlation between A and d_{50} (expressed in mm) $A = 0.21 d_{0.50}{}^{0.48}$.

Bernabeu et al. (2002) discussed a two-section equilibrium profile based on different dissipation processes acting on the beach for tidal environments (e.g., turbulence and

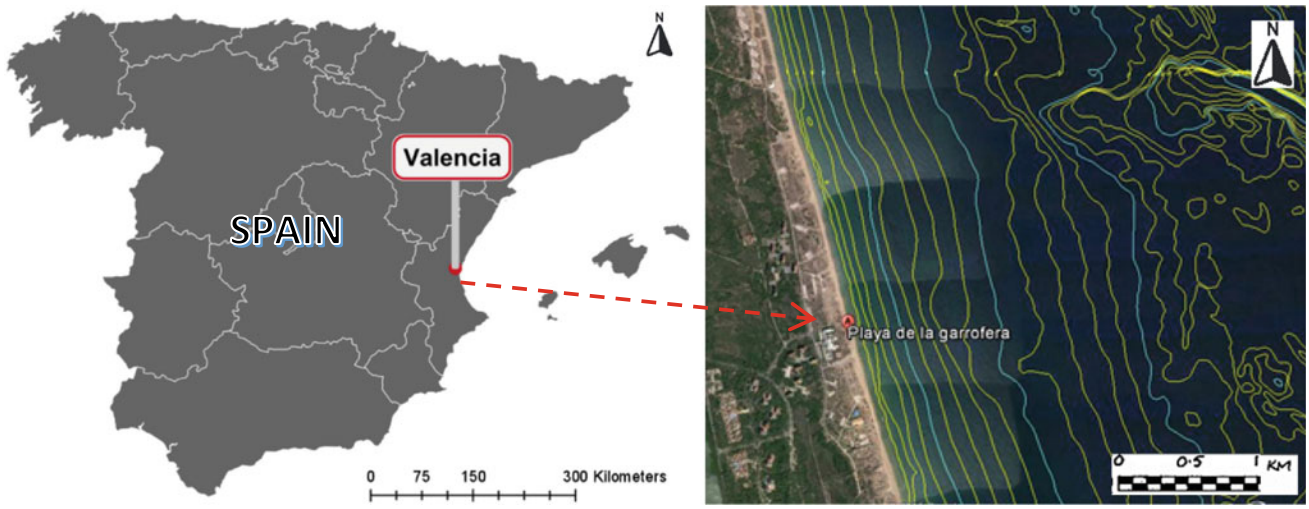

Fig. 1 Localization of La Garrofera beach and corresponding bathymetry

bottom friction). The profile is divided into a shoaling and a surf profile, and each section is treated independently. The developed expressions to characterize each profile section are presented in Eqs. (2) and (3):

$$x = \left(\frac{z}{a_1}\right)^{3/2} + \frac{a_2}{{a_1}^{3/2}} z^3 (\text{surfprofile}), \tag{2}$$

$$x = x_0 + \left(\frac{z}{a_3}\right)^{3/2} + \frac{a_4}{{a_3}^{3/2}} z^3 (\text{shoalingprofile}), \tag{3}$$

where the horizontal distance, x_0, depends on the tidal range, measured from the start of the surf profile and the virtual origin of the shoaling profile over the mean sea level. The coefficients a_1 and a_3 are associated with dissipation mechanisms, and the coefficients a_2 and a_4 are with energy reflection.

Both Dean and Bernabeu's profiles do not consider the existence of longshore bars. That shape can also represent an equilibrium profile, but few studies can be found concerning barred beaches. Yu and Slinn (2003) proposed the following expression to reproduce longshore uniform barred profiles:

$$z = k\left(1 - \frac{\beta_2}{\beta_1}\right)\tanh\left(\frac{\beta_1 x}{k}\right) + \beta_2 x - A_b \exp\left[-W_b\left(\frac{x - x_b}{x_b}\right)^2\right], \tag{4}$$

where x_b is the position of the bar crest and β_1 and β_2 are the nearshore and the offshore slopes, respectively, A_b is the bar amplitude, W_b is the bar width, and k is a calibration parameter.

3 Results

The numerical values of the input coefficients of Eqs. (1)–(4) were obtained by minimizing the differences between estimated and observed depth values. The results for the three models are shown in Fig. 2.

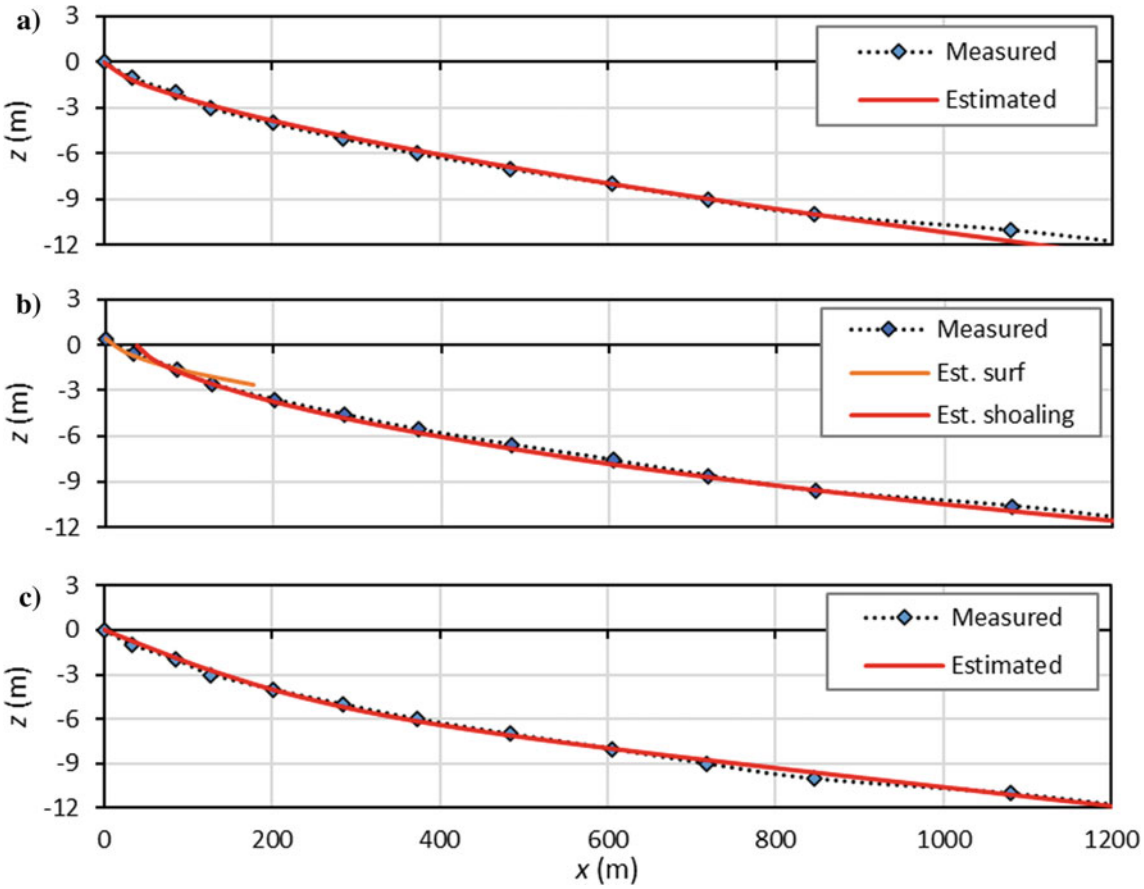

Fig. 2 Comparison of La Garrofera cross-shore profile with **a** Dean's, **b** Bernabeu et al.'s and **c** Yu and Slinn's models

4 Discussion

Dean's equilibrium beach profile theory assumes that the turbulence of breaking waves is the main destructive force acting on a beach. This assumption leads to developing a conceptual framework where the sediment of a given grain size can withstand wave energy dissipation per unit volume. It is noteworthy to mention that the obtained data, coming from a cartographic study of Valencia and Alicante regions made by DGCM, registers a relevant diameter for La Garrofera beach equal to $d_{50} = 0.27 \pm 0.4$ mm, confirming the value of $A = 0.111$. Therefore, it can be said that this beach adjusts reasonably well to Dean's equilibrium profile. Such adjustment is probably reflected in the stability revealed by the beach in the past decade.

Bernabeu et al. (2002) presented parameterization coefficients for nine locations along the Spanish Coast. In particular, for the Mediterranean Sea, values are given for El Vendrell beach ($a_1 = 0.14$, $a_2 = 0.05$, $a_3 = 0.2$ and $a_4 = 0.01$), which is located slightly north of La Garrofera beach. Our proposed values only differ for a_1 and a_3, which are proportional to the slope of the upper part of the surf and shoaling zones and are related to dissipation processes. By adopting $a_1 = A = 0.111$, the surf profile tends to the Dean profile, and the almost similar reasonable adjustment with $a_3 = 0.13$ suggests sand grain uniformity along with the cross-shore profile. The lower values of a_2 and a_4 suggest that this is a dissipative beach, and the reflection phenomenon is not so relevant.

Yu & Slinn (2003) expression shows an excellent adjustment to the La Garrofera beach profile. Furthermore, since there are no longshore bars, it is seen that their expression can be simplified, depending only on three parameters (β_1, β_2, k).

5 Concluding Remarks

This study analyses how several formulations representing equilibrium beach profiles adjust to the cross-shore profile of La Garrofera beach, located in Valencia (Spain).

The results show that the suggested Dean's equilibrium profile reasonably agrees with the La Garrofera beach cross-shore profile. Interestingly, it is seen that the observed concave curve can be obtained from the simple knowledge of the median grain size present on the beach. This good agreement probably reflects the beach stability observed in the past decade. Both Bernabeu et al.'s and Yu and Slinn's models provide good representations of the cross-shore profile as long the calibration parameters are correctly considered. Furthermore, it is possible to verify that Yu and Slinn's expression can also provide good estimations even if there are no longshore bars.

An understanding of equilibrium profiles is helpful in a few types of coastal engineering projects, helping to propose appropriate nourishment of beaches and other coastal management strategies.

Acknowledgements This research was made under the scope of the project SandTrack (PTDC/CTA-GEO/31779/2017) funded by FEDER, through COMPETE2020—Programa Operacional Competitividade e Internacionalização (POCI). We also acknowledge financial support to CESAM by FCT-MCTES (UIDP/50017/2020 + UIDB/50017/2020 + LA/P/0094/2020) through national funds.

References

Bernabeu, A. M., Medina, R., & Vidal, C. (2002). An equilibrium profile model for tidal environments. *Scientia Marina, 66*(4), 325–335.

Bruun, P. (1954). Coast erosion and the development of beach profiles. U.S. Army Beach Erosion Board Technical Memorandum, 44.

Dean, R. G. (1977). Equilibrium beach profiles: U.S. Atlantic and Gulf coasts. Ocean Engineering Report, 12, Dep. Civil Eng., University of Delaware, Newark, Delaware.

Dean, R. G. (1991). Equilibrium beach profiles: Characteristics and applications. *Journal of Coastal Research, 7*(1), 53–84.

Garcia, J. L. M. I., & Llorens, F. M. (2020). Rewilding urban areas to maintain ecosystem services and ecological tourism: The case of saler's devesa, València, Spain. *WIT Transactions on Ecology and the Environment, 248*, 177–189.

Yu, J., & Slinn, D. N. (2003). Effects of wave-current interaction on rip currents. *Journal of Geophysical Research, 108*(C3), 3088.

Numerical Validation of a Newly Developed River Morphological Prediction Software

Tew-Fik Mahdi

Abstract

UMHYSER-1D (Unsteady Model for the HYdraulics of SEdiments in Rivers 1D) is a one-dimensional hydro-morphodynamic software that computes water surface profiles in a single river or multiriver network for sub/supercritical flow regimes taking into account cohesive or non-cohesive sediment transport. UMHYSER-1D simulates steady and unsteady flows, with or without sediment transport. This paper presents numerical validation of UMHYSER-1D. By using a published study case of the US Bureau of Reclamation, the results of UMHYSER-1D are compared to those of the USBR software, SRH-1D. This study case is used to validate numerically UMHYSER-1D under unsteady flow and sediment transport conditions in a long reach of the Rio Grande River, more than 100 km long. UMHYSER-1D gives almost the same results as SRH-1D. The maximum differences observed at the two cross-sections are very acceptable. After its laboratory validation in a previous paper, the present work confirms that UMHYSER-1D is ready to be used as a numerical laboratory for fluvial hydraulics and/or a powerful tool to solve real engineering problems. UMHYSER-1D can be used for river morphological changes due to natural or human influences.

Keywords

One-dimensional model • UMHYSER-1D • Unsteady sediment transport • Bed geometry adjustment • Rio Grande River

1 Introduction

UMHYSER-1D, the Unsteady Model for the HYdraulics of SEdiments in Rivers 1D (AlQasimi & Mahdi, 2020), is a one-dimensional hydromorphodynamic software able to compute water surface profiles in a single river or a multi-river network, for sub/supercritical flow regimes, taking into account cohesive or non-cohesive sediment transport. UMHYSER-1D simulates steady and unsteady flows, with or without sediment transport.

It has been validated using laboratory experiments of Cantelli et al. (2004) and applied to natural river reaches (AlQasimi & Mahdi, 2019a, 2019b). This paper presents a numerical validation of UMHYSER-1D. For this end, a reach of the Rio Grande River in New Mexico, USA, is used. This choice is based on the existence of the extensive needed data published by Holmquist-Johnson (2005) and Padilla & Baird (2010). Moreover, this river reach was modelled by the US Bureau of Reclamation SRH-1D software (Greimann & Huang, 2018).

This case is used to validate numerically UMHYSER-1D under unsteady flow and sediment transport conditions in a long river reach. The results of SRH-1D and UMHYSER-1D are compared.

2 Materials and Methods

UMHYSER-1D (AlQasimi & Mahdi, 2020) is an unsteady one-dimensional model. It solves the one-dimensional water and solid phases. The de Saint–Venant equations are solved for the water phase, while the Exner/convection–diffusion equation is solved for the solid phase. The modelled river can have regular or irregular cross-sections, and its hydraulic structures are modelled using rating curves. The hydraulics computations are done using the NewC scheme (Kutija & Newett, 2002), assuring numerical stability in the transition sub/supercritical flows. Two methods are used for the de

T.-F. Mahdi (✉)
Department of Civil, Geological and Mining Engineering, Polytechnique Montréal, Montreal, QC, Canada
e-mail: tewfik.mahdi@polymtl.ca

A. Malheiro et al. (eds.), *Advances in Natural Hazards and Volcanic Risks: Shaping a Sustainable Future*, Advances in Science, Technology & Innovation, https://doi.org/10.1007/978-3-031-25042-2_34

Saint–Venant equations and the sediments. A non-equilibrium method is used for long-term computations, ignoring the unsteady terms of the continuity equation. In contrast, for short-term computations, a fractional step method (Yanenko, 1971) solves the convection–diffusion equation with a source term due to sediment erosion/deposition.

For each sediment size fraction, sediment transport is calculated, and for the bed composition accounting procedure, UMHYSER-1D uses the method of Bennet and Nordin (1977), which divides the bed into conceptual active/inactive layers. Finally, for cross-sectional adjustments, the user of UMHYSER-1D has the choice to use one of 3 minimization theories: energy slope (Chang, 1988), bed slope and total stream power (Yang, 1972). Moreover, riverbank retreat can be modelled using an angle of repose condition, and an extra option for bed geometry adjustments, using an equation between erosion width and flow rate, is incorporated in UMHYSER-1D.

In the study case, the reach of the Rio Grande from San Acacia Diversion Dam downstream to the Narrows of Elephant Butte Reservoir, a distance of 135 km, is shown in Fig. 1, along with the upstream hydrograph. UMHYSER-1D uses the input data of SRH-1D to simulate the historical period 1992–2002. This reach includes five lateral inflows with sediment (Fig. 2) and a downstream reservoir with variable water surface elevation (Fig. 3). The sediment rating curve at the upstream boundary condition is also shown in Fig. 3. All these input data, shown in these Figs. 1, 2 and 3, are derived from the SRH-1D input file of this case study (Greimann & Huang, 2018).

3 Results

The final longitudinal profiles and water surface elevations simulated by UMHYSER-1D and SRH-1D are shown in Fig. 4. The maximum differences occurring in two cross-sections, identified in Fig. 4 as XC-100 and XC-183, are shown in Fig. 5. Finally, Fig. 6 compares the two software's final simulated thalwegs and maximum water elevations.

4 Discussion

Figures 4 and 6 show that UMHYSER-1D and SRH-1D are almost the same. The ten-year simulations of this 135 km long reach produce comparable thalwegs and water surface elevations. Please note that the cross-section comparison gives the same conclusion since the vertical differences are

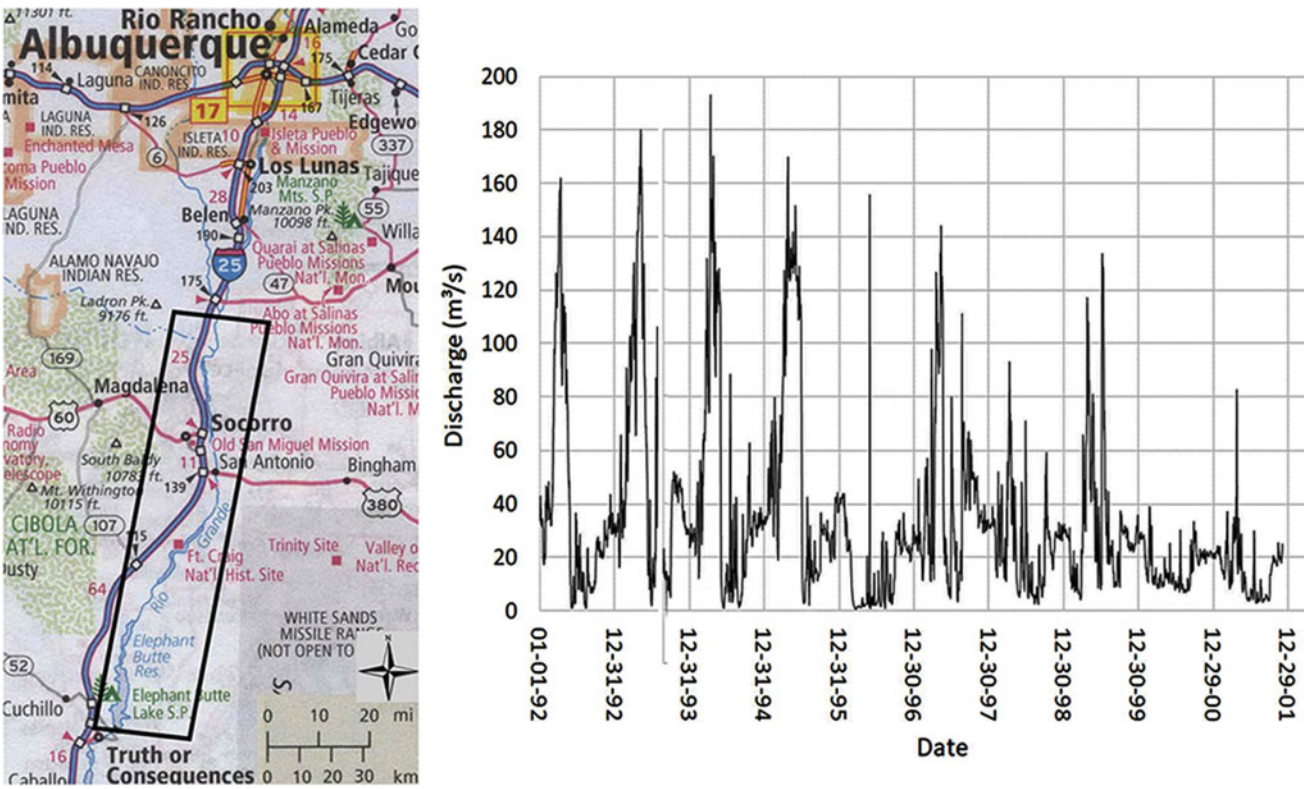

Fig. 1 Location of the modelled river reach: San Acadia to Elephant Butte Reservoir in New Mexico, USA (adapted from Maps of all US States, 2021), and the upstream hydrograph

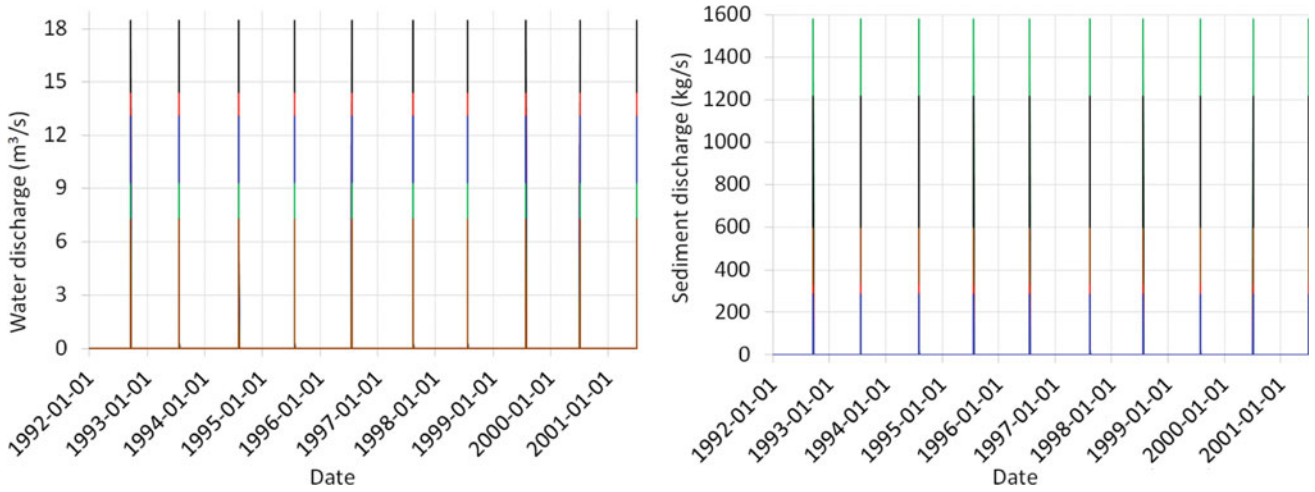

Fig. 2 Lateral water and sediment discharges. Inflows' positions are counted from downstream

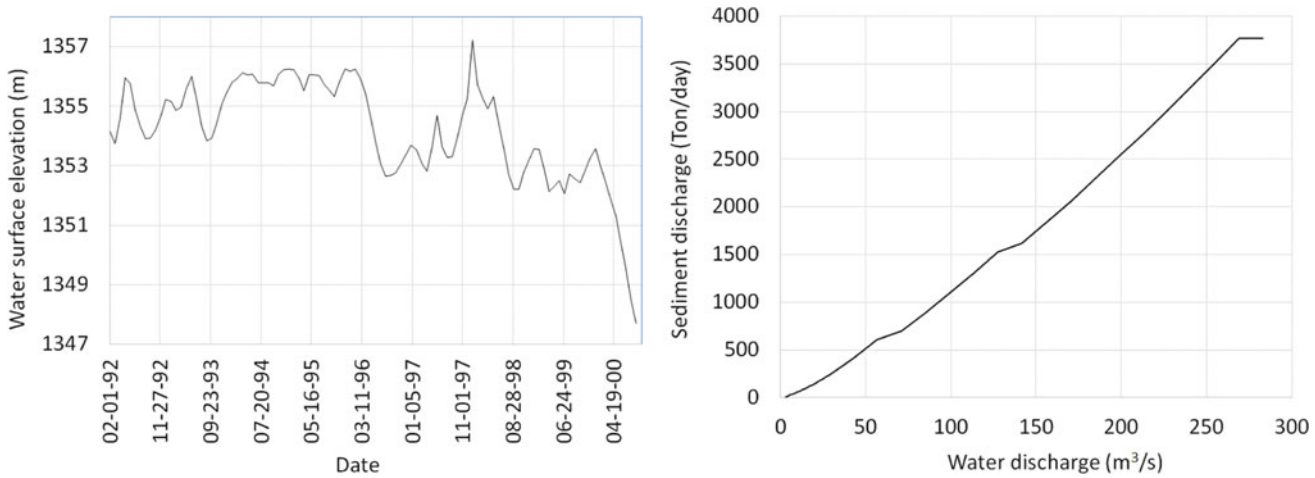

Fig. 3 Downstream boundary condition, variable water level, and sediment rating curve upstream boundary condition

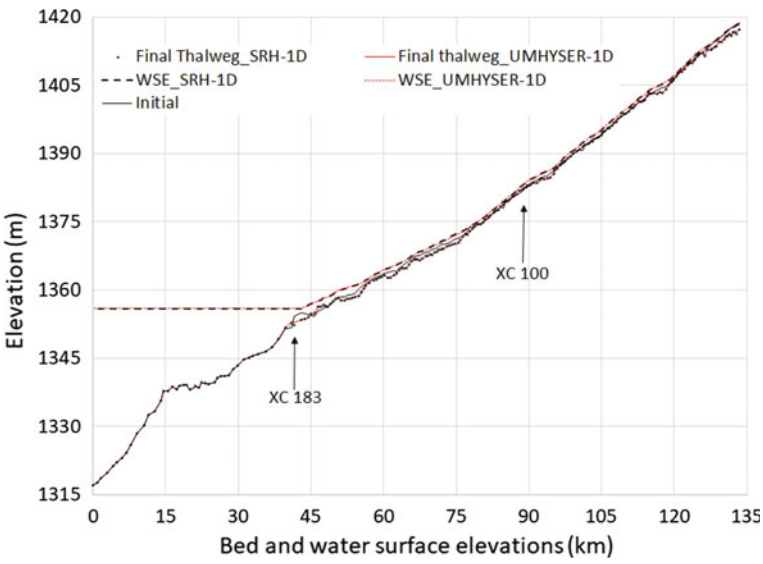

Fig. 4 Final longitudinal profiles and water surface elevations (WSE) simulated by UMHYSER-1D and SRH-1D

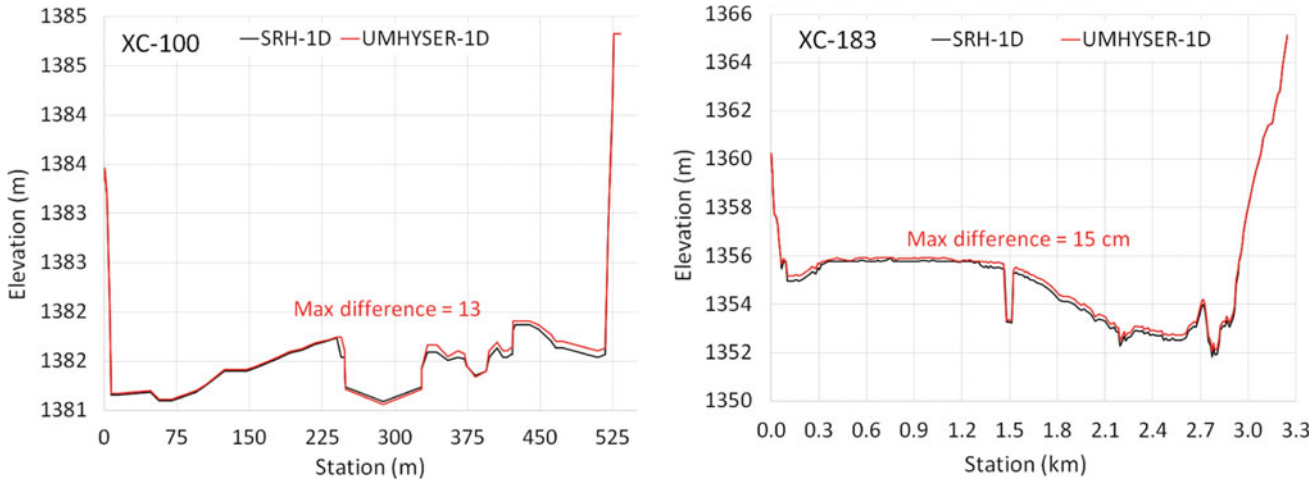

Fig. 5 Comparison of simulated cross-sections XC-100 and XC-183 by the two software

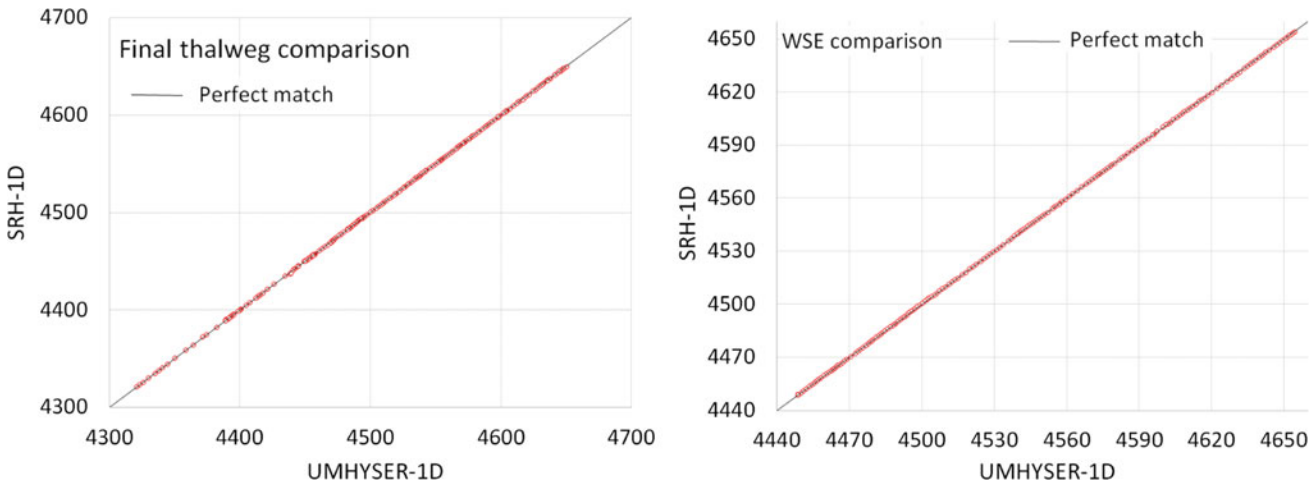

Fig. 6 Final thalweg and water surface elevation (WSE) comparisons

minor, less than 3 cm for all of them except cross-sections 100 and 183 (Fig. 4). The vertical differences are about 13 and 15 cm at these locations, respectively. The difference can explain these differences in the adopted numerical methods of the two software and the programming used algorithms. Unfortunately, the observed final thalweg and cross-sections at different locations are not available to compare with simulated results of SRH-1D and UMHYSER-1D and ultimately conclude on the more precise software.

5 Concluding Remarks

In this study, the numerical validation of the UMHYSER-1D model by comparison to the SRH-1D model, using the reach of the Rio Grande River from San Acacia Diversion Dam downstream to the Narrows of Elephant Butte Reservoir, a distance of 135 km. Furthermore, using the same input data for the two software allowed the comparison of their respective results.

Despite the differences at a few locations between the results of the two models, UMHYSER-1D reproduced the results of SRH-1D satisfactorily. In fact, the simulated thalwegs and cross-sections at different locations are in good agreement except at two locations, one at the reservoir entrance and the other 83 km upstream of the reservoir entrance, where the maximum differences are 15 cm and 13 cm, respectively. Even if, at this stage, it is unknown which software is better, it can be concluded that this case study demonstrates the numerical validity of UMHYSER-1D and shows its ability to simulate complex engineering real cases. Other validation study cases should be used to study more specific options of UMHYSER-1D, such as the implementation of sediment transport equations.

Acknowledgements This research was funded, in part, by the National Science and Engineering Research Council (NSERC) Discovery Grant, application No: RGPIN-2021-03272.

References

AlQasimi, E., & Mahdi, T. (2019a). Flooding of the Saguenay region in 1996: Part 1-Modeling a flooding in River Ha! Ha! *Natural Hazards, 96*(1), 1–15.

AlQasimi, E., & Mahdi, T. (2019b). Flooding of the Saguenay region in 1996: Part 2-Aux Sables River flood mitigation and environmental impact assessment. *Natural Hazards, 96*(1), 17–32.

AlQasimi, E., & Mahdi, T. F. (2020). A new one-dimensional numerical model for unsteady hydraulics of sediments in rivers. *SN Applied Sciences, 2*, 1480.

Bennet, J., & Nordin, C. (1977). Simulation of sediment transport and armoring. *Hydrological Sciences Bulletin, 22*, 555–569.

Cantelli, A., Paola, C., & Parker, G. (2004). Experiments on upstream-migrating erosional narrowing and widening of an incisional channel caused by dam removal. *Water Resources Research, 40*, W03304. https://doi.org/10.1029/2003WR002940

Chang, H. C. (1988). *Fluvial processes in river engineering*. Wiley.

Greimann, B., & Huang, J. V. (2018). SRH-1D 4.0 User's Manual (Sedimentation and River Hydraulics-One Dimension, Version 4.0). Technical Report SRH-2018-07, Technical Service Center, US Bureau of Reclamation, Denver (CO).

Holmquist-Johnson, C. (2005). Sediment Model for the Middle Rio Grande – Phase 1, San Acacia Diversion Dam to Elephant Butte Reservoir. US Bureau of Reclamation, Technical Service Center, Sedimentation & River Hydraulics Group, Denver, CO.

Kutija, V., & Newett, C. J. M. (2002). Modelling of supercritical flow conditions revisited, NewC Scheme. *Journal of Hydraulic Research, 40*(2), 145–152.

Maps of all US States. Retrieved December 13, 2021, from https://east-usa.com/new-mexico-parks-map.html

Padilla, R., & Baird, D. C. (2010). Channel changes and maintenance on the San Acacia Reach of the Middle Rio Grande. In *2nd Joint Federal Interagency Conferences*, Las Vegas, NV (pp. 1–11).

Yanenko, N. N. (1971). *The method of fractional steps: Solution of problems of mathematical physics in several variables*. Springer-Verlag.

Yang, C. T. (1972). Unit stream power and sediment transport. *ASCE Journal of the Hydraulics Division, 98*, 1805–1826.

Hydraulic Analysis of the Suitable Construction Solutions in the Middle Tiber River

Giuseppe Sappa and Giuseppe Mellace

Abstract

The hydraulic safety of the historic centre of Rome is guaranteed by preventing flooding events of the Tiber River by the embankment walls called "Muraglioni". For this reason, it is necessary to maintain the flood attenuation capacity ensured by the flooding of the floodplain areas upstream of the city. The urban developments of these areas are sustainable only by hydraulics engineering infrastructures aimed at controlling the flood in the floodplain areas in case of 100-year and 200-year return time meteoric and hydraulic extreme events. This work presents the engineering solutions and the results of the hydraulics analysis carried out on making compatible road infrastructures and flood protection infrastructures in the territory, such as river embankments and detention basins. The Tiber River has been studied to respect this target, setting up a one-dimensional numerical model using HEC-RAS and a two-dimensional model using SMS and BAS.E.MENT software. The numerical simulations of floods have been carried out with a 200-year return time in the several phases of construction of the infrastructures in the area. The analysis identified the most suitable design choices, saving the neighbouring Rome metropolitan area from increasing hydraulic risks.

Keywords

Flooding risk assessment • Middle Tiber River Valley • CAD • SMS • BAS.E.MENT

G. Sappa (✉) · G. Mellace
Department of Civil, Building and Environmental Engineering, La Sapienza University of Rome, Rome, Italy
e-mail: giuseppe.sappa@uniroma1.it

G. Sappa · G. Mellace
Consultant of Engineering, Rome, Italy

1 Introduction

In the past, flooding events of the Tiber river in Rome had occurred every twenty-five years (Frosini, 1977), causing epidemics and considerable economic damage. Between the end of XIX and the beginning of the XX century, the walls, called "muraglioni", were built up to convey floods comparable with the catastrophic flood wave in 1870, which inundated the monumental centre of the city.

Afterwards, embankments on the urban stretch were completed, and hydroelectric traverses and dams were built, including the Corbara dam with a reservoir of 190 million cubic meters (1959–1963). Still today, critical events in Rome come out due to the overflow of the embankments in the urban section, which corresponds to over 3,000 mc/s.

In case of flooding, the area between Orte and Castel Giubileo, upstream of Rome, is a natural reservoir of about 200 million cubic meters that decreases and delays the Tiber's flooding, allowing the outflow in advance of the Aniene river flood, the main tributary inside the city.

In the last decades, Rome's metropolitan area development processes have hugely transformed most of the flood plains (Manfreda et al., 2014; Nardi et al., 2013). On the other hand, climate change and global warming represent two additional factors affecting flooding risk due to the frequency increasing of high-intensity rainfall and the likelihood of river and surface water flooding (Piniewski et al., 2017).

In this framework, according to Italian Law 183/89 on soil protection, the Tiber River Basin Authority had anticipated the EU directive contents (2007/60) carrying out the Tiber River Basin Management Plan (PS1), which is a planning tool, approved in 1998, in order to: (i) contain the current hydraulic risk in Rome by preserving the reservoir capacity; (ii) minimise the risk to the population living in areas north of Rome. This planning tool deals with hydraulic risk assessment in the Middle River Tiber Valley (Sappa & Ferranti, 2020).

A. Malheiro et al. (eds.), *Advances in Natural Hazards and Volcanic Risks: Shaping a Sustainable Future*, Advances in Science, Technology & Innovation, https://doi.org/10.1007/978-3-031-25042-2_35

2 Methods and Materials

Currently, roads and hydraulic works are being planned and executed in the municipalities of Monterotondo and Castelnuovo di Porto, upstream of Rome's city, to respect the Tiber mentioned above River Basin Management Plan (PS1), as represented in Fig. 1.

This study represents the support analysis for constructing a viaduct for crossing the Tiber river and a road embankment connecting with the S.S. 4 Salaria to be transformed into a river embankment once the upstream expansion tank is completed.

To verify the hydraulic invariance in the area, different hydraulic simulations were performed relating to the different infrastructural configurations in the area with 200 years return period:

- Scenario 1—Free flooding of the watercourse without structures (pre-construction scenario).
- Scenario 2—Construction of road structures (transitory scenario).
- Scenario 3—Construction of road structures integrated with passive hydraulic safety structures (river embankments and non-return valves).
- Scenario 4—Construction of hydraulic safety structures (floodwater reservoir and river embankments) integrated with road structures.

The flood scenarios were simulated using, the first, a monodimensional hydraulic model for the river sections between the hydroelectric traverses of Nazzano and Castel Giubileo for a length of about 45 km, and subsequently through a 2D model for the study of local hydraulic conditions.

The following topographic campaigns were carried out to define the hydraulic models:

- topographic survey with traditional techniques (EuroGeos 1996–1997),
- laser scanning survey with the return of DEM with a regular 2 × 2 m mesh (Aquater),
- the campaign of baptismal and topographic surveys (DITS Sapienza University of Rome 2008–2009),

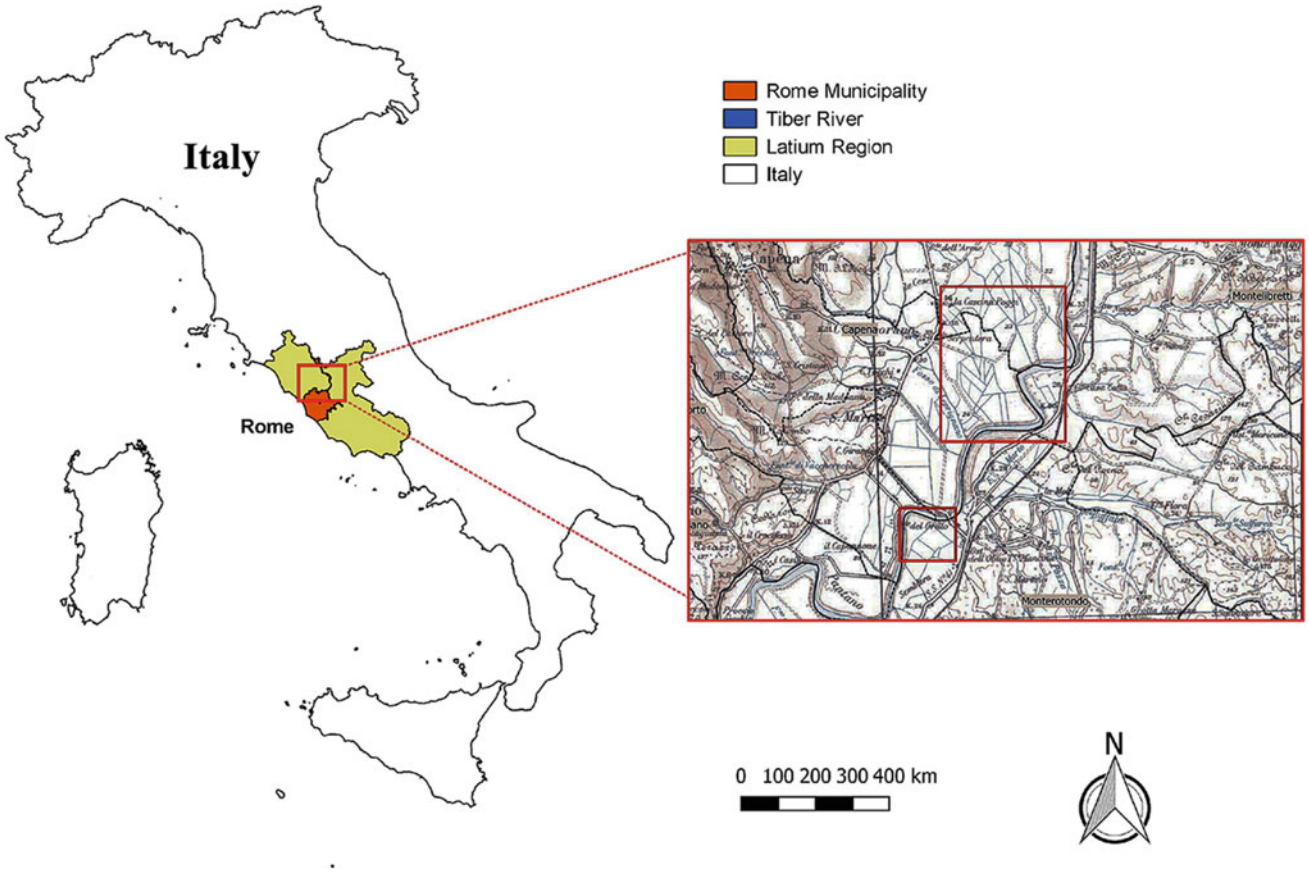

Fig. 1 Location of the study area

- the survey with the Multibeam methodology (DITS Sapienza University of Rome 2006).

The 1D model was implemented using the HEC-RAS software to analyse the river trunk between the hydroelectric crossings of Nazzano and Castel Giubileo, for a length of the river shaft equal to 43,853 km.

The computing domain consists of 1,093 cross-sections given by interpolating the sections detected with a 20 m pitch through the combined use of CAD software and the SMS 1D-Hyd module.

The statistical elaboration of 1000 years of historical precipitations series gave the 200 years return stream discharge by applying specific hydrological software because precipitations are the main parameter according to run-off, evapotranspiration, and groundwater recharge in a basin can be obtained (Natale & Savi, 2007). These elaborations have been carried out by applying "Modello TEVERE", the specific software set up, in early 2000, on behalf of the Tiber River Basin Authority (Calvo & Savi, 2009).

Afterwards, starting from data coming out from the 1D model, as represented in Fig. 2, an in-depth study of the hydrodynamic field was carried out at a local scale with a two-dimensional finite element calculation model.

The boundary conditions of the 2D model were imposed by inserting the values of water levels and flow rates obtained from the 1D model. In particular:

- upstream boundary condition: the hydrogram of the flow rates has been inserted at the bridge of the E-45 highway bridge;
- downstream boundary conditions: the rating curve, a relationship between stage and flow, was inserted at the E-35 highway bridge.

The simulations were obtained from the 2D unsteady flow model.

The SMS software was used for the pre-processing phase (set up of the calculation domain and the elevation model) and post-processing of the data (representation of the calculation domain of the hydraulic quantities of interest). While the numerical simulation software BAS.E.MENT, BASEplane module, was used to calculate the height of the water surface, the velocity and the tangential tension.

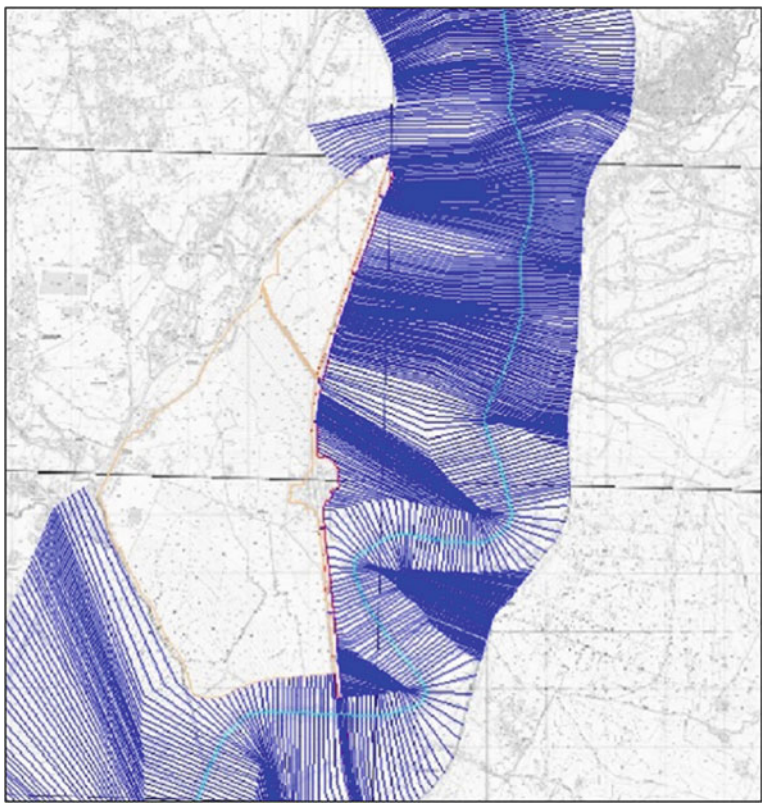

Fig. 2 Calculation cross-sections used for 1D model simulations

The computation domain is made up of an irregular grid (mesh) made of triangular (floodplain) and quadrangular (riverbed) nodes and elements. The elevation value to be associated with the domain was obtained through the constrained triangulation of the quoted points coming from the laser scanning survey, for the floodplain area, and from the Multibeam survey and bathymetric sections, for the riverbed.

Different soil characteristics (Manning coefficient and turbulent exchange coefficients) have been associated with each node and element of the grid.

The computation domain was built excluding the part of the embankment considered not surmountable by the flood, except where underpasses and manholes are present. The output of this processing step was exported in ASCII format to associate it with the calculation mesh during the pre-processing phase.

3 Results

The 2D model provided the values of levels, water depths, and velocities at each node. In addition, to reduce the impact of the new bridge on the hydraulic regime of the area, 16 ARMCO pipes were provided in the right embankment of the bridge.

In the transitional phase (scenario 2), the following assumptions have been provided to make the road embankment hydraulically transparent concerning the Tiber River's floods and those of the tributary ditches: n.1 manhole 3 × 3 m, n. 4 DN1500 and n. 1 DN2500.

For each section of the embankment, the maximum elevation of the water surface and the maximum velocity reached in the main channel during the flooding was calculated. In addition, values of flow and water levels, obtained from simulations for 50, 100, and 500 years return periods (T_r), were identified both upstream and downstream of the structures, and here they are represented in Table 1.

Table 1 Variations in flood flow rates downstream and upstream of the new structures

	ΔQ/Q (%)	
	P.te Grillo (downstream)	P.te Dir. A1 (upstream)
Tr = 50	−0.53	0.08
Tr = 200	−0.68	0.47
Tr = 500	−0.19	0.97

4 Discussion

A comparison of simulation results referred to scenarios 3 and 4 showed a maximum water level increase of 4 cm and a velocity increase, in the main channel, of 0.8%.

The one-dimensional hydraulic simulations, using the unsteady flow analysis, did not show sensitive differences in water surface elevation and velocity of water flow for the different scenarios investigated, as represented in Fig. 3, where one of these investigated scenarios is reported and zoomed in on one of its most critical points.

The execution of the proposed structures has been output as to be compatible from the hydraulic point of view. Furthermore, maintaining the flow rate at values below 2,945 m^3/s for the 4 different scenarios demonstrates the maintenance of the attenuation of the flood wave.

The simulation of the dynamic development of the flood event on the territory has confirmed the ability of the road underpasses to make "transparent" the road embankment in the project in scenario 2.

For every flood event characterised by a 50, 200 and 500 years return period, the realisation of the floodwater reservoir allows a substantial hydraulic invariance downstream of the hydraulic protection zone of the Monterotondo Scalo settlement.

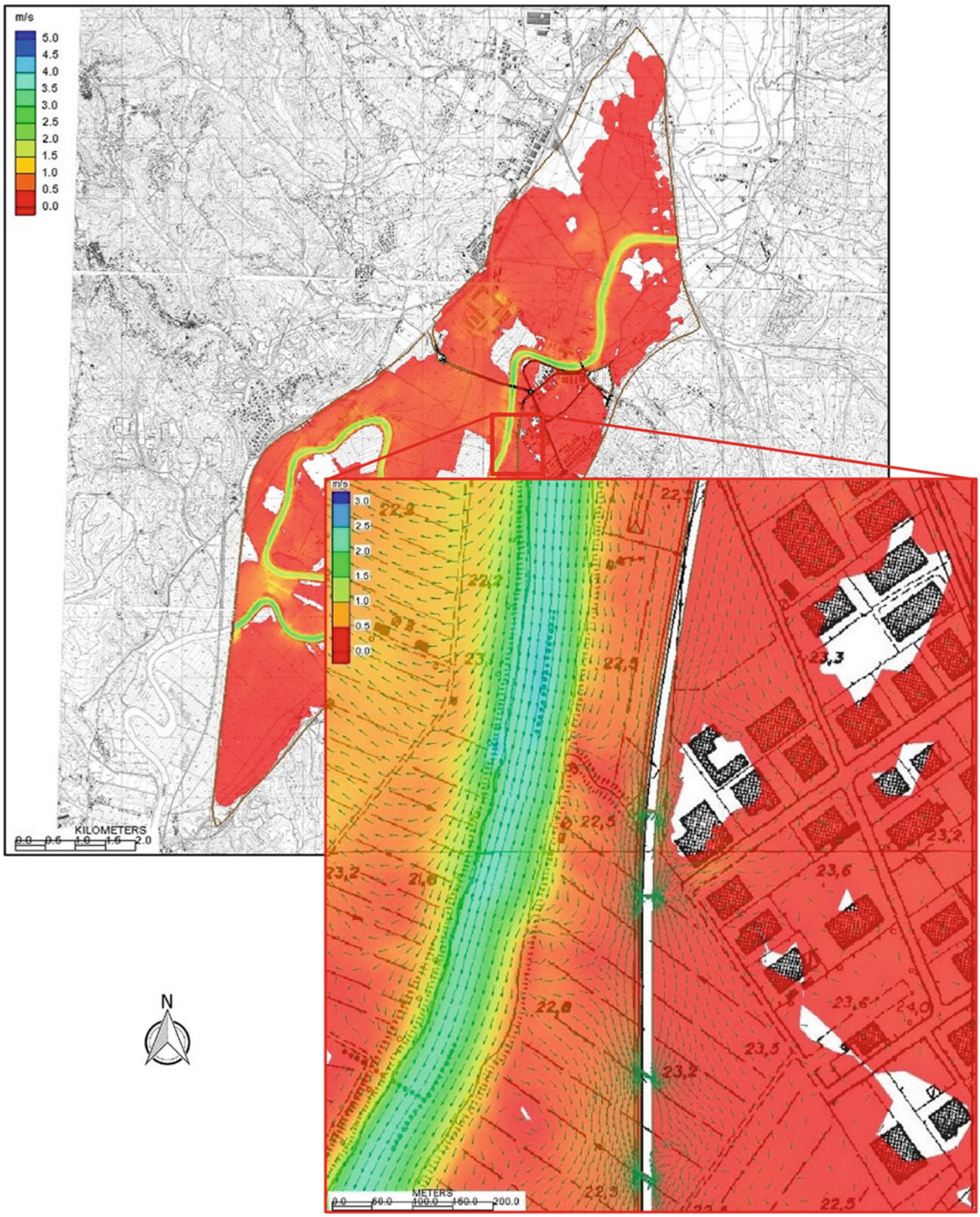

Fig. 3 Kinematic field and vector representation of velocities in the most critical area

5 Concluding Remarks

This study shows the outputs of the combined use of numerical models at different detail scales for the different scenarios of the realisation of road and hydraulic structures. Furthermore, the simulations' analysis lets us identify the most suitable design for works to maintain unchanged the lamination function of the areas located upstream of Rome.

References

Calvo, B., & Savi, F. (2009). Real-time flood forecasting of the Tiber river in Rome. *Natural Hazards, 50*(3), 461–477.

Frosini, F. (1977). *Il Tevere: Le inondazioni di Roma e i provvedimenti presi dal Governo Italiano per evitarle*. Accademia Nazionale dei Lincei.

Manfreda, S., Nardi, F., Samela, C., Grimaldi, S., Taramasso, A. C., Roth, G., & Sole, A. (2014). Investigation on the use of geomorphic approaches for the delineation of flood-prone areas. *Journal of Hydrology, 517*, 863–876.

Nardi, F., Biscarini, C., Di Francesco, S., Manciola, P., & Ubertini, L. (2013). Comparing a large-scale DEM-based floodplain delineation algorithm with standard flood maps: The Tiber river basin case study. *Irrigation and Drainage, 62*, 11–19.

Natale, L., & Savi, F. (2007). Monte Carlo analysis of probability of inundation of Rome. *Environmental Modelling Software, 22*(10), 1409–1416.

Piniewski, M., Mezghani, A., Szcześniak, M., & Kundzewicz, Z. W. (2017). Regional projections of temperature and precipitation changes: Robustness and uncertainty aspects. *Meteorologische Zeitschrift, 26*(2), 1–12.

Sappa, G., & Ferranti, F. (2020). Flooding risk assessment in the middle Tiber River valley with remediation proposal. In F. Fernandes, A. Malheiro, & H.I. Chaminé (Eds.), *Advances in natural hazards and hydrological risks: meeting the challenge* (pp. 111–115). ASTI Springer Series, Cham.

Terceira Island Geology and Geodiversity: Meeting Volcanological Hazards

Volcanic Geology of Terceira Island, Azores: A Field Guide to Geodiversity

Adriano Pimentel

Abstract

Terceira in the Azores archipelago is one of the most geologically diverse islands of the Atlantic Ocean and its geodiversity is due to the close relationship between tectonics and magmatism. This strong interaction is translated by the presence of large central volcanoes with calderas and a WNW-ESE-trending fissure zone that crosses them. The active tectonics of Terceira is well expressed by the Lajes Graben, which was the source of some of the more destructive earthquakes in the Azores. Moreover, the bimodal geochemistry of Terceira is recorded, on the one hand, by the numerous basaltic eruptions that punctuate the island and, on the other hand, by the less frequent but large trachytic (peralkaline) explosive eruptions of the central volcanoes. Among the latter, ignimbrite-forming eruptions are the most hazardous phenomena, and in case of such a future eruption the island would suffer catastrophic consequences. Historical eruptions have occurred on land (1761) and at sea offshore Terceira (1867 and 1998–2001), but with no record of casualties. This chapter highlights the diversity of geological structures found on Terceira Island, including tectonic faults, volcanoes and their products, volcanic caves, and geothermal areas, with attention to the associated volcanic hazards.

Keywords

Oceanic island • Volcanic caves • Volcanic hazards • Terceira Island

1 Introduction

Terceira Island is part of the archipelago of the Azores, located in the middle of the North Atlantic Ocean. It shows a remarkable diversity of geological structures for an oceanic volcanic island, which results from the strong interaction of tectonic and magmatic processes. Four overlapping central volcanoes with calderas (from west to east: Santa Bárbara, Pico Alto, Guilherme Moniz, and Cinco Picos—also called Serra do Cume-Ribeirinha) and a fissure zone form the island (Fig. 1). The two oldest central volcanoes, Cinco Picos and Guilherme Moniz, are believed to be extinct and together build the eastern and southern parts of Terceira, respectively. The northeast sector of Cinco Picos volcano is cut by NW–SE-oriented faults that mark the Lajes Graben. The other two central volcanoes, Pico Alto and Santa Bárbara, constitute the northern and western sectors of the island, respectively, while the fissure zone bisects Terceira from WNW to ESE and extends offshore. Pico Alto and Santa Bárbara volcanoes and the fissure zone are active systems with coeval activity in the last millennia (e.g., Pimentel et al., 2016, 2021; Self, 1976), see Fig. 2.

The stratigraphy of Terceira is organized into two main lithostratigraphic groups (Self, 1974) separated by the Lajes-Angra Ignimbrite, dated at ca. 25 cal ka BP, which corresponds to the main stratigraphic marker horizon of the island (Fig. 2). The Lower Terceira Group comprises all volcanic products older than 25 ka, including at least six main pyroclastic formations containing ignimbrites, associated with caldera-forming events of Pico Alto volcano and, possibly, Guilherme Moniz. On the other hand, the Upper Terceira Group includes all products younger than 25 ka of alternating eruptions of the fissure zone, Santa Bárbara, and Pico Alto volcanoes (e.g., Gertisser et al., 2010; Pimentel et al., 2021; Self, 1976).

A. Pimentel (✉)
Research Institute for Volcanology and Risk Assessment (IVAR), University of the Azores, Ponta Delgada, Azores, Portugal
e-mail: adriano.hg.pimentel@azores.gov.pt

Centre for Information and Seismovolcanic Surveillance of the Azores (CIVISA), Ponta Delgada, Azores, Portugal

A. Malheiro et al. (eds.), *Advances in Natural Hazards and Volcanic Risks: Shaping a Sustainable Future*, Advances in Science, Technology & Innovation, https://doi.org/10.1007/978-3-031-25042-2_36

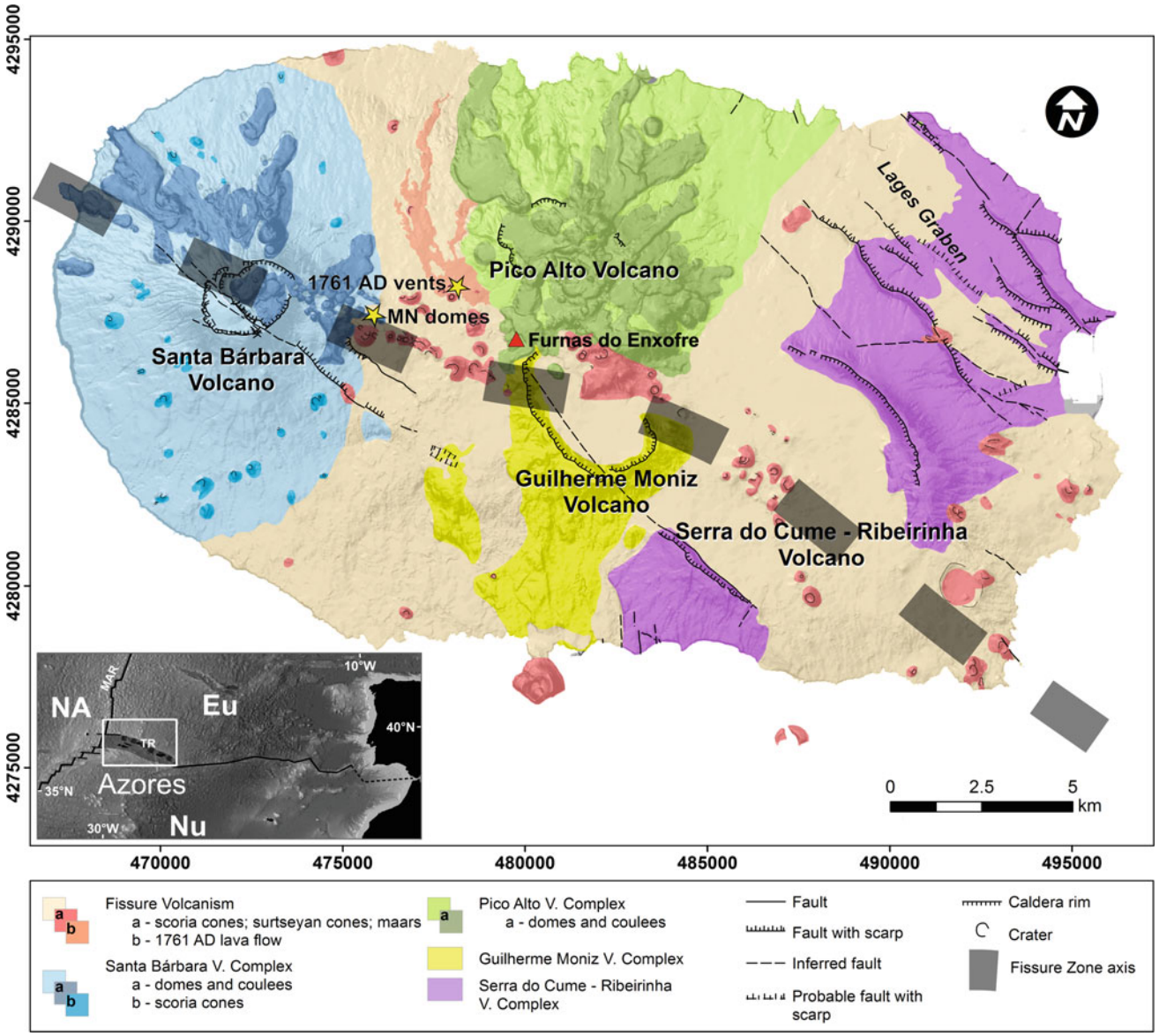

Fig. 1 Geological map of Terceira (modified from Madeira, 2005; in Pimentel et al., 2016), showing the site of the fumarolic field of Furnas do Enxofre, the basaltic lava flow and scoria cones of the 1761 eruption, and the Mistérios Negros (MN) lava domes. Inset illustrates the geodynamic setting of the Azores (NA: North American plate, MAR: Mid-Atlantic Ridge, Eu: Eurasian plate, Nu: Nubian plate, TR: Terceira Rift)

Historical eruptions (i.e., since the island's settlement around 1450) have occurred both on land and offshore. The first records of volcanic activity correspond to the 1761 events in the centre of Terceira (Fig. 1), with the extrusion of trachytic lava domes and a Hawaiian/Strombolian eruption that emitted a basaltic lava flow (Pimentel et al., 2016). Two other eruptions were reported in 1867 and in 1998–2001 on the Serreta submarine ridge, located off the west coast of the island, the latter of which produced basaltic lava balloons (Casas et al., 2018; Gaspar et al., 2003).

The field trip itinerary includes eight sites, starting from the older part of Terceira (east side) and ending in the younger part (west side) (Fig. 3), where it is possible to observe the main tectonic structures of the island, large calderas and their associated deposit (in particular ignimbrites), lava domes and coulées, as well as volcanic

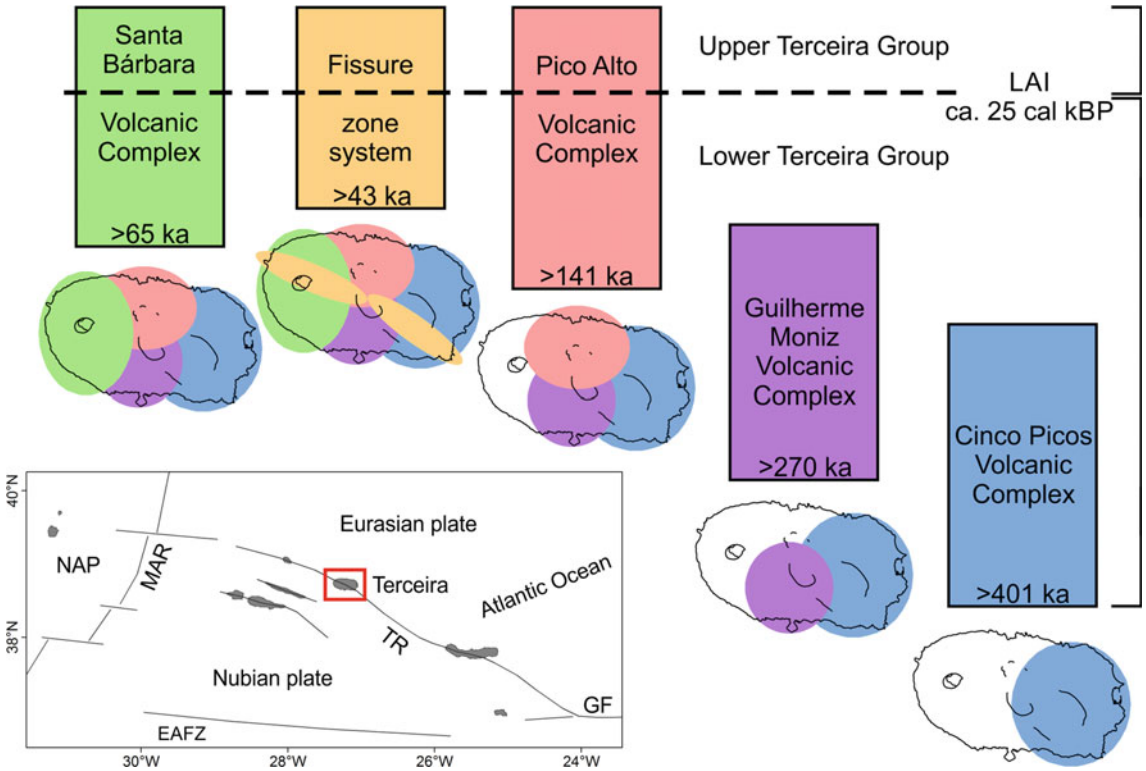

Fig. 2 Scheme of the stratigraphy and evolution of Terceira (after Pimentel et al., 2021) (LAI: Lajes-Angra Ignimbrite Formation). Oldest ages of volcanic systems are sourced from Calvert et al. (2006), Gertisser et al. (2010) and Hildenbrand et al. (2014). Inset illustrates the location of Terceira in the archipelago of the Azores and the main tectonic structures (NAP: North American plate, TR: Terceira Rift, MAR: Mid-Atlantic Ridge, GF: Gloria Fault, EAFZ: East Azores Fracture Zone)

features associated with recent and historical volcanism. The visit to the volcanic caves of Terceira undoubtedly marks this unique experience.

2 Sites of the Field Trip

2.1 Site A: Angra Do Heroísmo

The itinerary starts and finishes in Angra do Heroísmo, the main city of Terceira and a UNESCO World Heritage Centre. Angra do Heroísmo is known for its traditional architecture and archaeological heritage, despite severe damage resulting from the 1 January 1980 earthquake of magnitude 7.2. The city centre was successfully rebuilt in the following years and is now a colourful and vibrant place worth visiting.

2.2 Site 1: Serra Do Cume

Serra do Cume viewpoint is one of the best places to observe the older part of the island. The eastern third of Terceira is formed by the Cinco Picos volcano (Fig. 4), also known as Serra do Cume-Ribeirinha volcano, which is considered extinct. The eruptive history of Cinco Picos is still not fully understood, but it is thought to have started during the Pleistocene, and the caldera formation is estimated to have occurred less than 280 ka. From the top of Serra do Cume it is possible to observe the Cinco Picos caldera, with a diameter of approximately 7 km (the largest in the Azores). This central volcano is partially eroded and covered by younger products of adjacent volcanoes (Pico Alto and Guilherme Moniz), but the caldera walls are preserved in the northeast by Serra do Cume and in the southwest by Serra da Ribeirinha. The caldera is floored by basaltic lava flows and associated scoria cones related to the fissure zone (Fig. 5).

2.3 Site 2: Serra Do Facho

The oldest dated rocks of Terceira (401 ± 6 ka; Hildenbrand et al., 2014) crop out along the road from Praia da Vitória to the Serra do Facho viewpoint. These rocks correspond to a nearly horizontal sequence of basaltic lava flows on the east side of Cinco Picos volcano (Fig. 6). From the Serra do

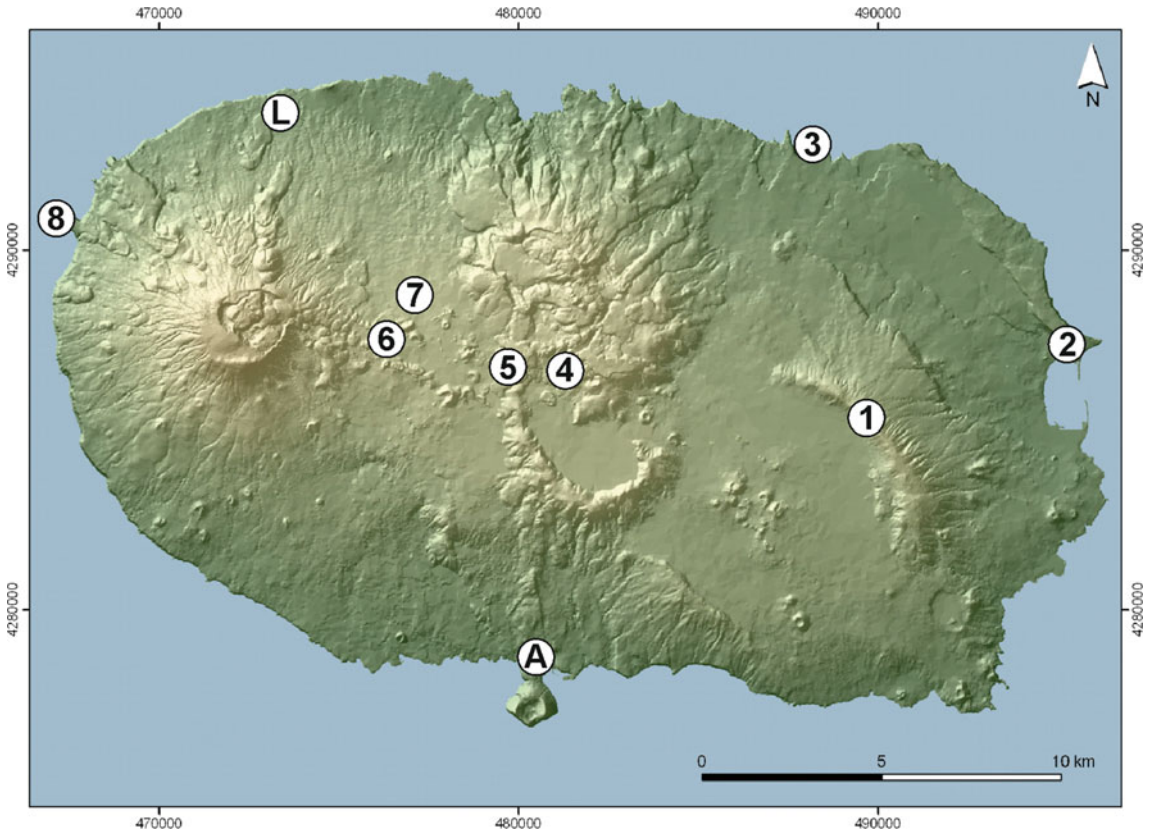

Fig. 3 Itinerary of field trip 2 of the NATHAZ22 Workshop. A: Angra do Heroísmo, 1: Serra do Cume, 2: Serra do Facho, 3: Ponta das Escaleiras, L: Lunch, 4: Algar do Carvão, 5: Furnas do Enxofre, 6: Gruta do Natal and Mistérios Negros, 7: 1761 Hawaiian/Strombolian eruption, 8: Ponta da Serreta

Facho viewpoint it is possible to observe the Lajes Graben, the main tectonic structure of Terceira, which cuts the older northeast sector of the island (Fig. 7). Two main normal-dextral faults trending NW–SE define the graben: the Lajes Fault to the northeast (SW-plunging) and the Fontinhas Fault to the southwest (NE-dipping). The Lajes Graben is 8 km long and 3 km wide in the subaerial part of the island, but it extends offshore for several kilometres. In addition, subsidiary faults cross the floor of the graben with the same NW–SE trend. The historical earthquakes that occurred on 24 May 1614 and 15 June 1841 generated surface ruptures in the graben faults, which caused great destruction and at least 200 deaths.

2.4 Site 3: Ponta Das Escaleiras

Ponta das Escaleiras on the north coast of Terceira is a key site to observe the old stratigraphy of the island (i.e., the Lower Terceira Group), particularly the main pyroclastic formations. These formations are dominated by ignimbrites of peralkaline silicic composition that were erupted within a limited period dated from ca. 86 ka to 25 cal ka BP (Fig. 8). These are closely related to caldera-forming events of Pico Alto and, possibly, also Guilherme Moniz. The outcrop at Ponta das Escaleiras starts with a basaltic lava flow, probably from the Cinco Picos volcano, which is covered by the Caldeira-Castelinho Ignimbrite Formation (71–83 ka),

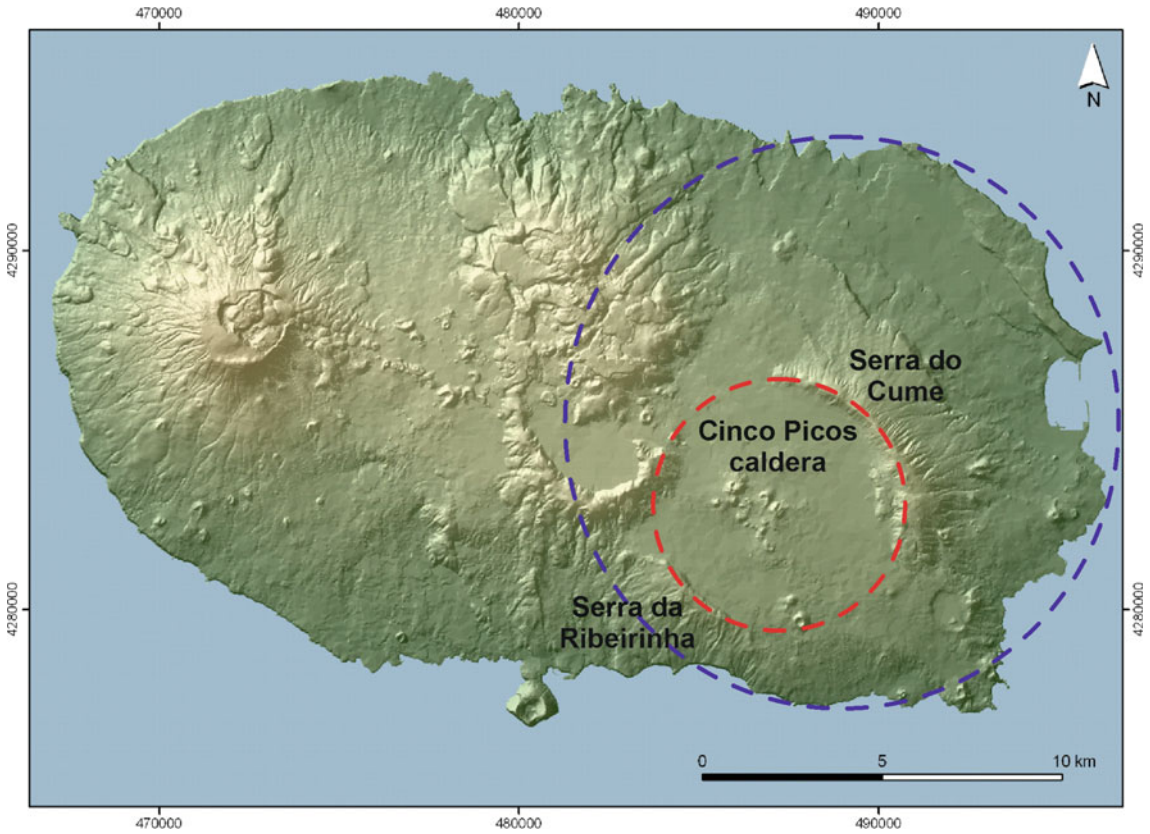

Fig. 4 Location of Cinco Picos central volcano in the eastern part of Terceira (blue dashed line marks the approximate subaerial extent of the volcano). Serra do Cume (at NE) and Serra da Ribeirinha (at SW) correspond to the preserved walls of the Cinco Picos caldera (red dashed line marks the reconstruction of the caldera)

Fig. 5 Panoramic view from the top of Serra do Cume looking to the floor of Cinco Picos caldera. Picos Alto (right side) and Guilherme Moniz (left side) are seen in the background, and a glimpse of Santa Bárbara behind them

Fig. 6 Old basaltic lava flows that form the east side of Cinco Picos volcano, cropping out on the southeast end of the Lajes Fault scarp

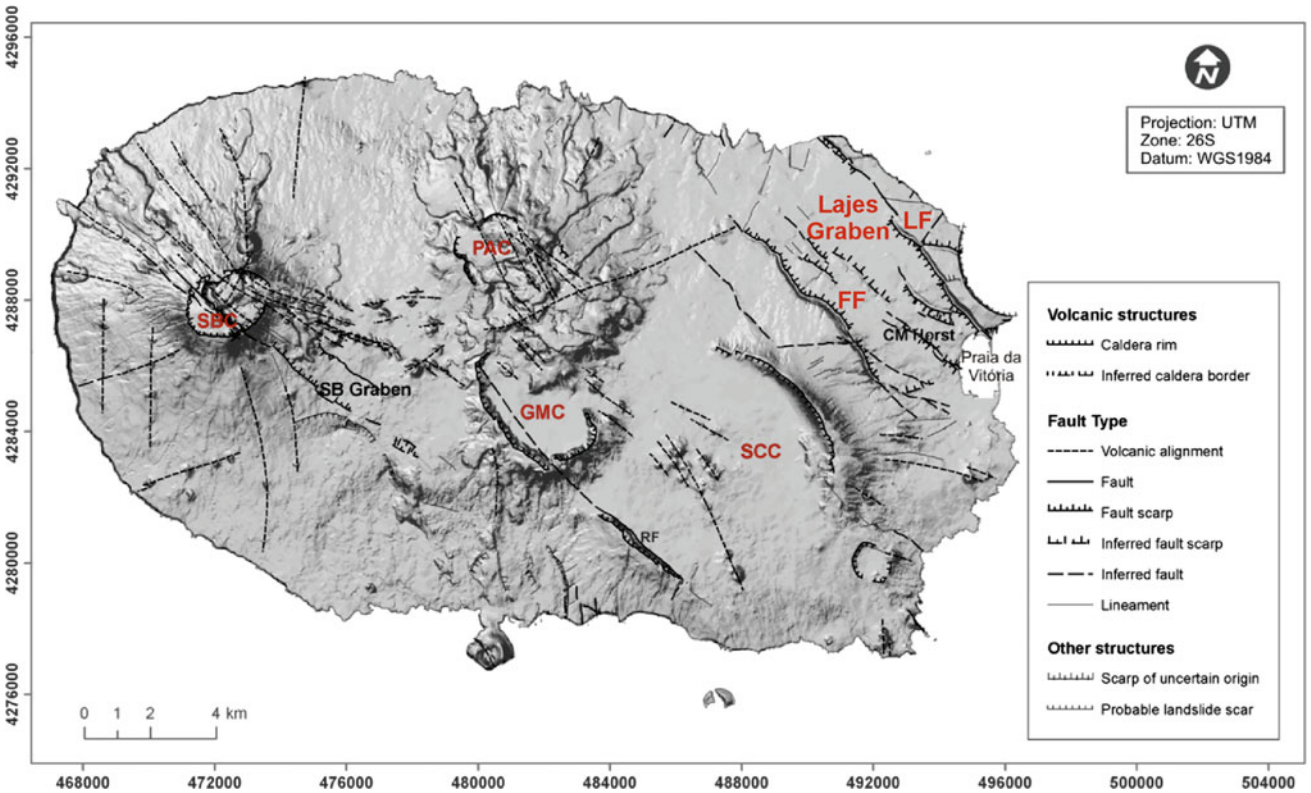

Fig. 7 Tectonic sketch of Terceira (after Madeira et al., 2015) (LF: Lajes Fault, FF: Fontinhas Fault, CM Horst: Cruz do Marco Horst, SCC: Serra do Cume-Ribeirinha Caldera, GMC: Guilherme Moniz Caldera, PAC: Pico Alto Caldera, SBC: Santa Bárbara Caldera, RF: Ribeirinha Fault, SB Graben: Santa Bárbara Graben)

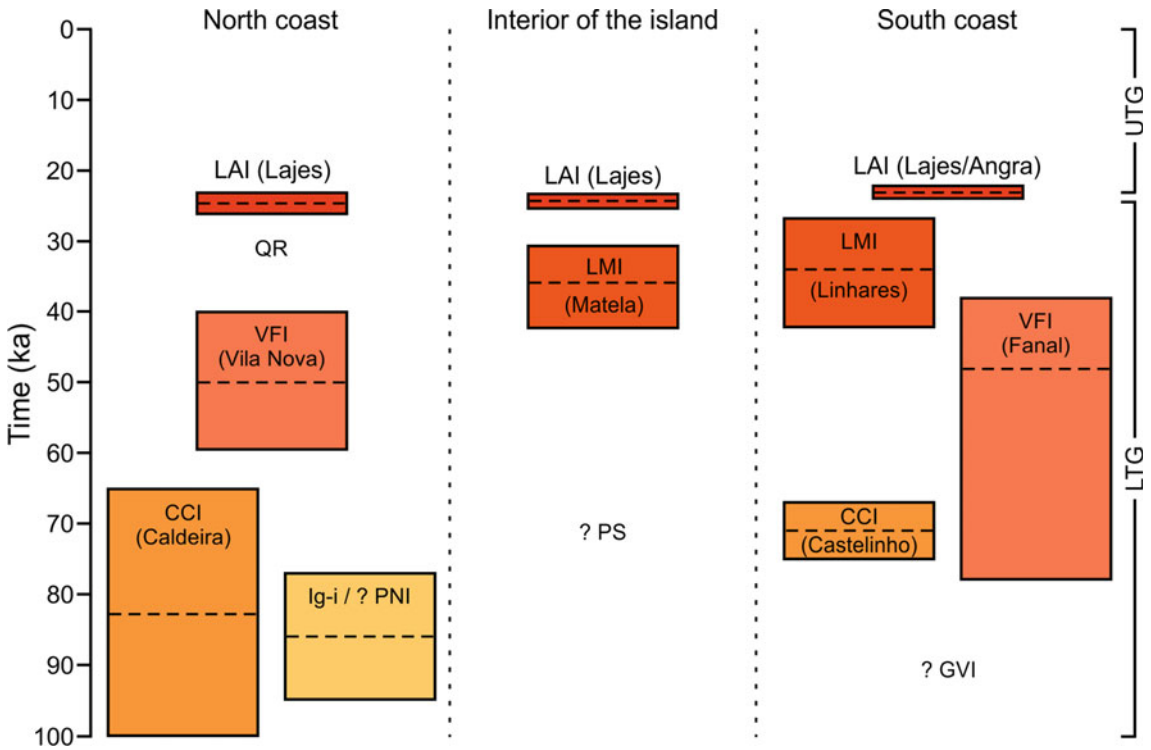

Fig. 8 Correlation scheme of Terceira's ignimbrite-bearing formations, with average ages (dashed lines) and maximum errors (size of the boxes is proportion to dating errors) (after Gertisser et al., 2010, in Pimentel et al., 2021). Ignimbrite members (in parenthesis) found in the north, south, and interior of the island are identified (LAI: Lajes-Angra Ignimbrite Formation, LMI: Linhares-Matela Ignimbrite Formation, QR: Quatro Ribeiras pyroclastic current deposit, VFI: Vila Nova-Fanal Ignimbrite Formation, CCI: Caldeira-Castelinho Ignimbrite Formation, PS: Posto Santo spatter-flow deposit, PNI: Pedras Negras Ignimbrite Formation, Ig-I: Ignimbrite I Formation, GVI: Grota do Vale Ignimbrite Formation)

followed by an undifferentiated sequence of tuffs and palaeosoils. This sequence is covered by the Vila Nova-Fanal Ignimbrite Formation (47–58 ka), which also contains some associated pumiceous fall beds, and is unconformably overlain by another undifferentiated sequence of tuffs and palaeosoils. At the top crops out the Lajes-Angra Ignimbrite Formation (ca. 25 cal ka BP), the youngest ignimbrite formation on the island (Fig. 9).

2.5 Site L: Lunch at Altares

Lunch at a traditional restaurant in the parish of Altares, located on the north coast of Terceira. Altares is known for its traditional rural architecture and typical Terceirean dishes such as Alcatra, Sopas do Espírito Santo and Arroz Doce.

2.6 Site 4: Algar Do Carvão

Algar do Carvão is a volcanic pit in the middle of the island, where the fissure zone intersects Pico Alto volcano. This volcanic pit was formed in two distinct phases. The older part is related to a peralkaline trachytic lava of Pico Alto with an age of ca. 3200 years, while the younger part of the cave corresponds to the drained conduit of a small scoria cone that erupted 1730 years ago, associated with the characteristic basaltic activity of the fissure zone (Fig. 10). This volcanic pit contains exceptional examples of silica stalactites and stalagmites that result from rainwater percolation through the trachytic country rock. A lake with clear blueish waters is found at the bottom of the volcanic pit, at approximately 80 m depth (Fig. 11).

2.7 Site 5: Furnas Do Enxofre

The fumarolic field of Furnas do Enxofre is one of the few examples of secondary manifestations of volcanism on Terceira Island (Fig. 12). It is situated in the middle of the island, on the southeast of Pico Alto, approximately 1.5 km west of Algar do Carvão volcanic pit. Furnas do Enxofre fumarolic field comprises two main zones with visible fumarolic emissions and temperature anomalies (up to 97 °C). The main zone sits atop an old trachytic lava dome (called Galhardo), which is surrounded by the branches of a younger

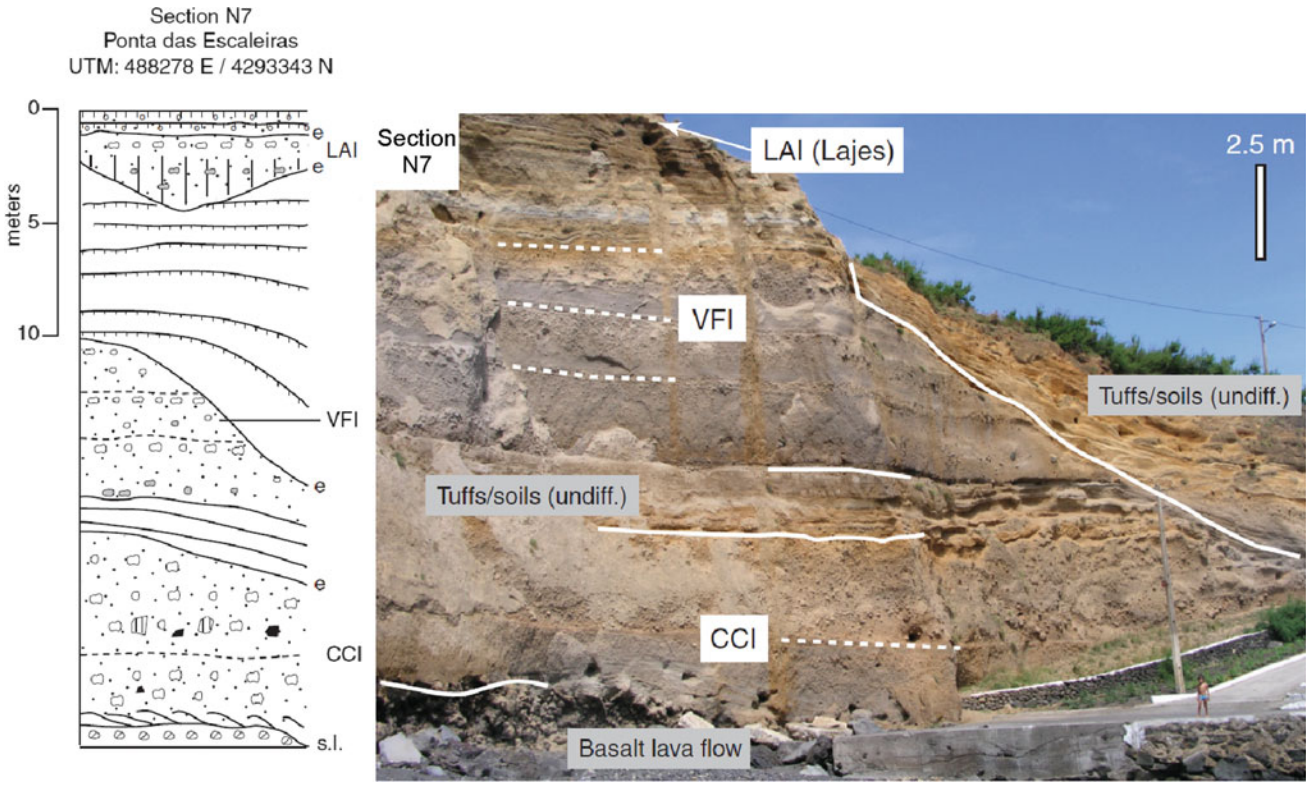

Fig. 9 Stratigraphic section at Ponta das Escaleiras coastal cliff showing a sequence of ignimbrite formations alternating with undifferentiated tuffs and palaeosoils (in Gertisser et al., 2010). Abbreviations are the same as in Fig. 8

Fig. 10 Interior of Algar do Carvão volcanic pit, showing the remnants of a thin film of basaltic lava covering the trachytic country rock (photo by Jorge Góis—gently shared by Associação Os Montanheiros)

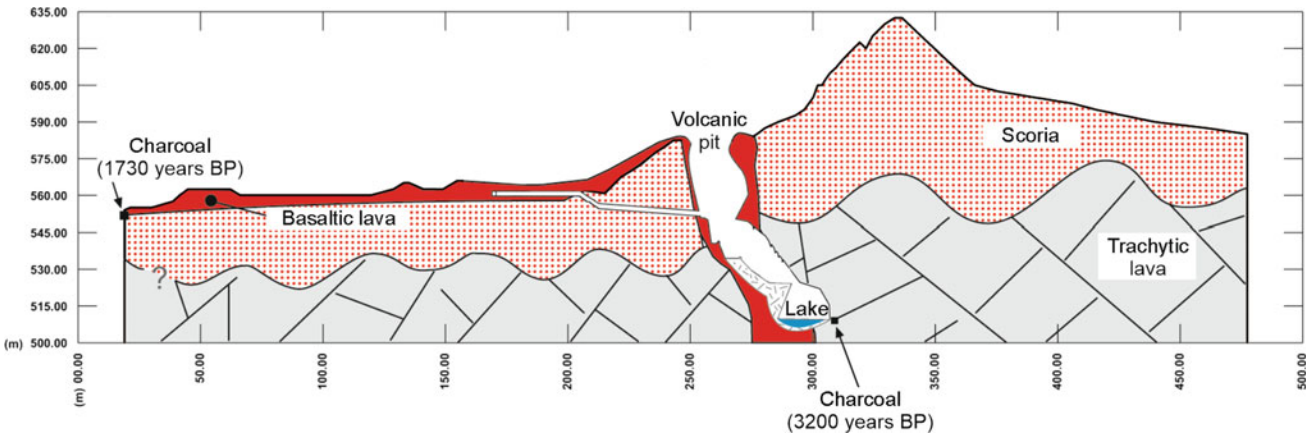

Fig. 11 Geologic profile of Algar do Carvão 1:2000 scale (after Associação Os Montanheiros)

Fig. 12 View of Furnas do Enxofre fumarolic field where it is possible to observe the area without vegetation, which is indicative of high soil temperature and CO_2 flux

coulée (known as Enxofre), while a smaller degassing zone is located at the contact between the dome and the southern branch of the coulée (Fig. 13). This geothermal area is crossed by a set of faults with different directions, trending NW–SE, E–W and NNE–SSW.

2.8 Site 6: Gruta Do Natal and Mistérios Negros

Gruta Natal is a volcanic cave consisting of a basaltic lava tube (Fig. 14) formed by the eruptive episode of the Pico do Gaspar fissure system less than 12,000 years ago (Nunes et al., 2014). This lava tube has a length of 700 m and a maximum height of 12 m (Fig. 15). In the cave's interior there are many interesting features, including lava stalactites, flow ledges or flow lines, and different lava textures. Since 1969, every year on Christmas day there is a religious celebration inside the cave and hence its present name (Natal meaning Christmas).

Outside of Gruta do Natal cave it is possible to see the Mistérios Negros, a chain of trachytic domes located on the east side of Santa Bárbara volcano (Fig. 16). Until recently, the age of these lava domes was a matter of debate. However, a new study (Pimentel et al., 2016) demonstrated that they were coeval with the 1761 Hawaiian/Strombolian eruption in the fissure zone. It is envisaged that the

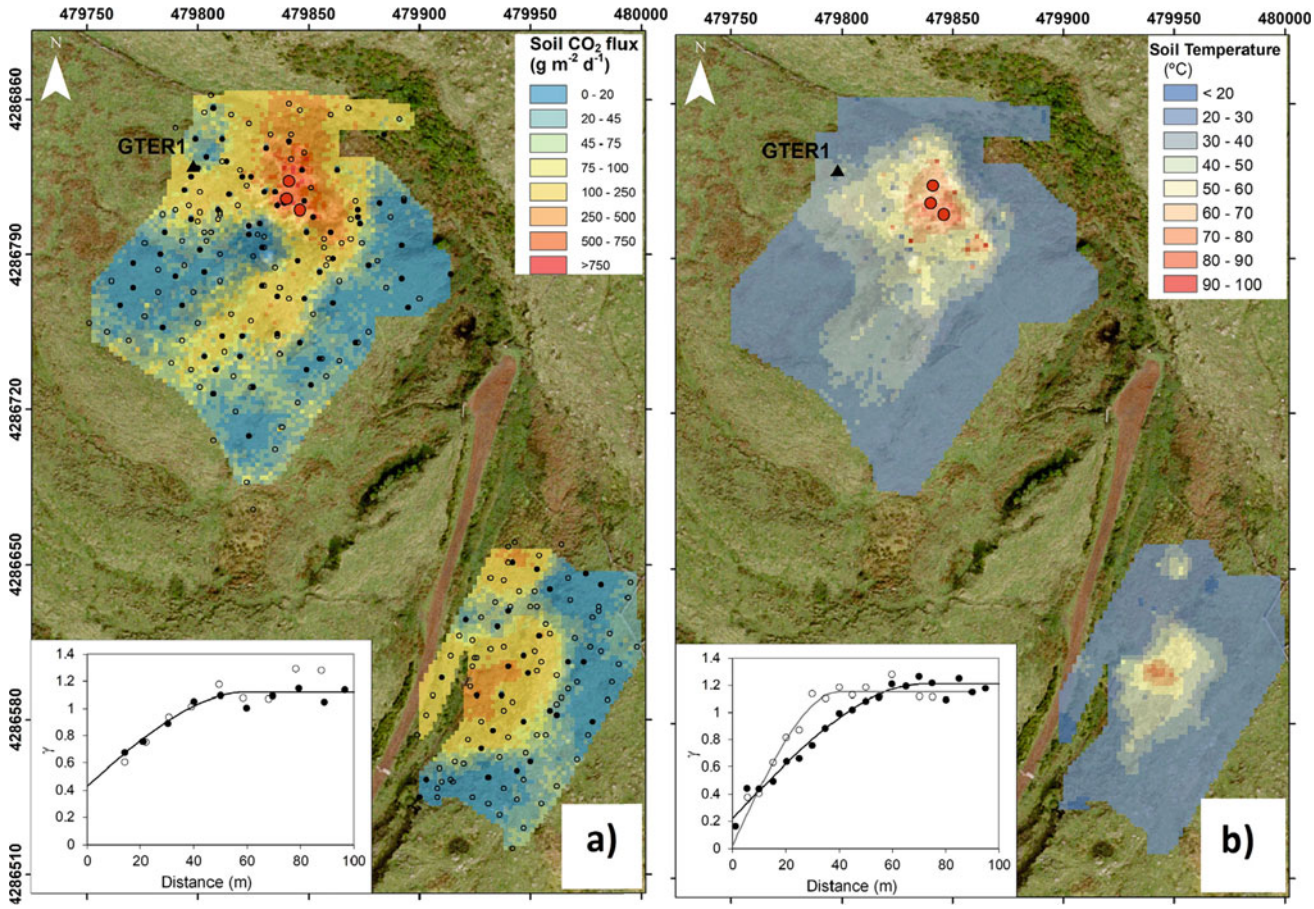

Fig. 13 Soil CO_2 flux (**a**) and temperature (**b**) maps for Furnas do Enxofre fumarolic filed (data from August 2014). Red circles correspond to fumaroles, while dots correspond to sampling sites (after Viveiros et al., 2020)

extrusion of the domes was triggered by changes in local stress due to a basaltic dike intrusion in the fissure zone. This intrusion created favourable stress conditions for the ascent of a partially degassed batch of trachytic magma stored beneath Santa Bárbara.

2.9 Site 7: 1761 Hawaiian/Strombolian Eruption

On 21 April 1761, a Hawaiian/Strombolian-style eruption started in the central area of the fissure zone, approximately 1 km ENE of Pico Gordo. This basaltic eruption produced a line of scoria cones (oriented ENE-WSW to E-W) and a lava flow that spread in different directions and reached the parish of Biscoitos in the north part of Terceira, where at least 27 houses were buried (Fig. 17). Small trachytic lava domes (Mistérios Negros) were also erupted in this period on the east side of Santa Bárbara (see site 6). At site 7, it is possible to see the line of scoria cones formed during this eruption, in particular, Pico Vermelho and Pico do Fogo (Fig. 18) and the basaltic lava flow that follows by the side of the road, which is locally called Mistério Novo (which means New God's Mystery). Pico Vermelho cone is almost entirely quarried out, but Pico do Fogo retains a preserved conical morphology.

2.9.1 Site 8: Ponta Da Serreta

Ponta da Serreta corresponds to a trachytic coulée that extends for approximately 800 m into the sea (Fig. 19). According to Self (1976), this highly viscous lava records one of the most recent eruptions of the Santa Bárbara volcano, which probably occurred just prior to the discovery of the island (i.e., sometime before 1450). Ponta de Serreta coulée exhibits various textures typical of trachytic lavas, including blocky surface, shear features, etc.

Looking inland, the west coast of Terceira can be observed at the same location, particularly the nearly horizontal sequence of basaltic lava flows and the remnants of a

Fig. 14 View of the lava tube of Gruta do Natal (photo by Jorge Góis—gently shared by Associação Os Montanheiros)

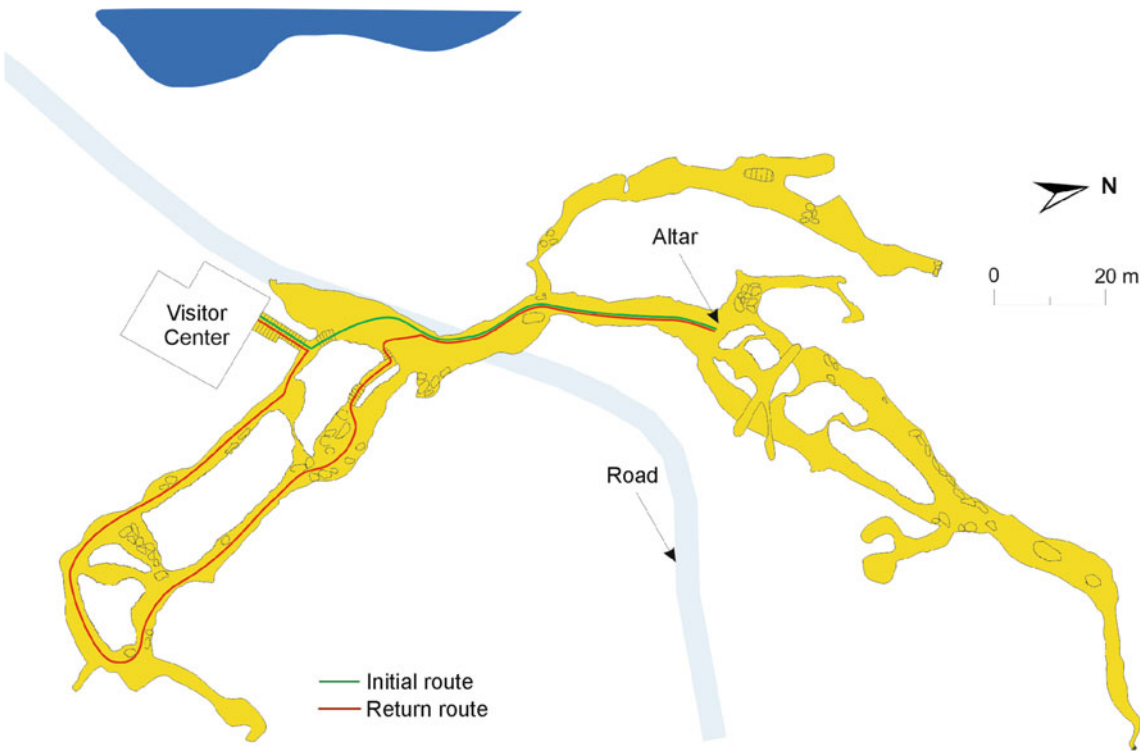

Fig. 15 Map of Gruta do Natal lava tube system with the location of the visitor centre and the road (after Associação Os Montanheiros)

Fig. 16 Alignment of lava domes known as Mistérios Negros (A) on the eastern flank of Santa Bárbara (after Pimentel et al., 2016)

scoria cone that form the older part (the shield stage) of Santa Bárbara volcano. Finally, looking offshore towards the west, approximately 10 km from land, is the site of the last volcanic eruption recorded in the archipelago of the Azores, which occurred in 1998–2001 on the Serreta submarine ridge and was characterized by the formation of lava balloons of basaltic composition that floated at the sea surface (Fig. 20).

3 Final Remarks

Terceira Island is noteworthy for its geodiversity, particularly in the context of oceanic volcanic islands. Its geological diversity results from the close interaction between tectonic and magmatic processes and the bimodal geochemistry of its rocks. The active tectonics of Terceira is well expressed by several NW–SE-oriented faults of the Lajes Graben, on the northeast sector of Cinco Picos volcano, but also by the volcanic fissure zone that crosses the entire island diagonally from WNW to ESE. In both cases, these geological structures extend far beyond the subaerial part of the island for several kilometres offshore. The Lajes Graben generated some of the most devastating earthquakes recorded in the Azores in historical times (1614 and 1841), and therefore its potential to generate future destructive earthquakes should not be overlooked.

Among the islands of the Azores, Terceira is the one with the highest production of peralkaline silicic magmas, which have erupted explosively, producing ignimbrites, and effusively, forming lava domes and coulées. Ponta das Escaleiras on the north coast is one of the best places to observe an extensive sequence of ignimbrite formations erupted from Pico Alto and, maybe, Guilherme Moniz. Ignimbrites result from the deposition of pumiceous pyroclastic density currents (i.e., fast-moving mixtures of volcanic particles and hot gases that flow along the topography under the influence of gravity) and are considered the most hazardous volcanic phenomena. Even small ignimbrite-forming eruptions can have devastating impacts on oceanic islands due to their small size and remote location, making risk mitigation and emergency management very challenging. On the other hand, when peralkaline silicic magmas erupt effusively, they form highly viscous lavas (domes or coulées), which are widely abundant on Pico Alto and Santa Bárbara volcanoes. Some of the best preserved examples of these trachytic lavas, containing pristine structures and textures, are the Mistérios Negros lavas domes (erupted in 1761) and the Ponta de Serreta coulée on the west coast of the island.

Historical volcanic eruptions on Terceira occurred both on land and at sea but always along the fissure zone that transects the island. The first in 1761 was in the central sector of the fissure zone, located between Santa Bárbara and Pico Alto, and was characterized by a Hawaiian/Strombolian-style eruption, accompanied by the inconspicuous eruption of the Mistérios Negros domes. While the 1867 and 1998–2001 eruptions were centred on the Serreta submarine ridge, which corresponds to the western offshore segment of the fissure zone. In all three cases, the eruptions did not cause victims, and there was only property loss in the parish of Biscoitos, where a lava flow destroyed approximately 27 houses.

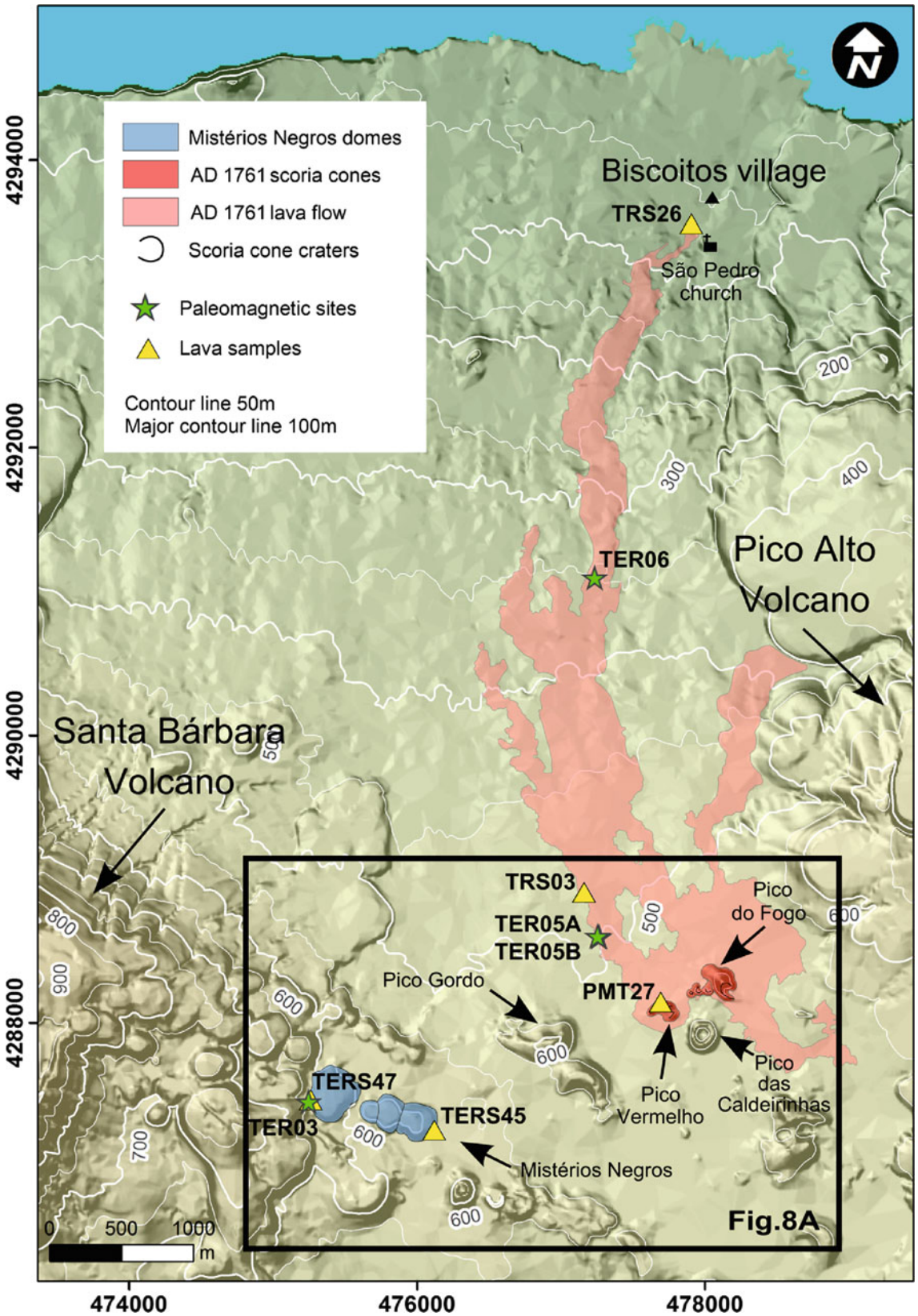

Fig. 17 Map showing the extent of 1761 basaltic lava flow and the associated Pico Vermelho and Pico do Fogo scoria cones. The lava domes of Mistérios Negros are also shown on the east slope of Santa Bárbara (in Pimentel et al., 2016)

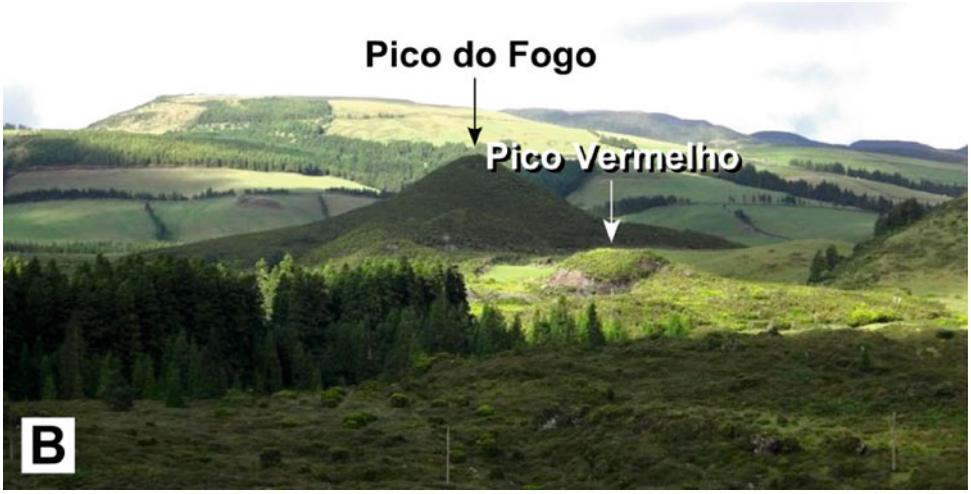

Fig. 18 Scoria cones formed during the 1761 Hawaiian/Strombolian eruption (B), with the Pico Vermelho cone (intensively quarried) in front of Pico do Fogo (after Pimentel et al., 2016)

Fig. 19 Google Earth image of Ponta da Serreta trachytic coulée

Finally, it is worth mentioning the Furnas do Enxofre fumarolic field as the main example of secondary manifestations of volcanism on the island, which corresponds to a geothermal area with high soil temperature and CO_2 flux. In addition, the volcanic caves of Terceira include easily visitable, world-class examples of different types and origin, such as the Gruta do Natal lava tube with its lava stalactites and flow ledges or the Algar do Carvão volcanic pit rich in silica stalactites and stalagmites, and a clear water lake.

Fig. 20 Aerial view of floating lava balloons (black spots) degassing at the sea surface during the Serreta submarine ridge eruption in 1998–2001 (after Gaspar et al., 2003)

References

Calvert, A. T., Moore, R. B., McGeehin, J. P., & Rodrigues da Silva, A. M. (2006). Volcanic history and 40Ar/39Ar and 14C geochronology of Terceira Island, Azores, Portugal. *Journal of Volcanology and Geothermal Research, 156*, 103–115.

Casas, D., Pimentel, A., Pacheco, J., Martorelli, E., Sposato, A., Ercilla, G., Alonso, B., & Chiocci, F. (2018). Serreta 1998–2001 submarine volcanic eruption, offshore Terceira (Azores): Characterization of the vent and inferences about the eruptive dynamics. *Journal of Volcanology and Geothermal Research, 356*, 127–140.

Gaspar, J. L., Queiroz, G., Pacheco, J. M., Ferreira, T., Wallenstein, N., Almeida, M. H., & Coutinho, R. (2003). Basaltic lava balloons produced during the 1998–2001 Serreta submarine ridge eruption (Azores). In J. D. L. White, J. L. Smellie, & D. A. Clague (Eds.), *Explosive subaqueous volcanism. AGU Geophysical Monograph, 140*, 205–212.

Gertisser, R., Self, S., Gaspar, J. L., Kelley, S. P., Pimentel, A., Eikenberg, J., Barry, T. L., Pacheco, J. M., Queiroz, G., & Vespa, M. (2010). Ignimbrite stratigraphy and chronology on Terceira Island, Azores. In: G. Groppelli, & L. Viereck-Goette (Eds.), *Stratigraphy and geology of volcanic areas*. GSA Special Paper 464 (pp. 133–154).

Hildenbrand, A., Weis, D., Madureira, P., & Marques, F. O. (2014). Recent plate re-organization at the Azores Triple junction: Evidence from combined geochemical and geochronological data on Faial, S. Jorge and Terceira volcanic islands. *Lithos, 210–211*, 27–39.

Madeira, J. (2005). The volcanoes of Azores Islands: A world-class heritage. Examples from Terceira, Pico and Faial Islands. In: *IV International Symposium ProGEO on the Conservation of the Geological Heritage - Field Trip Guidebook*. Universidade do Minho, Braga.

Madeira, J., Brum da Silveira, A., Hipólito, A., & Carmo, R. (2015). Active tectonics in the central and eastern Azores islands along the Eurasia-Nubia boundary: A review. In J. L. Gaspar, J. E. Guest, A. M. Duncan, F. J. A. S. Barriga, & D. K. Chester (Eds.), *Volcanic Geology of São Miguel Island (Azores Archipelago)* (pp. 15–32). Geological Society of London.

Nunes, J. C., Calvert, A., Medeiros, S., Lima, E. A., Pereira, F., Costa, M. P., Barcelos, P., & Carvalho, M. R. (2014). Geological mapping of the central area of Terceira Island (Azores, Portugal): Associated volcanostratigraphy, ages and genetic implications on the Malha-Balcões-Chamusca lava caves system. *Comunicações Geológicas, Lisbon, 101*, 283–288.

Pimentel, A., Self, S., Pacheco, J. M., Jeffery, A. J., & Gertisser, R. (2021). Eruption style, emplacement dynamics and geometry of peralkaline ignimbrites: Insights from the Lajes-Angra Ignimbrite Formation, Terceira Island, Azores. *Frontiers in Earth Science, 9*, 673686.

Pimentel, A., Zanon, V., de Groot, L. V., Hipólito, A., Di Chiara, A., & Self, S. (2016). Stress-induced comenditic trachyte effusion triggered by trachybasalt intrusion: Multidisciplinary study of the AD 1761 eruption at Terceira Island (Azores). *Bulletin of Volcanology, 78*, 22.

Self, S. (1974). *Recent volcanism on Terceira, Azores*. Imperial College, University of London, London (Ph.D. Thesis). http://hdl.handle.net/10044/1/20874

Self, S. (1976). The recent volcanology of Terceira, Azores. *Journal of the Geological Society of London, 132*, 645–666.

Viveiros, F., Chiodini, G., Cardellini, C., Caliro, S., Zanon, V., Silva, C., Rizzo, A. L., Hipólito, A., & Moreno, L. (2020). Deep CO_2 emitted at Furnas do Enxofre geothermal area (Terceira Island, Azores archipelago). An approach for determining CO_2 sources and total emissions using carbon isotopic data. *Journal of Volcanology and Geothermal Research, 401*, 106968.

Volcanological Features of Terceira Island (Azores): A Field Approach Around Hazards

João Carlos Nunes

Abstract

Terceira Island (400 km^2 area and the second most inhabited of the archipelago) comprises four polygenetic volcanoes with caldera (Cinco Picos, Guilherme Moniz, Santa Bárbara and Pico Alto central volcanoes) and an area of active fissural basaltic volcanism, split into two main sectors of the island, on its central and southeast zones. Impressive siliceous effusive volcanism products mark the island's geology and landscape as numerous domes and coulees: a total of about 160 eruptive centres of this type can be observed on the island, especially on the Santa Bárbara and Pico Alto volcanoes, with a clear morphological signature. Historical volcanism dates back to the eighteenth century, with land eruptions in 1761 (the "Mistérios Negros" and the "Mistério Novo" areas) and submarine eruptions in 1867 and 1998–2001, the latter in the Serreta submarine ridge. This work outlines a field trip on Terceira Island, emphasising its geological characteristics and geohazards.

Keywords

Polygenetic volcanoes • Domes and coulées • Active volcanism • Earthquakes • Terceira Island

1 Terceira Island General Volcano-Tectonic Framework

Terceira Island is located on a WNW-ESE spreading centre, named Terceira Rift, that extends for about 550 km along Graciosa, Terceira and São Miguel islands until south of the Formigas Trough, where it meets the GLORIA Fault (Fig. 1). The Terceira Rift generally establishes the northeast edge of the "Azores Block", a sheared area of the Azores Plateau that corresponds to a complex and non-linear boundary of the Azores Triple Junction (ATJ) between the Eurasian and the African tectonic plates. The Mid-Atlantic Ridge establishes the boundary between these two plates and the North American tectonic plate and corresponds to the western linear/discrete boundary of the ATJ.

Terceira Island comprises four central polygenetic volcanoes with a summit subsidence caldera (from east to west: Serra do Cume, Guilherme Moniz, Pico Alto and Santa Bárbara) and a Basaltic Fissural Zone, the latter mostly in the central and SE parts of the island (Fig. 2). Volcanic products extruded from these central volcanoes show a wide variety of rock compositions and include ignimbrites, pumice fall deposits, domes and coulée-type silicious lava flows, scoria and spatter deposits, surtseyan tuffs and basaltic lava flows.

The dominant monogenetic eruptive centres in Terceira Island are scoria cones of basaltic (s.l.) composition and domes, and coulées-type lava flows, as impressive thick siliceous (s.l.) lava flows, often with obsidian layers. Those landforms are especially abundant on the Santa Bárbara and Pico Alto volcanoes, either on their flanks or infilling almost completely its top calderas: a total of about 115 domes and coulées are emplaced on the flanks of those central volcanoes (Table 1), a unique feature of Azores Islands volcanism and a peculiar characteristic of Terceira Island geodiversity.

Figure 3 presents the itinerary of a field trip on Terceira Island, highlighting its main geological characteristics.

J. C. Nunes (✉)
Geosciences Department, Faculty of Sciences and Technology, University of Azores, Ponta Delgada, Azores, Portugal
e-mail: joao.cc.nunes@uac.pt

A. Malheiro et al. (eds.), *Advances in Natural Hazards and Volcanic Risks: Shaping a Sustainable Future*, Advances in Science, Technology & Innovation, https://doi.org/10.1007/978-3-031-25042-2_37

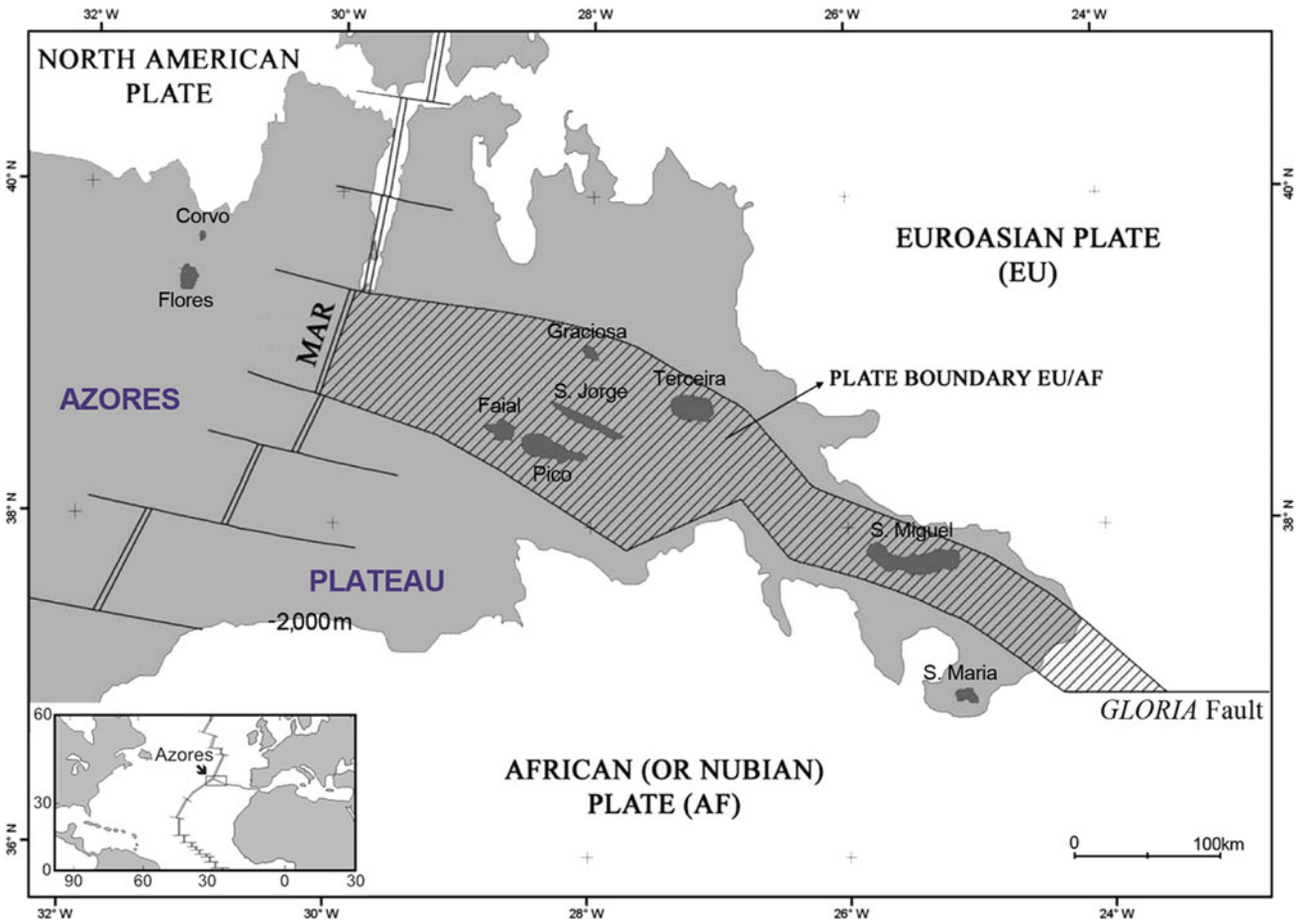

Fig. 1 Geotectonic framework of the Azores Triple Junction. *MAR*: Mid-Atlantic Ridge; gray area indicates the "Azores Plateau"; shaded area corresponds to the "Azores Block", the diffuse plate boundary between European and African plates

2 Description of Field Sites

Site 1: Angra do Heroísmo and Monte Brasil surtseyan tuff cone

Heavily damaged by the January 1st, 1980 earthquake (16h42 TMG; ML = 7.2; MMI = VIII/IX 61 deaths), the Angra do Heroísmo city was rebuilt, keeping its historical centre preserved, allowing its classification in 1983 as a UNESCO World Heritage Site, in recognition to its urban design with a Renaissance layout and its geostrategic importance in the "Carreira das Índias" sea corridor during the Portuguese discovery's epoch. Several normal faults with a general N–S trend, such as the Memória Fault, cross the urban area and its surroundings, often as fault scarps with a clear topographic signature (Figs. 4 and 5).

Overlooking the city, the Monte Brasil cone is the bigger Azorean cone formed by a basaltic submarine eruption of surtseyan type, which tuff material was used to build the São João Baptista fortress and the great wall that encircles the cone. Impressive moulds of the primitive and endemic flora of the area destroyed by the Monte Brasil Holocene eruption were preserved on the tuff deposit, which can be seen, together with other magnificent geological samples, at the "Museu Vulcanoespeleológico" (Volcanospeleological Musem) exhibition, of the "Os Montanheiros", a non-government organization association (NGO), in Angra do Heroísmo.

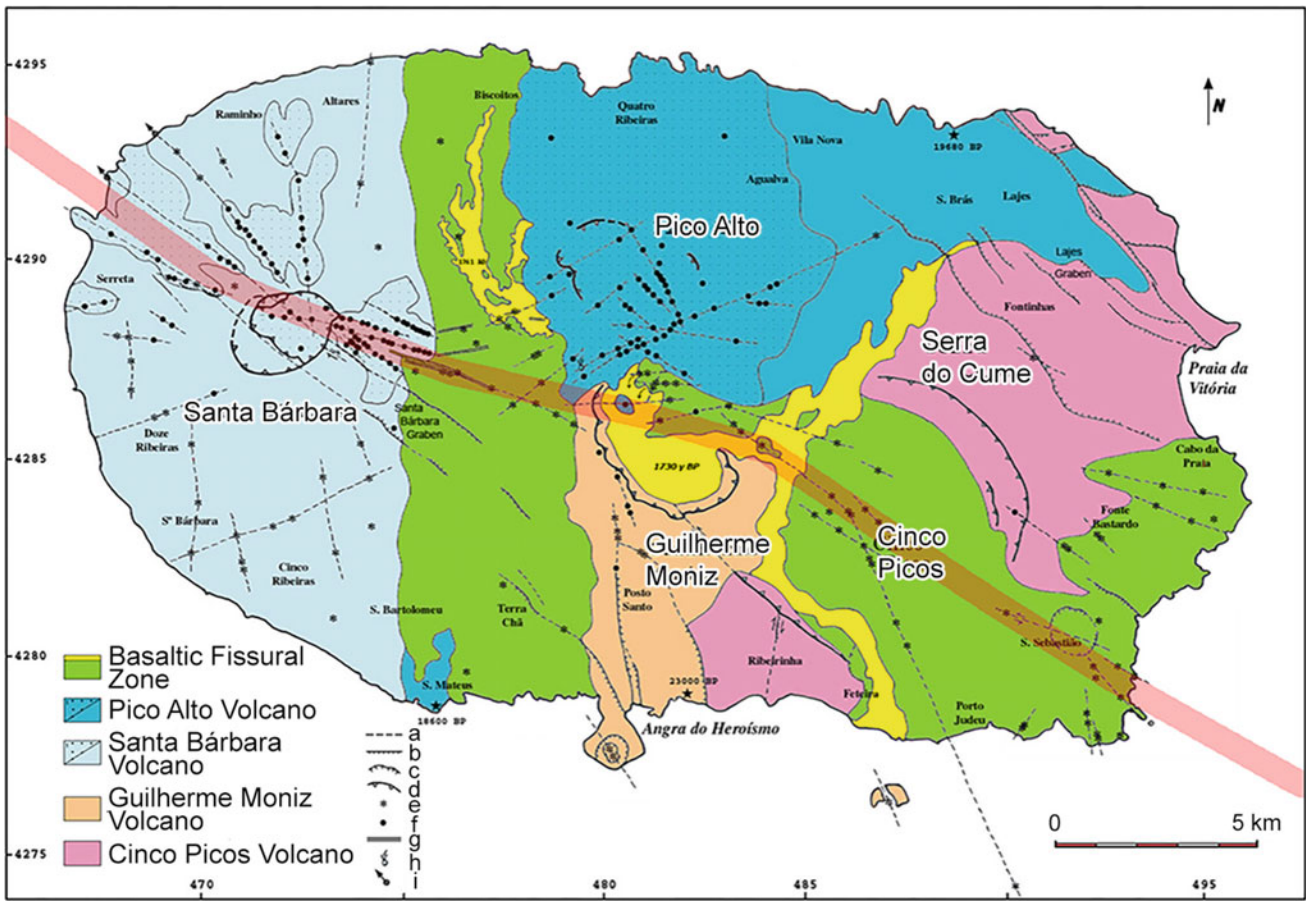

Fig. 2 Volcano-tectonic map of Terceira Island. "Basaltic Fissural Zone" includes the 1761 A.D. and the 1,730 years BP lava flows, in yellow. Dotted areas include domes and colées-type trachytic (s.l.) lava flows. a—volcano-tectonic lineaments; b—fault scarps; c—crater rim; d—caldera rim; e—basaltic (s.l.) eruptive centres (e.g. scoria cones); f—silicious eruptive centres (e.g. domes and coulées); g—eruptive fissures; h—Furnas do Enxofre fumarolic field; i—thermal springs. The shaded strip indicates the axis of the Terceira Rift. UTM coordinates in kilometres (updated from Nunes, 2000)

Site 2: Algar do Carvão volcanic pit

The "Algar do Carvão" volcanic pit is a remarkable structure emplaced in the central area of Terceira Island, classified as a Natural Monument and a geosite of international relevance of the Azores UNESCO Global Geopark due to its volcanic singularities and ecological and conservation value: siliceous stalactites and stalagmites of amorphous silica, refusion walls, obsidian formations and an underground lake are some of these singularities (Nunes et al., 2004a).

This peculiar volcanic pit had a double genesis and nature: it in part relates to the volcanic conduit of a scoria cone (with 2,115 years BP according to Zbyszewski et al., 1971) that belongs to the "Basaltic Fissural Area", but a substantial portion of the pit was previously developed in a trachytic dome and/or coulées associated to the Pico Alto polygenetic volcano (Fig. 6).

The ^{14}C age determinations and geological fieldwork reported by Nunes et al. (2004a) detail this double genesis of Algar do Carvão pit: (i) it was first formed on trachytic flows, dated about 3,200 years ago (Fig. 6) and, (ii) more recently (ca. 1,700 to 2,100 years ago) one, or more, basaltic eruptions happened here in this region with the extrusion of flooding lava flows that almost completely covered the Guilherme Moniz Volcano caldera floor (see Fig. 2), and also to local tectonic stress, this fluid lava drained inside its eruptive centre, allowing the formation of the Algar do Carvão nowadays pit.

Site 3: Serra do Cume caldera rim

The "Serra do Cume" and "Serra da Ribeirinha" hills mark the Cinco Picos collapse caldera rim of the older central volcano of the island nowadays. From this viewpoint, we see

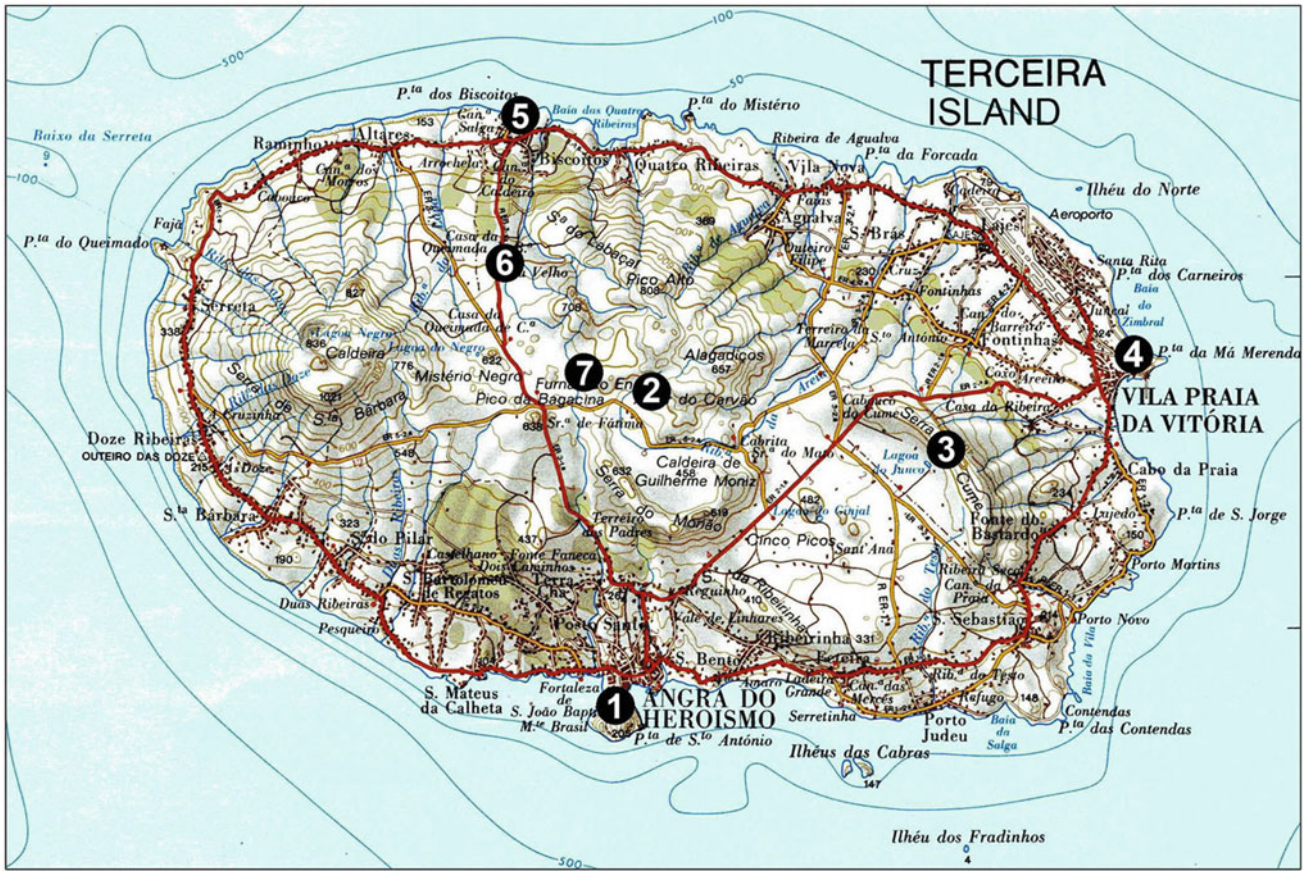

Fig. 3 Itinerary of the NATHAZ22 field trip sites. Topographic base map by Instituto Geográfico e Cadastral

Fig. 4 Panoramic view of Angra do Heroismo city, from the Monte Brasil tuff cone, including main volcanic systems of the island and major N–S fault scarps with a clear morphological signature (see also Fig. 2)

the all-caldera floor (the wider of the Azores archipelago, with a 7 km average diameter) as a vast plain dominated by green pasture lands and dark walls made of volcanic stones.

There are about 15 scoria cones in this vast plain, most aligned with an NW–SE trend and emplaced in the so-called "Cinco Picos" area. Those volcanic cones correspond to intra-caldera cones associated with recent basaltic eruptions of strombolian type along the basaltic fissure volcanism area (SE sector) of the island (Fig. 7) and mark the Terceira Rift fracture zone's signature on-land.

In the background, to the west of this caldera, stands the major central volcanoes of Terceira Island: the Guilherme Moniz, the Santa Bárbara and the Pico Alto polygenetic volcanoes.

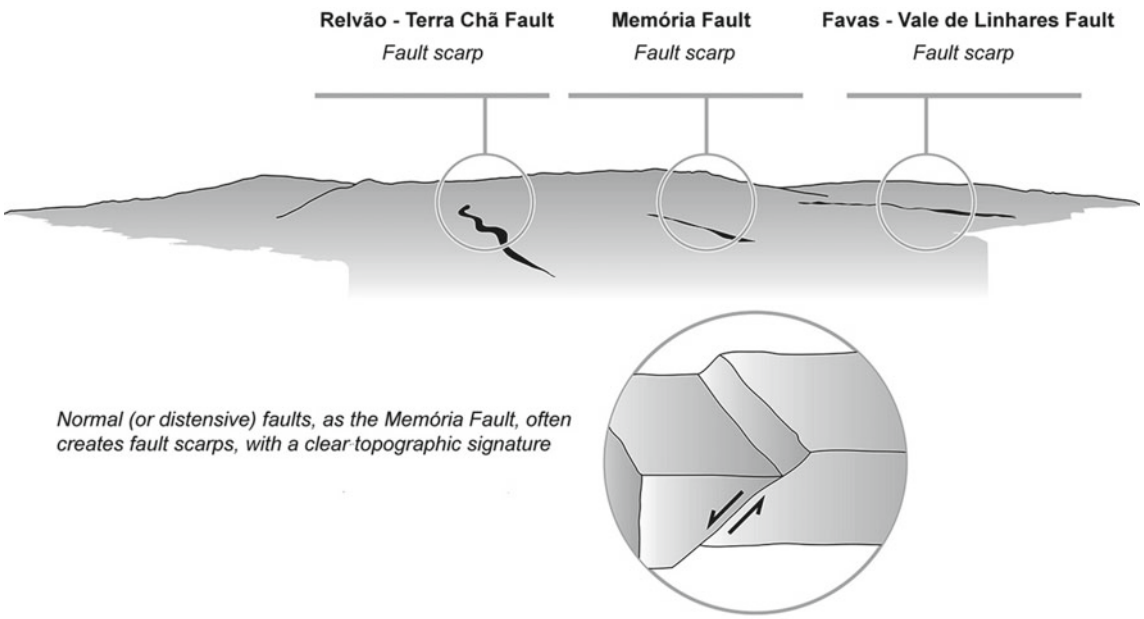

Fig. 5 Schematic representation of the main N–S normal faults that cross the Angra do Heroísmo urban area (see also Fig. 4)

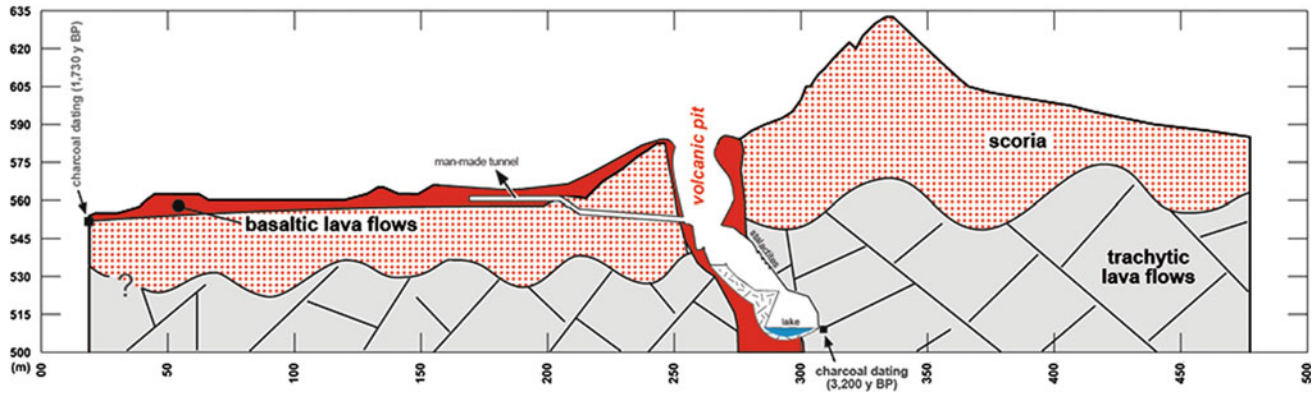

Fig. 6 Geological cross-section of Algar do Carvão volcanic pit area (adapted from Nunes et al., 2004a, 2004b)

Site 4: Lajes Graben

The Lajes Graben tectonic structure characterizes the morphology of the eastern part of Terceira Island (Moore & Silva, 2001; Self, 1974, 1976) together with the smooth slopes of Serra do Cume, and several basaltic scoria cones, like Pico das Favas, Pico das Cruzes and Pico do Capitão cones.

The tectonic structure designated as "Lajes Graben" spreads from the Praia da Vitória town to the Lajes village, with an NW–SE trend, and is bounded, in general terms, by the fault scarps of Serra de Santiago (at northeast) and Fontinhas—Pico Celeiro (at southwest)—Fig. 8. The Lajes Graben is marked by several fault scarps, with steep and usually forested slopes, that delimitate agriculture and flattened urban areas in between them: the airport, the Lajes village and the Praia da Vitória town occupy the central part of this tectonic depression.

The strong and destructive earthquakes of May, 24th 1614 and June, 15th 1841 A.D. (with MMI = IX and the first with more than 200 deaths) are testimonies of the seismic activity associated with this structure and its offshore sections.

Site 5: Biscoitos lava flow

The coastal area of Biscoitos includes the lava delta formed by the aa-type basaltic lava flows extruded about 4,500 years ago from Pico Gordo, a scoria cone located in the central part of Terceira Island (Calvert et al., 2006; Nunes et al., 2014).

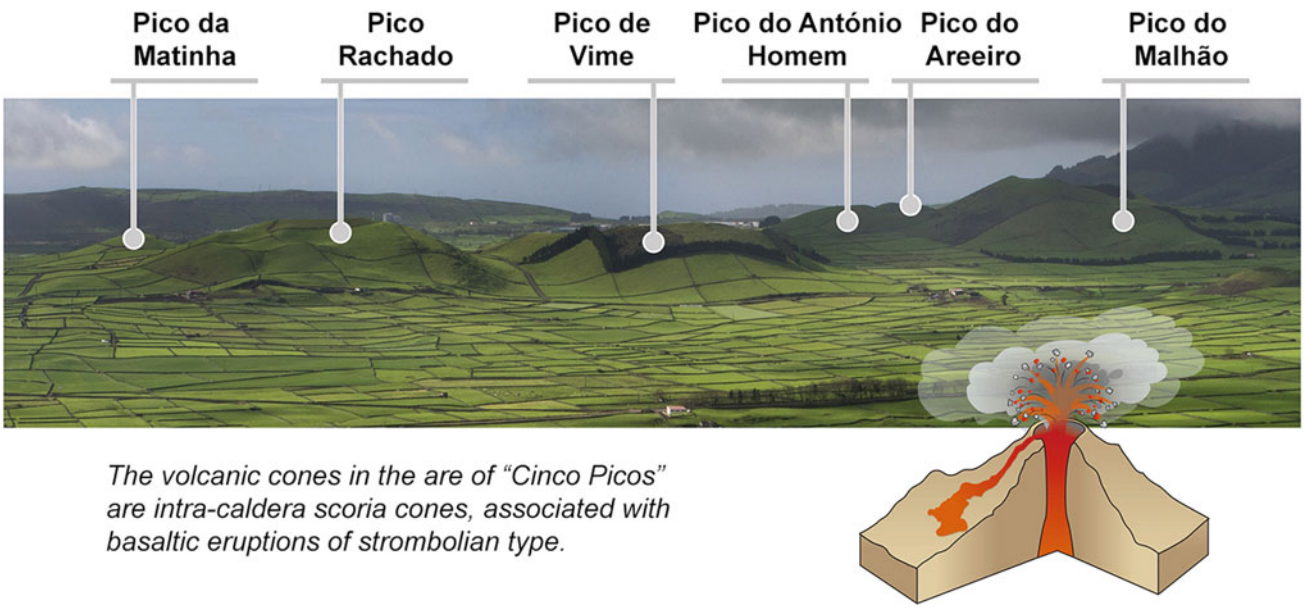

Fig. 7 Main strombolian-type cones of the "Cinco Picos" area

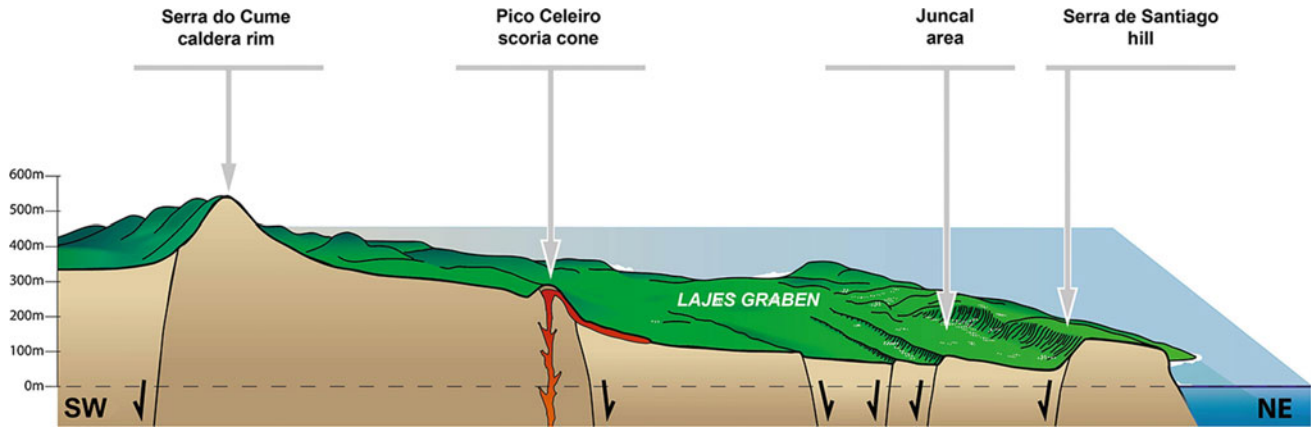

Fig. 8 Schematic cross-section of the Lajes Graben tectonic structure

The main lava flows emitted from that cone moved downslope almost 7 km and reached the sea, pushing the coastline further north for about 500 m, increasing the island's area and forming the several rocky points that characterize the lava delta area. As a result, the Biscoitos coastal front is bordered by a set of huge and convex ridges as "coastal lava cords", with a clear submarine signature (Fig. 9). Nowadays, the natural swimming pools of Biscoitos make a good profit from this peculiar littoral morphology.

Site 6: "Mistério Novo" 1761 A.D. lava flows

In 1761 A.D., two eruptive centres were active on Terceira Island: one associated with the trachytic domes of "Mistérios Negros" and another on the Basaltic Fissural Zone with vents nearby the Pico do Fogo scoria cone.

The latest is known as "Mistério Novo" and corresponds to a typical strombolian-type eruption, with the extrusion of basaltic scoria and lava flows. Those aa-type lava flows moved towards the north (Fig. 10) and, even not reaching the coast, destroyed several agricultural and fertile lands, affecting the inland and upper part of the Biscoitos parish.

The "Mistérios Negros" area is related to the initial phase of the 1761 A.D. historical eruption (that started in the morning of April 17th) and corresponds to domes of thick trachytic lava flows, with a rounded shape and with a black glassy surface of obsidian, thus its name ("negro", meaning black).

Fig. 9 Biscoitos coastal front, with the huge and convex ridges associated with the movement and cooling of the aa-type lava flow entering the ocean

Those domes are located on the east flank of the Santa Bárbara Volcano, Terceira Island, where several other alignments of trachytic lava domes and coulées set up important fractures with an NW–SE general trend under the influence of the so-called "Terceira Rift" tectonic structure (Figs. 2 and 10).

Site 7: Furnas do Enxofre fumarolic field

Furnas do Enxofre thermal area is known for the occurrence of several fumaroles dispersed over an area of around 6,500 m^2 on the south slopes of the Pico Alto polygenetic volcano, the most recent one on Terceira Island and here characterized by several domes and coulées (e.g. silicic lava flows), usually very thick and with obsidian layers.

This fumarolic field is associated with the high enthalpy fluids of the Pico Alto geothermal reservoir that easily arise from depth in this place, due to the presence of cracks, fissures, and hollows, in the dependency of the intersection of fractures with NNW–SSE and NE–SW trends (Fig. 11).

These hydrothermal surface manifestations are composed of water steam (dominant) and volcanic gases. The gas phase is essentially made of carbon dioxide ($\sim$98%), with minor concentrations of gases such as H_2S ($\sim$1%) and CH_4, N_2 and H_2 (Ferreira et al., 2014).

The ground in the fumaroles area (with temperatures up to 95–98 °C) has been deeply altered by hydrothermal processes of rock-water-gases interactions, which has resulted in a higher degree of clay enrichment and water retention capacity, thus its swampy and peat bog characteristics. These "thermal" andosoils are clearly differentiated in terms of their physical and chemical features, reflecting the influence of the thermal conditions on their development.

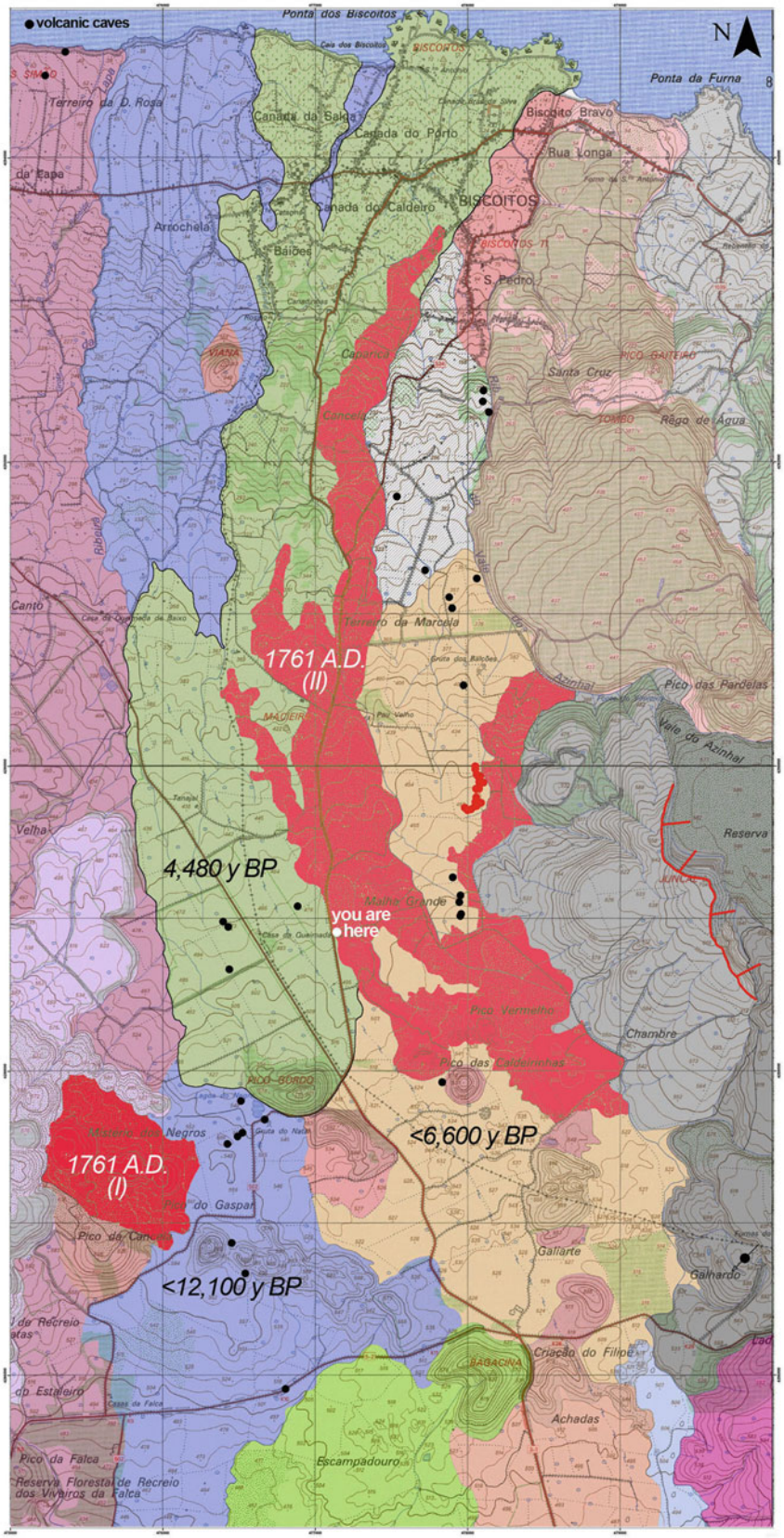

Fig. 10 Geological map of the Basaltic Fissural Zone central area (adapted from Nunes et al., 2014). "Mistérios Negros" domes are indicated as 1761 A.D. (I) and "Mistério Novo" basaltic lava flow is indicated as 1761 A.D. (II). Pico Gordo lava flow that formed the Biscoitos lava delta is dated 4,480 years BP. See also Fig. 2

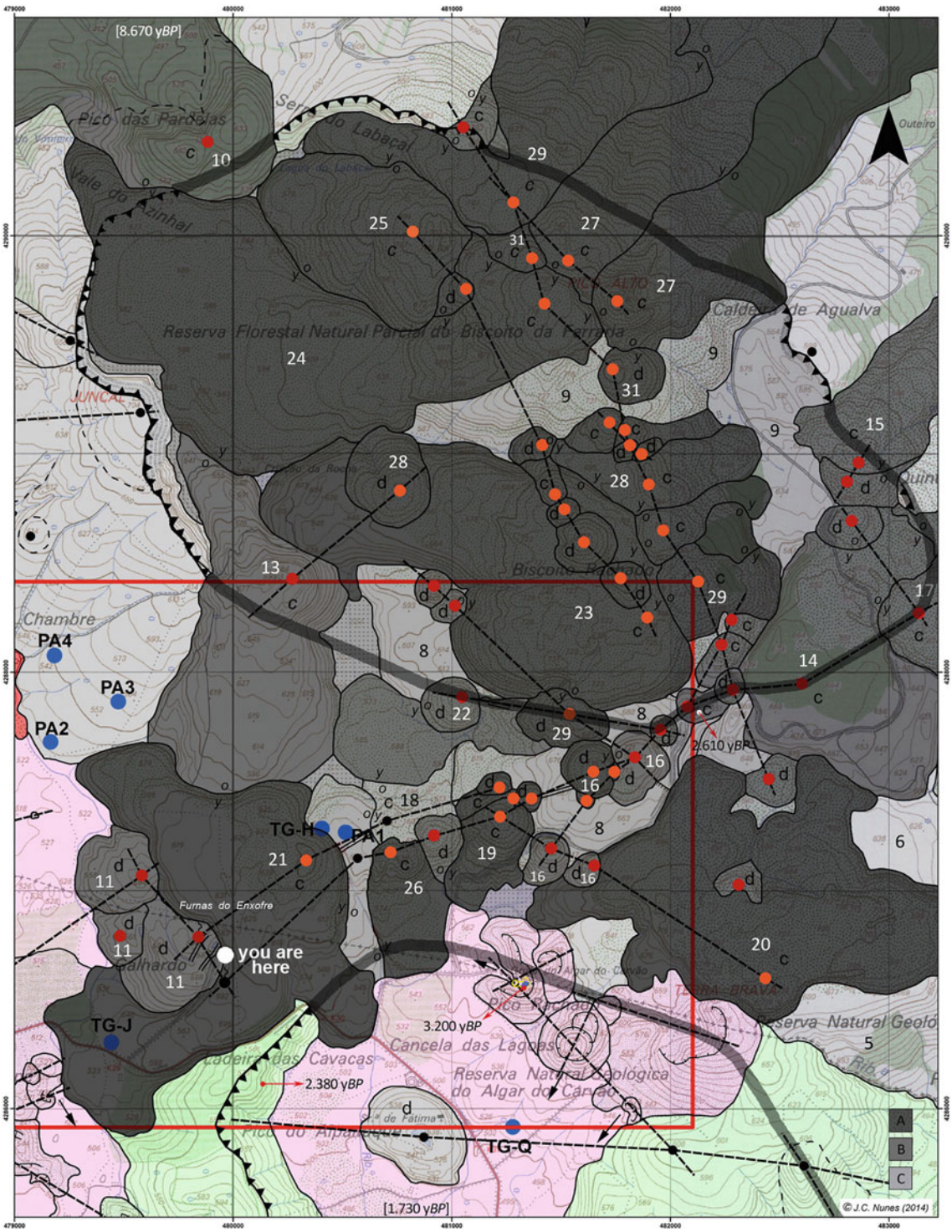

Fig. 11 Geological map of the Furnas do Enxofre fumarolic field and Pico Alto volcano caldera areas. Notations "PA" and "TG" refers to geothermal wells and thermo-gradient boreholes, respectively, of the Pico Alto geothermal field (after Nunes, 2017)

Table 1 Morphometric parameters and general characterization of Terceira Island volcanic systems (modified after Nunes et al., 2004b). MAR-Mid-Atlantic Ridge; a.s.l.—above the sea level; a.o.f.—above the ocean floor; s.l.—sea level; ka—thousand of years; Ma—millions of years; n.a.—non-applicable

	Volcanic system				
Parameters	Cinco Picos Volcano	Guilherme Moniz Volcano	Pico Alto Volcano	Santa Barbara Volcano	Basaltic Fissural area
Minimum distance to MAR (km)	251	244	243	234	240
Maximum elevation (a.s.l.) (m)	545	632	808	1021	637
High (a.s.l.) (m)	1900	2000	2200	2400	2000
Average base diameter (at s.l.) (km)	17.8	13.8	16.5	13.5	5.8*
Area (km^2)	54.8	24.2	90.7	101	130.6
Volume (km^3)	11	7	15	36	36
Top depression maximum diameter (km)	–	4.3	3.6	2.7	n.a
Top depression minimum diameter (km)	–	2.3	2.4	1.9	n.a
Top depression average diameter (km)	7	3.3	3.0	2.3	n.a
Top depression maximum depth (m)	267	174	258	198	n.a
Top depression maximum age (ka)	<300	23	19.6	25	n.a
Maximum known absolute age (Ma)	3.52	0.41	0.022	1.24	0.043
Maximum infered age (Ma)	–	–	0.1	–	0.05
Nr. Intracaldera Eruptive Centres	1	–	30	7	n.a
Nr. Intracaldera Scoria Cones	–	–	–	–	n.a
Nr. Intracaldera Pumice Cones	–	–	–	–	n.a
Nr. Intracaldera Domes	1	–	30	7	n.a
Nr. Intracaldera Maars	–	–	–	–	n.a
Nr. Intracaldera Tuff Cones/Rings	–	–	–	–	n.a
Nr. Flank Eruptive centres	1	14	39	104	5**
Nr. Flank Scoria cones	1	6	1	26	69
Nr. Flank Pumice cones	–	–	–	–	–
Nr. Flank Domes	–	5	38	78	1
Nr. Flank Maars	–	–	–	–	–
Nr. Flank Tuff cones/rings	–	3	–	–	–
Total of eruptive centres	2	14	69	111	75
Nr. historical eruptions	None	None	None	2	1
Last eruption (Y)	–	–	1,000 BP	1998/2001 A.D	1761 A.D
Death/injuries	–	–	–	0	0

3 Concluding Remarks

Four polygenetic volcanoes with subsidence caldera (Cinco Picos, Guilherme Moniz, Santa Bárbara and Pico Alto) and a basaltic fissural zone dominate the eruptive history of Terceira Island. Those central volcanoes are characterized by very heterogeneous volcanic rocks, from basalts to trachytes and comendites in composition (e.g., Gertisser et al., 2010; Pimentel, 2006; Pimentel et al., 2021). A remarkable feature of the Santa Bárbara and Pico Alto volcanoes, and also an iconic characteristic of the Terceira Island landscape, is the presence of thick and massive silicic lava flows as domes and coulées-type lava flows. In Terceira Island, the silicious volcanism associated with those landforms is dominantly effusive (about 80% of the extruded material being lava flows Self, 1976; Self & Gunn, 1976), in clear contrast with what happens on other silicious polygenetic Azorean volcanoes (namely in São Miguel, Graciosa and Faial islands) where pumice fall deposits-forming eruptions are dominant.

The Basaltic Fissural Zone, build-up by about 70 scoria cones and associated lava flows, occupies mostly the SE part of the island, including the São Sebastião pit-crater area (Montesinos et al., 2003) and also the central part of Terceira Island, in this case as a north–south strip, about 3–5 km wide and 50–100 m depth, as recent geothermal studies indicate (Nunes, 2017).

Geological hazards of Terceira Island include volcanic eruptions and earthquakes. Three historical volcanic eruptions took place on the island: (i) the on-land 1761 A.D. eruption had two different eruptive styles and sites, located east of Santa Bárbara Volcano: a first trachytic domes-building phase (at "Mistérios Negros") and afterwards a basaltic phase (at Pico do Fogo scoria cone area) with the extrusion of the "Mistério Novo" lava flows; (ii) the 1867 A.D. eruption was located on the sea, about 2.5 km NW of the island and, (iii) the 1998–2001 Serreta submarine volcano, located to NW of the island, about 8.5 km offshore. This was the last eruption in the Azores and an important milestone for the international volcanology community, with the first observations and interpretation of "Serretian-type" eruptions (details in Forjaz et al., 2001 and Gaspar et al., 2003).

Terceira Island has a track record of various destructive earthquakes, as the Praia da Vitória quakes in 1614 and 1841 and the January 1st, 1980 earthquake. Those earthquakes caused massive destruction around the island and more than 200 victims (e.g. 1614 A.D.) and 61 deaths in the case of the January 1st, 1980 earthquake.

Nevertheless, the more common natural hazards of Terceira Island are storms, river flooding and mass movement episodes, mostly associated with extreme and intense meteorological phenomena. Moreover, those hazards are often triggered or amplified either by inadequate human actions on streams' natural systems dynamics (e.g., affecting fluvial valleys drainage and sections) or by the dominant geological formations of the island (e.g. pumice fall deposits or loose unwelded ignimbrites unstable slopes), respectively. Even large-scale slope instabilities may also be present on oceanic islands like Terceira. However, no major landslide scars on large volcanic edifices areas have been found on Terceira Island (Marques et al., 2015).

References

Calvert, A. T., Moore, R. B., McGeehin, J. P., & Silva, A. M. R. (2006). Volcanic history and 40Ar/39Ar and 14C geochronology of Terceira Island, Azores, Portugal. *Journal of Volcanology and Geothermal Research, 156*, 103–115.

Ferreira, T., Medeiros, A., & CIVISA/CAD Team. (2014). Monitorização geofísica do campo geotérmico do Pico Alto (Ilha Terceira, Açores) durante os ensaios de produtividade dos poços geotérmicos PA2, PA3, PA4 e PA8. Relatório DTC 020/CVARG/CIVISA/14. Angra do Heroísmo (Unpublished Report).

Forjaz, V. H., França, Z., & Nunes, J. C. (2001). Serretian, a new type of submarine eruptions. In: *Abstracts Book "Cities on Volcanoes 2"*, Auckland, New Zealand: 39

Gaspar, J. L., Queiroz, G., Pacheco, J. M., Ferreira, T., Wallenstein, N., Almeida, M. H., & Coutinho, R. (2003). Basaltic lava balloons produced during the 1998–2001 Serreta submarine ridge eruption (Azores). In J.D.L. White, J.L. Smellie, & D.A. Clague (Eds.), *Explosive subaqueous volcanism. AGU Geophysical Monograph, 140*, 205–212.

Gertisser, R., Self, S., Gaspar, J. L., Kelley, S. P., Pimentel, A., Eikenberg, J., Barry, T. L., Pacheco, J. M., Queiroz, G., & Vespa, M. (2010). Ignimbrite stratigraphy and chronology on Terceira Island, Azores. In G. Groppelli & L. Viereck-Goette (Eds.), *Stratigraphy and geology of volcanic areas. GSA Special Paper, 464*, 133–154.

Marques, F. O., Catalão, J., Hildenbrand, A., & Madureira, P. (2015). Ground motion and tectonics in the Terceira Island: Tectonomagmatic interactions in an oceanic rift (Terceira Rift, Azores Triple Junction). *Tectonophysics, 651–652*, 19–34.

Montesinos, F. G., Camacho, A. G., Nunes, J. C., Oliveira, C. S., & Vieira, R. (2003). A 3-D gravity model for a volcanic crater in Terceira Island (Azores). *Geophysical Journal International, 154* (2), 393–406.

Moore, R. B., & Silva, A. M. R. (2001). Assessment of geologic hazards, Terceira island, Azores, Portugal. U.S. Geological Survey Open-File Report.

Nunes, J. C. (2000). Notas sobre a geologia da Ilha Terceira (Açores). *Açoreana, 9*(2), 205–215.

Nunes, J. C. (2017). Cartografia vulcanoestratigráfica do campo geotérmico do Pico Alto (Ilha Terceira, Açores). *Açoreana, 11*(1), 59–88.

Nunes, J. C., Barcelos, P., Pereira, F., Forjaz, V. H., & Borges, P. A. (2004a). Monumento Natural Regional do Algar do Carvão (Ilha Terceira): Biodiversidade e geodiversidade. *Atlântida, 49*, 279–286.

Nunes, J. C., Calvert, A., Medeiros, S., Lima, E. A., Pereira, F., Costa, M. P., Barcelos, P., & Carvalho, M. R. (2014). Geological mapping of the central area of Terceira Island (Azores, Portugal): Associated volcanostratigraphy, ages and genetic implications on the Malha-Balcões-Chamusca lava caves system. *Comunicações Geológicas, Lisbon, 101*, 283–288.

Nunes, J. C., França, Z., Forjaz, V. H., Macedo, R., & Lima, E. A. (2004b). Poligenetic volcanoes of Azores archipelago (Portugal): Size, nature, eruptive styles and related volcanic hazard. In *Abstracts Book (part 1) 32nd International Geological Congress*, Firenze, Italy (p. 336).

Pimentel, A. H. G. (2006). Domos e *coulées* da ilha Terceira (Açores): contribuição para o estudo de mecanismos de instalação. Azores University, Ponta Delgada (M.Sc. Dissertation). http://hdl.handle.net/10400.3/507

Pimentel, A., Self, S., Pacheco, J. M., Jeffery, A. J., & Gertisser, R. (2021). Eruption style, emplacement dynamics and geometry of peralkaline ignimbrites: Insights from the Lajes-Angra Ignimbrite Formation, Terceira Island, Azores. *Frontiers in Earth Science, 9*, 673–686.

Self, S. (1974). *Recent volcanism on Terceira, Azores*. Imperial College, University of London, London (Ph.D. Thesis). http://hdl.handle.net/10044/1/20874

Self, S. (1976). The recent volcanology of Terceira, Azores. *Journal of the Geological Society of London, 132*, 645–666.

Self, S., & Gunn, B. M. (1976). Petrology, volume and age relations of alkaline and saturated peralkaline volcanics from Terceira, Azores. *Contributions to Mineralogy and Petrology, 54*, 293–313.

Zbyszewski, G., Medeiros, A. C., & Ferreira, O. V. (1971). Carta Geológica de Portugal na escala de 1:50000. Notícia explicativa da Folha Ilha Terceira (Açores). Serviços Geológicos de Portugal, Lisboa.

Author Index

A. Malheiro et al. (eds.), *Advances in Natural Hazards and Volcanic Risks: Shaping a Sustainable Future*,
Advances in Science, Technology & Innovation, https://doi.org/10.1007/978-3-031-25042-2